Molecular cloning and expression analysis of ADAMs and cadherins during chicken embryonic development

Dissertation

zur Erlangung des akademischen Grades Doctor rerum naturalium (Dr. rer. nat.) vorgelegt dem Rat der Biologisch-Pharmazeutischen Fakultät der Friedrich-Schiller-Universität Jena

von

Juntang Lin

Master of Science in Zoologie (M.Sc.)

geboren am 08 August 1976

in der Provinz Henan, China

Molecular cloning and expression analysis of ADAMs and cadherins during chicken embryonic development

Dissertation

for obtaining the degree of Doctor rerum naturalium (Dr. rer. nat.) at the Faculty of Biology and Pharmacy, Friedrich-Schiller-University Jena

submitted by

Juntang Lin

Master of Science in Zoology (M.Sc.)

Born on 08 August 1976

in Henan Province, China

Reviewers:

Prof. Dr. Dr. Christoph Redies
Institute of Anatomy I
Friedrich-Schiller-University Jena, School of Medicine
Teichgraben 7
07740 Jena, Germany

Prof. Dr. Jürgen Bolz
Institute of General Zoology and Animal Physiology
Faculty for Biology and Pharmaceutics
Friedrich-Schiller-University Jena
Erbert Str. 1
07743 Jena, Germany

Prof. Dr. Karina Reiss
Department of Dermatology and Allergology
University Hospital Schleswig-Holstein
Schittenhelm Str. 7
24105 Kiel, Germany

Day of the public defence: 16.12.2008

Contents

ABBREVIATIONS

ADAM	A disintegrin and metalloprotease
APP	Amyloid precursor protein
BBB	Blood-brain barrier
bp	Base pair
CAM	Cell adhesion molecule
CD	Cluster of differentiation
Cdh	Cadherin
cDNA	Complementary deoxyribonucleic acid
C. elegans	Caenorhabditis elegans
CHL1	Cell adhesion molecule with homology to L1CAM
CNS	Central nervous system
cRNA	Complementary ribonucleic acid
CTF	C-terminal fragment
CX3CL	CX3 chemokine ligand
DNA	Deoxyribonucleic acid
dsRNA	Double-stranded RNA
E	Embryonic day
E-Cdh	Epithelial cadherin
EGF	Epithelial growth factor
EGFP	Enhanced green fluorescence protein
EGFR	Epithelial growth factor receptor
ER	Endoplasmic reticulum
Fig.	Figure
Fn	Fibronectin
GAPDH	Glyceraldehyde-3-phosphate dehydrogenase
GBSS	Gey’s buffered salt solution
GFP	Green fluorescence protein
Golgi	Golgi compartment
HB-EGF	Heparin-binding epidermal growth factor-like growth factor
HBSS	Hepes-buffered saline solution
IGFBP	Insulin-like growth factor-binding protein

IgG	Immunoglubulin G
IL	Interleukin
ISH	In situ hybridization
MBP	Myelin basic peptide
MDC	Metalloprotease/disintegrin/cysteine-rich
min	Minute
MMP	Matrix metalloproteinase
mRNA	Message ribonucleic acid
ms	Milli-second
N-Cdh	Neural cadherin
ne	Neuroepithelium
NTF	N-terminal fragment
ORF	Open reading frame
P-Cdh	Placental cadherin
PBS	Phosphate-buffered saline
Pcdh	Protocadherin
PCR	Polymerase chain reaction
Pe	Periventricular stratum
PFA	Paraformaldehyde
PK	Protease K
PKC	Protein kinase C
PSGL	P-selectin glycoprotein ligand
R-Cdh	Retinal cadherin
RACE	Rapid amplification of cDNA ends
RCAS	Replication competent avian splice
RNA	Ribonucleic acid
RNAi	Ribonucleic acid interference
RT-PCR	Reverse transcriptase polymerase chain reaction
SAC	Stratum album centrale of the tectum
sec	Second
S.E.M	Standard error of the mean
SGC	Stratum griseum centrale of the tectum
SGFS	Stratum griseum et fibrosum superficiale of the tectum

siRNA	Small interfering RNA
SMA	Alpha smooth muscle actin
SSC	Standard sodium citrate
TACE	TNF-alpha converting enzyme
TBS	Tris-buffered saline
Tect	Tectum
TEM	Transmission electron microscopy
TIMP	Tissue inhibitor of metalloproteinase
TM	Transmembrane domain
TNF	Tumor necrosis factor
TNFR	Tumor necrosis factor receptor
VE-Cdh	Vascular endothelial cadherin

1. INTRODUCTION

This present dissertation explores the expression patterns of members of the ADAM and cadherin gene families in the chicken embryo. Section 1.1 of the Introduction introduces the chicken embryo as an experimental system in developmental biology. Section 1.2 is an outline about the superfamily of cell adhesion molecules, which includes the ADAM and cadherin families. Sections 1.3 and 1.4 give an overview on the functions of ADAMs and cadherins in cell adhesion and related developmental processes, especially during nervous system development. Section 1.5 describes the molecular interactions between ADAMs and cadherins and underlines the motivation to study both families of genes in this work. Section 1.6 outlines the aim and experimental approach of the present dissertation.

1.1 The chicken as an experimental model organism

The chicken (*Gallus gallus*) is an important model organism for biomedical research, embryonic development, and molecular biology (Hamburger and Hamilton, 1951; Bellairs and Osmond, 2005). The chicken embryo has served as one of the most widely used experimental animals for both teaching and research for more than a century, for the following reasons: (1) fertilized eggs are cheap and available in large numbers at any time; (2) chicken embryonic development is fast in comparison with most mammalian embryos, lasting only 21 days, which is similar to that of the mouse; (3) the physiology of the chicken embryo is not complicated by the presence of a placenta; (4) chicken genetics are known well, both for normal embryos and for different mutant forms; and (5) as an amniote, chicken development resembles that of mammals in its broad outline (Bellairs and Osmond, 2005). The recent completion of the sequencing of the chicken genome has enhanced the importance of this species in embryology and developmental biology (http://www.ncbi.nlm.nih.gov/projects/genome/guide/chicken/). More recently, the chicken embryo has also been used broadly in the field of molecular biology and has provided an important model system for studies of gene regulation. Although chicken gene “knock out” is impractical because embryonic stem cells are elusive and generation times in the hen’s reproductive organ are long (Brown et al., 2003), the application of plasmid-based RNA interference (RNAi) in conjunction with in vivo (in ovo or ex ovo) electroporation makes loss-of-function studies possible (Das et al., 2006). In conjunction with gene overexpression (gain-of-function) mediated by the in ovo or ex ovo electroporation of

recombinant plasmids, the chicken embryo allows to fully explore gene function regionally and temporally (Muramatsu et al., 1997, 1998; Luo and Redies, 2004, 2005).

The Redies laboratory has extensive experience in chicken embryonic development, especially in the development of the central nervous system (CNS), both in the context of descriptive studies (Arndt et al., 1998; Fushimi et al., 1997; Redies et al., 1997, 2001, 2002a, b; Arndt and Redies, 1996, 1998; Gänzler-Odenthal and Redies, 1998; Wöhrn et al., 1998, 1999; Gerhardt et al, 1999, 2000a, b; Becker and Redies, 2003; Kovjanic and Redies, 2003; Heyers et al., 2003, 2004; Müller et al., 2004; Ju et al., 2004) and experimental research using in vivo electroporation (Treubert-Zimmermann et al., 2002; Luo and Redies, 2004, 2005; Luo et al., 2004, 2006). For these reasons, I chose the chicken embryo as the experimental animal model in my doctoral research.

1.2 Developmental processes mediated by cell adhesion molecules (CAMs)

The development of an organism like the chicken embryo is a highly complex process. Vertebrate embryos share fundamentally similar developmental mechanisms during early embryogenesis. Multiple cleavage divisions generate a large number of cells from the fertilized oocyte. In a temporally and spatially highly orchestrated fashion, different genes regulate the proliferation, differentiation, migration, adhesion, fate determination and apoptosis of cells (Bellairs and Osmond, 2005).

In developmental processes, cell adhesion molecules (CAMs) play an important role. Many CAMs are glycoproteins located on the external surface of the cytoplasmic membrane. These proteins interact either with other CAMs on adjacent cells or with proteins of the extracellular matrix, to mediate cell-cell and cell-extracellular matrix adhesion, respectively. There are a number of classifications for CAMs. Initially, they were named after the tissue, in which they were first identified. It is now clear that most CAMs are expressed rather widely and not limited to single tissues or organs. For example, N-cadherin (N-Cdh), which was first discovered in the neural tissues, is also found in diverse epithelia and mesenchymal cells; E-cadherin (E-Cdh), which was initially discovered in the epithelium, has also been localized to non-epithelial tissues (Takeichi, 1988; Redies, 2000); and R-cadherin (R-Cdh), which was confirmed in the retina at first, is also expressed strongly in brain (Arndt and Redies, 1996). Later, based on homologies and phylogenetic comparisons, CAMs were separated into several superfamilies, which each contain a number of smaller subgroups. The superfamilies of CAMs include the immunoglobulins, cadherins, integrins, selectins, proteoglycans (including the syndecan

subfamily of adhesion molecules) (Kerrigan et al., 1998). ADAMs (a disintegrin and metalloproteases) can also be viewed as a subfamily of CAMs because of their disintegrin domain, which can bind integrin to mediate cell-cell or cell-extracelluar matrix interaction (Lu et al., 2007). Moreover, ADAMs contain a cysteine-rich domain and an epidermal growth factor (EGF)-like domain, both of which are able to mediate cell-cell adhesion as well (Zhao et al., 2004; Zigrino et al., 2007). In addition, some ADAMs can shed other trans-membrane proteins through their metalloprotease activity. For example, ADAM10 sheds N-Cdh, E-Cdh, protocadherin (Pcdh)-C3 and vascular endothelial cadherin (VE-Cdh), to regulate their functions (Reiss et al., 2005, 2006; Maretzky et al., 2005, 2008; Schulz et al., 2008). The current project focuses mainly on the expression patterns and possible functions of ADAMs and cadherins during chicken embryonic development.

1.3 ADAMs play versatile roles during embryonic development

1.3.1 Structure and potential functions of ADAMs

ADAMs belong to type I trans-membrane proteins. Some members of the ADAM family have also been named MDC, which stands for metalloprotease/disintegrin/cysteine-rich. Members of this protein family possess a multi-domain structure and are composed of a signal peptide, a prodomain, a metalloprotease domain, a disintegrin domain, a cysteine-rich domain, an EGF-like domain, a trans-membrane domain and a cytoplasmic tail (Black and White, 1998; Schlöndorff and Blobel, 1999; Stone et al., 1999; Primakoff and Myles, 2000; Lu et al., 2007). The possession of these multiple domains suggests that ADAMs are potentially involved in proteolysis, adhesion, cell fusion and cell signaling (Blobel, 2002, 2005). The domain structure and the potential function of each domain are shown in Figure 1. Specific biological processes, in which ADAMs have been implicated, include sperm-

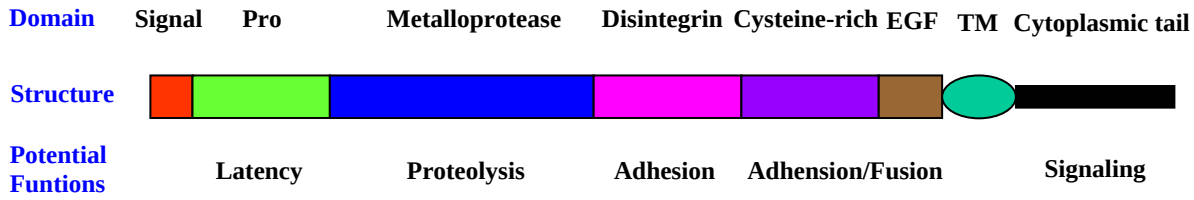

Fig. 1. A schematic diagram for the domain structure and potential functions of ADAMs. EGF, EGF-like domain; TM, trans-membrane domain. Revised after Black and White (1998), Duffy et al. (2003), and Seals and Courtneidge (2003).

egg fusion, somatic cell-cell adhesion, ectodomain shedding, and developmental processes, for example, myoblast fusion and neurogenesis.

Emerging data suggest that ADAMs are probably synthesized in the rough endoplasmic reticulum (ER) and processed to produce their mature form in the Golgi compartment; maturation involves the removal of the prodomain from the ADAM precursor protein (Seals and Courtneidge, 2003; see Fig. 3 in Part 1.5). Most ADAMs possess a putative furin recognition sequence between the prodomain and the metalloprotease domain, which agrees with the finding that ADAMs are possibly activated by a furin-like protein convertase enzyme (Anders et al., 2001; Duffy et al., 2003).

ADAMs have been found in vertebrates, as well as in *Caenorhabditis elegans* (*C. elegans*) and *Drosophila*. However, they are not present in *Escherichia coli*, *Saccharomyces cerevisiae*, or plants. So far, more than 35 members of the ADAM family have been cloned and confirmed in different species. Not every ADAM family member possesses proteolytic function, though all of them have a metalloprotease domain. Only those members, which contain the remarkably conserved sequence HExxHxxGxxHD in the metalloprotease domain, are predicted to have catalytic activation. This is the case for approximately half of all members of the ADAM family. The presently known ADAMs and their potential functions and characteristics are listed in Table 1.1 (http://people.virginia.edu/~jw7g/ Table_of_the_ ADAMs.html).

Table 1.1. Members of the ADAM family

ADAM	**Other name**	**Characteristics and potential functions**	**Organism**
ADAM1	PH-30 alpha; Fertilin alpha	Spermatogenesis, sperm-egg fusion	Human, mouse, rat
ADAM2	PH-30 beta; Fertilin beta	Sperm-egg binding via integrins, testis-specific	Human, mouse, rat
ADAM3	Cyritestin; tMDC I	Sperm-egg adhesion and fusion, testis-specific	Human, mouse, rat
ADAM4	tMDC V	Primarily expressed in testis	Mouse, rat
ADAM5	tMDC II	Primarily expressed in testis	Mouse
ADAM6	tMDC IV	Primarily expressed in testis	Human, mouse, rat
ADAM7	EAP I, GP-83	Sperm maturation, androgen-regulated	Human, mouse, rat
ADAM8	MS2, CD156	Neutrophil infiltration, osteoclast stimulating factor	Human, mouse
ADAM9	MDC9, meltrin gamma	Cleaves HB-EGF, APP, secretase activity, myogenesis	Human,mouse,*Xenopus*,**chicken**
ADAM10	MADM; kuzbanian	Neurogenesis, alpha-secretase activity, axon extension	Many including **chicken**
ADAM11	MDC	Candidate tumor suppressor for breast cancer	Human, mouse, *xenopus*
ADAM12	Meltrin alpha	Myoblast fusion, osteogenesis, cleaves IGFBP-3	Human, mouse, **chicken**
ADAM13		Neural crest cell migration	*Xenopus*, **chicken**
ADAM14	adm-1, UNC-71	Expressed on sperm	*Caenorhabditis elegans*
ADAM15	Metargidin; MDC 15	Blood vessel function, binds integrin	Human, mouse, rat
ADAM16	MDC 16	Spermatogenesis, fertilization, testis-specific	*Xenopus*
ADAM17	TACE	Cleaves pro-TNF-alpha , TNF receptor, L-selectin,	Human, mouse, rat, **chicken**

		APP	
ADAM18	tMDC III	Expressed on sperm, testis-specific	Human, mouse, rat
ADAM19	Meltrin beta	Myogenesis, osteoblast differentiation	Human, mouse
ADAM20		Spermatogenesis, testis-specific	Human
ADAM21	ADAM31	Spermatogenesis, testis-specific	Human, mouse
ADAM22	MDC 2	Expressed predominantly in brain	Human,mouse,*Xenopus*,**chicken**
ADAM23	MDC 3	Expressed predominantly in brain	Human, mouse, **chicken**
ADAM24	Testase-1	Testis-specific	Mouse
ADAM25	Testase-2	Testis-specific	Mouse
ADAM26	Testase-3	Testis specific	Mouse
ADAM27	ADAM18	Expressed on sperm, testis-specific	Human, mouse, rat
ADAM28	eMDCII, MDC-Ls	Expressed in human lymphocytes	Human, mouse, rat
ADAM29	svph1	Testis-specific	Human, mouse
ADAM30	svph4	Testis-specific	Human, mouse
ADAM31	ADAM21	Spermatogenesis testis-specific	Human, mouse
ADAM32		Testis-predominent	Human, mouse, rat
ADAM33		Asthma susceptibility gene, airway remodeling	Human, mouse
ADAM34	Testase-4	Testis-specific	Mouse
ADAM35	Meltrin epsilon	Expressed in epithelial tissues	**Chicken**

Note: This table was derived from data originating in the White laboratory and was referenced in recent publications (Duffy, et al., 2003; Watabe-Uchida et al, 2004; Publication 1). Underlined ADAMs possess the consensus metalloprotease sequence HExGHxxGxxHD that indicates potential metalloprotease activity. "Chicken" highlights the ADAMs that have been identified in chicken. For abbreviations, see the list of abbreviation on page III-V.

ADAMs have been confirmed to play a critical role during fertilization and embryonic development. Altered expression of individual ADAMs has been associated with a number of diseases including inflammation, asthma, arthritis, Alzheimer's disease, atherosclerosis and cancer (Wolfsberg et al., 1995a,b; Primakoff and Myles, 2000; Kheradmand and Werb, 2002; Duffy et al., 2003; Novak, 2004; Yang et al., 2006). From our own results, it is clear that some ADAMs are expressed in a highly restricted pattern in particular types of tissues or cells whereas other ADAMs are expressed more widely throughout the developing organism.

1.3.2 Expression and role of ADAMs in embryonic development

In embryonic development, ADAMs were shown to play a role in spermatogenesis, fertilization, myogenesis and morphogenesis. The processes mediated by ADAMs in embryonic development include ectodomain shedding of cell membrane-binding proteins via the metalloprotease domain, cell-cell and cell-matrix adhesion via the disintegrin and the cysteine-rich domain, and direct or indirect intracellular signaling through the

cytoplasmic domain (Blobel, 2002, 2005). For example, ADAM1 and ADAM2 (also called fertilin-alpha and -beta) are sperm-surface proteins and participate in sperm migration into the oviduct, the dispersal of cumulus cells, and sperm binding to the zona pellucida (Wolfsberg et al., 1993; Nishimura et al., 2004). ADAM24-ADAM27 mRNAs are transcribed in spermatogenic cells in a regulated pattern at a specific developmental stage (Zhu et al., 1999). ADAM12 shows strong expression in neonatal skeletal muscle, bones, nervous system, and is involved in myoblast fusion and differentiation (Yagami-Hiromasa et al., 1995; Gilpin et al., 1998; Bernstein et al, 2004), in pathological processes of muscular dystrophy (Kronqvist et al., 2002), and in adipogenesis (Kawaguchi et al., 2002). Moreover, ADAM12 is expressed in a restricted fashion in the developing chicken brain (Publication 4). Chicken ADAM10 is expressed in the developing dermatome and myotome, in epidermis, endoderm, the epithelial tissues of the kidney, liver, heart, and in neural crest cells. The expression patterns and protein distribution of ADAM10 suggest that it may play a significant role in the morphogenesis of several epithelial tissues (Hall and Erickson, 2003). Moreover, by shedding the Notch ligand Delta from the cell surface in *Drosophila*, ADAM10 (also named Kuzbanian in *Drosophila*) is involved in the Notch signaling pathway that regulates numerous cell fate decisions in invertebrates and vertebrates (Sotillos et al., 1997; Hartmann et al., 2002; Six et al., 2003). ADAM15 has a role in neovascularization in mice under pathological conditions (Horiuchi et al., 2003, 2005), whereas ADAM19 is essential for cardiovascular morphogenesis (Kurohara et al., 2004; Zhou et al., 2004). *Xenopus* ADAM13 is expressed in somitic mesoderm and cranial neural crest cells during gastrulation and neurulation (Alfandari et al., 1997; Gunn et al., 2002). Alteration of its expression in cranial neural crest cells results in the failure of their migration along the branchial pathways (Alfandari et al., 2001). The expression of ADAM13 in the chicken embryo was shown to be temporally and spatially regulated in different organs and tissues (Publication 1). ADAM35 is also expressed in epithelial tissues during chicken embryogenesis (Watabe-Uchida et al., 2004). ADAM17 (also called TNF-alpha converting enzyme or TACE) shows a restricted expression in embryonic development. The absence of ADAM17 activity in mouse allows the generation of cells with an osteoclastic phenotype, but prevents their migration into the core of the diaphysis and the subsequent formation of a marrow cavity (Boissy et al., 2003). ADAM17 is the only ADAM described so far to be expressed in human skin, and its expression was seen throughout all layers of the epidermis, the hair follicles, eccrine ducts and glands, and sebaceous glands (Kawaguchi et al., 2004).

1.3.3 ADAMs in the developing nervous system

To date, 17 members of ADAMs have been identified in the CNS (Novak, 2004). Table 1.2 lists these ADAMs and their metalloprotease characteristics. During nervous system development, ADAMs play versatile roles in neurogenesis, neuronal migration, axonal extension and plasticity, through mediating signal transduction, cell-cell adhesion, and ectodomain shedding. Some ADAM knock-out mice have been shown to cause defects in the structure and/or function of the central nervous system. For example, ADAM10-mutant mice die at embryonic day 9.5 (E9.5) because of major and multiple morphological defects in the cardiovascular system and in the developing brain, such as growth retardation, shortened forebrain primordium, abnormal hindbrain flexure, and an irregular neuroepithelial wall (Hartmann et al., 2002). In ADAM11-deficient mice, brain or spinal cord is apparently normal with no major histological abnormalities, but learning and motor coordination are affected (Takahashi et al., 2006). In ADAM22-deficient mice, ataxia and prominent hypomyelination of the peripheral nerves was observed (Sagane et al., 2005). ADAM23-deficient mice suffer from tremor and ataxia and die during early postnatal times (Mitchell et al., 2001). ADAM17- and ADAM19-deficient mice die at birth because of multiple cardiovascular defects (Horiuchi et al., 2005), but an analysis of their nervous system has not been reported. In contrast, ADAM8-mutant mice have no major defects in the CNS during development or in adult tissues, despite the fact that this molecule is expressed prominently in the developing brain and spinal cord (Kelly et al., 2005). ADAM9 and ADAM15 knock-out mice also do not exhibit obvious morphological deficits in the nervous system (Weskamp et al., 2002; Horiuchi et al., 2003), despite their wide expression in the brain. Possibly, other ADAMs compensate for the absence of these ADAMs.

Table 1.2. ADAMs present in the nervous system and their known substrates

ADAMs	Location in the nervous system	References	Substrate
ADAM1	Pyramidal neurons of the hippocampus	Gerst et al., 2000	Unknown
ADAM2	Pyramidal neurons of the hippocampus, ependymal cells	Gerst et al., 2000; Yang et al., 2005	Inactive
ADAM3	Astrocytes around the third ventricle	Yang et al., 2005	Inactive
ADAM4	mRNA detected in the brain	Wolfsberg et al., 1995a,b	Inactive
ADAM5	mRNA detected in the brain	Wolfsberg et al., 1995a,b	Inactive

ADAM8	Neurons, astrocytes, and oligodendrocytes	Chantry et al., 1992; Schlomann et al., 2000	APP, CHL1, CD16, CD23, CX3CL1, L-selectin, MBP, PSGL-1, TGF-alpha, CD163, IL-1-RII, TNFR1
ADAM9	Ubiquitous expression in the CNS, with higher expression in the hippocampus, hypothalamus, and cerebellum	Weskamp et al., 2002 Hotoda et al., 2002	APP, pro-HB-EGF
ADAM10	Neurons in cerebral cortex, hippocampus, ventral hypothalamus, and cerebellar cortex, oligodendrocytes	Kärkkäinen et al., 2000; Marcinkiewicz and Seidah, 2000; Ortiz et al., 2005; Reiss et al., 2005, 2006	APP, pro-HB-EGF, pro-EGF, Notch, Delta, ephrins, L1, type-IV collagen, cellular prion precursor, CD44, N-Cdh,E-Cdh,Pcdh-C3,VE-Cdh
ADAM11	Neurons throughout the cerebrum, hippocampus, cerebellum, and spinal cord, as well as sensory ganglia	Rybnikova et al., 2002; Sagane et al., 1999	Inactive
ADAM12	Pyramidal neurons and oligodendrocytes	Bernstein et al., 2004	Pro-HB-EGF, insulin-like growth factor binding proteins 3 and 5, S carboxymethylated transferrin
ADAM15	Neurons in the brain and spinal cord, Schwann cells in the peripheral nerve	Bosse et al., 2000	Type-IV collagen, gelatine, CD23
ADAM17	Astrocytes and endothelial cells or neurons	Goddard et al., 2001; Skovronsky et al., 2001	APP, pro-TNF-alpha, pro-HB-EGF, pro-androgen receptor, Notch, EGFR ligand, TNF receptor I and II, pro-amphiregulin, cellular prion precursor…
ADAM19	Ventral horn of the spinal cord and the dorsal root ganglia	Kurisaki et al., 1998; Tanabe et al., 2007	APP, pro-neuroregulin-1
ADAM21	Ependyma, tanycytes, growing neurons and processes	Yang et al., 2005	Unknown
ADAM22	Neurons throughout the brain and spinal cord	Sagane et al., 2005	Inactive
ADAM23	Neurons throughout the brain, with higher expression in the hippocampal formation, basal ganglia and Purkinje and granule cells of the cerebellum	Goldsmith et al., 2004; Leighton et al., 2001; Mitchell et al., 2001	Inactive
ADAM33	Granule neurons of the dentate gyrus and cerebellum	Gunn et al., 2002	Unknown

Note: Revised after Yang et al. (2006). For abbreviations, see the list of abbreviation on page III-V.

Various functions of different ADAMs have been identified in the nervous system. ADAMs play a role not only in axon guidance, but also in neural crest cell migration. The axon pathways in *Drosophila* embryos with a loss-of-function mutation of ADAM10/Kuzbanian exhibit dramatic defects with many axons stalling and failing to extend through the nerve cord. These data suggest that proteolysis by the ADAM10/Kuzbanian metalloprotease activity is required at the growth cone for axon extension (Fambrough et al., 1996). ADAM10 was confirmed to regulate the guidance of retinal axons in *Xenopus laevis* (Chen et al., 2007). Moreover, ADAM10/Kuzbanian

induces the shedding of ephrin-A2 from the cell surface, which results in axon repulsion (Hattori et al., 2000). In *C. elegans*, UNC-71, a homolog of human ADAM14, regulates motor axon guidance and probably functions in a combinatorial manner with integrins and UNC-6/netrin (Huang et al., 2003). ADAM13 is expressed in the somitic mesoderm and neural crest cells during development of *Xenopus laevis* (Alfandari et al., 1997). The protease activity of ADAM13 plays a critical role in neural crest cell migration along defined pathways. It has been proposed that the ADAM13-dependent modification of extracellular matrix and/or other guidance molecules is a key step in the directed migration of the neural crest cells (Alfandari et al., 2001). Recently, it was reported that ADAM2 promotes the migration of neuroblasts in the rostral migratory stream to the olfactory bulb (Murase et al., 2008).

ADAMs are expressed widely in the adult nervous system. In adult rodent CNS, at least 17 ADAM mRNAs are expressed in strikingly different expression patterns (Table 1.2). For example, it has been shown that ADAM10 mRNA expression is widespread, while ADAM17 shows a spatially more restricted expression pattern. The wide and differential expression of ADAM mRNAs suggests versatile roles for ADAMs in the adult CNS (Kärkkäinen et al, 2000). However, little is known about the expression of ADAMs during development, especially during the embryonic development of the nervous system. In order to provide a basis for experimental studies on the role of ADAMs in CNS development, I analyzed the spatiotemporal expression pattern of five ADAMs in detail in the embryonic chicken brain (Publication 4). I also show that the overexpression of ADAM17 in the chicken tectum causes an enlargement of blood vessels due to an increasing number of pericytes (Additional Results).

1.4 Cadherins are important to embryonic development

1.4.1 Structure and functions of cadherins

Cadherins are a family of trans-membrane proteins, which are composed of an extracellular domain, a trans-membrane domain and a cytoplasmic domain. The main characteristics of this protein family are about 100 amino acid-long “cadherin repeats” or “cadherin domains” in the extracellular domain. So far, more than 100 members of the cadherin superfamily were confirmed from vertebrate to invertebrate species (*Drosophila* and *C. elegans*). These members were classified into several subfamilies according to conserved amino acid motifs in their extracellular domain as well as cytoplasmic domain. The subfamilies are the classic cadherins, desmosomal cadherins, Flamingo cadherins, fat-

like cadherins and protocadherins (Hirano et al., 2003; Redies et al., 2005; Takeichi, 2007; Suzuki and Takeichi, 2008; see Fig. 2 for models on the molecular structure of cadherins, cited after Hirano et al., 2003).

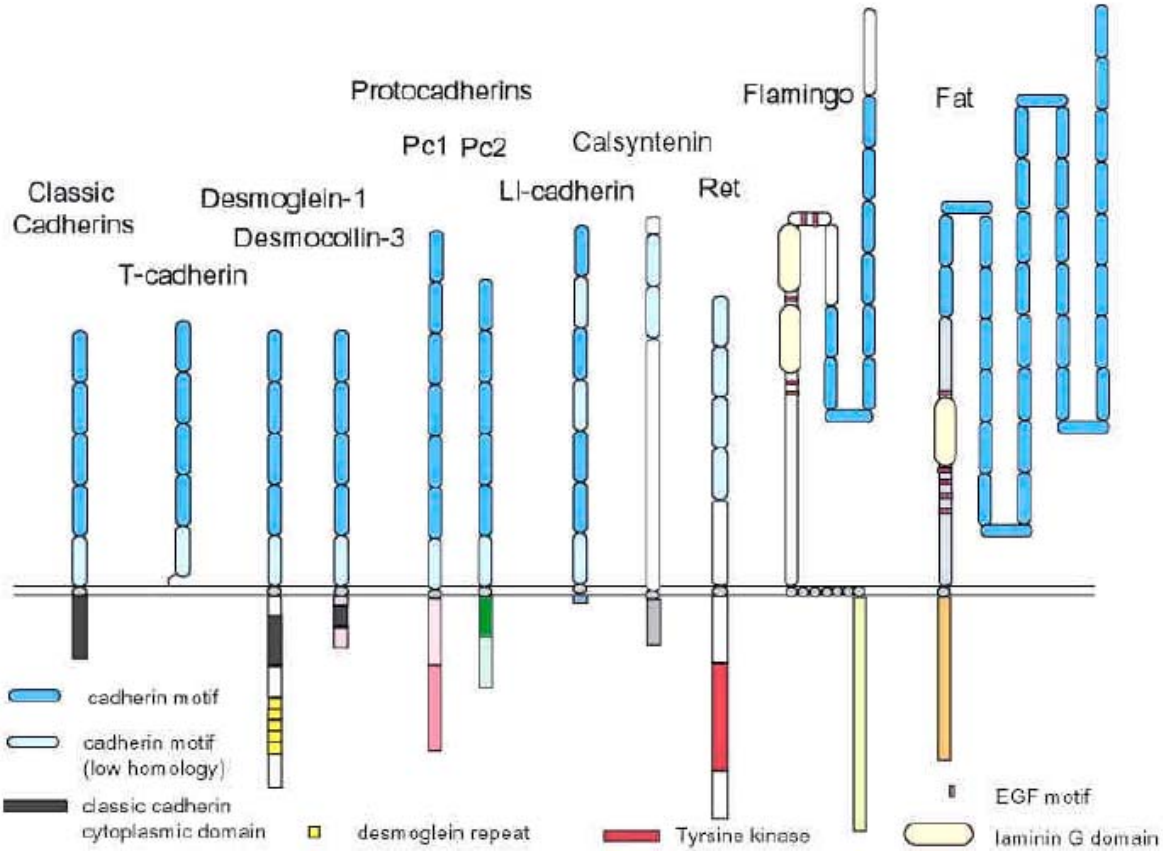

Fig. 2. Members of the cadherin family. Shown are the domain structures of representative members of the cadherin family of vertebrates. Note that, in most cases, the cytoplasmic domains are completely different from each other. This feature suggests that members of different cadherin subfamilies participate in distinct signaling pathways and protein interactions. Reproduced from Hirano et al. (2003).

The present thesis project mainly focuses on classic cadherins (Cdh). Classic cadherins are composed of five conserved extracellular domains, of which the fifth domain shows lower homology than the other domains. On basis of characteristic amino acid sequences in the cytoplasmic domain, classic cadherins can be further divided into type I and type II classic cadherins. Type I classic cadherins, which share five extracellular cadherins repeats, have been named according to the organ or tissue, in which they were first identified. For example, E-Cdh is expressed in epithelia, N-Cdh in neural tissue, P-Cdh in the placenta, and R-Cdh in the retina. The expression of these cadherins, however, is not restricted to these tissues (see above). Type II classic cadherins, which differ from

type I cadherins in specific amino acid sequences, were numbered by the order of their discovery (Hirano et al., 2003). So far, type II cadherins include Cdh5 (VE-Cdh), Cdh6, Cdh7, Cdh8, Cdh9, Cdh10, Cdh11, Cdh12, Cdh18, Cdh19, and Cdh20; these genes were identified in human, mouse, rat, chicken, or *Xenopus*.

As adhesion molecules, the principal function of cadherins is in cell-cell adhesion. Cadherins preferentially bind to the same cadherin subtype (homophilic adhesion). For example, E-Cdh interacts with E-Cdh, whereas N-Cdh interacts with N-Cdh (Hirano et al., 2003). This binding specificity is thought to provide a molecular basis for the sorting of cells and/or their processes during embryonic development (Takeichi, 1995; Redies et al., 1997, 2000; Hirano et al., 2003). The strength of cadherin-mediated adhesion can be regulated by a number of proteins, including catenins, which serve to bind cadherins to the cytoskeleton (Hirano et al., 2003; Takeichi, 2007). Apart from cell-cell adhesion, cadherins have been implicated in a number of signaling pathways, as well as in cell proliferation and differentiation.

Cadherins play an important role in the morphogenesis of many organs and tissues. Abnormal alteration of cadherin function results in malformation and tumorgenesis (Takeichi, 1995; Vleminckx and Kemler, 1999; Peinado et al., 2004). The differential expression of cadherins has been considered as a potential marker for epithelial to mesenchymal transformation during tumor progression (Agiostratidou et al., 2007).

1.4.2 Cadherins in embryonic development

Cadherins play various roles during embryonic development and are major players for regulating morphogenesis. Developmental mechanisms, which are mediated by cadherins, include epithelial-mesenchymal transition, gastrulation movements, tubulogenesis, somite morphogenesis, morphogenesis of the heart and neural tube, vasculogenesis, as well as neurogenesis (Thiery, 2003). E-Cdh and N-Cdh are of critical importance as adhesive molecules in early development. N-Cdh-deficient mouse embryos die around E10.5 with multiple defects, including malformed somites and neural tube, although the death is caused mainly by severe heart defects (Luo et al., 2001). The heart phenotype can be rescued partially by expressing either N-Cdh or E-Cdh under the control of muscle-specific promoters (Luo et al., 2001; Thiery, 2003).

A number of organs express multiple classic cadherins in spatiotemporally highly regulated patterns that reflect complex tissue morphogenesis, for example the brain (Redies, 2000; Hirano et al., 2003) and the kidney (Perantoni, 1999). Several cadherins are

also expressed in the developing inner ear, for instance, N-Cdh, R-Cdh and Cdh11 exhibit distinct spatiotemporal patterns of expression during otic vesicle morphogenesis of zebrafish (Novince et al., 2003), but the spatial relationship of their expression patterns and their relation to cochlear morphogenesis remains largely unclear. I therefore investigated 8 classic cadherins (N-Cdh, R-Cdh, Cdh6, Cdh7, Cdh8, Cdh11, Cdh19 and Cdh20) in the developing chicken cochlea, and demonstrated that most of these cadherins show differential and restricted expression profiles during chicken cochlear development (Publication 2).

1.4.3 Cadherins in the developing and adult CNS

Development of the nervous system is the process, during which the relatively simple neuroepithelium of the neural tube is transformed into a highly complex set of divisions that become functionally connected to form neural circuits. During this process, a large number of cadherins are expressed in a regionally restricted fashion in the embryonic and functional subdivisions of the CNS (Redies, 2000; Hirano et al., 2003). The vast majority of cadherins are expressed during the formation, regionalization, and maintenance of brain segments, brain nuclei, gray matter, and cortical layers (Redies and Takeichi, 1996; Redies, 2000; Hirano et al., 2003). In the nervous system, cadherins were shown to be involved in cell proliferation, differentiation, and migration (Winklbauer et al., 1992; Nakagawa and Takeichi, 1998; Goichberg and Geiger, 1998), in axonal outgrowth, fasciculation, and pathfinding (Riehl et al., 1996; Treubert-Zimmermann et al., 2002), as well as in synaptogenesis and synaptic plasticity (Fannon and Colman, 1996; Tanaka et al., 2000; Suzuki et al., 2007; Takeichi, 2007). Cadherin-mediated adhesive specificity may thus provide a molecular code for early embryonic CNS regionalization as well as for the development and maintenance of functional structures in the CNS (Redies, 2000; Redies et al., 2003; Hertel et al., 2008; Krishna et al., 2008). In the adult CNS, some cadherins seem to be involved in synapse formation and plasticity and neuronal survival. However, the biological role of most cadherins in the adult remains largely unknown (Takeichi, 2007).

The vast complexity of developing brain structures is reflected in a similarly complex expression of genes, such as cadherins (Redies, 2000; Hirano et al., 2003). Complex molecular expression patterns can be established not only by the expression of multiple genes, but also by the expression of multiple mRNA isoforms of the same molecule. In contrast to some protocadherins, for example δ-protocadherins (Vanhalst et al., 2005; Redies et al., 2005), which possess numerous isoforms, there are only single or

very few isoforms for most classic cadherins. With few exceptions (rat Cdh8, Kido et al., 1998; chicken Cdh7, Kawano et al., 2002; and chicken Cdh20, Shirabe et al., 2005), little is known about the spatiotemporal expression patterns of these mRNA isoforms. In this work, I identified three isoforms of Cdh8 in chicken and studied their temporal and spatial expression patterns during development of the embryonic chicken brain (Publication 3).

1.5 Interaction between ADAMs and cadherins

The principal function of cadherins is in cell-cell adhesion. One of the mechanisms, which regulates adhesiveness, is the release of the extracellular cadherin domain. The ectodomain cleavage of cadherins can be inhibited with the matrix metalloproteinase (MMP) inhibitors, including the tissue inhibitors of metalloproteinases (TIMPs; Ho et al., 2001). This finding suggests that a metalloprotease is responsible for the ectodomain shedding of cadherins. Because about half of all ADAMs possess a predicted metalloprotease activity, ADAMs have been considered candidate proteases to shed cadherins and thereby regulate cadherin-mediated cell-cell adhesion. This notion was confirmed by demonstrating that ADAM10

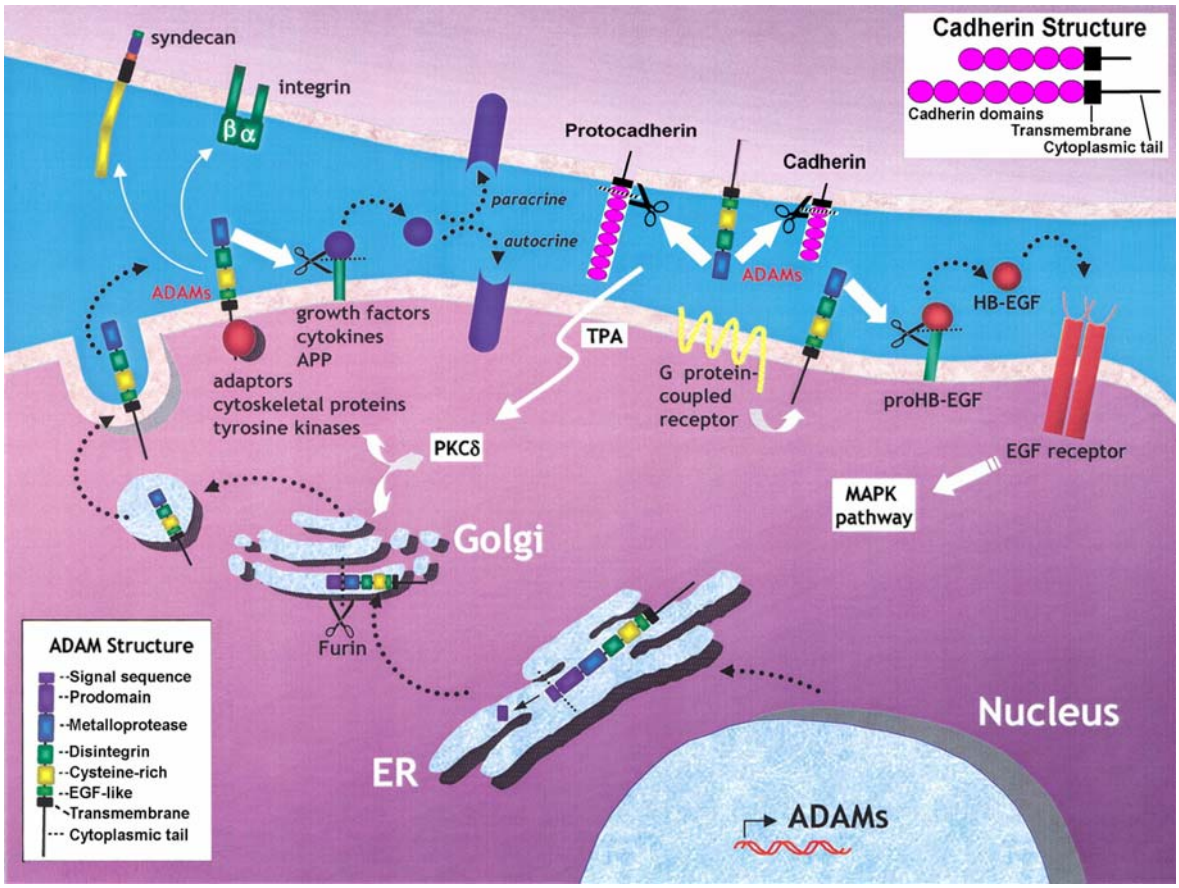

Fig. 3. The structure and function of ADAMs and cadherins as well as their interaction. Revised after Seals and Courtneidge (2003) and Reiss et al. (2005, 2006)

can shed N-Cdh, E-Cdh, Pcdh C3 and VE-Cdh (Reiss et al., 2005, 2006; Maretzky et al., 2005, 2008; Schulz et al., 2008). The postulated interaction between members of the ADAM family and the cadherin family is illustrated in Figure 3.

ADAM10 and N-Cdh are co-localized in different regions of the embryo, such as in the somites, heart and neural tube, giving support for the notion that both proteins are functionally linked. ADAM10 is the major protease responsible for N-Cdh ectodomain cleavage in fibroblasts and neuronal cells. The cell-cell adhesion mediated by N-Cdh is upregulated in ADAM10-deficient fibroblasts. Therefore, ADAM10 is responsible for the initial and crucial proteolytic processing of N-Cdh, leading to the generation of the C-terminal fragment (CTF1) and thereby modulating cell-cell adhesion as well as signal transduction through influencing the cytoplasmic β-catenin pool (Reiss et al., 2005). The coordinated interaction of ADAM10 and N-Cdh may be significant for the coordinated interplay between cell-cell adhesion, cell detachment, cell proliferation and cell survival during embryogenic development (Reiss et al., 2005). ADAM10 is responsible for the shedding of not only N-Cdh, but also E-Cdh in fibroblasts and keratinocytes. ADAM10-mediated E-Cdh shedding affects epithelial cell-cell adhesion as well as cell migration (Maretzky et al., 2005). The shedding of E-Cdh by ADAM10 modulates β-catenin subcellular localization and downstream signaling (Maretzky et al., 2005). Moreover, the release of ADAM10-mediated E-Cdh is regulated by proinflammatory cytokinase and modulates keratinocyte cohesion in eczematous dermatitis (Maretzky et al., 2008). Also, ADAM10 was confirmed to shed γ-protocadherin C3 (Pcdh-C3) and Pcdh-B4 and to regulate their function in fibroblasts and neuronal cells (Reiss et al., 2006). In contrast to N-Cdh that was activated by N-methyl-D-aspartic acid receptor activation in neuronal cells, γ-Pcdh shedding was induced by alpha-amino-3-hydroxy-5-methylisoxazole-4-propionic acid hydrate stimulation, which suggests that the regulatory mechanism of cadherin-mediated function at the synapse differs for the two types of cadherins (Reiss et al., 2006). VE-Cdh, which plays an essential role in the regulation of endothelial permeability, vascular integrity, leukocyte transmigration, and angiogenesis, is the major adhesion molecule at the endothelial adherence junction. Recently, it was reported that VE-Cdh is specifically cleaved by ADAM10 (Schulz et al., 2008). Interestingly, similar to the case of N-Cdh, the cleavage of other cadherins or protocadherins by ADAM10 releases a soluble fragment and generates a carboxyl-terminal membrane-bound stub (see the model of ADAM10-induced shedding of N-Cdh in Figure 4; cited after Reiss et al., 2005).

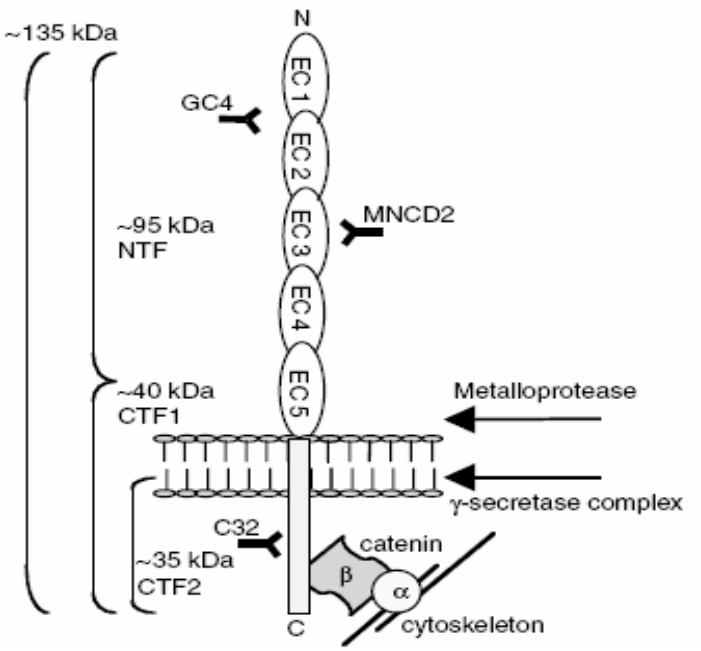

Fig. 4. Schematic representation of the N-Cdh cleavage sites and different antibody binding regions (for antibodies GC4, MNCD2 and C32). Full-length 135 kDa N-Cdh is cleaved by metalloprotease activity into an N-terminal 95 kDa fragment (NTF) and a C-terminal 40 kDa fragments (CTF1), which can be further processed by gamma-secretase-like activity into a soluble 35kDa fragment (CTF2). It was confirmed that the metalloprotease is ADAM10. Reproduced from Reiss et al. (2005).

Moreover, ADAM15 co-localizes with VE-Cdh at the cell-cell boundaries between endothelial cells. VE-Cdh can drive surface expression of ADAM15, which suggests that ADAM15 may be a novel component of adherence junctions and thus could play a role in endothelial adhesive function (Ham et al., 2002). It is likely that many other interactions between ADAMs and cadherins remain unexplored.

1.6 Aims of the study and experimental approach

The expression of members of the ADAM and the cadherin superfamilies can vary considerably. A more precise picture of their spatiotemporal expression profiles would be very useful to explore their possible interactions and functions. The expression patterns of classic cadherins and protocadherins have been studied well in the nervous system of different vertebrate species, such as the rat, the mouse, and the chicken (for reviews, see Redies, 2000; Hirano et al., 2003). Nevertheless, the expression of many members of this trans-membrane protein family remains unexplored, especially in organs other than the brain, for example, the cochlea.

Compared to cadherins, the expression patterns of ADAMs are much less explored during embryonic development. In particular, virtually no details on expression patterns are known for the chicken. ADAM expression during vertebrate development remains poorly documented. Amongst the few studies published in this area are the work by Asayesh et al. (2005) that described the restricted expression of ADAM9, ADAM10, and ADAM17 in divergent pancreatic compartments of the mouse, and the work by Kärkkäinen et al (2000) who found strikingly different expression patterns for individual ADAM mRNAs in the adult mouse CNS.

The aims and the experimental approaches of my study are as follows:

1. Cloning of cDNA fragments, ORFs, or full-length cDNAs of some ADAMs and cadherins from chicken, according to the predicted chicken sequences or homologous sequences from other vertebrate species. The cDNA fragments or ORF of selected ADAMs and cadherins of chicken are cloned into pCR-II vector that will be used to synthesize cRNA probes for in situ hybridization (ISH) of sections through the chicken embryo.

2. The expression patterns of members of the ADAM family and cadherin family are investigated during chicken embryonic development, especially in the CNS and in the cochlea (Publications 1, 2, 3 and 4).

3. For selected ADAM and cadherin genes, the ORFs are subcloned into a suitable vector for gene overexpression (gain-of-function studies) by in ovo or ex ovo electroporation in the chicken embryo, in order to investigate the possible function of these genes during the development. In particular, ADAM17 is overexpressed by ex ovo electroporation in the developing chicken tectum (Additional Results).

2. PUBLICATION OVERVIEW

2.1 Regionalized expression of ADAM13 during chicken embryonic development. Juntang Lin, Christoph Redies, Jiankai Luo. *Developmental Dynamics*, 2007, 236:862-870.

The full-length cDNA of chicken ADAM13 was cloned in this study. The temporal expression profile of chicken ADAM13 was studied by semi-quantitative RT-PCR, and its expression pattern was investigated by section and whole mount in situ hybridization during chicken embryonic development. Our results extend the previous results from *Xenopus* for early stages of development and show in detail that ADAM13 is expressed temporally and spatially at later stages of embryonic development as well.

Own contribution to the manuscript:
1. Cloning and identification of chicken ADAM13
2. Analysis of the temporal expression profile of ADAM13 during chicken embryonic development with semi-quantitative RT-PCR
3. Analysis of the temporal and spatial expression pattern of ADAM13 during chicken embryonic development by section and whole-mount in situ hybridization
4. Data evaluation, and interpretation and representation of the results

2.2 Cadherin expression in the developing chicken cochlea. Jiankai Luo, Hong Wang, Juntang Lin, Christoph Redies. *Developmental Dynamics*, 2007, 236:2331-2337.

In this study, we focused on the chicken embryo as the experimental animal model to investigate the expression patterns of eight classic cadherins (N-Cdh, R-Cdh, Cdh6B, Cdh7, Cdh8, Cdh11, Cdh19 and Cdh20) in the cochlea during late stages of embryonic development with in situ hybridization and fluorescence immunostaining. We also cloned and identified the full-length sequences of Cdh8 and Cdh19, and the open reading frame of Cdh20. Our results show that each cadherin is expressed in one or more cochlear regions, and reversely, two or three cadherins can be co-distributed in one region. These results suggest that cadherins play a role in the development of the cochlea, for example, in the formation of hair cells or in the guidance of neurites from the acoustic ganglion to the hair cells.

Own contribution to the manuscript:
1. Cloning and identification of chicken Cdh8, Cdh19 and Cdh20
2. Bioinformatics analysis of chicken Cdh8 and Cdh19
3. Participation in probes synthesis, section preparation, and the performance of some in situ hybridization experiments on sections
4. Participation in data evaluation and in the interpretation and representation of the results

2.3 Molecular cloning and expression analysis of three cadherin-8 isoforms in the embryonic chicken brain. Juntang Lin, Jiankai Luo, Christoph Redies. *Brain Research*, 2008, 1201:1-14.

We cloned three types of full-length cDNAs of chicken cadherin-8 by the RACE method in this study. Semi-quantitative RT-PCR with type-specific primers showed that the transcription of the three isoforms was temporally and spatially regulated in different parts of the embryonic chicken brain. In situ hybridization results for the long isoform showed that Cdh8 expression is restricted to a subset of brain nuclei, regions and layers in all major parts of the brain. The spatiotemporally regulated restriction of gene expression suggests that the three Cdh8 isoforms likely play different roles during brain development.

Own contribution to the manuscript:
1. Cloning and identification of the three isoforms of chicken Cdh8
2. Analysis of the temporal and regional expression profile of the three Cdh8 isoforms during chicken embryonic brain development with semi-quantitative RT-PCR
3. Analysis of the regional and temporal expression profile of the long Cdh8 isoform in developing chicken brain by in situ hybridization
4. Data evaluation and interpretation and representation of the results

2.4 Differential expression of five members of the ADAM family in the developing chicken brain. Juntang Lin, Jiankai Luo, Christoph Redies. *Neuroscience*, 2008 (in press).

In this study, we cloned the open reading frames of ADAM9, ADAM10 and ADAM23 by RT-PCR, and the full-length cDNAs of ADAM12 and ADAM22 by the RACE method, from chicken embryonic brain. We analyzed their evolutionary relationship by bioinformatics analysis, and investigated their expression patterns in the embryonic chicken brain by in situ hybridization for the first time. Our results show that each of the five ADAMs investigated is expressed in a spatially restricted and temporally regulated expression pattern, but the general types of structures that express the individual ADAMs are rather different. This result suggests that different ADAMs play versatile roles during brain development.

Own contribution to the manuscript:

1. Cloning and identification of the ORFs of ADAM9, ADAM10 and ADAM23 by RT-PCR, and the full-length cDNAs of ADAM12 and ADAM22 by RACE
2. Brain section preparation and in situ hybridization for the five investigated ADAMs in the developing chicken brain
3. Anatomical analysis of the in situ results for the five investigated ADAMs
4. Data evaluation and interpretation and representation of the results

3.1

Regionalized expression of ADAM13 during chicken embryonic development

Juntang Lin, Christoph Redies, Jiankai Luo

Developmental Dynamics, 2007, 236:862-870.

Pages 21-29

DEVELOPMENTAL DYNAMICS 236:862–870, 2007

Regionalized Expression of ADAM13 During Chicken Embryonic Development

Juntang Lin, Christoph Redies, and Jiankai Luo*

ADAMs are a family of membrane proteins possessing a disintegrin domain and a metalloprotease domain, which have functions in cell–cell adhesion, cell–matrix adhesion, and protein shedding, respectively. ADAMs are involved in morphogenesis and tissue formation during embryonic development. In the present study, chicken ADAM13 was cloned and identified, and its expression was investigated by semiquantitative reverse transcriptase-polymerase chain reaction and in situ hybridization during chicken embryonic development. Our results show that ADAM13 expression is temporally and spatially regulated in chicken embryos. At early developmental stages, ADAM13 is expressed in the head mesenchyme, which later develops into the craniofacial skeleton, in the branchial arches, and in the meninges surrounding the brain. Furthermore, ADAM13 mRNA was also detected in several tissues and organs, such as the somites and their derived muscles, the meninges surrounding the spinal cord, the dorsal aorta, the developing kidney, and several digestive organs. *Developmental Dynamics 236:862–870, 2007.* © 2007 Wiley-Liss, Inc.

Key words: ADAM; gene expression pattern; neural crest; somite; dorsal aorta; branchial arch; meninges; limb; kidney; esophagus; proventriculus; gizzard; intestine; development

Accepted 20 December 2006

INTRODUCTION

Members of the ADAM (a disintegrin and metalloprotease) family are membrane-anchored metalloproteases that are expressed widely in many organs, tissues, and cells (Wolfsberg et al., 1995). ADAMs have multiple domains as well as multiple functions. Their metalloprotease domain can shed other transmembrane proteins and cleave matrix proteins. The disintegrin domain as well as the cysteine-rich domain have adhesive activities in cell–cell and cell–matrix interaction. The cytoplasmic domain of ADAMs is involved in intracellular signal transduction. ADAMs are candidates for modulating proteolysis, cell adhesion and fusion, and for cell signaling (Seals and Courtneidge, 2003; White, 2003; Blobel, 2005; Huang et al., 2005; Maretzky et al., 2005; Reiss et al., 2006).

The meltrin subfamily of ADAMs comprises ADAM9, 12, 19, and 35. These genes are involved in muscle development (Yagami-Hiromasa et al., 1995; Weskamp et al., 1996; Lewis et al., 2004; Watabe-Uchida et al., 2004). The expression of some members of the meltrin subfamily has been described in avian embryos (Lewis et al., 2004; Watabe-Uchida et al., 2004). In the quail, ADAM12 is expressed in the cranial ganglia, in the mesenchyme of the limb bud, and in the mesenchyme surrounding the dorsal aorta, whereas ADAM19 is expressed in the cranial and dorsal root ganglia and in the allantois (Lewis et al., 2004). ADAM35 is expressed in the chicken myotome and several epithelial tissues, such as the otic vesicles and gut epithelia (Watabe-Uchida et al., 2004). The full-length sequence of chicken ADAM9 was reported, but its expression pattern has not been described to date (Caldwell et al., 2005).

Xenopus ADAM13, which is similar to members of the meltrin subfamily and to ADAM33, is expressed in somitic mesoderm and cranial neural crest cells during gastrulation and neurulation of *Xenopus* (Alfandari et al., 1997; Gunn et al., 2002). Alteration of its expression in cranial neural crest cells results in the failure of

The Supplementary Material referred to in this article can be found at http://www.interscience.wiley.com/jpages/1058-8388/suppmat

Institute of Anatomy I, Friedrich Schiller University of Jena, Jena, Germany
***Correspondence to: Jiankai Luo, Institute of Anatomy I, Friedrich Schiller University of Jena, Teichgraben 7, D-07743 Jena, Germany. E-mail: tluo@mti.uni-jena.de**

DOI 10.1002/dvdy.21071
Published online 23 January 2007 in Wiley InterScience (www.interscience.wiley.com).

their migration along the branchial and hyoid pathways (Alfandari et al., 2001). In the present study, a cDNA encoding an ortholog of *Xenopus* ADAM13 was identified in the chicken embryo. Its expression pattern was analyzed during embryonic development by semiquantitative reverse transcriptase-polymerase chain reaction (RT-PCR) and, in detail, by in situ hybridization in different tissues and organs.

RESULT AND DISCUSSION

Cloning and Sequence Analysis of a cDNA Encoding Chicken ADAM13

To obtain a cDNA encoding the chicken ortholog of *Xenopus* ADAM13, RT-PCR was performed using a pair of specific primers. A cDNA fragment of 1,278 bp was obtained. Based on the sequence of this fragment, a rapid amplification of cDNA ends (RACE) reaction was performed and a molecule with a full-length sequence encoding 947 amino acids was obtained (see Supplementary Figure S1, which can be viewed at http://www.interscience.wiley.com/jpages/1058-8388/suppmat). This chicken cDNA sequence was analyzed in three steps. First, we searched for highly similar sequences with the NCBI BLAST program (http://www.ncbi.nlm.nih.gov/BLAST). The BLAST result demonstrated that, on the nucleotide level, the chicken cDNA sequence shares a high similarity with the predicted sequence of chicken ADAM13 published in GenBank (NCBI GenBank accession no. XM_420886). On the amino acid level, the protein sequence deduced from the full-length cDNA sequence shows highest similarity to *Xenopus* ADAM13 protein (57% identities and 70% positives; NCBI GenBank accession no. U66003). Second, based on the alignment of the chicken and *Xenopus* amino acid sequences of ADAM13, the chicken protein possesses domains that are characteristic of the ADAM family, such as a signal peptide (38% identity to *Xenopus* ADAM13), a prodomain (48% identity), a metalloprotease domain (80% identity), a disintegrin domain (77% identity), a cysteine-rich domain (62% identity), an EGF-like domain (77% identity), a transmembrane domain (27% identity), and a cytoplasmic domain (36% identity; see Supplementary Figure S1). Third, the amino acid sequence deduced from the obtained chicken cDNA was compared with other meltrin subfamily members and to ADAM33. The obtained chicken gene shares a relatively high identity with ADAM33 and ADAM19, respectively (Fig. 1A). Based on the sequence analysis described above, we designated the obtained molecule as chicken ADAM13. The complete sequence has been submitted to GenBank (NCBI GenBank accession no. EF136663).

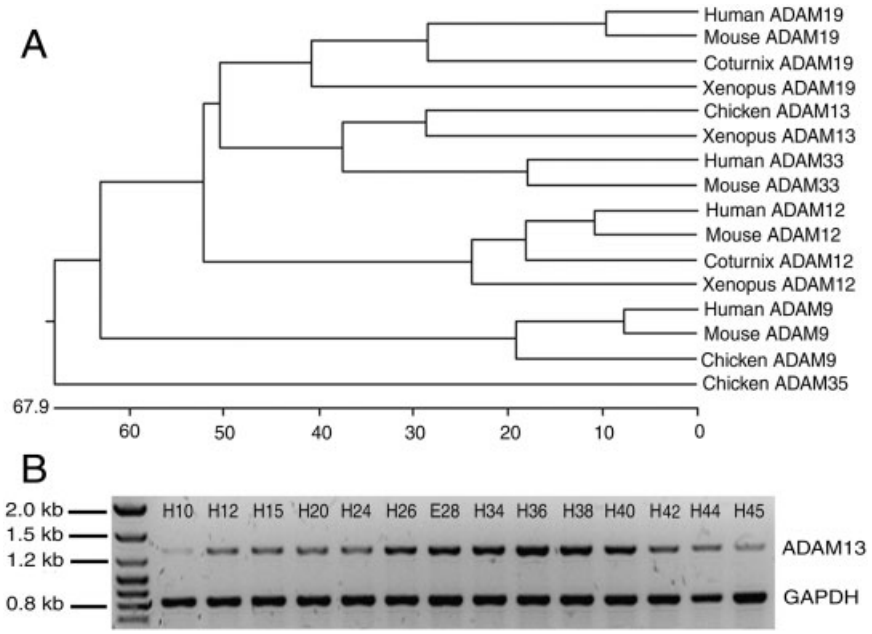

Fig. 1. Phylogenetic tree and semiquantitative reverse transcriptase-polymerase chain reaction (RT-PCR) of ADAM13. **A:** Phylogenetic tree illustrating the relationship between chicken ADAM13 and *Xenopus* ADAM13, the other members of the meltrin subfamily of ADAMs, and ADAM33. The numbers below indicate the percentage difference between the various amino acid sequences. **B:** Detection of ADAM13 expression using semiquantitative RT-PCR at different stages of chicken embryonic development. Glyceraldehyde-3-phosphate dehydrogenase (GAPDH) was used as an internal control to monitor the amount of RNA.

Expression Analysis of ADAM13 at Different Stages by RT-PCR

To study ADAM13 transcription, we performed semiquantitative RT-PCR from stage 10, when the neural crest begins to develop, to stage 45. Our results showed that ADAM13 began to be transcribed weakly at stage 10 (Fig. 1B). As the embryo developed, the transcription of ADAM13 increased gradually, reaching the highest level at around stage 36, and then decreased gradually until stage 45, when ADAM13 was still detectable (Fig. 1B). This result suggested that the expression of ADAM13 was temporally regulated during chicken embryonic development.

Expression of ADAM13 in Structures Derived From Cranial Neural Crest

To study the expression pattern of ADAM13 in detail, we performed in situ hybridization at different stages (from stage 10 to 36) during chicken development using antisense cRNA probes. Sense cRNA probe was used as a negative control for in situ hybridization (data not shown). At stage 10, weak ADAM13 expression was detected in the dorsal cranial area (arrowhead in Fig. 2A) but not in the trunk region. At stage 13, ADAM13 transcript was revealed in the mesenchyme surrounding the brain and the eyes, and also in the branchial arches (Fig. 2D,J–L). Note that, at this stage, the ADAM13-positive neural crest cells were still in migration from dorsal to ventral in the area around the

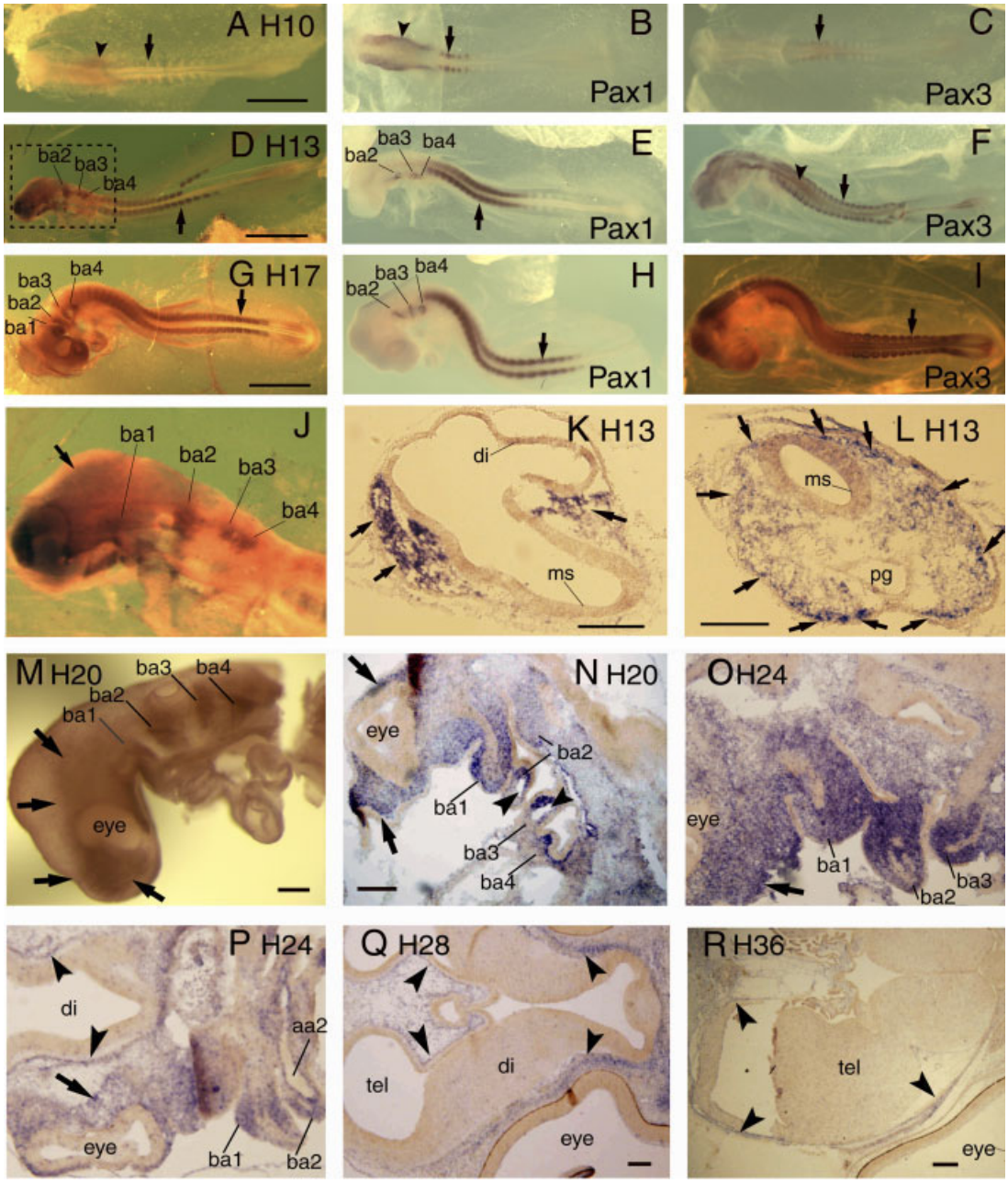

Fig. 2. ADAM13 transcript in structures derived from cranial neural crest cells. **A–I:** Whole-mount in situ hybridization at stage 10 (A–C), stage 13 (D–F), and stage 17 (G–I) using antisense probes for ADAM13 (A,D,G), Pax1 (B,E,H), and Pax3 (C,F,I). The arrows indicate the somites. The arrowheads in A, B, and F indicate the dorsal cranial area, head mesenchyme, and neural tube, respectively. **J–R:** ADAM13 is transcribed in the mesenchyme (arrows in J–O) derived from head cranial neural crest around the forebrain and the eyes, in the branchial arches 1–4 (ba1-4; J, M–P), and in the meninges surrounding the diencephalon (di) and telencephalon (tel; arrowheads in P–R) at different stages (marked). J shows the magnification of the area boxed in D. The arrowheads in N point to branchial arch arteries (aa). K, L, P show transverse sections, and Q and R frontal sections. M–O represent lateral views. ms, mesencephalon; pg, pharynx. Scale bars = 200 μm in K,L,M, in N (applies to N–P); 500 μm in Q,R; 1.2 mm in A (applies to A–C); 2.0 mm in D (applies to D–F); 2.5 mm in G (applies to G–I).

pharynx, where the branchial arches are forming (Fig. 2L). At stage 17, ADAM13 transcription was strong with clear boundary between the different migratory streams in the branchial arches (Fig. 2G); expression was maintained until stage 26 at least (Figs. 2M–O, 3K). The neural crest at the level from the mesencephalon to rhombomere 2 contributes to the mesenchyme around the brain and the eyes and will later develop into parts of the craniofacial skeleton, and into the first branchial arch. The neural crest at the level of rhombomeres 3 to 7 and their adjacent paraxial mesoderm gives rise to branchial arches 2, 3, and 4 (Lumsden et al., 1991; Le Douarin et al., 2004; Noden and Trainor, 2005). In the branchial arches, ADAM13-expressing cells were located more peripherally and enveloped the branchial myogenic cores derived from the paraxial meso-

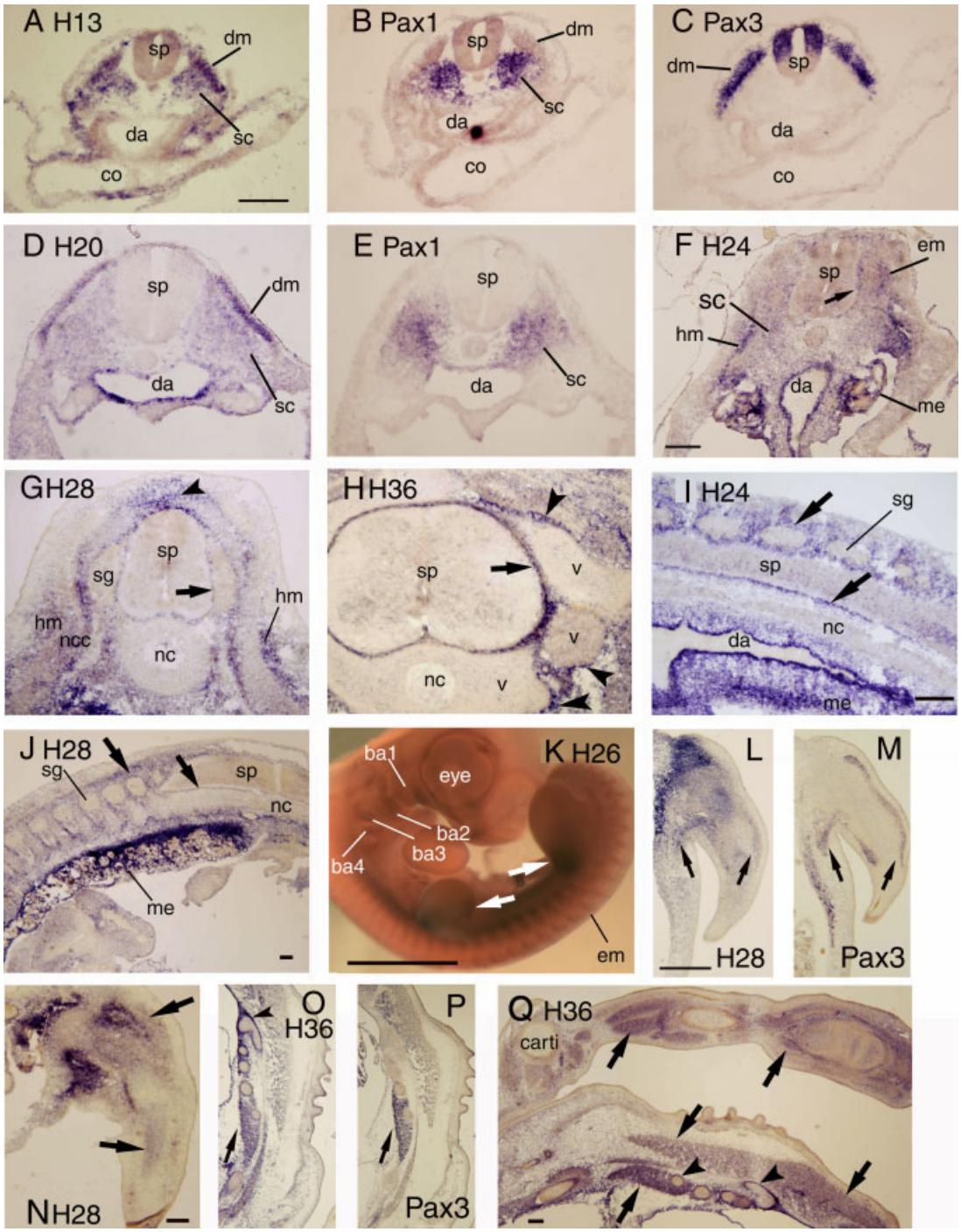

Fig. 3. ADAM13, Pax1, and Pax3 transcription in somites and in somite-derived musculature. **A,D,F–L,N,O,Q:** ADAM13 is expressed in the somites (A,D,F,G; transverse sections), in the meninges around the spinal cord (sp) and spinal ganglia (sg; arrows in F–H, transverse section; in I and J, parasagittal sections), and by muscles (arrows in K,L,N,O,Q) at different stages (marked). **B,E:** Pax1 is expressed in the sclerotome at stage 13 (B) and stage 20 (E). **C,M,P:** Pax3 is transcribed in the dermomyotome (dm; C) and in muscles (arrows in M, P) at stage 13 (C), stage 28 (M), and stage 36 (P). The arrowheads in G indicate ADAM13-expressing neural crest cells. The arrowheads in H, O, and Q show chondroblasts around the vertebrae (v) and the ribs, respectively. carti, cartilage; co, coelom; da, dorsal aorta; em, epaxial myotome; hm, hypaxial myotome; me, mesonephros; nc, notochord; ncc, neural crest cell; sc, sclerotome; tel, telencephalon. Scale bars = 50 μm in L (applies to L,M,O,P); 200 μm in A (applies to A–E,H); in F (applies to F,G) and in I,N; 500 μm in J,Q; 5 mm in K.

derm (Fig. 2D,G,M–O; Noden and Trainor, 2005). Therefore, compared with the expression patterns of the myogenic regulatory genes *Myf5*, *MyoD*, and *Pax1*, the transcript of ADAM13 in the branchial arches was more widespread (Fig. 2D,E,G,H; Barnes et al., 1996; Hacker and Guthrie, 1998; Noden and Trainor, 2005). The ectoderm and the endoderm of the head did not express ADAM13. In the prospective craniofacial skeleton at

stage 36, ADAM13 mRNA was transcribed in the prospective premaxilla, maxilla, nasal conchae, and mandibular cartilage (data not shown). A similar expression pattern was seen in *Xenopus* where ADAM13 is expressed in the structures of the mandibular crest segment, the hyoid crest, and the anterior and posterior branchial crest (Alfandari et al., 1997). In chicken, we found ADAM13 to be expressed also in the mesenchyme around the brain and the eyes, which develops later into parts of the craniofacial skeleton. The expression of ADAM13 in cranial neural crest cells suggested that ADAM13 might play a role in cranial neural crest cell migration and differentiation.

Expression of ADAM13 in the Meninges

During development, the meninges around the forebrain originate from the cranial neural crest, whereas the meninges around the mesencephalon and the more caudal CNS, including the spinal cord, derive from mesoderm-originated mesenchymal cells (Halata et al., 1990; Le Douarin et al., 2004). At stage 24 of chicken development, ADAM13 mRNA was expressed in a thin layer of mesenchyme that condensated around the forebrain and corresponded to the prospective meninges (arrowheads in Fig. 2P). At stage 28, strong expression of ADAM13 was maintained around the forebrain (arrowheads in Fig. 2Q). Expression then decreased gradually but was still visible at stage 36 (arrowheads in Fig. 2R). At stage 28, ADAM13 transcript was also found surrounding the mesencephalon and hindbrain (data not shown). In the meninges around the spinal cord and spinal ganglia, ADAM13 mRNA was expressed from stage 24 (arrows in Fig. 3F,I) and expression persisted at stage 28 (Fig. 3G,J) and stage 36 (Fig. 3H).

Expression of ADAM13 in the Somites and Derived Structures

In whole-mount embryos, ADAM13 mRNA was detected in the somites along the entire cranial–caudal axis at stage 13 (Fig. 2D) and was expressed strongly at stage 17 (Fig. 2G). Expression was absent at stage 10 (Fig. 2A). In transverse sections of stage 13 embryos, ADAM13 transcription was prominent in the dermomyotome and the sclerotome, where Pax3 and Pax1 were also expressed, respectively (Fig. 3A–C). As the somites differentiated, the expression of ADAM13 remained strong in the dermomyotome, but it became more widespread and diffuse around the sclerotome at stage 20 (Figs. 3D, 4A). From stage 24 to 28, ADAM13 was expressed strongly in the epaxial and hypaxial myotome and weakly in the sclerotome (Fig. 3F,G).

Because the epaxial and hypaxial myotomes develop into skeletal musculature, and the sclerotome gives rise to the skeleton of the trunk, we also investigated the expression patterns of ADAM13 in their derivatives. From stage 26, ADAM13 transcript was found in the limb buds (arrows in Fig. 3K) where it was expressed by developing muscles, which coexpressed Pax3 (arrows in Fig. 3L–N; Bendall et al., 1999). At stage 36, ADAM13 mRNA was transcribed widely in muscles, e.g., of the limbs, the thorax, and the abdominal wall (arrows in Fig. 3O,Q). The muscles of the thorax and the abdominal wall also coexpressed Pax3 (arrow in Fig. 3P; Bendall et al., 1999). Furthermore, at stage 36, ADAM13 mRNA was found also in condensed sheets of chondroblasts around cartilage, e.g., around the vertebrae (arrowheads in Fig. 3H) and the ribs and the sternum (arrowheads in Figs. 3O,Q, 4K), but it was not observed in the perichondrium of limb skeleton elements (Fig. 3Q). Expression of ADAM13 in somitic mesoderm was also described in *Xenopus*, but only at early stages of development and not in somite-derived structures (Alfandari et al., 1997). In the present study, we demonstrate expression of ADAM13 also at relatively late stages. Our data show that the skeletal muscles of the limbs and the trunk also expressed ADAM13 mRNA.

ADAM13 Expression in Dorsal Aorta and Developing Kidney

During the initial phase of blood vessel formation, nascent endothelial tubes are established from mesodermal precursor cells. During aortic development, the endothelia of the aorta originate from two different precursor pools: the splanchnopleura and the somite. After fusion of the paired aortae, the vessels are renewed by replacing the initial endothelium derived from the splanchnopleural cells by the cells derived from the somites (Pouget et al., 2006). Furthermore, cells derived from the somites differentiate into smooth muscle cells of the aorta (Pouget et al., 2006). At stages 20 and 24 of chicken development, ADAM13 mRNA was detected in the wall of the dorsal aorta, including the epithelium and the surrounding mesenchyme (Fig. 4A,B). The boundaries of ADAM13 expression between the dorsal aorta and adjacent structures, such as the nephrogenic ridges (mesonephros) and the scleromyotome, were vague (Fig. 4A,B). At stages 28 and 36, the expression of ADAM13 in the wall of the dorsal aorta persisted (Fig. 4C,D). At stage 36, aortic expression was stronger dorsally than ventrally at thoracic levels (insert in Fig. 4E). The ADAM13-expressing cells may correspond to cardiac neural crest cells, which contribute to the formation of the cardiac ganglion and the aortico-pulmonary septum (Verberne et al., 1998). Moreover, in transverse sections at cervical levels, ADAM13 mRNA was expressed strongly throughout the wall of the carotid arteries (Fig. 4E).

During vertebrate development, the intermediate mesoderm forms the nephrogenic mesenchyme, which extends down the trunk and contributes to the developing kidneys (pronephros, mesonephros, and metanephros). At stage 20, ADAM13 mRNA was expressed in the primordia of the glomeruli and in the mesenchyme around the mesonephric tubules (Fig. 4A). As the kidney develops (stages 24 to 36), the expression of ADAM13 became restricted gradually to the glomeruli, the mesenchyme around the mesonephric tubules, and the nephric duct (Fig. 4B–D,F). The glomeruli, which express ADAM13 strongly, were located in the dorsal and medial side of the mesonephros (Fig. 4B–D,F). At the hindlimb level, ADAM13 mRNA was strongly transcribed in the mesenchyme of the met-

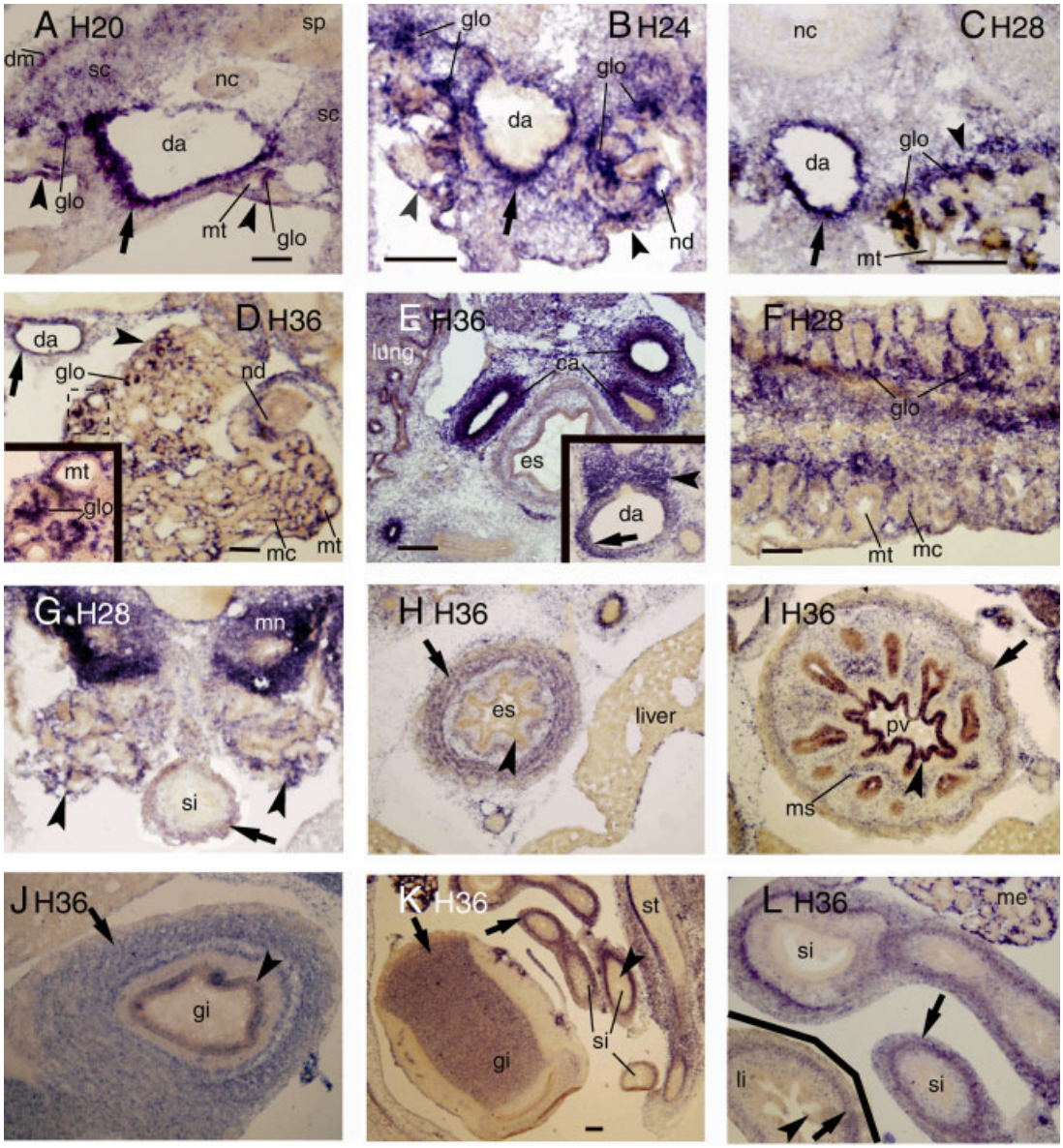

Fig. 4. Expression of ADAM13 in the dorsal aorta, the developing kidney, and digestive organs. **A–G:** ADAM13 is expressed in the dorsal aorta (da, arrows in A–E, transverse sections) and the developing kidneys (arrowheads in A–D,G) at different stages (marked). Note that the boundary of ADAM13 expression between the dorsal aorta and the adjacent sclerotome (sc) and the mesonephros (me) was not clear (A,B). The arrowhead in the insert of E points to the mesenchyme at the dorsal side of the dorsal aorta. The insert in D shows a magnification of the area boxed in D. **H–L:** ADAM13 is transcribed in the epithelium (arrowheads) of the proventriculus (I) and the gizzard (J) and in the mesenchymal layer (arrows) of several digestive organs at stage 36. Transverse sections are shown. ca, carotid artery; dm, dermomyotome; es, esophagus; gi, gizzard; glo, glomerulus; li, large intestine; mc, mesenchyme of the mesonephric tubules; mn, metanephros; ms, mesenchyme; mt, mesonephric tubules; nc, notochord; nd, nephric duct; pv, proventriculus; si, small intestine; sp, spinal cord; st, sternum. Scale bars = 50 μm in A; 100 μm in F (applies to F,G); 200 μm in B–D; and E (applies to E,H–J,L); 500 μm in K.

anephros, which was located at the caudal and dorsal side of the mesonephros (Fig. 4G). At stage 36, the expression of ADAM13 was restricted to the glomeruli and the mesenchyme around the mesonephric tubules and the nephric duct (Fig. 4D and insert). Note that the expression of ADAM13 in the glomeruli seemed to be related to the vascular tuft. Whether ADAM13 expression in the mesenchyme around the mesonephric tubules and the nephric duct is associated with blood vessels, remains to be studied.

Expression of ADAM13 in Digestive Organs

At around stage 28, the gut of the chicken has developed into several parts, such as the esophagus, the proventriculus, the gizzard, and the intestines. Each of these organs consists of an epithelium and a surrounding mesenchyme (connective tissue and smooth muscle layers), which are derived from endoderm and mesoderm, respectively. From stage 28, weak expression of ADAM13 in the digestive organs can be detected in the mesenchymal layer (Fig. 4G; data not shown). At stage 36, ADAM13 mRNA

was transcribed distinctly in the esophagus, the proventriculus, the gizzard, and the intestines, with slightly different expression patterns (Fig. 4H–L). In the esophagus, ADAM13 was expressed in mesoderm-derived tissues only, including the connective tissue and the muscle layers (Fig. 4H). In the proventriculus, ADAM13 was transcribed in scattered epithelial cells and, more weakly, in the surrounding mesenchyme (Fig. 4I). In the gizzard, ADAM13 was expressed in the epithelium and the muscle layers, especially in the latter (Fig. 4J,K). During chicken development, the proventricular epithelium invades the surrounding mesenchyme and begins to form proventricular glands, which later secrete pepsin and hydrochloric acid. This differentiation of gland epithelium depends on an interaction between epithelial cells and mesenchyme and may involve genes such as BMP2, Sox2, and GATA5 (Fukuda and Yasugi, 2005). Whether the restricted expression of ADAM13 in the gizzard epithelial cells plays a role in this interaction remains to be elucidated. In the small and large intestines, the expression of ADAM13 mRNA was restricted to mesenchymal cells and the muscle layers (Fig. 4K,L, and insert in 4L).

Concluding Remarks

In conclusion, during chicken embryonic development, ADAM13 expression is temporally and spatially regulated in different organs and tissues, most of which are of mesenchymal origin. In the head, expression is prominent in the mesenchymal components of the branchial arches, the craniofacial skeleton, and the meninges. In the trunk, ADAM13 is expressed in the somites and several tissues of somitic origin, for example, by the skeletal and intestinal musculature, by the mesoderm-derived components of the kidney and digestive organs, by the meninges of the spinal cord, and by the dorsal aorta. Our results extend previous results from *Xenopus* for early stages of development (Alfandari et al., 1997, 2001) and show in detail that ADAM13 is expressed also at later stages of development.

EXPERIMENTAL PROCEDURES

Animals

Fertilized eggs of White Leghorn chicken (*Gallus domesticus*) were obtained from a local farm and incubated in a forced-draft incubator (Ehret, Emmendingen, Germany) at 37°C and 65% humidity. Embryos were studied at stages 10, 12, 13, 15, 17, 20, 24, 26, 28, 34, 36, 38, 40, 42, 44, and 45 (according to Hamburger and Hamilton, 1951; at least 3 embryos for each stage). After deep anesthesia was induced by cooling on ice, the embryos were removed from the eggs. For RT-PCR analysis, the embryos were quickly immersed in liquid nitrogen and stored in a −80°C freezer. For in situ hybridization of sections, embryos were fixed in 4% formaldehyde solution on ice for 6 to 24 hr, depending on the size of the embryo. For whole-mount in situ hybridization, embryos were dehydrated in a graded series of methanol solutions (25%, 50%, 75% [v/v] in phosphate buffered saline [PBS]) and stored in 100% methanol at −20°C until further use.

cDNA Cloning, RACE, and Sequences Analysis

To obtain chicken ADAM13 cDNA, total RNA of chicken brain at stage 40 was extracted with TRIzol reagent (Invitrogen, Karlsruhe, Germany). First-strand cDNA was synthesized in vitro using the SuperScript First-Strand Synthesis System (Invitrogen). For PCR performance, a pair of specific primers was designed with the Lasergene software (DNASTAR, Inc., Madison, WI), based on the comparison of the *Xenopus* ADAM13 sequence with the predicted ADAM13 sequence of chicken from GenBank (NCBI GenBank accession no. XM_420886). The sequence of the forward primer was A13-F: 5′-CGATGCCAACGCCACGCTCTG-3′ and that of the reverse primer was A13-R: 5′-ATGCTGCACGGGGCCACTGTCC-3′. The PCR template was denatured for 2 min at 94°C, followed by 35 cycles of amplification (denaturing for 20 sec at 94°C, annealing for 30 sec at 64°C, and extension for 2 min at 68°C). After the last cycle, the reaction product was extended finally for 15 min at 68°C. The PCR fragment obtained was cloned into pCR II-TOPO vector with the TA-cloning kit (Invitrogen). The plasmid was purified using the Plasmid Maxi Kit (Qiagen, Hilden, Germany) and sequenced by a commercial company (SeqLab, Göttingen, Germany).

To obtain the full-length sequence of chicken ADAM13, 5′- and 3′-end RACE reactions were performed with the SMART RACE cDNA Amplification Kit (Takara Bio Europe/Clontech, Saint-Germain-en-Laye, France). The specific primers for RACE were chosen from the obtained 1,278-bp fragment according to the instructions of the RACE Kit User Manual. The primers for 5′-end RACE PCR were as follows: 5′-GCGTCTCAGTATAGCCTGGTGCCAGCA-3′ (A13-antisense-1), and 5′-TGCAGATGGTCCCAGCCACCTTCAGC-3′ (A13-antisense-2). The primers used for 3′-end RACE PCR were 5′-GTTGGGCTCCTCCATACTGCGAGAAGC-3′ (A13-sense-1) and 5′-GGACCTGGTGGTGGGACGGAAATGTG-3′ (A13-sense-2). The touchdown PCR for 5′- and 3′-end RACE amplification was performed using the A13-antisense-1 and A13-sense-1 primers together with the Universal Primer Mix, respectively. For the first 5 cycles, the touchdown PCR was performed at 94°C for 30 sec, at 72°C for 3 min, then for second 5 cycles at 94°C for 30 sec, at 70°C for 30 sec, and at 72 for 3 min. At last, for further 27 cycles, PCR was performed at 94°C for 30 sec, at 68°C for 30 sec, and at 72°C for 3 min. To get more specific bands, nested PCR was subsequently carried out with the primers A13-antisense-2 and A13-sense-2 together with the Nested Universal Primer for 5′- and 3′-end cDNA amplification, respectively. The PCR template was denatured for 1 min at 95°C, followed by 20 cycles of amplification (denaturing for 30 sec at 95°C, annealing and extension for 3 min at 68°C). After the last cycle, the reaction product was extended finally for 3 min at 68°C. The PCR products were cloned into pCR II-TOPO vector (Invitrogen) and sequenced by a commercial company (MWG, Ebersberg, Germany). The full-length nucleotide sequence encoding 947 amino acids was obtained by splicing both the 5′- and 3′-end se-

quences together with the previously obtained 1,278-bp fragment.

Chicken cDNAs encoding *Pax1* (NCBI GenBank accession no. NM_204269) and *Pax3* (NCBI Genbank accession no. U22046) were obtained using the same method described as above (RT-PCR). The forward primer for *Pax1* was 5′-AGATCCTGGCCCGCTACAACGAGA-3′, and the reverse primer was 5′-TGGGCGGAAGGGAAGGCAGTC-3′. The forward primer of *Pax3* was 5′-GCATCCGGCCCTGTGTCATCTC-3′, and the reverse primer was 5′-GCTCCTGCCTGCTTCCTCCATCT-3′.

Semiquantitative RT-PCR

Total RNA of chicken embryos (stages 10, 12, 15, 20, 24, 26, 28, 34, 36, 38, 40, 42, 44, and 45) were extracted with TRIzol reagent (Invitrogen). For early embryonic stages (stage 10 to stage 24), whole embryos were homogenized directly in TRIzol reagent. For later stages, the embryos were ground in liquid nitrogen and total mRNA was extracted from the resulting powder. The glyceraldehyde-3-phosphate dehydrogenase (GAPDH) was used as an internal control to monitor the amount of RNA in the semiquantitative RT-PCR. The forward primer for GAPDH was 5′-GGGCTCATCTGAAGGGTGGTGCTA-3′ and the reverse primer was 5′-GTGGGGGAGACAGAAGGGAACAGA-3′. The semiquantitative RT-PCR was performed using the One Step RT-PCR Kit (Qiagen) by adding ADAM13 primers (A13-F and A13-R) together with the primers for GAPDH in one tube. The ratio of primer concentration of ADAM13 and GAPDH was 6:1. The one-step RT-PCR reaction was started at 50°C for 30 min for reverse transcription and at 95°C for 15 min for denaturing, followed by 30 cycles of amplification (denaturing for 45 sec at 94°C, annealing for 45 sec at 62°C, and extension for 1.5 min at 72°C). The RT-PCR fragments were analyzed on agarose gels.

In Situ Hybridization

Digoxigenin-labeled sense and antisense cRNA probes were transcribed using plasmids containing cDNA fragments for ADAM13, Pax1, and Pax3 as templates, according to the manufacturer's instructions for probe synthesis (Roche, Mannheim, Germany). Sense cRNA probe was used as a negative control for in situ hybridization. The protocol for in situ hybridization on cryosections was according to Redies et al. (1993). In brief, 20-μm-thick cryostat sections were fixed with 4% formaldehyde in PBS and were pretreated with proteinase K and acetic anhydride. Sections were hybridized overnight with cRNA probe at a concentration of 3 ng/μl at 70°C in hybridization solution (50% formamide, 3× standard saline citrate, 1× Denhardt's solution, 250 μg/ml yeast transfer RNA, and 250 μg/ml salmon sperm DNA). After the sections were washed and the unbound cRNA was removed by RNAse, the sections were incubated with alkaline phosphatase–coupled anti-digoxigenin Fab fragments (Roche) at 4°C overnight. For visualization of the labeled mRNA, a substrate solution of nitroblue tetrazolium salt and 5-bromo-4-chloro-3-indoyl phosphate was added. The sections were viewed and photographed under a microscope (Olympus BX40, Hamburg, Germany) equipped with a digital camera (Olympus DP70). Whole-mount in situ hybridization was performed on chicken embryos as described by Riddle et al. (1993) using the digoxigenin-labeled cRNA probes described above.

REFERENCES

Alfandari D, Wolfsberg TG, White JM, DeSimone DW. 1997. ADAM 13: a novel ADAM expressed in somitic mesoderm and neural crest cells during *Xenopus laevis* development. Dev Biol 182:314-330.

Alfandari D, Cousin H, Gaultier A, Smith K, White JM, Darribère T, DeSimone DW. 2001. *Xenopus* ADAM 13 is a metalloprotease required for cranial neural crest-cell migration. Curr Biol 11:918-930.

Barnes GL, Hsu CW, Mariani BD, Tuan RS. 1996. Chicken Pax-1 gene: structure and expression during embryonic somite development. Differentiation 61:13-23.

Bendall AJ, Ding J, Hu G, Shen MM, Abate-Shen C. 1999. Msx1 antagonizes the myogenic activity of Pax3 in migrating limb muscle precursors. Development 126:4965-4976.

Blobel CP. 2005. ADAMs: key components in EGFR signalling and development. Nat Rev Mol Cell Biol 6:32-43.

Caldwell RB, Kierzek AM, Arakawa H, Bezzubov Y, Zaim J, Fiedler P, Kutter S, Blagodatski A, Kostovska D, Koter M, Plachy J, Carninci P, Hayashizaki Y, Buerstedde JM. 2005. Full-length cDNAs from chicken bursal lymphocytes to facilitate gene function analysis. Genome Biol 6:R6.

Fukuda K, Yasugi S. 2005. Molecular mechanisms of stomach development in vertebrates. Dev Growth Differ 47:375-382.

Gunn TM, Azarani A, Kim PH, Hyman RW, Davis RW, Barsh GS. 2002. Identification and preliminary characterization of mouse ADAM33. BMC Genet 3:2.

Hacker A, Guthrie S. 1998. A distinct developmental programme for the cranial paraxial mesoderm in the chick embryo. Development 125:3461-3472.

Halata Z, Grim M, Christ B. 1990. Origin of spinal cord meninges, sheaths of peripheral nerves, and cutaneous receptors including Merkel cells. An experimental and ultrastructural study with avian chimeras. Anat Embryol (Berl) 182:529-537.

Hamburger V, Hamilton HL. 1951. A series of normal stages in the development of the chick embryo. J Morphol 88:49-92.

Huang J, Bridges LC, White JM. 2005. Selective modulation of integrin-mediated cell migration by distinct ADAM family members. Mol Biol Cell 16:4982-4991.

Le Douarin NM, Creuzet S, Couly G, Dupin D. 2004. Neural crest cell plasticity and its limits. Development 131:4637-4650.

Lewis SL, Farlie PG, Newgreen DF. 2004. Isolation and embryonic expression of avian ADAM 12 and ADAM 19. Gene Expr Patterns 5:75-79.

Lumsden A, Sprawson N, Graham A. 1991. Segmental origin and migration of neural crest cells in the hindbrain region of the chick embryo. Development 113:1281-1291.

Maretzky T, Reiss K, Ludwig A, Buchholz J, Scholz F, Proksch E, de Strooper B, Hartmann D, Saftig P. 2005. ADAM10 mediates E-cadherin shedding and regulates epithelial cell-cell adhesion, migration, and beta-catenin translocation. Proc Natl Acad Sci U S A 102:9182-9187.

Noden DM, Trainor PA. 2005. Relations and interactions between cranial mesoderm and neural crest populations. J Anat 207:575-601.

Pouget C, Gautier R, Teillet MA, Jaffredo T. 2006. Somite-derived cells replace ventral aortic hemangioblasts and provide aortic smooth muscle cells of the trunk. Development 133:1013-1022.

Redies C, Engelhart K, Takeichi M. 1993. Differential expression of N- and R-cadherin in functional neuronal systems and other structures of the developing chicken brain. J Comp Neurol 333:398-416.

Reiss K, Maretzky T, Haas IG, Schulte M, Ludwig A, Frank M, Saftig P. 2006. Regulated ADAM10-dependent ectodomain shedding of gamma-protocadherin C3 modulates cell-cell adhesion. J Biol Chem 281:21735-21744.

Riddle RD, Johnson RL, Laufer E, Tabin C. 1993. Sonic hedgehog mediates the po-

larizing activity of the ZPA. Cell 75:1401-1416.
Seals DF, Courtneidge SA. 2003. The ADAMs family of metalloproteases: multidomain proteins with multiple functions. Genes Dev 17:7-30.
Verberne ME, Gittenberger-deGroot AC, Poelmann RE. 1998. Lineage and development of the parasympathetic nervous system of the embryonic chick heart. Anat Embryol (Berl) 198:171-184.
Watabe-Uchida M, Masuda A, Shimada N, Endo M, Shimamura K, Yasuda K, Sehara-Fujisawa A. 2004. Novel metalloprotease-disintegrin, meltrin (ADAM35), expressed in epithelial tissues during chick embryogenesis. Dev Dyn 230:557-568.
Weskamp G, Kratzschmar J, Reid MS, Blobel CP. 1996. MDC9, a widely expressed cellular disintegrin containing cytoplasmic SH3 ligand domains. J Cell Biol 132: 717-726.
White JM. 2003. ADAMs: modulators of cell–cell and cell–matrix interactions. Curr Opin Cell Biol 15:598–606.
Wolfsberg TG, Straight PD, Gerena RL, Huovila AP, Primakoff P, Myles DG, White JM. 1995. ADAM, a widely distributed and developmentally regulated gene family encoding membrane proteins with a disintegrin and metalloprotease domain. Dev Biol 169:378-383.
Yagami-Hiromasa T, Sato T, Kurisaki T, Kamijo K, Nabeshima Y, Fujisawa-Sehara A. 1995. A metalloprotease-disintegrin participating in myoblast fusion. Nature 377:652-656.

3.2

Cadherin expression in the developing chicken cochlea

Jiankai Luo, Hong Wang, Juntang Lin, Christoph Redies

Developmental Dynamics, 2007, 236:2331-2337.

Pages 31-37

Cadherin Expression in the Developing Chicken Cochlea

Jiankai Luo,[1,2]* Hong Wang,[3] Juntang Lin,[1] and Christoph Redies[1]

In this study, we demonstrate that eight classic cadherins are differentially expressed in distinct anatomical regions of the cochlea during late stages of chicken embryonic development. Cadherin-6B is expressed in hair cells and spindle-shaped cells, while cadherin-8 mRNA is found only in supporting cells. Cadherin-11 is widely expressed not only in mesenchymal cell around the cochlea, but also in supporting cells and homogene cells. N-cadherin is found in the sensory epithelium, the neurons of the acoustic ganglion and on their neurites that target the hair cells. Three closely related cadherins (cadherin-7, cadherin-19, and cadherin-20) are expressed in a partially complementary manner in spindle-shaped cells and acoustic ganglion cells. R-cadherin is observed in homogene cells, acoustic ganglion cells, and their projections to hair cells. The expression of classic cadherins in the developing cochlea suggests a role for cadherins in the development of the cochlea. *Developmental Dynamics 236:2331–2337, 2007.*

Key words: cadherin; cochlea; gene expression pattern; chicken development

Accepted 31 May 2007

INTRODUCTION

The inner ear is a complex sensory organ that is responsible for sound detection and body balance. It arises from a simple embryonic structure, the otic vesicle, which originates in a transient epithelial thickening of cranial ectoderm at the level of the hindbrain. During embryonic development, the epithelium of the otic vesicle differentiates into distinct anatomical domains of the mature inner ear (Cohen and Fermin, 1978). The ventromedial part of the otic epithelium gives rise to the cochlea and the laterodorsal region to the vestibular organ (Torres and Giraldez, 1998). The formation of the mature inner ear is regulated by a combinatorial action of genes (Brigande et al., 2000) and a balanced interplay between different signaling mechanisms acting from inside and outside the otic vesicle (Riccomagno et al., 2002, 2005; Bok et al., 2003; Ozaki et al., 2004). Remarkably, the mutation of many genes (at least 35 known genes) can lead to hearing loss in hereditary deafness (Holme and Steel, 1999).

Cell adhesion molecules, including cadherins, are suggested to be involved in the genesis of the cochlea (Richardson et al., 1987; Raphael et al., 1988; Kelley, 2003; Novince et al., 2003). Cadherins are Ca^{2+}-dependent adhesion molecules and play important roles in the regulation of morphogenesis and tissue formation during embryo development (Redies, 1995, 2000; Takeichi, 1995). Several cadherins were found to be expressed during the development of the cochlea. In the zebrafish, cadherin-2 (Cad2 or N-Cad) and cadherin-4 (Cad4 or R-Cad) are transcribed only in the sensory patches and in the statoacoustic ganglion, while cadherin-11 (Cad11) mRNA is expressed widely in the early otic placode and restricted later to a subset of cells, including hair cells (Novince et al., 2003). In the chicken, N-Cad and E-cadherin (E-Cad) are coexpressed first in the epithelium of the otic vesicle and subsequently, N-Cad

The Supplementary Material referred to in this article can be found at http://www.interscience.wiley.com/jpages/1058-8388/suppmat

[1]Institute of Anatomy I, Friedrich Schiller University Jena, Jena, Germany
[2]Neurobiological Laboratory, Department of Neurology, University of Rostock, Rostock, Germany
[3]Department of Otorhinolaryngology, Friedrich Schiller University Jena, Jena, Germany
***Correspondence to: Jiankai Luo, Neurobiological Laboratory, Department of Neurology, University of Rostock, Gehlsheimerstrasse 20, D-18147 Rostock, Germany. E-mail: jiankai.luo@uni-rostock.de**

DOI 10.1002/dvdy.21248
Published online 24 July 2007 in Wiley InterScience (www.interscience.wiley.com).

TABLE 1. Primers of PCR or RACE and the PCR Parameters for Different Cadherins[a]

Name	Primer (PCR or RACE)	PCR parameter
Cad8	5′-aacaaacctctggagcctc-3′	30 sec at 94°C, 30 sec at 50°C
	5′-cggaattctcrtanggnggngcngt-3′	3 min at 68°C
Cad11	5′-gctctagagatgctgccgcctctgct-3′	15 sec at 94°C, 30 sec at 55°C
	5′-gctctagacctgcttacatttcttctggattc-3′	3.5 min at 68°C
Cad19	5′-aatgcccggctgctttaca-3′	30 sec at 94°C, 30 sec at 54°C
	5′-ctcaccacctccttcatcatcata-3′	2 min at 68°C
Cad20	5′-ggaattcgtktggaaycarttytt-3′	15 sec at 94°C, 30 sec at 51°C
	5′-ggaattcrtabctctgsagggartc-3′	2.5 min at 68°C
Cad8-anti-1	5′-gaatgttggctgcttctaccttcagag -3′	
Cad8-anti-2	5′-ggcttctctgtccatgttgggaagagc-3′	
Cad19-anti-1	5′-ggtggattgtcattgacgtcagagagg-3′	
Cad19-anti-2	5′-gctcctgcttgtccaaccatatctttgg-3′	
Cad8-sense-1	5′-cctcctaagtttgcgcagagtctgtatc-3′	
Cad8-sense-2	5′-gaaccacagtcaagtgtcccgggtgc-3′	
Cad19-sense-1	5′-ctgtcactgtctgtgactgtgatactg-3′	
Cad19-sense-2	5′-gcataagacagcagaggaagaagactc-3′	

[a]PCR, polymerase chain reaction; RACE, rapid amplification of cDNA ends.

is maintained in the sensory epithelia of the basilar papilla, whereas E-Cad is detected in the nonsensory epithelia (Richardson et al., 1987; Raphael et al., 1988). During rat cochlear ontogeny, truncated-cadherin (T-Cad) is present in fibrocytes and in the subdomains of the pillar cells. E-Cad is expressed in cochlear epithelial cells except for the inner hair cells (IHCs). N-Cad appears first in the developing IHCs and then in the neighboring Kölliker's organ (Simonneau et al., 2003). Furthermore, protocadherin-15 (Pcdh15) and cadherin-23 (Cad23) are involved in the formation of the stereociliary bundles of the hair cells during mouse cochlear development and may regulate the mechanoelectrical transduction in the hair cells (Alagramam et al., 2001a,b; Siemens et al., 2004). Mutation of the Pcdh15 and Cad23 genes results in defects of the hair cells and causes a recessive deafness in mice (Hampton et al., 2003; Noben-Trauth et al., 2003; Adato et al., 2005; El-Amraoui and Petit, 2005).

The distribution and function of cadherins in the developing cochlea have still remained largely unexplored. In the present study, we investigated the relationship between cadherin expression patterns and developing cochlear structures at late embryonic stages in the chicken. Our results show that the expression of each of eight different classic cadherins is restricted to distinct parts and cell types of the cochlea, although the expression patterns overlap partially.

RESULTS

Cloning and Sequence Analysis of Chicken cDNAs Encoding Cadherins

To obtain cDNAs encoding chicken Cad8, Cad11, Cad19, and Cad20, reverse transcriptase-polymerase chain reaction (RT-PCR) was performed using pairs of specific or degenerate primers under optimal parameters (see Table 1). The PCR fragments were subcloned into pBluescript-SK(+) or pCRII-TOPO vectors, and the clones were sequenced. A search of the NCBI GenBank database (http://www.ncbi.nlm.nih.gov) using the BLAST program revealed that two fragments of 2,850 bp and 2,055 bp, respectively, had the same nucleotide sequences as the published chicken Cad11 (GenBank accession no. NM_001004371) and Cad20 (GenBank accession no. NM_204134). Two other fragments of 1,759 bp and 1,407 bp, respectively, shared highest similarity with the predicted sequence Cad8 (GenBank accession no. XM_425125) and Cad19 (GenBank accession no. XM_419115) of chicken. To identify whether these two fragments were chicken Cad8 and Cad19, rapid amplification of cDNA ends (RACE) was carried out using different primers (see Table 1). Two full-length sequences encoding 799 amino acids (see Supplementary Figure S1, which can be viewed at http://www.interscience.wiley.com/jpages/1058-8388/suppmat) and 776 amino acids (see Supplementary Figure S2) were obtained, respectively. On the nucleotide level, these two full-length sequences share highest similarity with the predicted chicken Cad8 and Cad19 sequences, respectively. On the amino acid level, the proteins deduced from the two full-length sequences show highest similarity to human Cad8 (90% identity; GenBank accession no. BC113416) and to human Cad19 (57% identity; GenBank accession no. AJ007607), respectively. Alignment of the amino acid sequences between the obtained chicken molecules and known cadherins revealed that the deduced chicken proteins possess the domains characteristic of the classic cadherin family (see Supplementary Figures S1 and S2). Taken together, the two molecules obtained were identified as chicken Cad8 and Cad19, respectively. The complete sequences of chicken Cad8 (accession no: EF608154) and Cad19 (accession no: EF608155) have been submitted to NCBI GenBank.

Expression of Cadherins in the Developing Cochlea

We investigated the gene expression patterns of eight classic cadherins in

transverse sections through midregions of the cochlea from 11 days of incubation (E11; stage 37), when hearing in chicken embryo begins (Saunders et al., 1973; Jackson and Rubel, 1978; Jones et al., 2006), to the prehatching stage (E18). At E11, different types of cells in distinct anatomical regions can be recognized in the embryonic cochlea (Cohen and Fermin, 1978; Tanaka and Smith, 1978). For example, sensory hair cells and supporting cells are located in the basilar papilla, and ganglion cells in the acoustic ganglion (Fig. 1A,B). The three cell types can be visualized by their Islet-1 expression (Li et al., 2004) (Fig. 1C). Homogene cells are found adjacent to the superior fibrocartilaginous plate and spindle-shaped cells are distributed between the acoustic ganglion cells and the sensory epithelium (Fig. 1A). In the following paragraphs, we will describe the expression of each cadherin in the different cell types and tissues associated with the cochlea.

Cad6B mRNA was detectable at E11 and E14 (Fig. 1D,E) in the spindle-shaped cells and the acoustic ganglion cells, but disappeared at E18 (Fig. 1F). From E14, Cad6B began to be expressed in the tall hair cells (Fig. 1E–G). Cad8 mRNA was extremely abundant in the supporting cells at the inferior edge of the basilar papilla at E11 and E14 (Fig. 1H,I) and was distributed homogeneously at E18 (Fig. 1J).

For Cad11, previous studies have indicated that this molecule is expressed widely by neural cells as well as by mesenchymal cells. Cad11 is involved in various morphogenetic events, e.g., neurogenesis and chondrogenesis, during embryonic development (Simonneau et al., 1995; Simonneau and Thiery, 1998; Vallin et al., 1998). In our study, strong expression of Cad11 was found in the chondroblast cells and the mesenchymal cells around the cochlea. Furthermore, Cad11 was found in the supporting cells and the homogene cells from E11 to E18 (Fig. 1K–M). N-Cad was expressed abundantly in the hair cells, in the supporting cells of the sensory epithelium, and in acoustic ganglion cells at E11 and E14 (Figs. 1N,O, 3F,J) and was retained at E18 (Fig. 1P).

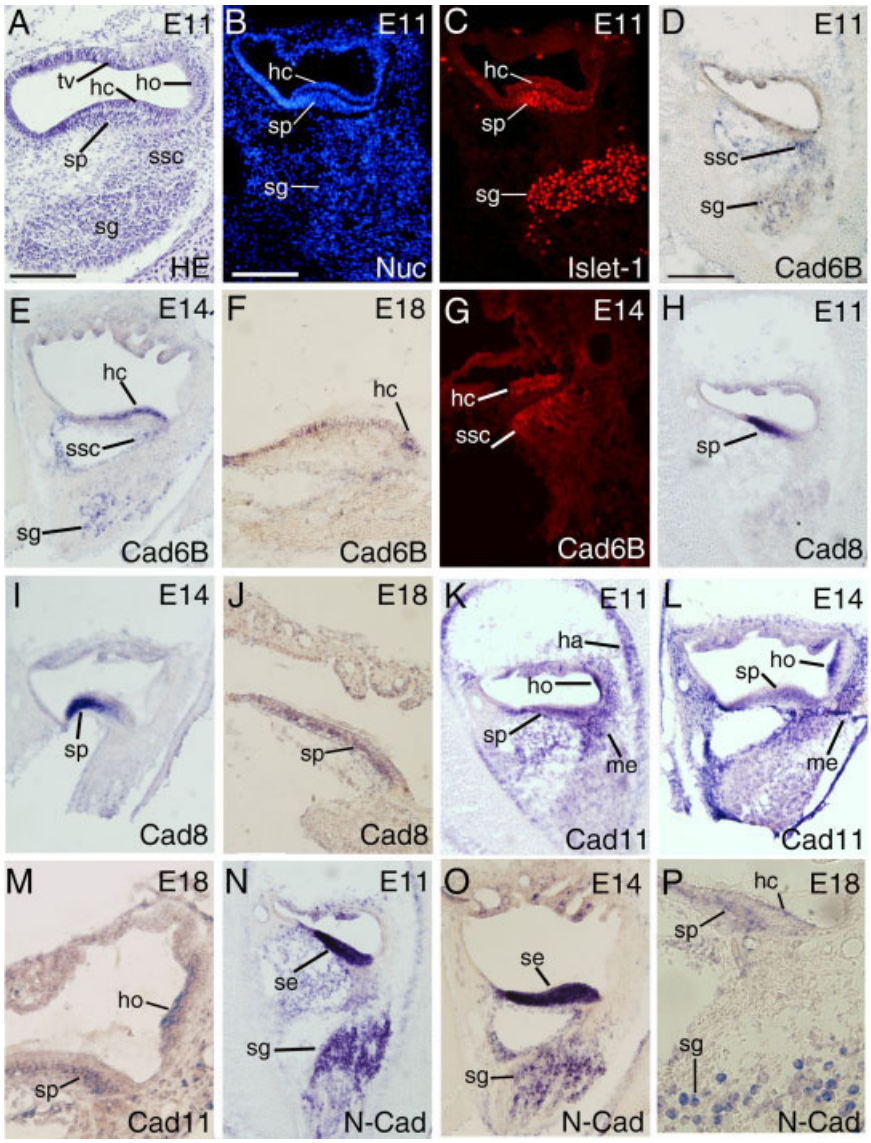

Fig. 1. Expression of Islet-1 and cadherins in transverse sections through the midregion of the developing chicken cochlea. **A:** Hematoxylin and eosin (HE) staining at embryonic day (E) 11. **B,C:** Nuclear stain using dye Hoechst 33258 (Nuc, B) and immunostaining for Islet-1 for revealing hair cells (hc), supporting cells (sp), and acoustic ganglion cells (sg) at the same section of E11 (C). **D–P:** In situ hybridization (D–F,H–P) and immunostaining (G) for Cad6B (D–G), Cad8 (H–J), Cad11 (K–M), and N-Cad (N–P) at different stages (marked). Adjacent sections are shown in D, H, K, and N, and in E, I, L, and O, respectively. ho, homogene cells; me, mesenchymal cells; se, sensory epithelium; ssc, spindle-shaped cells; tv, tegmentum vasculosum. Scale bars = 50 μm in A, 100 μm in B (applies to B,C,F,G,J,M,P), 200 μm in D (applies to D,E,H,I,K,L,N,O).

Cad7 was expressed in the spindle-shaped cells and the acoustic ganglion cells at both the mRNA and protein level from E11 to E18 (Figs. 2A–D, 3C,D). Cad19 mRNA was found in the spindle-shaped cells (Fig. 2E–G), while Cad20 transcript was present in the acoustic ganglion cells (Fig. 2H–J).

R-Cad expression was present in the homogene cells and the acoustic ganglion cells at E11 and E14 (Figs. 2K,L, 3I) and was reduced in the homogene cells and disappeared in the acoustic ganglion cells at E18 (Fig. 2M).

In summary, the expression of each of the eight cadherins was restricted to different types of cells and distinct anatomic structures of the cochlea, with partial overlap (Fig. 2N).

Furthermore, the neurites of the acoustic ganglion were also studied. By immunostaining against neurofilament (NF), a specific marker for differentiated neurons and their processes (Hatta

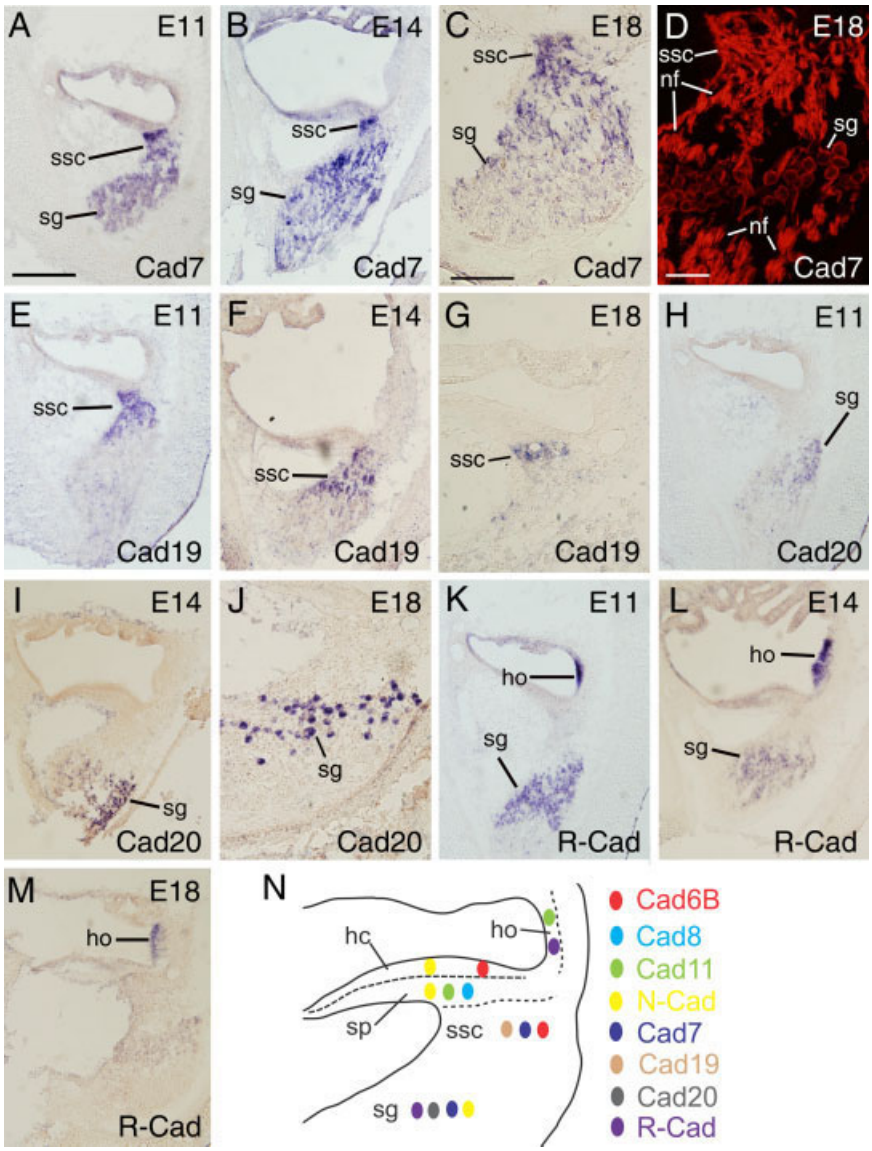

Fig. 2. Expression of cadherins in transverse sections through the midregion of the developing chicken cochlea. **A–M:** In situ hybridization (A–C,E–M) and immunostaining (D) for Cad7 (A–D), Cad19 (E–G), Cad20 (H–J), and R-Cad (K–M) at different stages (marked). Adjacent sections are shown in A, E, H, and K, and in B, F, I, and L, respectively. N summarizes schematically the expression of cadherins in the cochlea at E14. ho, homogene cells; nf, neural fibers; sg, acoustic ganglion cells; sp, supporting cells; ssc, spindle-shaped cells. Scale bars = 50 μm in D, 100 μm in C (applies to C,G,J), 200 μm in A (applies to A,B,E,F,H,I,K–M).

et al., 1987), and β-tubulin III (Tuj-1), a marker for neurons, axons, and chicken hair cells (Cheng et al., 2003), the neurites of the acoustic ganglion cells (nf in Fig. 3B,E) and their terminals that contact the hair cells (arrows in Fig. 3B,E and insert in 3E) were visualized. The neurites of the acoustic ganglion cells expressed Cad7 (nf in Figs. 2D, 3C,D), N-Cad (nf in Fig. 3F), and R-Cad (nf in Fig. 3I). Moreover, N-Cad and R-Cad were coexpressed in the contact areas between the neurite terminals and the hair cells (arrows in Fig. 3F,G,I,J).

DISCUSSION

Cadherins in the Sensory Epithelia and the Differentiation of Hair Cells and Supporting Cells

In the present study, expression of Cad6B and N-Cad was demonstrated in the hair cells (Fig. 1E–G,N–P), while Cad8, Cad11, and N-Cad mRNAs were present in the supporting cells of the basilar papilla (Fig. 1H–P). During chicken cochlear development, hair cells and supporting cells share a common progenitor cell (Weisleder et al., 1995; Fekete et al., 1998). Supporting cells can differentiate into hair cells when hair cells are destroyed by acoustic noise or ototoxic drugs (Girod et al., 1989; Adler and Raphael, 1996; Roberson et al., 2004; Yamagata et al., 2006). It is remarkable that N-Cad signaling can induce cell proliferation of both hair cells and supporting cells. Blocking the function of N-Cad results in an inhibition of the proliferation of both hair cells and supporting cells (Warchol, 2002). Therefore, the expression of cadherins in the supporting cells and the hair cells may have an effect on the differentiation of the supporting cells and the hair cells during normal chicken cochlear development.

Cadherins in Homogene Cells, Spindle-Shaped Cells, and Acoustic Ganglion Cells

Cad11 and R-Cad were exclusively expressed by the homogene cells of the chicken cochlea (Figs. 1K–M, 2K–M), which are involved in the formation of the tectorial membrane during chicken cochlear development (Tanaka and Smith, 1975; Cohen and Fermin, 1985). The temporal profile of Cad11 and R-Cad expression in the homogene cells may relate to the generation of the tectorial membrane.

The human homologues of Cad7, Cad19, and Cad20 are closely related and found at the same chromosomal location of the human genome (Kools et al., 2000). Of interest, they were expressed in an overlapping manner during cochlear development in the chicken. Cad19 was transcribed by the spindle-shaped cells, Cad20 in the acoustic ganglion cells, and Cad7 in both of them (Fig. 2A–J). This result suggests that the regulation of gene expression for the three cadherins is only partially diverged in the cochlea and may coregulate the development of the spindle-shaped cells and the acoustic ganglion cells.

In the cochlea, the projection of peripheral receptive regions onto auditory structures of the central nervous system is tonotopically organized. The guidance of the nerve fibers mediating this tonotopic projection is therefore of special interest. Several cell adhesion

molecules have been found to be involved in the guidance of the extension of the neurites from the acoustic ganglion to their target hair cells (Richardson et al., 1987; Kajikawa et al., 1997). The present study reveals that Cad7, N-Cad, and R-Cad are coexpressed by the neurites of the acoustic ganglion axons (nf in Figs. 2D, 3F,I) and that N-Cad and R-Cad are also coexpressed in the areas of contact between the neurite terminals and the hair cells (arrows in Fig. 3I–K). Previous studies have demonstrated that Cad7, N-Cad, and R-Cad play an important role in neurite outgrowth and fasciculation, in synaptogenesis and/or in synaptic plasticity during embryonic development (Redies et al., 1992, Redies, 1995; Fannon and Colman, 1996; Riehl et al., 1996; Tanaka et al., 2000; Treubert-Zimmermann et al., 2002). Therefore, the three cadherins may be involved in the guidance of neurites from the acoustic ganglion to the sensory epithelium and in synaptogenesis with the target cells.

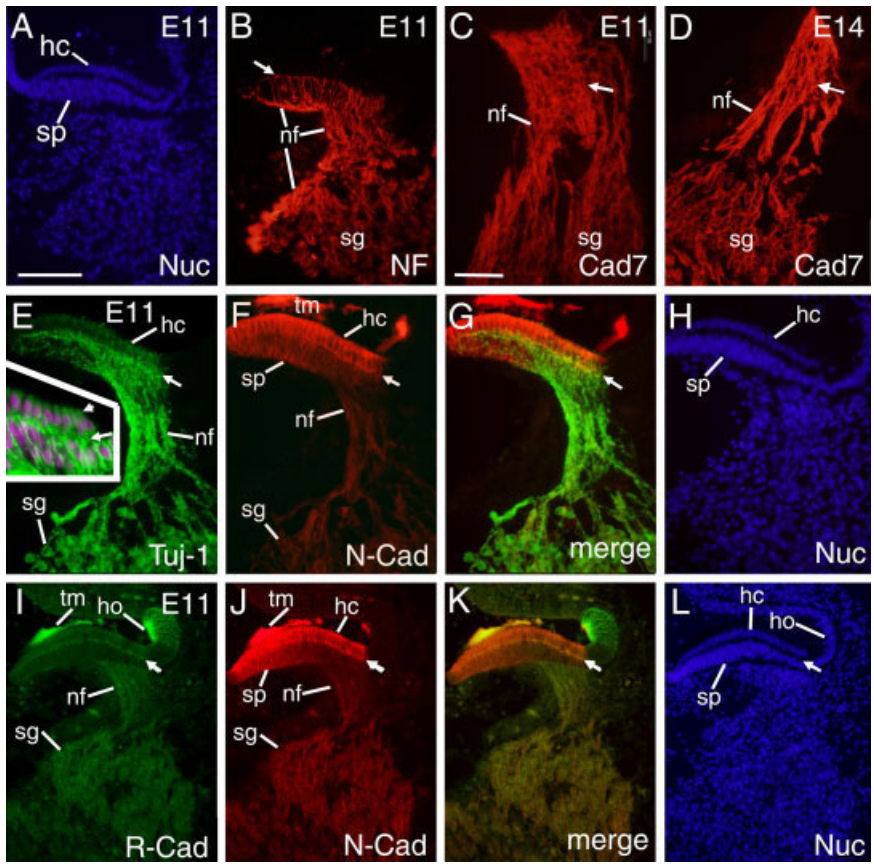

Fig. 3. Expression of cadherins in transverse sections through the midregion of the developing chicken cochlea. **A,B:** Nuclear stain using dye Hoechst 33258 (Nuc; A) and immunostaining for neurofilament (NF; B) to reveal nerve fibers (nf) targeting the sensory epithelium. The arrow indicates the neurites at the bottom of the hair cells. **C,D:** Cad7 is expressed in the acoustic ganglion cells (sg) and their projections (nf). The arrow points to spindle-shaped cells. **E–H:** Double immunostaining for β-tubulin III (Tuj-1; green, E) and N-Cad (red, F) in the cochlea at embryonic day (E) 11. G: The merged image of E and F is shown. H: A nuclear stain using dye Hoechst 33258. The arrows indicate the bottom of the hair cells, where the neurites contact the hair cells to form synapses. The insert in E shows a magnification of a sensory epithelial region. The arrowhead indicates the hair cells (hc). The nuclei of the hair cells and the supporting cells (sp) are represented by the violet color. **I–L:** Double immunostaining of R-Cad (green, I) and N-Cad (red, J) in the cochlea at E11. K: The merged image of I and J is shown. L: A nuclear stain. The arrows indicate the bottom of the hair cells. ho, homogene cells; tm, tectorial membrane. Scale bars = 50 μm in C, 100 μm in A (applies to A,B,D–L).

EXPERIMENTAL PROCEDURES

Animals, Antibodies, and cRNA Probes

Eggs from White Leghorn chicken (*Gallus domesticus*) were incubated in a forced-draft incubator (BSS160, Ehret, Germany) at 37°C under 60% humidity. Chicken embryos were staged according to Hamburger and Hamilton (1951). After the embryos were deeply anesthetized by cooling on ice, they were removed from the shell and perfused through the heart with 4% formaldehyde in 0.1 M cacodylate buffer (Roth, Karlsruhe, Germany; containing 1 mM Ca^{2+} and 1mM Mg^{2+}). Cochleae were separated and collected for this study at E11, E14, and E18 (stages 37, 40, and 44, respectively; at least six cochleae for each stage). The experiments were carried out under an approved institutional protocol according to the National Institutes of Health Guide for the Care and Use of Laboratory Animals.

For immunohistochemistry, primary mouse and rat monoclonal antibodies raised against Cad6B (CCD6B-1) and Cad7 (CCD7-1; Nakagawa and Takeichi, 1998), N-Cad (NCD-2; Hatta and Takeichi, 1986), R-Cad (RCD-2; Redies et al., 1992), Islet-1 (Li et al., 2004), neurofilament (Hatta et al., 1987), and β-tubulin III (Tuj-1; Sigma) were used. CCD6-1, CCD7-1, NCD-2, RCD-2, and neurofilament antibodies were kind gifts of Dr. S. Nakagawa and Dr. M. Takeichi (RIKEN Center for Developmental Biology, Kobe, Japan). Antibodies against Islet-1 were obtained from the Developmental Studies Hybridoma Bank developed under the auspices of the NICHD and maintained by The University of Iowa, Department of Biological Sciences (Iowa City, IA 52242).

For in situ hybridization, purified plasmids containing the full-length sequences encoding chicken Cad6B, Cad7, N-Cad, and R-Cad (kind gifts of Dr. S. Nakagawa and Dr. M. Takeichi), and the RT-PCR fragments encoding chicken Cad8, Cad11, Cad19, and Cad20 were used as templates for the in vitro synthesis of cRNA probes. Digoxigenin-labeled sense and antisense cRNA probes were transcribed according to the manufacturer's instructions (Roche, Mannheim, Germany). Sense cRNA probes were applied as a negative control for in situ hybridization.

RT-PCR and RACE Reaction

To obtain chicken cDNAs encoding cadherins (Cad8, Cad11, Cad19, and Cad20), mRNA from E14 (stage 40)

chicken brain was purified using Micro-FastTrack 2.0 mRNA Isolation Kit (Invitrogen, Karlsruhe, Germany) and first-strain cDNA was synthesized in vitro with the SuperScript First-Strand Synthesis System (Invitrogen). Then PCR was performed with a pair of specific or degenerate primers (see Table 1). The PCR templates were denatured for 2 min at 94°C, followed by 35 cycles of amplification with optimal denaturing, annealing, and extension conditions for each cadherin (see Table 1). After the last cycle, the reaction was extended finally for 15 min at 72°C. The PCR fragments obtained were cloned into pBluescript-SK(+) vector (for Cad8, Cad11, and Cad20) or into pCR II-TOPO vector using the TA-cloning kit (Invitrogen; for Cad19). The plasmids were purified using the Plasmid Maxi Kit (Qiagen, Hilden, Germany) and sequenced by a commercial company (MWG, Ebersberg, Germany).

To obtain the full-length sequences of chicken Cad8 and Cad19, 5- and 3-end RACE reactions were performed with the SMART RACE cDNA Amplification Kit (Takara Bio Europe/Clontech, Saint-Germain-en-Laye, France). The specific primers for RACE were chosen from the obtained PCR fragments according to the instructions of the RACE Kit User Manual. The primers for 5-end RACE PCR (Cad8-anti-1 and Cad8-anti-2 for chicken Cad8; Cad19-anti-1 and Cad19-anti-2 for chicken Cad19) and 3-end RACE PCR (Cad8-sense-1 and Cad8-sense-2 for Cad8; Cad19-sense-1 and Cad19-sense-2 for Cad19) are shown in Table 1. The touch-down PCR for 5- and 3-end RACE amplification was performed using the 5- and 3-end RACE PCR primers (Cad8-anti-1 and Cad19-anti-1 for 5-end RACE; Cad8-sense-1 and Cad19-sense-1 for 3-end RACE, respectively) together with the Universal Primer Mix. For the first 5 cycles, the touch-down PCR was performed at 94°C for 30 sec and at 72°C for 3 min. The next 5 cycles were performed at 94°C for 30 sec, 70°C for 30 sec, and 72°C for 3 min. At last, another 27 cycles were performed at 94°C for 30 sec, at 68°C for 30 sec, and at 72°C for 3 min. To obtain more specific bands, nested PCR was performed following the touch-down PCR for 5- and 3-end cDNA amplification with the primers (Cad8-anti-2 and Cad19-anti-2 for 5-end RACE; Cad8-sense-2 and Cad19-sense-2 for 3-end RACE) together with the Nested Universal Primer, respectively. The PCR templates were denatured for 1 min at 95°C, followed by 20 cycles of amplification (denaturing for 30 sec at 95°C, and annealing and extension for 3 min at 68°C). The PCR products were cloned into pCR II-TOPO vector (Invitrogen) and sequenced by a commercial company (MWG). After ligating the RACE sequences with the obtained RT-PCR fragment sequences, two molecules with the full-length nucleotide sequences were obtained.

Immunohistochemistry

To detect the expression of cadherins in the cochlea, fluorescent immunostaining was performed on sections of chicken cochleae according to the protocol described previously (Luo and Redies, 2004). In brief, after post-fixation with 4% formaldehyde, cryostat sections of 20 μm thickness were preincubated with blocking solution (5% skimmed milk, 0.3% Triton X-100 in TBS) at room temperature for 60 min. Then the sections were incubated overnight at 4°C with the primary antibody against cadherin, followed by Alexa 488-labeled or Cy3-labeled secondary antibody against mouse or rat IgG (Dianova, Hamburg, Germany) at room temperature for 1 hr. Finally, cell nuclei were counterstained with dye Hoechst 33258 (Molecular Probes, Eugene, OR). Fluorescence was imaged under a fluorescence microscope (BX40, Olympus, Hamburg, Germany) equipped with a digital camera (DP70, Olympus).

For double-label fluorescent immunohistochemistry, sections were first immunostained with antibodies against R-Cad or β-tubulin III using the method described above. Subsequently, immunostaining for N-Cad was performed.

In Situ Hybridization

In situ hybridization on cryosections was performed according to the protocol described previously (Redies and Takeichi, 1993). In brief, after post-fixation with 4% formaldehyde in phosphate-buffered saline, cryostat sections of 20 μm thickness were pretreated with proteinase K and acetic anhydride and hybridized overnight with cRNA probe at a concentration of approximately 1–5 ng/μl at 70°C in hybridization solution (50% formamide, 3× SSC, 1× Denhardt's solution, 250 μg/ml yeast transfer RNA, and 250 μg/ml salmon sperm DNA). After the unbound cRNA was removed by RNAse, the sections were incubated with alkaline phosphatase-conjugated anti-digoxigenin Fab fragments (Roche) at 4°C overnight. For visualization of the labeled mRNA, a substrate solution of nitroblue tetrazolium salt (NBT) and 5-bromo-4-chloro-3-indoyl phosphate (BCIP) was added. The color reactions were analyzed under a microscope (BX40, Olympus) and photographed with a digital camera (DP70, Olympus).

ACKNOWLEDGMENTS

We thank Dr. S. Nakagawa and Dr. M. Takeichi for their kind gifts of plasmids and antibodies, and Ms. S. Hänβgen for technical assistance.

REFERENCES

Adato A, Michel V, Kikkawa Y, Reiners J, Alagramam KN, Weil D, Yonekawa H, Wolfrum U, El-Amraoui A, Petit C. 2005. Interactions in the network of Usher syndrome type 1 proteins. Hum Mol Genet 14:347–356.

Adler HJ, Raphael Y. 1996. New hair cells arise from supporting cell conversion in the acoustically damaged chick inner ear. Neurosci Lett 205:17–20.

Alagramam KN, Murcia CL, Kwon HY, Pawlowski KS, Wright CG, Woychik RP. 2001a. The mouse Ames waltzer hearing-loss mutant is caused by mutation of Pcdh15, a novel protocadherin gene. Nat Genet 27:99–102.

Alagramam KN, Yuan H, Kuehn MH, Murcia CL, Wayne S, Srisailpathy CR, Lowry RB, Knaus R, Van Laer L, Bernier FP, Schwartz S, Lee C, Morton CC, Mullins RF, Ramesh A, Van Camp G, Hageman GS, Woychik RP, Smith RJ. 2001b. Mutations in the novel protocadherin PCDH15 cause Usher syndrome type 1F. Hum Mol Genet 10:1709–1718.

Bok D, Galbraith G, Lopez I, Woodruff M, Nusinowitz S, BeltrandelRio H, Huang W, Zhao S, Geske R, Montgomery C, Van Sligtenhorst I, Friddle C, Platt K, Sparks MJ, Pushkin A, Abuladze N, Ishiyama A, Dukkipati R, Liu W, Kurtz I. 2003. Blindness and auditory impairment caused by loss of the sodium bicarbonate cotransporter NBC3. Nat Genet 34:313–319.

Brigande JV, Kiernan AE, Gao X, Iten LE, Fekete DM. 2000. Molecular genetics of

pattern formation in the inner ear: do compartment boundaries play a role? Proc Natl Acad Sci U S A 97:11700–11706.

Cheng AG, Cunningham LL, Rubel EW. 2003. Hair cell death in the avian basilar papilla: characterization of the in vitro model and caspase activation. J Assoc Res Otolaryngol 4:91–105.

Cohen GM, Fermin CD. 1978. The development of hair cells in the embryonic chick's basilar papilla. Acta Otolaryngol 86:342–358.

Cohen GM, Fermin CD. 1985. Development of the embryonic chick's tectorial membrane. Hear Res 18:29–39.

El-Amraoui A, Petit C. 2005. Usher I syndrome: unravelling the mechanisms that underlie the cohesion of the growing hair bundle in inner ear sensory cells. J Cell Sci 118:4593–4603.

Fannon AM, Colman DR. 1996. A model for central synaptic junctional complex formation based on the differential adhesive specificities of the cadherins. Neuron 17:423–434.

Fekete DM, Muthukumar S, Karagogeos D. 1998. Hair cells and supporting cells share a common progenitor in the avian inner ear. J Neurosci 18:7811–7821.

Girod DA, Duckert LG, Rubel EW. 1989. Possible precursors of regenerated hair cells in the avian cochlea following acoustic trauma. Hear Res 42:175–194.

Hamburger V, Hamilton HL. 1951. A series of normal stages in the development of the chick embryo. J Morphol 88:49–92.

Hampton LL, Wright CG, Alagramam KN, Battey JF, Noben-Trauth K. 2003. A new spontaneous mutation in the mouse Ames waltzer gene, Pcdh15. Hear Res 180:67–75.

Hatta K, Takeichi M. 1986. N-cadherin adhesion molecules associated with early morphogenetic events in chick development. Nature 320:447–449.

Hatta K, Takagi S, Fujisawa H, Takeichi M. 1987. Spatial and temporal expression pattern of N-cadherin cell adhesion molecules correlated with morphogenetic processes of chicken embryos. Dev Biol 120:215–222.

Holme RH, Steel KP. 1999. Genes involved in deafness. Curr Opin Genet Dev 9:309–314.

Jackson H, Rubel EW. 1978. Ontogeny of behavioral responsiveness to sound in the chick embryo as indicated by electrical recordings of motility. J Comp Physiol Psychol 92:682–696.

Jones TA, Jones SM, Paggett KC. 2006. Emergence of hearing in the chicken embryo. J Neurophysiol 96:128–141.

Kajikawa H, Umemoto M, Taira E, Miki N, Mishiro Y, Kubo T, Yoneda Y. 1997. Expression of neurite outgrowth factor and gicerin during inner ear development and hair cell regeneration in the chick. J Neurocytol 26:501–509.

Kelley MW. 2003. Cell adhesion molecules during inner ear and hair cell development, including notch and its ligands. Curr Top Dev Biol 57:321–356.

Kools P, Van Imschoot G, van Roy F. 2000. Characterization of three novel human cadherin genes (CDH7, CDH19, and CDH20) clustered on chromosome 18q22–q23 and with high homology to chicken cadherin-7. Genomics 68:283–295.

Li H, Liu H, Sage C, Huang M, Chen ZY, Heller S. 2004. Islet-1 expression in the developing chicken inner ear. J Comp Neurol 477:1–10.

Luo J, Redies C. 2004. Overexpression of genes in Purkinje cells in the embryonic chicken cerebellum by in vivo electroporation. J Neurosci Methods 139:241–245.

Nakagawa S, Takeichi M. 1998. Neural crest emigration from the neural tube depends on regulated cadherin expression. Development 125:2963–2971.

Noben-Trauth K, Zheng QY, Johnson KR. 2003. Association of cadherin 23 with polygenic inheritance and genetic modification of sensorineural hearing loss. Nat Genet 35:21–23.

Novince ZM, Azodi E, Marrs JA, Raymond PA, Liu Q. 2003. Cadherin expression in the inner ear of developing zebrafish. Gene Expr Patterns 3:337–339.

Ozaki H, Nakamura K, Funahashi J, Ikeda K, Yamada G, Tokano H, Okamura HO, Kitamura K, Muto S, Kotaki H, Sudo K, Horai R, Iwakura Y, Kawakami K. 2004. Six1 controls patterning of the mouse otic vesicle. Development 131:551–562.

Raphael Y, Volk T, Crossin KL, Edelman GM, Geiger B. 1988. The modulation of cell adhesion molecule expression and intercellular junction formation in the developing avian inner ear. Dev Biol 128:222–235.

Redies C. 1995. Cadherin expression in the developing vertebrate CNS: from neuromeres to brain nuclei and neural circuits. Exp Cell Res 220:243–256.

Redies C. 2000. Cadherins in the central nervous system. Prog Neurobiol 61:611–648.

Redies C, Takeichi M. 1993. Expression of N-cadherin mRNA during development of the mouse brain. Dev Dyn 197:26–39.

Redies C, Inuzuka H, Takeichi M. 1992. Restricted expression of N- and R-cadherin on neurites of the developing chicken CNS. J Neurosci 12:3525–3534.

Riccomagno MM, Martinu L, Mulheisen M, Wu DK, Epstein DJ. 2002. Specification of the mammalian cochlea is dependent on Sonic hedgehog. Genes Dev 16:2365–2378.

Riccomagno MM, Takada S, Epstein DJ. 2005. Wnt-dependent regulation of inner ear morphogenesis is balanced by the opposing and supporting roles of Shh. Genes Dev 19:1612–1623.

Richardson GP, Crossin KL, Chuong CM, Edelman GM. 1987. Expression of cell adhesion molecules during embryonic induction. III. Development of the otic placode. Dev Biol 119:217–230.

Riehl R, Johnson K, Bradley R, Grunwald GB, Cornel E, Lilienbaum A, Holt CE. 1996. Cadherin function is required for axon outgrowth in retinal ganglion cells in vivo. Neuron 17:837–848.

Roberson DW, Alosi JA, Cotanche DA. 2004. Direct transdifferentiation gives rise to the earliest new hair cells in regenerating avian auditory epithelium. J Neurosci Res 78:461–471.

Saunders JC, Coles RB, Gates GR. 1973. The development of auditory evoked responses in the cochlea and cochlear nuclei of the chick. Brain Res 63:59–74.

Siemens J, Lillo C, Dumont RA, Reynolds A, Williams DS, Gillespie PG, Muller U. 2004. Cadherin 23 is a component of the tip link in hair-cell stereocilia. Nature 428:950–955.

Simonneau L, Thiery JP. 1998. The mesenchymal cadherin-11 is expressed in restricted sites during the ontogeny of the rat brain in modes suggesting novel functions. Cell Adhes Commun 6:431–450.

Simonneau L, Kitagawa M, Suzuki S, Thiery JP. 1995. Cadherin 11 expression marks the mesenchymal phenotype: towards new functions for cadherins? Cell Adhes Commun 3:115–130.

Simonneau L, Gallego M, Pujol R. 2003. Comparative expression patterns of T-, N-, E-cadherins, beta-catenin, and polysialic acid neural cell adhesion molecule in rat cochlea during development: implications for the nature of Kolliker's organ. J Comp Neurol 459:113–126.

Takeichi M. 1995. Morphogenetic roles of classic cadherins. Curr Opin Cell Biol 7:619–627.

Tanaka K, Smith CA. 1975. Structure of the avian tectorial membrane. Ann Otol Rhinol Laryngol 84:287–296.

Tanaka K, Smith CA. 1978. Structure of the chicken's inner ear: SEM and TEM study. Am J Anat 153:251–271.

Tanaka H, Shan W, Phillips GR, Arndt K, Bozdagi O, Shapiro L, Huntley GW, Benson DL, Colman DR. 2000. Molecular modification of N-cadherin in response to synaptic activity. Neuron 25:93–107.

Torres M, Giraldez F. 1998. The development of the vertebrate inner ear. Mech Dev 71:5–21.

Treubert-Zimmermann U, Heyers D, Redies C. 2002. Targeting axons to specific fiber tracts in vivo by altering cadherin expression. J Neurosci 22:7617–7626.

Vallin J, Girault JM, Thiery JP, Broders F. 1998. Xenopus cadherin-11 is expressed in different populations of migrating neural crest cells. Mech Dev 75:171–174.

Warchol ME. 2002. Cell density and N-cadherin interactions regulate cell proliferation in the sensory epithelia of the inner ear. J Neurosci 22:2607–2616.

Weisleder P, Tsue TT, Rubel EW. 1995. Hair cell replacement in avian vestibular epithelium: supporting cell to type I hair cell. Hear Res 82:125–133.

Yamagata M, Weiner JA, Dulac C, Roth KA, Sanes JR. 2006. Labeled lines in the retinotectal system: markers for retinorecipient sublaminae and the retinal ganglion cell subsets that innervate them. Mol Cell Neurosci 33:296–310.

3.3

Molecular cloning and expression analysis of three cadherin-8 isoforms in the embryonic chicken brain

Juntang Lin, Jiankai Luo, Christoph Redies

Brain Research, 2008, 1201:1-14.

Pages 39-52

available at www.sciencedirect.com

ScienceDirect

www.elsevier.com/locate/brainres

BRAIN RESEARCH

Research Report

Molecular cloning and expression analysis of three cadherin-8 isoforms in the embryonic chicken brain

Juntang Lin[a], *Jiankai Luo*[a,b], *Christoph Redies*[a,*]

[a]*Institute of Anatomy I, Friedrich Schiller University Jena, Teichgraben 7, D-07743 Jena, Germany*
[b]*Neurobiological Laboratory, Department of Neurology, University of Rostock, Gehlsheimerstrasse 20, D-18147 Rostock, Germany*

ARTICLE INFO

Article history:
Accepted 26 January 2008
Available online 9 February 2008

Keywords:
Cadherin
RACE
Isoform
Expression pattern
Brain development
In situ hybridization

ABSTRACT

Three types of full-length cDNAs encoding chicken *cadherin-8* (*Cdh8*) were identified and their expression in the embryonic chicken brain was investigated. The longest type of cDNA is closely similar to that of other classic cadherins, and the predicted protein shows a high similarity to rat and human Cdh8. The second type of cDNA is considerably shorter. The deduced protein lacks the cytoplasmic tail and the transmembrane domain, and contains a truncated fifth cadherin repeat in the extracellular domain (EC5; 68 amino acids), suggesting that it is a soluble isoform. The third type resembles the second one but is even shorter (only 30 amino acids in EC5). All types contain unique short sequences at their C terminus. Genomic analysis demonstrated that all of the three Cdh8 isoforms are located on chromosome 11, and consist of 12, 10, and 9 exons, respectively. Semi-quantitative RT-PCR with type-specific primers showed that the transcription of the three Cdh8 isoforms was temporally and spatially regulated in different parts of the embryonic chicken brain. The distinct regulation of gene expression suggested that the three isoforms likely play different roles during brain development. Northern blot analysis revealed that the transcription of the long isoform was much stronger than that of the two shorter ones. In situ hybridization showed that the long isoform of Cdh8 is expressed by a specific subset of brain nuclei, regions and layers in all major parts of the brain.

1. Introduction

Cadherins are a large family of transmembrane proteins that mediate Ca^{2+}-dependent cell–cell adhesion. They play important roles in regulating morphogenesis and tissue formation during embryonic development, also in the central nervous system (CNS) (for reviews, see Redies (2000); and Takeichi (2007)). Cadherin subfamilies are the classic cadherins (type I and type II), the protocadherins, the desmosomal cadherins, etc. (Nollet et al., 2000). So far, more than a dozen classic cadherins have been reported in various tissues of different organisms. In general, classic cadherins share common properties. For example, at the N-terminal side, the extracellular domain is composed of five so-called cadherin repeats. Following the transmembrane domain, there is a highly conserved cytoplasmic domain at the C-terminal side. The expression of most classic cadherins, for example, of N-cadherin, R-cadherin, cadherin-6 (Cdh6), Cdh7, Cdh8, Cdh11, and Cdh20, is restricted to specific developing gray matter regions, fiber tracts and synapses in the CNS (for reviews, see Redies (2000); and Hirano et al. (2003)).

* *Corresponding author*. Fax: +49 3641 938512.
E-mail address: redies@mti.uni-jena.de (C. Redies).

Abbreviations: Cdh, cadherin; EC, extracellular domain; GAPDH, glyceraldehyde-3-phosphate dehydrogenase; PBS, phosphate-buffered saline; ORF, open reading frame; RACE, rapid amplification of cDNA ends

0006-8993/$ – see front matter © 2008 Elsevier B.V. All rights reserved.
doi:10.1016/j.brainres.2008.01.071

Cdh8, a type II classic cadherin, has been identified in human (Shimoyama et al., 2000), mouse (Korematsu and Redies, 1997a,b), rat (Kido et al., 1998) and chicken (Luo et al., 2007). The expression of this cadherin has been studied in detail in the mouse brain (Korematsu and Redies, 1997a,b; Korematsu et al., 1998). An analysis of *Cdh8* knock-out mice revealed that *Cdh8* is essential for establishing the physiological coupling between cold-sensitive sensory neurons and their target dorsal horn neurons (Suzuki et al., 2007).

It was also reported that rat Cdh8 is expressed in two forms, a complete form and a truncated form without a transmembrane domain and a cytoplasmic tail (Kido et al., 1998). Splicing variants of type II cadherins have been reported also for Cdh22 (PB-cadherin; Sugimoto et al., 1996), Cdh11 (Kawaguchi et al., 1999), and Cdh7 (Kawano et al., 2002). The variant forms of these cadherins represent truncated transmembrane proteins with a short cytoplasmic domain that differs from the full-length forms. In contrast, the short variant of Cdh20 (MN-cadherin) lacks the EC1 and EC2 domains in the extracellular region (Shirabe et al., 2005). The function of these short variants remains to be elucidated. Variant forms of some protocadherins have been reported as well (Makarenkova et al., 2005; Vanhalst et al., 2005).

Little is known about variant *Cdh8* forms and the expression of *Cdh8* in chicken. In the present study, we have successfully cloned and identified two novel truncated isoforms of chicken Cdh8 by RACE (rapid amplification of cDNA ends). The two isoforms lack the transmembrane domain and the cytoplasmic tail, but both have short unique sequences at the C terminus. The gene and protein structures of the three *Cdh8* isoforms were analyzed by appropriate bioinformatics software. The expression of the three isoforms was studied at different developmental stages and in various parts of the brain by semi-quantitative RT-PCR. Our results show that the expression of the Cdh8 isoforms is temporally and spatially regulated during brain development. The expression pattern of the long isoform was mapped by in situ hybridization in the embryonic chicken brain.

2. Results

2.1. *Cloning and identification of novel chicken Cdh8 isoforms*

Based on the predicted sequence of chicken Cdh8 (GenBank accession No. XM_425125), a 1759 bp fragment was cloned previously (Luo et al., 2007). By nested RACE PCR, one band of about 1500 bp in length was obtained from the 5 end and two bands of about 600 bp and 750 bp in length from the 3 end, respectively. After sequencing and alignment of these RACE products with the 1759 bp fragment, two full-length sequences with polyadenylation sites were obtained. The length of one sequence was 2570 bp, and of the other sequence was 2771 bp. An alignment of these two sequences with Cdh8 from other animals revealed a very high similarity with Cdh8 from human (NM_001796), mouse (NM_007667) and rat (NM_053393) (more than 80% sequence identity), but they were much shorter than the complete Cdh8 sequences of the other species. Therefore, these two sequences represented truncated isoforms of chicken Cdh8, and were named Cdh8-1 and Cdh8-2. The long Cdh8 isoform that included a 3676 bp sequence with a polyadenylation site was similar in length to human, mouse or rat Cdh8. It was confirmed as chicken Cdh8 (Luo et al., 2007) and named Cdh8-3. The sequences of these three isoforms of chicken Cdh8 have been submitted to NCBI GenBank (Cdh8-1, GenBank accession No. EU035636; Cdh8-2, GenBank accession No. EU035637; and Cdh8-3, GenBank accession No. EF608154).

Next, primers were designed to amplify unique fragments of the three isoforms for use in semi-quantitative RT-PCR, Northern blotting and in situ hybridization (ISH). Bands of 466 bp length (for Cdh8-1), 575 bp length (for Cdh8-2) and 697 bp length (for Cdh8-3) were obtained (Fig. 1A) and cloned into

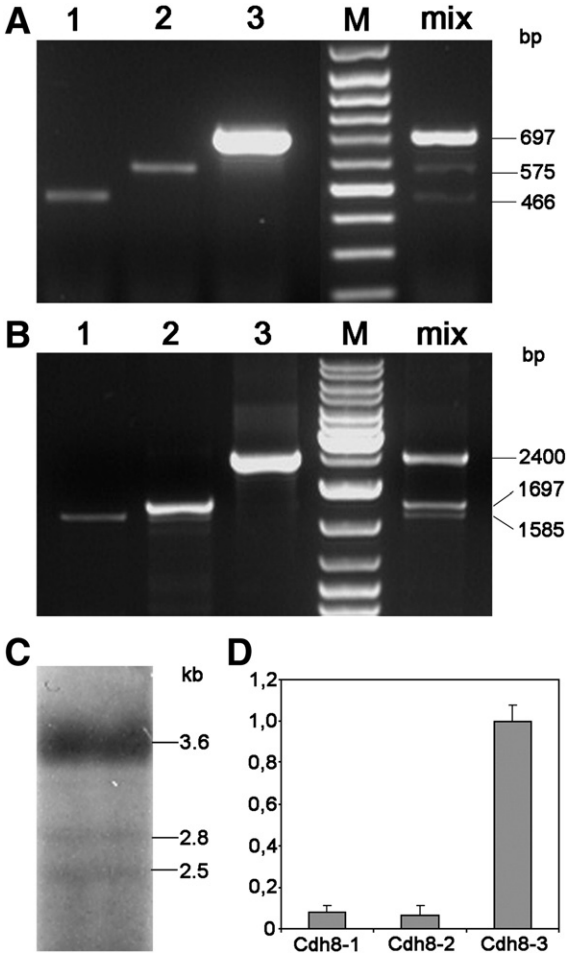

Fig. 1 – A. Visualization of the unique PCR products that correspond to the three isoforms of Cdh8. 1, Cdh8-1 (466 bp); 2, Cdh8-2 (575 bp); 3, Cdh8-3 (697 bp); M, DNA molecular weight marker; mix, mixture of all three unique PCR products. B. ORFs of the three Cdh8 isoforms. 1, Cdh8-1 (1585 bp); 2, Cdh8-2 (1697 bp); 3, Cdh8-3 (2400 bp); M, DNA molecular weight marker; mix, mixture of all three ORF. C. Results from Northern blot analysis showing the relative transcript amounts of the three Cdh8 isoforms (Cdh8-1, 2.5 kb; Cdh8-2, 2.8 kb; and Cdh8-3, 3.6 kb) at E18. D. The measured intensity values of the bands are normalized to the Cdh8-3 value. The error bars represent means +/− s.e.m. (n=3).

Topo II vector. The position of the primers and the unique fragments is shown in the alignment of the three isoforms (Suppl. Fig. S1).

To confirm the existence of the three Cdh8 isoforms, their ORFs were cloned by RT-PCR (Fig. 1B). Bands of the predicted size were obtained (Cdh8-1, 1585 bp; Cdh8-2, 1697 bp; and Cdh8-3, 2400 bp).

Northern blot was performed to confirm the existence of three Cdh8 isoforms in the E18 chicken brain. Results revealed three bands of 2.5 kb, 2.8 kb and 3.6 kb in length corresponding to Cdh8-1, Cdh8-2 and Cdh8-3, respectively (Fig. 1C). These findings are compatible with results from RACE and RT-PCR. The intensity of the bands was quantified with appropriate software (ImageQuant TL). Result showed that the expression levels of Cdh8-1 and Cdh8-2 were similar. Expression of Cdh8-3 was about 15 times stronger than that of the two shorter isoforms (Fig. 1D). Similar results were obtained for chicken brain at E7 and E12 (data not shown).

2.2. *Gene structure and characterization of the three isoforms*

The three sequences of chicken Cdh8 were blasted against the chicken genome (http://www.ncbi.nlm.nih.gov/blast). Results showed that Cdh8-1 has 9 exons, Cdh8-2 has 10 exons, and Cdh8-3 has 12 exons, respectively (Fig. 2A). The 8 exons of the 5 end are identical in the three isoforms. The remaining exons at the 3 end differ from each other, especially in the UTR. The lengths of the exons and introns are shown in Table 1. *Cdh8* is located on chromosome 11 of the chicken genome in a region that represents a synteny block on chromosome 16 in the human genome (Martin et al., 2004). Chicken *Cdh8* and human *Cdh8* both have 12 exons. The exon sizes and the intron/exon boundaries for chicken *Cdh8* are very similar, if not identical, compared to those of human *Cdh8*. Differences exist only in the first exon and in the last exon; the 3-UTR and 5-UTR of chicken *Cdh8* both are much longer than in human *Cdh8*. However, the length of the introns shows large differences between chicken and human *Cdh8* (Table 1).

A comparison of the unique sequences of Cdh8-1, Cdh8-2 and the truncated isoform of rat Cdh8 indicates that there is a consensus sequence (AA[G]ATAT) at the boundary between the complete type of Cdh8 and the truncated ones (Suppl. Fig. S1). This result suggests that these truncated types are produced by alternative mRNA splicing (Kido et al., 1998). The possible alternative splicing sites are indicated by arrowheads in Supplementary Fig. S1. Furthermore, Cdh8-1, but not Cdh8-2, shares a sequence (AAATATCCATGTT) with the truncated Cdh8 isoform from rat, suggesting that Cdh8-1 is the chicken orthologue of this isoform.

The ORF of the three isoforms of Cdh8 were obtained with the ORF Finder program at the NCBI website (http://www.ncbi.nlm.nih.gov/gorf/gorf.html). The putative proteins have the following lengths: Cdh8-1 526 aa, Cdh8-2 564 aa, and Cdh8-3 799 aa. An alignment of the three isoforms was carried out with the Clustal X 1.83 program. Results displayed in Supplementary Fig. 2 demonstrate that the two shorter isoforms of chicken Cdh8 each have a unique 13 aa-long sequence at the C terminus in EC5. The molecular weight of Cdh8-1, Cdh8-2 and Cdh8-3 is 58.45 kDa, 62.81 kDa, and 88.38 kDa, respectively. The three isoforms have a similar isoelectric point around p*I* 4.6 (analyzed with the DNASTAR Protean program).

A protein blast (http://www.ncbi.nlm.nih.gov/blast) of the three isoforms of Cdh8 indicated that Cdh8-1, Cdh8-2 and Cdh8-3 show a high similarity to human Cdh8 (NP_001787), mouse Cdh8 (NP_031693) and rat Cdh8 (NP_445845; Table 2). Cdh8-3 possesses all domains of a classic cadherin (5 extracellular repeats, a transmembrane domain and a cytoplasmic tail). Cdh8-1 and Cdh8-2 lack the transmembrane domain and the cytoplasmic tail; the fifth extracellular cadherin domain (EC5) contains only 68 aa and 30 aa in Cdh8-2 and Cdh8-1, respectively (Fig. 2B and Suppl. Fig. S2).

Signal peptide analysis was performed with the SignalP 3.0 program (http://www.cbs.dtu.dk/services/SignalP/) and revealed

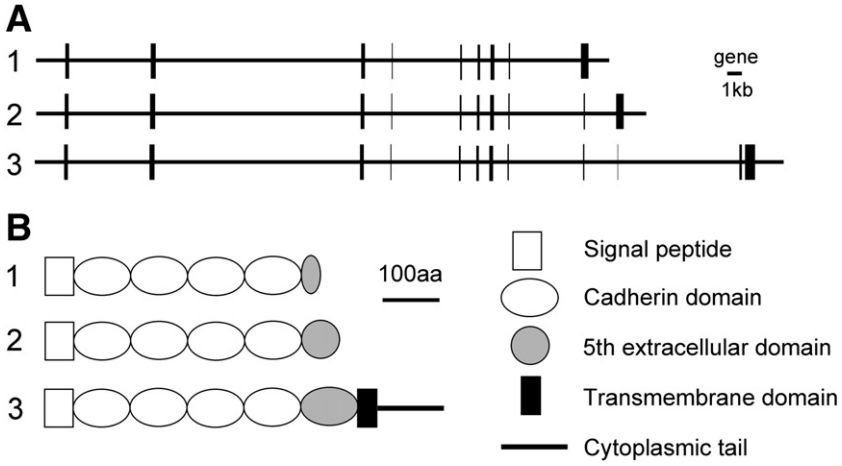

Fig. 2 – A. Genomic organization of chicken *Cdh8* and exon/intron structure of the three cloned isoforms. Vertical lines represent exons and horizontal lines represent introns between the exons. Cdh8-1 (1) consists of 9 exons and 8 introns, Cdh8-2 (2) consists of 10 exons and 9 introns, and Cdh8-3 (3) consists of 12 exons and 11 introns. B. Schematic representation of the putative chicken *Cdh8* products. Cdh8-1 (1) lacks the transmembrane domain and cytoplasmic tail and contains a truncated fifth extracellular repeat (EC5; only 30 aa). Cdh8-2 (2) is similar to Cdh8-1, but has 68 aa in the truncated EC5. Cdh8-3 (3) is the complete isoform of chicken Cdh8.

Table 1 – The exon and intron sizes of the three isoforms of chicken *Cdh8* and human *Cdh8* (H-Cdh8)

	Exon (bp)	Intron (bp)
Cdh8-1	1 (323)	1 (17052)
	2 (446)	2 (43032)
	3 (297)	3 (22557)
	4 (121)	4 (13924)
	5 (172)	5 (3889)
	6 (188)	6 (2722)
	7 (258)	7 (3497)
	8 (140)	8 (16309)
	9 (255)	
Cdh8-2	1 (323)	1 (17052)
	2 (446)	2 (43032)
	3 (297)	3 (22557)
	4 (121)	4 (13924)
	5 (172)	5 (3889)
	6 (188)	6 (2722)
	7 (258)	7 (3497)
	8 (140)	8 (16309)
	9 (126)	9 (6873)
	10 (697)	
Cdh8-3	1 (323)	1 (17052)
	2 (446)	2 (43032)
	3 (297)	3 (22557)
	4 (121)	4 (13924)
	5 (172)	5 (3889)
	6 (188)	6 (2722)
	7 (258)	7 (3497)
	8 (140)	8 (16309)
	9 (126)	9 (6873)
	10 (116)	10 (26635)
	11 (253)	11 (1088)
	12 (1229)	
H-Cdh8	1 (54)	1 (14586)
	2 (449)	2 (119663)
	3 (300)	3 (44044)
	4 (121)	4 (32105)
	5 (172)	5 (4067)
	6 (188)	6 (3194)
	7 (258)	7 (27117)
	8 (140)	8 (62134)
	9 (123)	9 (13134)
	10 (122)	10 (58111)
	11 (253)	11 (1366)
	12 (773)	

a most likely cleavage site between positions M29 and A30. This cleavage position is the same for all three isoforms, suggesting that the putative Cdh8 proteins have a common signal peptide of 29 aa at the N terminus. Similar results were obtained for human, mouse and rat Cdh8 (data not shown). The signal peptide is highlighted by purple color in Supplementary Fig. 2.

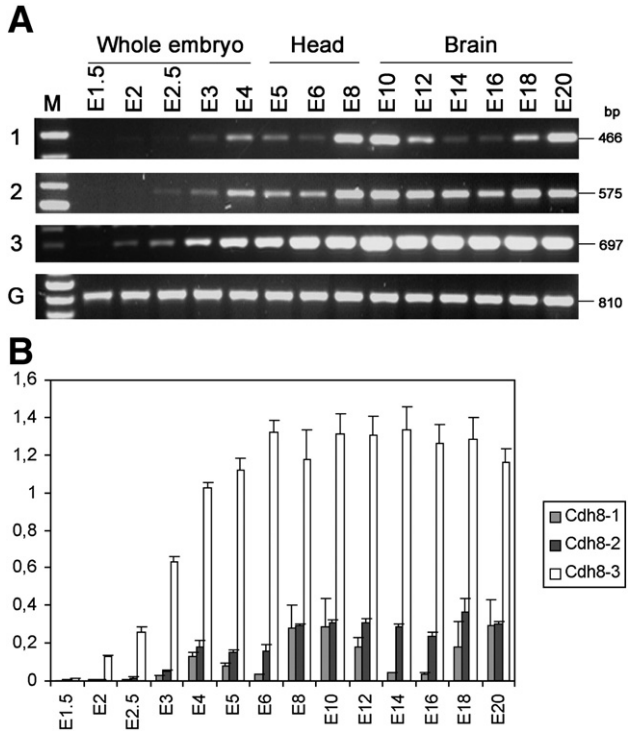

Fig. 3 – A. Results from semi-quantitative RT-PCR analysis showing the expression of the Cdh8 isoforms (1, Cdh8-1; 2, Cdh8-2, and 3, Cdh8-3) at different stages of chicken embryonic development (E1.5–E4, whole embryos; E5–E8, whole head; E10–E20, brain); GAPDH (G) served as an internal control to monitor the amount of RNA. Note that the intensity of the bands of Cad8-1 and Cad8-2 was increased to visualize the weakest ones (compare the bands of the marker that was used at the same concentration in all panels). B. The measured intensity values of the bands are normalized to the GAPDH value. The error bars represent means +/– s.e.m. (n=3).

2.3. *Expression of Cdh8 isoforms during chicken embryonic development*

To study the transcription of the three chicken Cdh8 isoforms in the chicken embryo, we performed semi-quantitative RT-PCR from E1.5 to E20 (Fig. 3A). Results for Cdh8-3 and GAPDH, which served as an internal control, were from multiplex RT-PCR. However, multiplex RT-PCR did not work for Cdh8-1 and Cdh8-2 in conjunction with Cdh8-3 or GAPDH. The bands were quantified by using appropriate software (ImageQuant TL). The

Table 2 – Percent identity and similarity (positives) between the chicken Cdh8 isoforms and human Cdh8, mouse Cdh8, and rat Cdh8

	Human NP_001787	Mouse NP_031693	Rat NP_445845
Cdh8-1	Identities 87% (451/513)	Identities 86% (446/513)	Identities 86% (446/513)
	Positives 93% (478/513)	Positives 92% (475/513)	Positives 92% (475/513)
Cdh8-2	Identities 88% (485/551)	Identities 86% (479/551)	Identities 86% (479/551)
	Positives 93% (515/551)	Positives 92% (512/551)	Positives 92% (512/551)
Cdh8-3	Identities 90% (725/802)	Identities 89% (718/799)	Identities 89% (717/799)
	Positives 94% (761/802)	Positives 94% (758/799)	Positives 94% (757/799)

measured values were normalized to the corresponding GAPDH values (Fig. 3B). Negative controls (water and no enzyme) did not yield any band (data not shown).

Results showed that Cdh8-3 begins to be transcribed weakly at E2 in whole embryos. As the embryo develops, the transcription of Cdh8-3 increases gradually in the embryos until E4. In the head, expression is relatively high from E4 to E6 and, in the brain, from E10 to E20. Cdh8-1 and Cdh8-2 are expressed more weakly than Cdh8-3. Transcript of Cdh8-2 is detected from E2.5 and increases until E4 in whole embryos. In the head, expression is higher at E8 than at E5 and E6. In the brain, expression is relatively prominent from E10 to E20. Expression of Cdh8-1 is similar to Cdh8-2. Transcript is first detected at E3 in whole embryos. Expression in the head peaks at E8 and, in the brain, it decreases from E10 to E14, and increases again until E20. These results suggest that the expression of each of the Cdh8 isoforms is individually regulated during chicken embryonic development.

2.4. *Regional expression of the three isoforms in chicken embryonic brain*

To analyze the expression of the Cdh8 isoforms in brain by semi-quantitative RT-PCR at the regional level, brains of E7, E12 and

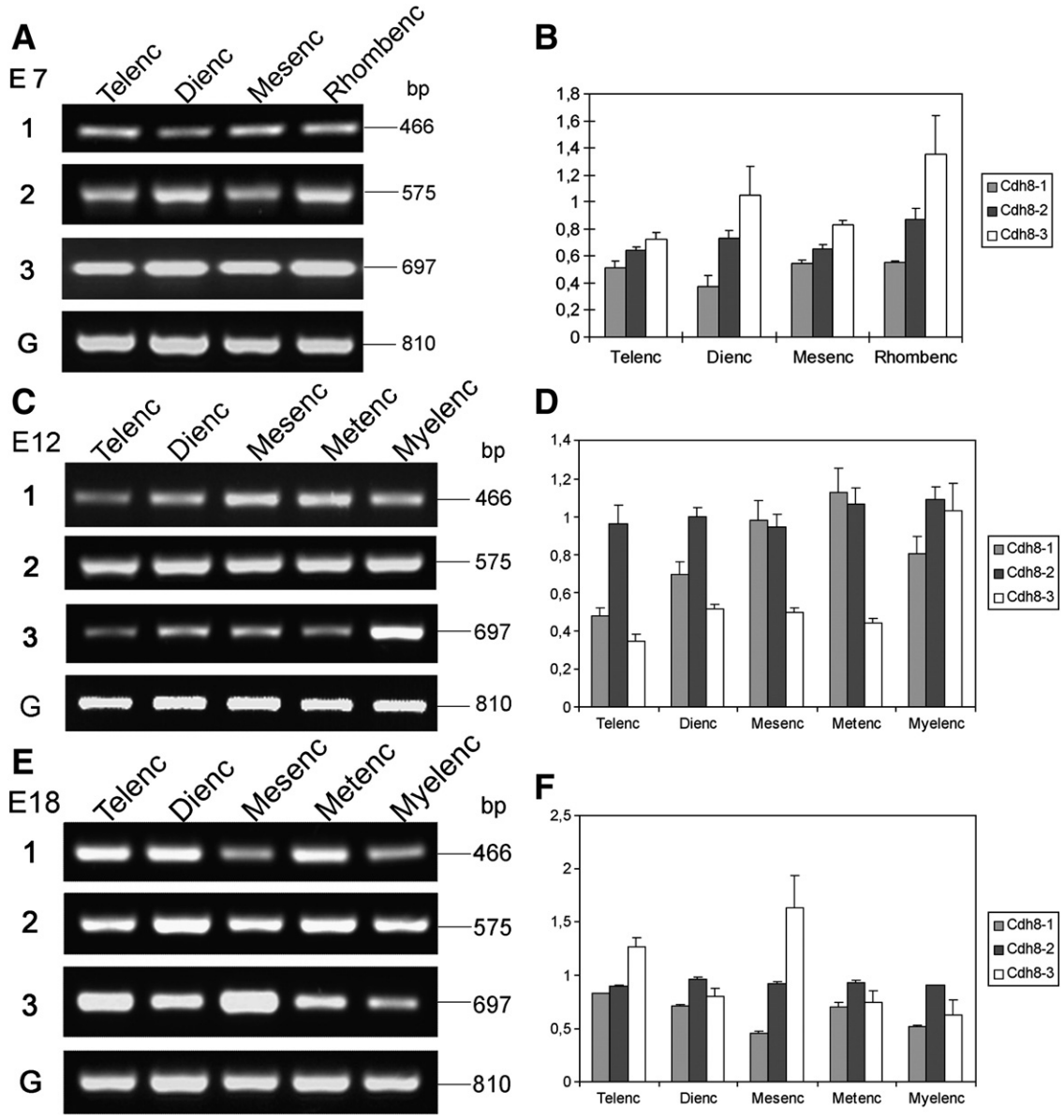

Fig. 4 – A, C and E. Results from semi-quantitative RT-PCR analysis for regional expression of the three Cdh8 isoforms (1, Cdh8-1; 2, Cdh8-2, and 3, Cdh8-3) in brain at E7 (A), E12 (C) and E18 (E). The same amount of total RNA was used in each case. Note that 35 PCR cycles were used for Cdh8-1 and Cdh8-2, but 25 cycles only for Cdh8-3 and GAPDH. B, D and F. The measured intensity values of the bands are normalized to the GAPDH value for E7 (B), E12 (D) and E18 (F). The error bars represent means +/−s.e.m. (n=3). Dienc, diencephalon; Mesenc, mesencephalon; Metenc, metencephalon; Myelenc, myelencephalon; Rhombenc, rhombencephalon; and Telenc, telencephalon.

E18 embryos were separated into telencephalon, diencephalon, mesencephalon, metencephalon and myelencephalon (for E7 brains, the metencephalon and myelencephalon were not separated leaving the rhombencephalon intact). GAPDH served as an internal control. Because expression of Cdh8-1 and Cdh8-2 was overall weaker (see Figs. 1C, D and 3A, B), the number of RT-PCR cycles used was higher than that for Cdh8-3 and GAPDH amplification. For each isoform, regional differences in transcription can be detected. For example, at E7, the expression of Cdh8-2 and Cdh8-3 is stronger in the rhombencephalon than telencephalon and mesencephalon (Figs. 4A and B). Regional differences in transcription are also seen at E12, especially for Cdh8-1 and Cdh8-3. For example, the telencephalon expresses Cdh8-1 more weakly than the metencephalon. However, the expression of Cdh8-3 is stronger in myelencephalon. Cdh8-2 is stably expressed in all brain parts (Figs. 4C and D). At E18, Cdh8-1 is expressed more weakly in the mesencephalon than in the telencephalon. Cadh8-3 expression in the mesencephalon is stronger than in the myelencephalon (Figs. 4E and F). In conclusion, the expression of the three isoforms is regulated not only temporally but also regionally in the embryonic brain.

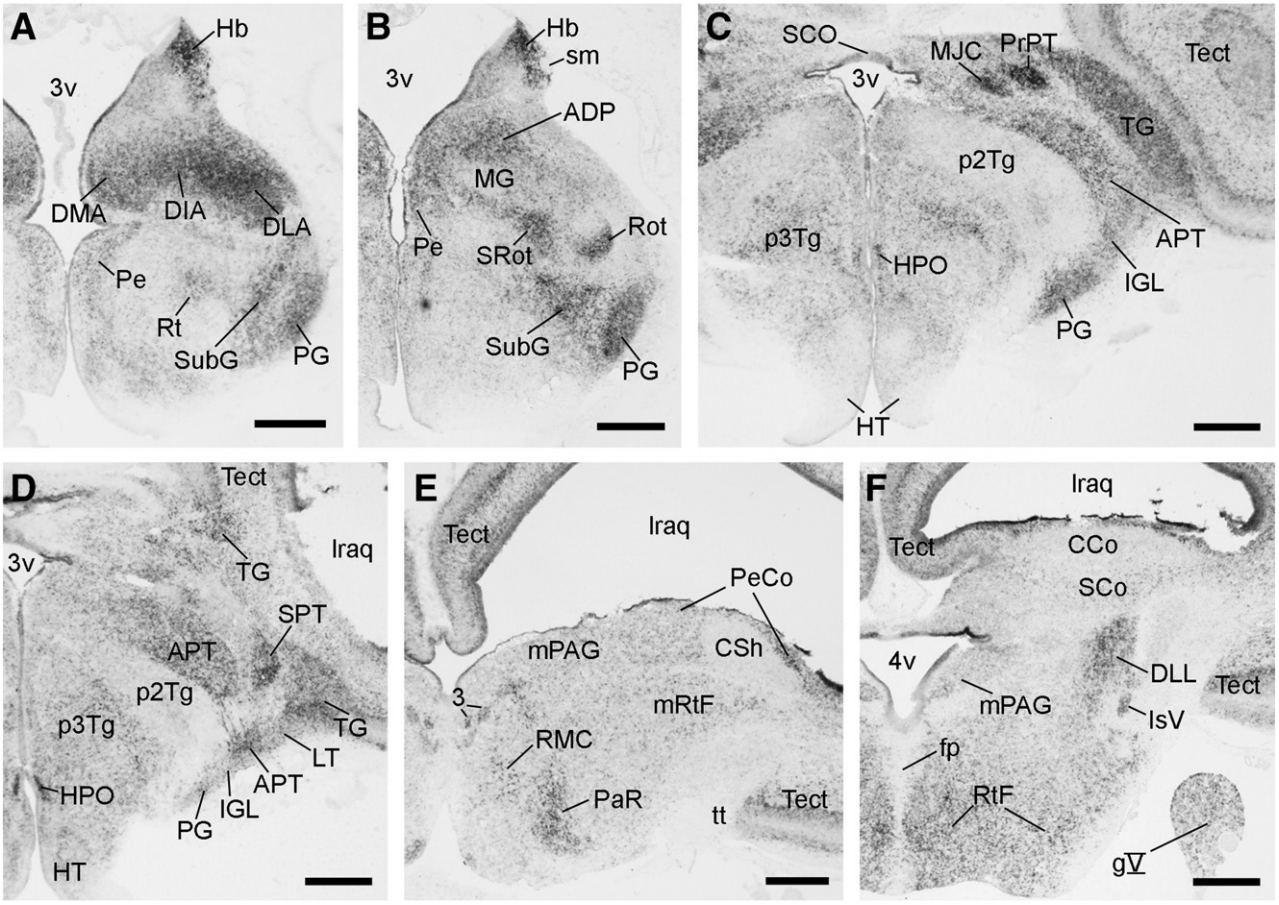

Fig. 5 – Results from in situ hybridization visualizing Cdh8-3 expression in the embryonic day 10 brain of the chicken. Frontal sections through the rostral diencephalon (A and B), the caudal diencephalon (C and D), the midbrain (E) and the mid-/hindbrain transition area (F) are shown in a rostral-to-caudal sequence. Abbreviations: 3, oculomotor nucleus; 3v, third ventricle; 4v, fourth ventricle; ADP, dorsoposterior nuclear complex of the thalamus; APT, anterior pretectal nucleus; CCo, central core part of the midbrain auditory torus; CSh, central shell part of the midbrain auditory torus; DIA, dorsal intermediate anterior nucleus of the thalamus; DLA, dorsolateral anterior nucleus of the thalamus; DLL, dorsal nucleus of the lateral lemniscus; DMA, dorsomedial anterior nucleus of the thalamus; fp, floor plate; gV, trigeminal ganglion; Hb, habenula; HPO, hypothalamic periventricular organ; HT, hypothalamus; IGL, intergeniculate leaflet; IsV, ventral isthmic nucleus; Iraq, lateral recess of the aqueduct; LT, lateral terminal nucleus (pretectum); MG, medial geniculate nucleus (nucleus ovoidalis); MJC, medial juxtacommissural nucleus of the pretectum; mPAG, mesencephalic periaqueductal gray; mRtF, mesencephalic reticular formation; p2Tg, prosomere 2 tegmentum (prerubral field); p3Tg, prosomere 3 tegmentum (Forel's field); PaR, pararubral nucleus; Pe, periventricular stratum; PeCo, periventricular core part of the midbrain auditory torus; PG, pregeniculate nucleus (formerly ventral geniculate nucleus); PrPT, principal pretectal nucleus; RMC, red nucleus, magnocellular part (mesencephalon); Rot, rotundus nucleus (thalamus); Rt, reticular nucleus (prethalamus); RtF, reticular formation; SCo, superficial core part of the midbrain auditory torus; SCO, subcommissural organ; SCo, superficial core part of the midbrain auditory torus; sm, stria medullaris; SPT, subpretectal nucleus; SRot, subrotundus nucleus of the thalamus; SubG, subgeniculate nucleus of the prethalamus (ventrolateral nucleus); Tect, tectum; TG, tectal gray; tt, tectothalamic tract. Scale bar, 500 μm.

2.5. *Results from in situ hybridization*

Next, we studied expression of Cdh8 by in situ hybridization. Expression of Cdh8-1 and Cdh8-2 was too weak to be detected (no data shown), even with a more sensitive method of in situ hybridization (tyramide amplification; Van Heusden et al., 1997). The expression of Cdh8-3 was studied at E8, E10, E12, E14 and E18 in consecutive series of frontal brain sections. Representative results are displayed in Fig. 5 for E10, in Fig. 6 for E12 and in Fig. 7 for E18 (data for E8 and E14 are not shown). Results indicate that Cdh8-3 expression is restricted to a specific subset of gray matter structures in all major brain divisions, from the telencephalon to the hindbrain. At the regional level, expression is remarkably stable from E8 to E18. If the expression pattern changes in a given brain region, these changes usually reflect regional gray matter differentiation. In the following paragraphs, we will describe Cdh8-3 expression on a regional basis in a rostral-to-caudal sequence for representative stages.

2.5.1. *Telencephalon*

In the medial pallium, Cdh8-3 is expressed in the hippocampus (Hi in Fig. 6A) and the parahippocampal area (PHiI, PHiL and PHiCL in Figs. 6A,B; and 7A,B) at E12. At E18, expression persists only in the lateral and caudolateral part of the parahippocampal area (PHiL and PHiCL). In the caudolateral parahippocampal area (PHiCL), patches of Cdh8-3 expression are observed in the superficial layers (Figs. 6B; 7A,B). Similar patches were described before for Cdh7 expression (Kovjanic and Redies, 2003). In the dorsal pallium, expression in the apical hyperpallium (HA in Fig. 6A) is especially prominent. The boundary between the lateral and ventral pallium, the ventral pallial lamina, is weakly Cdh8-3 positive (vpl in Fig. 6A). In the ventral pallium, the caudolateral region of the nidopallium shows strong Cdh8-3 signal (NCL in Figs. 6A,B,D; and 7D). Other positive regions include the core nucleus and the intermedioanterior nucleus (ACo, AIA in Figs. 7D, and 6B) in the amygdala (Amy) and the lateral septal area (LS in Figs. 6A–C; and 7C). Scattered cells in the nuclei of the horizontal and ventral limb of the diagonal band (HDB in Fig. 6D and VDB in Fig. 7C) are also positive. In the subpallium, the medial striatum (MSt in Fig. 6A), the ectopic part of the pallidum (PalE in Figs. 6B,C) and other pallidal regions (Pal in Figs. 6B–D, and 7C) express Cdh8-3.

2.5.2. *Diencephalon*

Cdh8-3 is expressed by a subset of diencephalic nuclei. In the epithalamus, both the medial and lateral habenular complexes show strong signal (Hb in Figs. 5A,B; and 6E; MHb, LHb in Fig. 7E). In the prethalamus (prosomere 3), expression is especially prominent in the subgeniculate nucleus (SubG in Figs. 5A,B; and 6D,E), and the reticular nucleus (Rt, RtD in Figs. 5A; and 6D, E). In the thalamus (prosomere 2), Cdh8-3 is expressed by a large portion of the dorsal thalamic nuclei (DMA, DIA, DLA, DP, DSS in Figs. 5A,B; 6E; and 7E). Moreover, part of the rotundus nucleus (Rot), the subrotundus nucleus (SRot) and the intrageniculate leaflet (IGL) show signal (Figs. 5B–D). In the pretectum (prosomere 1), the principal pretectal nucleus (PrPT) and the subpretectal nucleus (SPT) are positive, as well as the medial juxtacommissural nucleus (MJC) and the anterior pretectal nucleus (APT). The perigeniculate nucleus (PG), which derives from all three prosomeres, also expresses Cdh8-3 (Figs. 5A–D; 6E,F).

At E10, the tegmental (ventral) area of the diencephalon shows weak staining in prosomere 2 (p2Tg in Figs. 5C,D). This is contrasted with much stronger signal in prosomere 3 (p3Tg) and in prosomere 1 (APT; Figs. 5C,D). In the hypothalamus (HT in Figs. 5C,D; 6D; and 7E,F), the periventricular organ (HPO in Figs. 5C,D) expresses Cdh8-3 strongly.

2.5.3. *Mesencephalon*

Cdh8-3-positive midbrain structures include the oculomotor nucleus (3 in Figs. 5E; 6G; and 7F), the trochlear nucleus (4 in Figs. 7G,H), the interfascicular nucleus (IF in Fig. 7F), the interpeduncular nucleus (IP in Figs. 6G; and 7G), the pedunculotegmental nucleus (PTg in Fig. 6G), the pararubral nucleus (PaR in Figs. 5E; and 7F), the dorsal nucleus of the lateral lemniscus (DLL in Fig. 7E), the midbrain reticular formation (mRtF in Figs. 5E; 7F), the periaquaeductal gray (mPAG in Figs. 5E,F), and the red nucleus (RMC in Fig. 5E).

In the midbrain auditory torus, the periventricular core part (PeCo in Figs. 5E; and 6G) and the superficial core part (SCo in Figs. 5F; and 6G) express Cdh8-3, unlike the central shell and core parts (CSh, CCo in Figs. 5E,F; and 6G). The tectal gray (TG in Figs. 5C; and 6F) shows strong signal for Cdh8-3. The tectum (Figs. 6F,H; 7G) includes scattered Cdh8-3-positive projection neurons in the stratum griseum centrale (SGC). A deep sublamina of the stratum griseum et fibrosum superficiale (SGFS) expresses Cdh8-3 also.

In the (pre-)isthmic region, the ventral isthmic nucleus (IsV in Fig. 5F) is positive. The isthmic parvicellular nucleus (IsPC in Fig. 7G) and the magnocellular preisthmic nucleus (MCPI in Fig. 7G) are negative.

2.5.4. *Cerebellum and hindbrain*

The cerebellar cortex contains parasagittal domains of Cdh8-3-positive Purkinje cell clusters; other positive structures in the cerebellar system are the medial cerebellar nucleus (Med in Fig. 7I), parts of the lateral and intermediate cerebellar nuclei and parts of the inferior olivary complex (F. Neudert and C. Redies, unpublished data). In the hindbrain, a rostral part of the raphe nucleus (R in Fig. 7H), the reticular formation (RtF in Figs. 5F; and 7G,H,J,K), the superior olive (OS in Fig. 7J), the medial pontine nucleus (MPn in Fig. 7J), and the medial vestibular nucleus (MVe in Figs. 7J,K) express Cdh8 more strongly than their surround. Cdh8-3 is expressed also by a subset of neurons in the trigeminal ganglion (gV in Fig. 5F).

3. Discussion

3.1. *Isoforms and gene structure of chicken Cdh8*

Cdh8 has been identified in human (Shimoyama et al., 2000), mouse (Korematsu and Redies, 1997a,b), and rat (Kido et al., 1998). In this study, we have successfully cloned three sequences of chicken Cdh8 by RACE; all of them have a polyadenylation tail. After sequence analysis and alignment with human, mouse and rat Cdh8, the three sequences were confirmed as isoforms of chicken Cdh8. The three isoforms can be all found on chromosome 11 of the chicken genome, a region of synteny to 16q22.1 of

the human genome where human *Cdh8* is located (Kremmidiotis et al., 1998; Martin et al., 2004). Moreover, most of the 5 end sequence is identical. These results indicate that the three isoforms represent splice variants transcribed from a single gene. The complete sequence of chicken Cdh8 (Cdh8-3) has been published previously by our group (Luo et al., 2007), but the two shorter isoforms (Cdh8-1 and Cdh8-2) are described here for the first time. Chicken *Cdh8-3* cDNA has high similarity with human, mouse, and rat *Cdh8* (80% identities and higher); similarity to human *Cdh8* is highest (Luo et al., 2007). The structural similarity between the *Cdh8* genes of these species demonstrates that *Cdh8* is a gene highly conserved between higher vertebrates. The even higher conservation at the protein level (more than 86% identity, Table 2) between human, mouse, rat and chicken suggests that Cdh8 has similar functions in these species.

It was reported that, in rat, Cdh8 is expressed in two isoforms, a complete isoform and a truncated isoform that lacks the transmembrane domain and the cytoplasmic tail (Kido et al., 1998). The truncated isoform of rat Cdh8 is terminated near the N terminus of EC5 with a short unique sequence of 19 aa at the C terminus. Likewise, the two truncated isoforms of chicken Cdh8 both have unique sequences of 13 aa in EC5 at the C terminus (S2) and are truncated in the same domain (EC5) as the rat isoform. Cdh8-1 shares four amino acids (NISM) with rat truncated type at the beginning of the unique sequences. However, the other residues of the unique sequences differ from each other in rat and chicken. Isoforms of some other type II classic cadherins have been reported (see Introduction). The function of all these short variants of classic cadherins remains to be investigated.

The cytoplasmic domain is essential for the association of classic cadherins with catenins. This association plays a crucial role in the binding of cadherins to the cytoskeleton, which contributes to cell–cell adhesion, and in signal transduction (for reviews, see Hirano et al. (2003); and Takeichi (2007)). Consequently, the three isoforms are likely to differ in their adhesive function and interaction with cytoplasmic proteins. Moreover, the two shorter isoforms are predicted to represent secreted forms of Cdh8 because they lack the transmembrane domain and have a truncated EC5 domain. The soluble endogenous form of another classic cadherin, N-cadherin, is generated by proteolysis; this soluble form retains its biological function in promoting cell adhesion and neurite outgrowth (Paradies and Grunwald, 1993). T-cadherin is the only classic cadherin known to lack the cytoplasmic and transmembrane domains constitutively (Ranscht and Dours-Zimmermann, 1991).

Shimoyama et al. (2000) have demonstrated that, like other classic cadherins, the long isoform of Cdh8 regulates cell–cell binding. The two short isoforms of chicken Cdh8 might also have adhesive function because the extracellular domain of classic cadherins serves as the interface for cell–cell binding and determines binding specificity (Takeichi, 1991). Structural analysis revealed that the extracellular domains form structural units whose dimerization is crucial for adhesive activity (Shapiro et al., 1995; Nagar et al., 1996; Elste and Benson, 2006; Pokutta and Weis, 2007). Whether the short unique sequences that are found in the short isoforms at the site of truncation have a special role in cell adhesion or other functions of Cdh8 remains unclear. For rat Cdh8, Kido et al. (1998) did not demonstrate an adhesive function for the truncated isoform because they failed to express it in L cells.

3.2. *Expression analysis of chicken Cdh8*

In order to explore the possibility that the three isoforms of chicken Cdh8 have different functions during the embryonic development, we studied their expression patterns by semi-quantitative RT-PCR, Northern blotting and in situ hybridization, respectively.

First, we designed unique primers to detect separately the transcript of the three isoforms (Fig. 1A). Second, we confirmed the existence of the ORFs corresponding to the three Cdh8 isoforms by RT-PCR with a different set of unique 3 end primers (Fig. 1B). Third, we analyzed the relative amount of each isoform by Northern blotting. Cdh8-3 is transcribed around 15 times more strongly than Cdh8-1 and Cdh8-2 (Figs. 1C, D).

Fig. 6 – Results from in situ hybridization visualizing Cdh8-3 expression in the embryonic day 12 brain of the chicken. Frontal sections through the rostral telencephalon (A and B), the caudal telencephalon (C), the tel-/diencephalic transition area (D), the rostral diencephalon (E), the caudal diencephalon (F), the mid-/hindbrain transition area (G), and the tectum (H) are shown in a rostral-to-caudal sequence. The asterisks indicate artefacts. Abbreviations: 3, oculomotor nucleus; 3v, third ventricle; ac, anterior commissure; ACo, amygdala, core nucleus; AIA, amygdala, intermedioanterior nucleus; APT, anterior pretectal nucleus; csm, corticoseptomesencephalic tract; CCo, central core part of midbrain auditory torus; DIA, dorsal intermediate anterior nucleus of the thalamus; DLA, dorsolateral anterior nucleus of the thalamus; DMA, dorsomedial anterior nucleus of the thalamus; DSS, dorsal somatosensory nucleus of the thalamus; EP, neuroepithelium; HA, apical hyperpallium; Hb, habenula; HDB, nucleus of the horizontal limb of the diagonal band; Hi, hippocampus; IP, interpeduncular nucleus; HT, hypothalamus; lfb, lateral forebrain bundle; LPall, lateral pallium; lraq, lateral recess of the aquaeduct; LS, lateral septum; LSt, lateral striatum; lv, lateral ventricle; MSt, medial striatum; MV, mesopallium, ventral part; NCcp, nidopallium, caudal part, corticoid plate; NCL, nidopallium, caudal part, lateral region; NICe, nidopallium, intermediate part, central region; Pal, pallidum; PalE, ectopic (intrastriatal) part of pallidum; pch, choroid plexus; Pe, periventricular stratum; PeCo, periventricular core part of the midbrain auditory torus; PG, pregeniculate nucleus (formerly ventral geniculate nucleus); PHiCL, parahippocampal area, caudolateral part; PHiL, parahippocampal area, lateral part; PrPT, principal pretectal nucleus; psp, pallial-subpallial boundary; PTg, pedunculotegmental nucleus; Rt, reticular nucleus (prethalamus); RtD, reticular nucleus, dorsal part (prethalamus); SAC, stratum album centrale; SCo, superficial core part of the midbrain auditory torus; SGC, stratum griseum centrale; SGFS, stratum griseum et fibrosum superficiale; sm, stria medullaris; SPC, superficial parvicellular nucleus of the thalamus; SubG, subgeniculate nucleus of the prethalamus (ventrolateral nucleus); Tect, tectum; TG, tectal gray; Tu, olfactory tubercle; VPall, ventral pallium; vpl, ventral pallial lamina. Scale bar, 500 μm (in A-G) and 200 μm (in H).

This result may explain why the in situ hybridization signal of Cdh8-1 and Cdh8-2 was too weak to be detected. Fourth, we analyzed expression levels of the three isoforms by semi-quantitative RT-PCR in whole embryos, heads and brain (Fig. 3) and in different brain regions (Fig. 4). The difference in the temporal and regional expressions between the three isoforms indicates that the transcription of each isoform is regulated individually during embryonic development of chicken embryo and brain. Results confirm that the expression of Cdh8-1 and Cdh8-2 was considerably weaker than that of Cdh8-3.

Fifth, the expression of the three isoforms was studied by in situ hybridization. However, the signal for Cdh8-1 and Cdh8-2 was too weak to be detected. The fact that RT-PCR is more sensitive than in situ hybridization (Wakamatsu et al., 2007) may explain why Cdh8-1 and Cdh8-2 can be revealed by RT-PCR, but not by in situ hybridization. Nevertheless, because Cdh8-1 and Cdh8-2 may represent soluble forms of Cdh8 (see 2.2 and 3.1), it will still be interesting to explore their possible expression and function in future studies in detail.

The in situ hybridization study revealed a restricted pattern of Cdh8 expression in a subset of gray matter structures in the late embryonic chicken brain (Figs. 5–7). Other classic cadherins are expressed in a similarly restricted pattern in the embryonic chicken brain, for example Cdh3 (N-cadherin), Cdh4 (R-cadherin), Cdh6B, Cdh7 (Redies et al., 2000, 2001), and Cdh10 (Fushimi et al., 1997). The Cdh8-3 expression pattern is different from that of

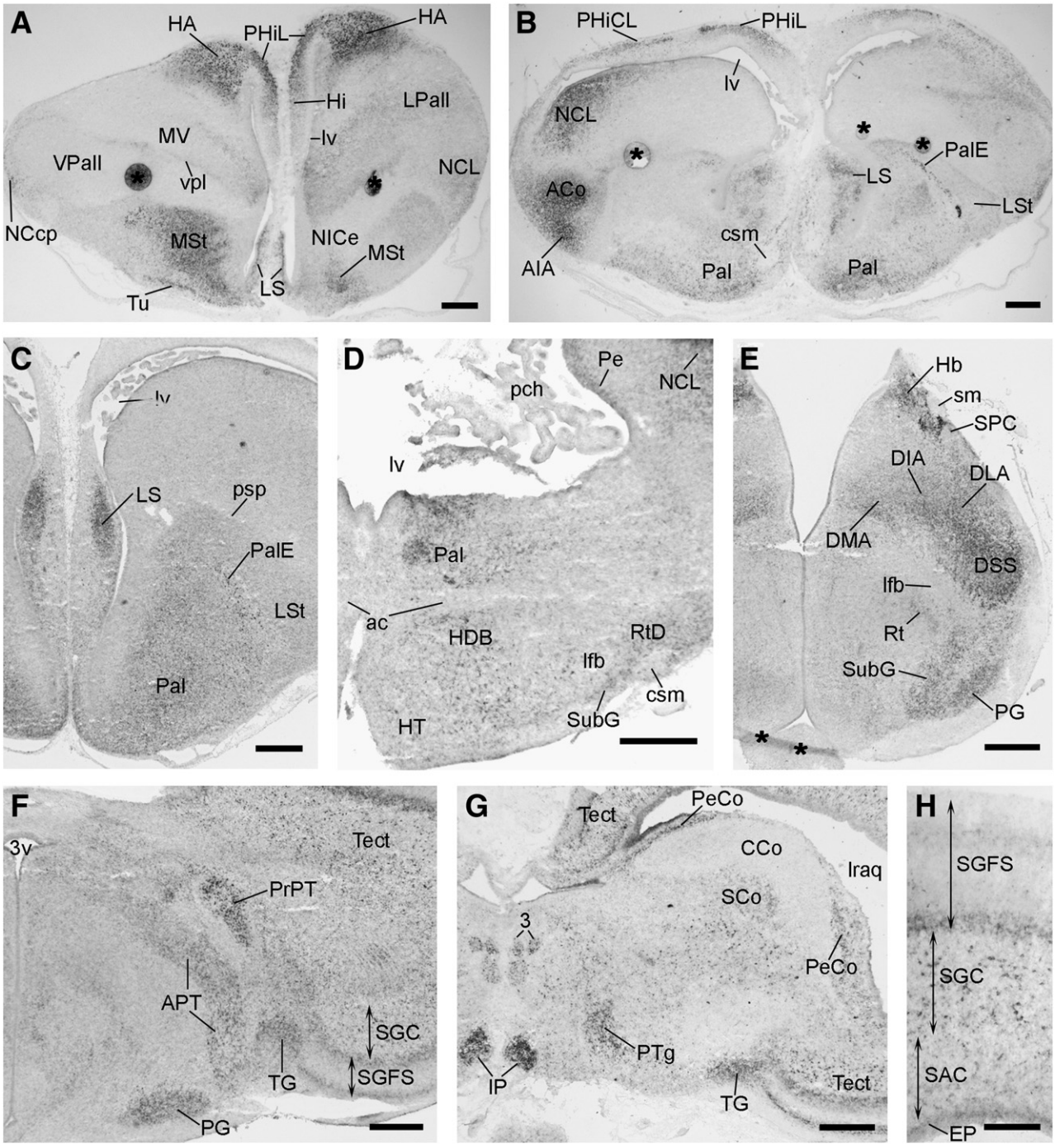

these other cadherins, although a partial overlap can be noted in some areas. Cdh8 expression in the mouse (Korematsu and Redies, 1997a,b; Suzuki et al., 1997) is also restricted regionally.

A comparison of the expression patterns in chicken and mouse brains reveals that a number of brain structures express this molecule in both species. Examples in the telencephalon include the hippocampus, the caudolateral parahippocampal area that likely corresponds to the entorhinal cortex in mouse (Kovjanic and Redies, 2003), the septal nuclei, the amygdala, the striatum and parts of the pallidum. In the diencephalon, the medial and lateral habenula, large parts of the dorsal thalamic complex, the dorsolateral thalamic nucleus, the reticular nucleus and the anterior pretectal nucleus express Cdh8 in both species. Additional examples are found in the cerebellar system (Purkinje cell domains and deep cerebellar nuclei) and in the mesencephalon (tectum, interpeduncular nucleus, and medial raphe). In the hindbrain, cross-species expression is observed in the inferior olive, the pontine nuclei and the vestibular nucleus. Together, these results suggest a relatively large degree of phylogenetic conservation of Cdh8 expression between chicken and mouse.

In summary, Cdh8 can contribute to the adhesive code that is postulated to regulate morphogenesis and functional differentiation of the chicken brain during embryogenesis (for a review, see Redies (2000)). A function of Cdh8 in neural circuit formation and synaptogenesis has recently been demonstrated in the somatosensory system of Cdh8-deficient mice (Suzuki et al., 2007). Their results showed that Cdh8 is essential for establishing the physiological coupling between cold-sensitive sensory neurons and their target neurons in dorsal horn of the spinal cord. It will be interesting to analyze the possible functions of the three Cdh8 isoforms during chicken embryonic development by appropriate experimental methods also in chicken, for example with gene over-expression or knock down in conjunction with in vivo electroporation.

4. Experimental procedures

4.1. *Animals*

Fertilized eggs of White Leghorn chicken (*Gallus gallus domesticus*) were obtained from a farm and incubated in a forced-draft incubator (Ehret, Emmendingen, Germany) at 37 °C and 65% humidity. Embryos were studied at embryonic day 1.5 (E1.5), E2, E2.5, E3, E4, E5, E6, E7, E8, E10, E12, E14, E16, E18, and E20 (at least 3 embryos for each stage). After deep anesthesia was induced by cooling on ice, the embryos were removed from the eggs. For RT-PCR analysis, the embryos, heads or brains were put directly into liquid nitrogen and stored at −80 °C. For regional analysis by RT-PCR, brains of E7, E12, and E18 embryos were cut into different parts and washed with phosphate-buffered saline (PBS). Specimens were immersed in liquid nitrogen and stored at −80 °C. For in situ hybridization, embryos were fixed in 4% formaldehyde solution on ice for 6 to 24 h, depending on the size of the embryos. Specimens were embedded in TissueTec O.C.T. compound (Science Services, München, Germany), frozen in liquid nitrogen and stored at −80 °C, as described previously (Redies and Takeichi, 1993).

4.2. *RNA isolation, RT-PCR and RACE reaction*

Total RNA from whole chicken embryos or embryonic brains was prepared using TRIzol reagent according to the manufacturer's instruction (Invitrogen, Karlsruhe, Germany). For E1.5, E2, E2.5, E3 and E4, total RNA was isolated from whole embryos; for E5, E6 and E8, total RNA was extracted from the heads only; and for E10, E12, E14, E16, E18 and E20, total RNA was extracted from isolated brains. To analyze the regional expression of the three isoforms of Cdh8 in chicken, the brains of E12 and E18 embryos were separated into telencephalon, diencephalon, mesencephalon, metencephalon and myelencephalon. For E7 brains, the metencephalon and myelencephalon were not separated (rhombencephalon). The quality of total RNA was examined by ethidium bromide-stained denature agarose gel electrophoresis and its concentration determined by a spectrophotometer for the following experiments.

To obtain the full-length sequences of chicken Cdh8, 5 and 3 end RACE reactions were performed with the SMART RACE cDNA Amplification Kit (Clontech, Saint-Germain-en-Laye, France). The selection of the specific primers for RACE was based on the sequence of a PCR-fragment of chicken Cdh8 obtained previously (Luo et al., 2007), according to the instructions of the RACE Kit User Manual. Touch-down PCR for 5 and 3 end RACE amplification was performed using the 5 and 3 end

Fig. 7 – Results from in situ hybridization visualizing Cdh8-3 expression in the embryonic day 18 brain of the chicken. Frontal sections through the caudolateral parahippocampal area (A, B), the septal area (C), the amygdaloid complex (D), the rostral diencephalon (E), the mesencephalon (F and G), the midbrain tegmentum (H), the cerebellum (I), and the hindbrain at the level of the superior olive (OS; J) and of the cochlear commissure (xc; K) are shown in a rostral-to-caudal sequence. B shows a thionin stain of a section adjacent to A. The asterisks indicate artefacts. Abbreviations: 3, oculomotor nucleus; 3n, oculomotor nerve; 3v, third ventricle; 4, trochlear nucleus; 4v, fourth ventricle; ACo, amygdala, core nucleus; Amy, amygdala; Cb, cerebellum; CbC, cerebellar cortex; DLA, dorsolateral anterior nucleus of the thalamus; DLL, dorsal nucleus of the lateral lemniscus; HT, hypothalamus; IF, interfascicular nucleus; IP, interpeduncular nucleus; ir, infundibular recess; IsPC, isthmic parvicellular nucleus; LHb, lateral habenular nucleus; LS, lateral septum; lv, lateral ventricle; MCPI, magnocellular preisthmic nucleus; Med, medial cerebellar nucleus; MHb, medial habenular nucleus; MPn, medial pontine nucleus; mRtF, mesencephalic reticular formation; MS, medial septal nucleus; MVe, medial vestibular nucleus; NCIF, nidopallium, caudal part, island field; NCL, nidopallium, caudal part, lateral region; OS, superior olive; Pal, pallidum; PaR, pararubral nucleus; pch, choroid plexus; PH, parahippocampal area; PHiCL, parahippocampal area, caudolateral part; PHiL, parahippocampal area, lateral part; R, raphe nucleus; RtF, reticular formation; SAC, stratum album centrale; SGC, stratum griseum centrale; sm, stria medullaris; SPC, superficial parvicellular nucleus of the thalamus; Tect, tectum; TG, tectal gray; VDB, nucleus of the ventral limb of the diagonal band; xc, cochlear decussation. Scale bars, 200 μm (in A and B) and 500 μm (in C-K).

RACE PCR primers (Cdh8-antisense-1 for 5 end RACE; Cdh8-sense-1 for 3 end RACE) together with the Universal Primer Mix. For the first 5 cycles, the touch-down PCR was performed at 94 °C for 30 s and at 72 °C for 3 min. The next 5 cycles were performed at 94 °C for 30 s, 70 °C for 30 s and 72 °C for 3 min. At last, another 27 cycles were performed at 94 °C for 30 s, at 68 °C for 30 s and at 72 °C for 3 min. To obtain more specific bands, nested PCR was performed following the touch-down PCR for 5 and 3 end cDNA amplification with the primers (Cdh8-antisense-2 for 5 end RACE; and Cdh8-sense-2 for 3 end RACE) together with the Nested Universal Primer, respectively. The PCR templates were denatured for 1 min at 95 °C, followed by 20 cycles of amplification (denaturing for 30 s at 95 °C, and annealing and extension for 3 min at 68 °C). The PCR products were cloned into pCR II-TOPO vector (Invitrogen) and sequenced by a commercial company (MWG, Ebersberg, Germany). After combining the RACE sequences with the previously obtained RT-PCR fragment sequence, two sequences similar to Cdh8 were obtained, but they were much shorter than the complete Cdh8 cDNAs obtained in other species. The complete sequence of chicken Cdh8 was obtained by RACE as well (Luo et al., 2007). The primers for 5 end RACE PCR were as follows: Cdh8-antisense-1: 5′-GAATGTTGGCTGCTTCTACCTTCAGAG-3′, and Cdh8-antisense-2: 5′-GGCTTCTCTGTCCATGTTGGGAAGAGC-3′. The primers used

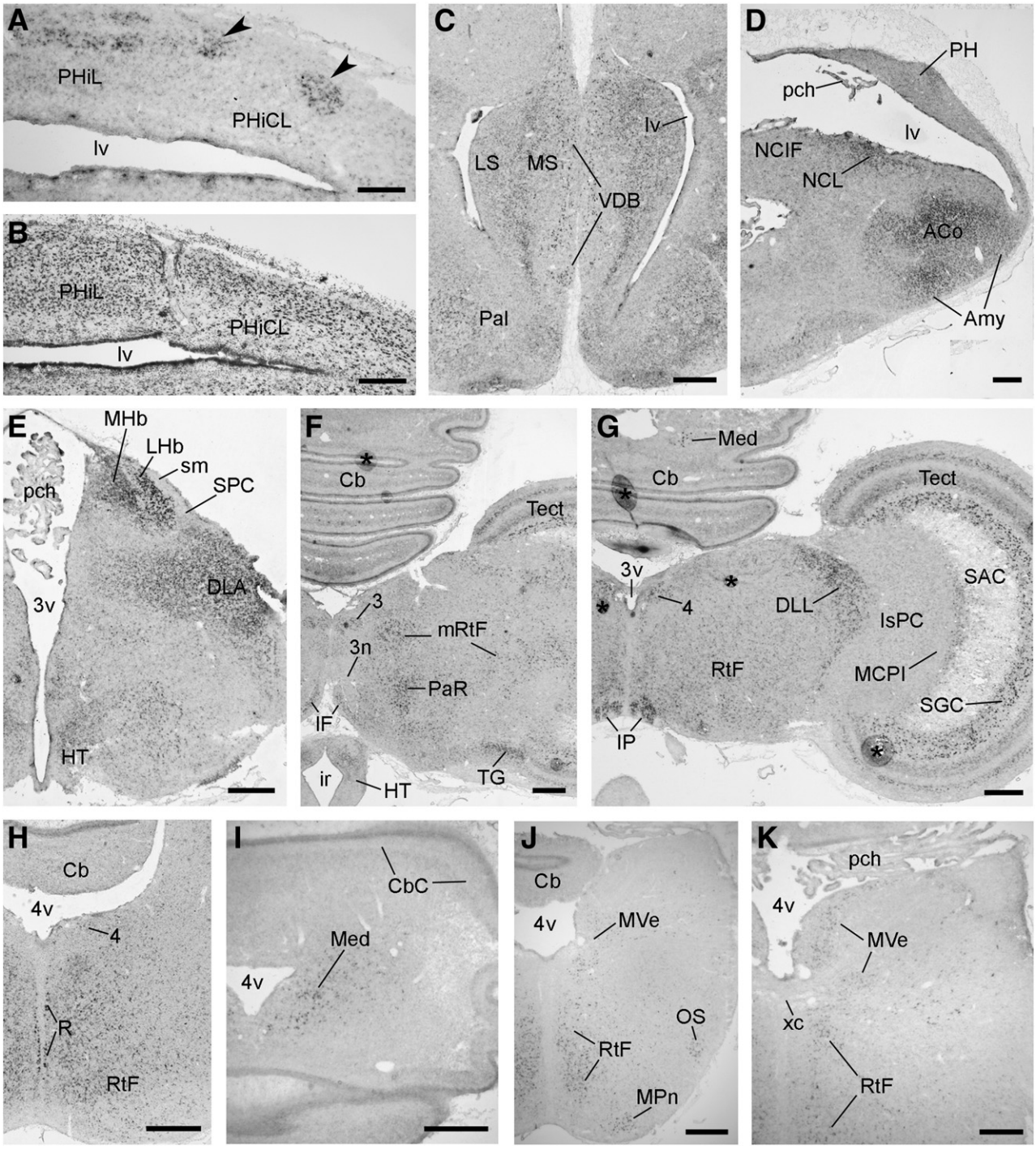

for 3 end RACE PCR were Cdh8-sense-1: 5′-CCTCCTAAGTTTGCG-CAGAGTCTGTATC-3′; and Cdh8-sense-2: 5′-GAACCACAGT-CAAGTGTCCCGGGTGC-3′.

4.3. *Bioinformatic analysis of the three full-length sequences of Cdh8*

Sequence alignments were performed with the Clustal X 1.83 program. ORF finding, translation and molecular mass calculation of the predicted protein of the full-length sequences for the three isoforms were carried out with the Lasergene software (DNASTAR, Madison, WI) and the ORF Finder (http://www.ncbi.nlm.nih.gov/gorf/gorf.html). BLAST was done at the NCBI server for nucleotide, protein, and genome analysis (http://www.ncbi.nlm.nih.gov/blast), while structural analysis of the predicted proteins for the three isoforms was carried out by the SignalP 3.0 program at the following website: (http://www.cbs.dtu.dk/services/SignalP/).

4.4. *Cloning of the unique nucleotide sequences and the ORFs of the three isoforms*

To clone the unique sequences of the three isoforms of Cdh8, appropriate primers were chosen from the unique sequences of the 3 ends, respectively. For the shortest Cdh8 isoform (Cdh8-1), the forward primer was 5′-ATGTTGTATAATTTAGAGTGTTAG-3′ and the reverse primer was 5′-AATTATCTTAGAAAAGTGAG-TAAG-3′ (expected fragment length 466 bp). For the short Cdh8 isoform (Cdh8-2), the forward primer was 5′-AGATATAAAATG-TATGTAATATGTG-3′ and the reverse primer was 5′-ACTGTG-CATGAAATTCCACTTC-3′ (expected fragment length 575 bp). For the long Cdh8 isoform (Cdh8-3), the forward primer was 5′-CATAATGGATTCAGTCGGCAG-3′ and the reverse primer was 5′-CAACTGAGTAAAGTTCTCCAAG-3′ (expected fragment length 697 bp). The three unique sequences (466 bp, 575 bp and 696 bp) amplified with the above primers were all intron-spanning (see Suppl. Fig. S1 and Table 1). The one step RT-PCR reaction was performed first at 50 °C for 30 min for reverse transcription and at 95 °C for 15 min for denaturing, followed by 30 cycles of amplification (denaturing for 45 s at 94 °C, annealing for 45 s at 56 °C [for Cdh8-1 and Cdh8-2] or 59 °C [for Cdh8-3], and extension for 1.5 min at 72 °C). The RT-PCR fragments were analyzed on 1.5% agarose gels. The PCR fragments of the three isoforms obtained were cloned into pCR II-TOPO vector with the TA-cloning kit (Invitrogen) for synthesis of unique probes for each isoform.

To clone the open reading frame (ORF) of the three types of Cdh8, primers that included the start codon or stop codon, which was derived from the full-length sequences of the three isoforms, were chosen. The forward primer was same for the three sequences: 5′-ATGCCAGAAAGACTAACGGAAATG-3′. The lower primer for Cdh8-1 was 5′-CATTCTAACACTCTAAATTA-TACAAC-3′; for Cdh8-2 5′-ATTCAGGTAAATATTACACATAT-TAC-3′; and for Cdh8-3 5′-TCAAGTTTCTTTGTCACTTTCTCC-3′. The expected length of the sequences was 1585 bp, 1697 bp and 2400 bp, respectively. First strand cDNA was synthesized in vitro with the SuperScript First-Strand Synthesis System (Invitrogen) from chicken E10 brain total RNA. The first strand cDNA served as the PCR template and was denatured for 2 min at 94 °C, followed by 35 cycles of amplification (denaturing for 20 s at 94 °C, annealing for 30 s at 62 °C, and extension for 2 min at 68 °C). After the last cycle, the reaction product was extended finally for 15 min at 68 °C. The RT-PCR results were visualized on 1% agarose gel.

4.5. *Semi-quantitative RT-PCR*

Semi-quantitative RT-PCR was performed using the One Step RT-PCR Kit (Qiagen, Hilden, Germany). Samples with water only or without reverse transcriptase (RT) were served as negative controls. The same amount of total RNA was used for each reaction. Glyceraldehyde-3-phosphate dehydrogenase (GAPDH) was used as an internal control to monitor the amount of RNA. The forward primer for GAPDH was 5′-GGGCTCATCTGAAGGG-TGGTGCTA-3′ and the reverse primer was 5′-GTGGGGGAGACA-GAAGGGAACAGA-3′ (expected length 810 bp). The one step RT-PCR reaction was performed first at 50 °C for 30 min for reverse transcription and at 95 °C for 15 min for denaturing, followed by 30 cycles of amplification (denaturing for 45 s at 94 °C, annealing for 45 s at 56 °C [for Cdh8-1 and Cdh8-2] or 59 °C [for Cdh8-3 and GAPDH], and extension for 1.5 min at 72 °C). For brain regional semi-quantitative RT-PCR, 35 PCR cycles were used for Cdh8-1 and Cdh8-2, and 25 cycles for Cdh8-3 and GAPDH. Cdh8-3 and GAPDH were amplified by multiplex RT-PCR with the One Step RT-PCR Kit (Qiagen) following the instructions supplied with the kit. The ratio between the primer concentrations for Cdh8-3 and GAPDH was 5:1. This and multiple other ratios were used for multiplex RT-PCR with Cdh8-1 or Cdh8-2 primers but did not yield any bands. The RT-PCR fragments were analyzed on 1.5% agarose gels.

4.6. *In situ hybridization*

Digoxigenin-labeled sense and antisense cRNA probes were transcribed in vitro from the purified plasmids containing the unique fragments of the three isoforms, according to the manufacturer's instructions for probe synthesis (Roche, Mannheim, Germany). Sense cRNA probes were used as a negative control for in situ hybridization. In situ hybridization on cryosection was performed according to Redies and Takeichi (1993). In brief, cryostat sections of 20 μm thickness were fixed with 4% formaldehyde in PBS and were then pretreated with proteinase K and acetic anhydride. Sections were hybridized overnight with cRNA probe at a concentration of about 3 ng/μl at 70 °C in hybridization solution (50% formamide, 3× SSC, 10 mM EDTA, 10% dextran sulfate, 1× Denhardt's solution, 42 μg/ml yeast transfer RNA and 42 μg/ml salmon sperm DNA). After the sections were washed and the unbound cRNA was removed by RNase, the sections were incubated with alkaline phosphatase-coupled anti-digoxigenin Fab fragments (Roche) at 4 °C overnight. For visualization of the labeled mRNA, a substrate solution of nitroblue tetrazolium salt and 5-bromo-4-chloro-3-indoyl phosphate was added. The sections were viewed and photographed under a transmission light microscope (Olympus BX40, Hamburg, Germany) equipped with a digital camera (Olympus DP70). Photomicrographs, including those for gels, were adjusted in contrast and brightness by the Photoshop software (Adobe, Mountain View, CA) for optimal display of the staining patterns in the figures. For identification and terminology of

neuroanatomical structures, the atlas by Puelles et al. (2007) was followed.

Fluorescent in situ hybridization with tyramide amplification was performed according to the protocol by Van Heusden et al. (1997).

4.7. *Northern blot analysis*

Northern blot analysis was performed according to the protocol by Sambrook and Russell (2001), with some modifications. In brief, 20 μg each of total RNA from E7, E12 and E18 chicken brains were electrophoresed in denaturing 1.5% agarose formaldehyde gel, and transferred onto Hybond nylon membrane (Amersham Biosciences, Freiburg, Germany). The same digoxigenin-labeled antisense cRNA probes as used for in situ hybridization (see 4.6) were hybridized to the membrane at 65 °C. After washing, the membrane was reacted with a substrate solution containing nitroblue tetrazolium salt and 5-bromo-4-chloro-3-indoyl phosphate (see 4.6), until mRNA bands were clearly visible.

4.8. *Statistical analysis*

The intensity of individual bands from semi-quantitative RT-PCR and Northern blotting was quantified using the software ImageQuant TL (Amersham Biosciences). The intensity value of each band was normalized to the value of the corresponding GAPDH band. Each experiment was repeated at least three times ($n=3$). In the figures, all data are shown with the standard error of the mean (s.e.m). Statistical analysis was performed by one-way analysis of variance (ANOVA) and two-tailed *t* test using PRISM 4 software (GraphPad, San Diego, CA, USA). A value of $p<0.05$ was considered significantly different.

Acknowledgments

We thank Ms. Franziska Neudert for contributing to the analysis of Cdh8 expression, Mr. Krishna K. for his assistance with the tyramide-amplified in situ hybridization, Dr. Zhenhua Wang for the help with the statistical analysis, and members of the laboratory for the critical reading of the manuscript. This work was supported by a grant from the German Research Council (Re 616/4-4).

Appendix A. Supplementary data

Supplementary data associated with this article can be found, in the online version, at doi:10.1016/j.brainres.2008.01.071.

REFERENCES

Elste, A.M., Benson, D.L., 2006. Structural basis for developmentally regulated changes in cadherin function at synapses. J. Comp. Neurol. 495, 24–35.

Fushimi, D., Arndt, K., Takeichi, M., Redies, C., 1997. Cloning and expression analysis of cadherin-10 in the CNS of the chicken embryo. Dev. Dyn. 209, 269–285.

Hirano, S., Suzuki, S.T., Redies, C., 2003. The cadherin superfamily in neural development: diversity, function and interaction with other molecules. Front. Biosci. 8, d306–d355.

Kawaguchi, J., Takeshita, S., Kashima, T., Imai, T., Machinami, R., Kudo, A., 1999. Expression and function of the splice variant of the human cadherin-11 gene in subordination to intact cadherin-11. J. Bone Miner. Res. 14, 764–775.

Kawano, R., Matsuo, N., Tanaka, H., Nasu, M., Yoshioka, H., Shirabe, K., 2002. Identification and characterization of a soluble cadherin-7 isoform produced by alternative splicing. J. Biol. Chem. 277, 47679–47685.

Kido, M., Obata, S., Tanihara, H., Rochelle, J.M., Seldin, M.F., Taketani, S., Suzuki, S.T., 1998. Molecular properties and chromosomal location of cadherin-8. Genomics 48, 186–194.

Korematsu, K., Redies, C., 1997a. Cadherin-8 mRNA expression in the developing mouse central nervous system. J. Comp. Neurol. 387, 291–306.

Korematsu, K., Redies, C., 1997b. Restricted expression of cadherin-8 in segmental and functional subdivisions of the embryonic mouse brain. Dev. Dyn. 208, 178–189.

Korematsu, K., Nishi, T., Okamura, A., Goto, S., Morioka, M., Hamada, J., Ushio, Y., 1998. Cadherin-8 protein expression in gray matter structures and nerve fibers of the neonatal and adult mouse brain. Neuroscience 87, 303–315.

Kovjanic, D., Redies, C., 2003. Small-scale pattern formation in a cortical area of the embryonic chicken telecephalon. J. Comp. Neurol. 456, 95–104.

Kremmidiotis, G., Baker, E., Crawford, J., Eyre, H.J., Nahmias, J., Callen, D.F., 1998. Localization of human cadherin genes to chromosome regions exhibiting cancer-related loss of heterozygosity. Genomics 49, 467–471.

Luo, J., Wang, H., Lin, J., Redies, C., 2007. Cadherin expression in the developing chicken cochlea. Dev. Dyn. 236, 2331–2337.

Makarenkova, H., Sugiura, H., Yamagata, K., Owens, G., 2005. Alternatively spliced variants of protocadherin 8 exhibit distinct patterns of expression during mouse development. Biochim. Biophys. Acta 1681, 150–156.

Martin, J., Han, C., Gordon, L.A., Terry, A., Prabhakar, S., She, X., Xie, G., Hellsten, U., Chan, Y.M., Altherr, M., Couronne, O., Aerts, A., Bajorek, E., Black, S., Blumer, H., Branscomb, E., Brown, N.C., Bruno, W.J., Buckingham, J.M., Callen, D.F., Campbell, C.S., Campbell, M.L., Campbell, E.W., Caoile, C., Challacombe, J.F., Chasteen, L.A., Chertkov, O., Chi, H.C., Christensen, M., Clark, L.M., Cohn, J.D., Denys, M., Detter, J.C., Dickson, M., Dimitrijevic-Bussod, M., Escobar, J., Fawcett, J.J., Flowers, D., Fotopulos, D., Glavina, T., Gomez, M., Gonzales, E., Goodstein, D., Goodwin, L.A., Grady, D.L., Grigoriev, I., Groza, M., Hammon, N., Hawkins, T., Haydu, L., Hildebrand, C.E., Huang, W., Israni, S., Jett, J., Jewett, P.B., Kadner, K., Kimball, H., Kobayashi, A., Krawczyk, M.C., Leyba, T., Longmire, J.L., Lopez, F., Lou, Y., Lowry, S., Ludeman, T., Manohar, C.F., Mark, G.A., McMurray, K.L., Meincke, L.J., Morgan, J., Moyzis, R.K., Mundt, M.O., Munk, A.C., Nandkeshwar, R.D., Pitluck, S., Pollard, M., Predki, P., Parson-Quintana, B., Ramirez, L., Rash, S., Retterer, J., Ricke, D.O., Robinson, D.L., Rodriguez, A., Salamov, A., Saunders, E.H., Scott, D., Shough, T., Stallings, R.L., Stalvey, M., Sutherland, R.D., Tapia, R., Tesmer, J.G., Thayer, N., Thompson, L.S., Tice, H., Torney, D.C., Tran-Gyamfi, M., Tsai, M., Ulanovsky, L.E., Ustaszewska, A., Vo, N., White, P.S., Williams, A.L., Wills, P.L., Wu, J.R., Wu, K., Yang, J., Dejong, P., Bruce, D., Doggett, N.A., Deaven, L., Schmutz, J., Grimwood, J., Richardson, P., Rokhsar, D.S., Eichler, E.E., Gilna, P., Lucas, S.M., Myers, R.M., Rubin, E.M., Pennacchio, L.A., 2004. The sequence and analysis of duplication-rich human chromosome 16. Nature 432, 988–994.

Nagar, B., Overduin, M., Ikura, M., Rini, J.M., 1996. Structural basis of calcium-induced E-cadherin rigidification and dimerization. Nature 380, 360–364.

Nollet, F., Kools, P., van Roy, F., 2000. Phylogenetic analysis of the cadherin superfamily allows identification of six major

subfamilies besides several solitary members. J. Mol. Biol. 299, 551–572.
Paradies, N.E., Grunwald, G.B., 1993. Purification and characterization of NCAD90, a soluble endogenous form of N-cadherin, which is generated by proteolysis during retinal development and retains adhesive and neurite-promoting function. J. Neurosci. Res. 36, 33–45.
Pokutta, S., Weis, W.I., 2007. Structure and mechanism of cadherins and catenins in cell–cell contacts. Annu. Rev. Cell Dev. Biol. 23, 237–261.
Puelles, L., Martinez-de-la-Torre, M., Paxinos, G., Watson, C., Martinez, S., 2007. The chick brain in stereotaxic coordinates. An Atlas Featuring Neuromeric Subdivisions and Mammalian Homologies. Academic Press, San Diego.
Ranscht, B., Dours-Zimmermann, M.T., 1991. T-cadherin, a novel cadherin cell adhesion molecule in the nervous system, lacks the conserved cytoplasmic region. Neuron 7, 391–402.
Redies, C., 2000. Cadherins in the central nervous system. Prog. Neurobiol. 61, 611–648.
Redies, C., Takeichi, M., 1993. Expression of N-cadherin mRNA during development of the mouse brain. Dev. Dyn. 197, 26–39.
Redies, C., Ast, M., Nakagawa, S., Takeichi, M., Martínez-de-la-Torre, M., Puelles, L., 2000. Morphologic fate of diencephalic prosomeres and their subdivisions revealed by mapping cadherin expression. J. Comp. Neurol. 421, 481–514.
Redies, C., Medina, L., Puelles, L., 2001. Cadherin expression by embryonic divisions and derived gray matter structures in the telencephalon of the chicken. J. Comp. Neurol. 438, 253–285.
Sambrook, J., Russell, D.W., 2001. Molecular Cloning (third edition). Cold Spring Harbor Laboratory Press, New York.
Shapiro, L., Fannon, A.M., Kwong, P.D., Thompson, A., Lehmann, M.S., Grubel, G., Legrand, J.F., Als-Nielsen, J., Colman, D.R., Hendrickson, W.A., 1995. Structural basis of cell–cell adhesion by cadherins. Nature 374, 327–337.
Shimoyama, Y., Tsujimoto, G., Kitajima, M., Natori, M., 2000. Identification of three human type-II classic cadherins and frequent heterophilic interactions between different subclasses of type-II classic cadherins. Biochem. J. 349, 159–167.
Shirabe, K., Kimura, Y., Matsuo, N., Fukushima, M., Yoshioka, H., Tanaka, H., 2005. MN-cadherin and its novel variant are transiently expressed in chick embryo spinal cord. Biochem. Biophys. Res. Commun. 334, 108–116.
Sugimoto, K., Honda, S., Yamamoto, T., Ueki, T., Monden, M., Kaji, A., Matsumoto, K., Nakamura, T., 1996. Molecular cloning and characterization of a newly identified member of the cadherin family, PB-cadherin. J. Biol. Chem. 271, 11548–11556.
Suzuki, S.C., Furue, H., Koga, K., Jiang, N., Nohmi, M., Shimazaki, Y., Katoh-Fukui, Y., Yokoyama, M., Yoshimura, M., Takeichi, M., 2007. Cadherin-8 is required for the first relay synapses to receive functional inputs from primary sensory afferents for cold sensation. J. Neurosci. 27, 3466–3476.
Suzuki, S.C., Inoue, T., Kimura, Y., Tanaka, T., Takeichi, M., 1997. Neuronal circuits are subdivided by differential expression of type-II classic cadherins in postnatal mouse brains. Mol. Cell. Neurosci. 9, 433–447.
Takeichi, M., 1991. Cadherin cell adhesion receptors as a morphogenetic regulator. Science 251, 1451–1455.
Takeichi, M., 2007. The cadherin superfamily in neuronal connections and interactions. Nat. Rev., Neurosci. 8, 11–20.
Van Heusden, J., de Jong, P., Ramaekers, F., Bruwiere, H., Borgers, M., Smets, G., 1997. Fluorescein-labeled tyramide strongly enhances the detection of low bromodeoxyuridine incorporation levels. J. Histochem. Cytochem. 45, 315–319.
Vanhalst, K., Kools, P., Staes, K., van Roy, F., Redies, C., 2005. d-protocadherins: a gene family expressed differentially in the mouse brain. Cell. Mol. Life Sci. 62, 1247–1259.
Wakamatsu, N., King, D.J., Seal, B.S., Brown, C.C., 2007. Detection of Newcastle disease virus RNA by reverse transcription-polymerase chain reaction using formalin-fixed, paraffin-embedded tissue and comparison with immunohistochemistry and in situ hybridization. J. Vet. Diagn. Invest. 19, 396–400.

3.4

Differential expression of five members of the ADAM family in the developing chicken brain

Juntang Lin, Jiankai Luo, Christoph Redies

Neuroscience, accepted on 26 Aug 2008 (in press).

Pages 54-94

Letter for paper acceptance

Von: "Neuroscience, Editorial" neuroscience@journal-office.com
Datum: 26. August 2008 07:25:12 MESZ
An: redies@mti.uni-jena.de
Cc: gerfenc@mail.nih.gov
Betreff: Acceptance of NSC-08-875

Ms. No.: NSC-08-875
Title: Differential expression of five members of the ADAM family in the developing chicken brain

Dear Dr. Redies,

We are pleased to inform you that your manuscript referenced above has been accepted for publication in Neuroscience. We hope that the review has been a positive experience and that your manuscript has been improved by the process.

The misprints should be corrected in the proofs.

Many thanks for submitting your fine paper to Neuroscience. We look forward to receiving additional papers from your laboratory in the future.

Kind regards,

Dr. Ole Petter Ottersen
Chief Editor
Neuroscience

Dr. Charles R. Gerfen
Section Editor
Neuroscience

Differential expression of five members of the ADAM family in the developing chicken brain

Juntang Lin,[a] Jiankai Luo,[a,b] and Christoph Redies[a*]

[a] Institute of Anatomy I, Friedrich Schiller University Jena, Teichgraben 7, D-07743 Jena, Germany

[b] Albrecht-Kossel-Institute for Neuroregeneration, Centre for Mental Health Disease, University of Rostock, Gehlsheimerstrasse 20, D-18147 Rostock, Germany

*Corresponding author:
Christoph Redies, Institute of Anatomy I, Friedrich Schiller University of Jena, Teichgraben 7, D-07743 Jena, Germany. Tel: +49-3641-938511, Fax: +49-3641-938512, E-mail: redies@mti.uni-jena.de

Section Editor: Dr. Charles R. Gerfen

Abbreviations: ADAM, a disintegrin and metalloprotease; E, embryonic day; EGF, epidermal growth factor; Galc, galactocerebroside; HBSS, Hepes-buffered salt solution; ORF, open reading frame; PBS, phosphate-buffered saline; RACE, rapid amplification of cDNA ends; RT-PCR, reverse transcriptase-polymerase chain reaction; TBS, Tris-buffered saline; Thio, thionine.

Abbreviations used in the figures[1]

3	oculomotor nucleus
3n	oculomotor nerve
3v	third ventricle
4	trochlear nucleus
4v	fourth ventricle
6C	abducens nucleus, caudal part
10	dorsal motor nucleus of the vagus nerve
AA	anterior amygdaloid area
ac	anterior commissure
ACo	amygdala, core nucleus
AHi	amygdalohippocampal area
Ang	angular cochlear nucleus
APT	anterior pretectal nucleus
aq	mesencephalic aqueduct
ATn	amygdaloid taenial nucleus
BCS	brachium of the superior colliculus
Bv	blood vessel
Cb	cerebellum
cc	central canal
CDL	caudodorsolateral pallium (*dorsolateral corticoid area*)
chp	choroid plexus
csm	corticoseptomesencephalic tract
DA	dorsal anterior nuclei of thalamus
Di	diencephalon
DLG	dorsal lateral geniculate nucleus (*lateroanterior nucleus*)
DP	dorsal posterior nuclei of thalamus
DR	dorsal raphe nucleus
draq	dorsal recess of the mesencephalic aqueduct
EA	extended amygdala
EGL	external granular layer
ET	epithalamus

EW	Edinger-Westphal nucleus
Fl	flocculus
fp	floor plate
GP	globus pallidus (*paleostriatum primitivum*)
Gr	granule cell layer of the cerebellum
HA	apical hyperpallium
Hb	habenula
HBr	hindbrain
Hi	hippocampus
HPO	hypothalamic periventricular organ
HT	hypothalamus
InP	intrapeduncular nucleus (*central part of striatopallidal area*)
IO	inferior olivary nucleus
IPC	interpeduncular nucleus, caudal subnucleus
IsO	isthmooptic nucleus
IsPC	isthmic parvicellular nucleus
Lat	lateral cerebellar nucleus
LP	lateral pallium
lr4v	lateral recess of fourth ventricle
lraq	lateral recess of the mesencephalic aqueduct
LS	lateral septal nucleus
lv	lateral ventricle
LVe	lateral vestibular nucleus
M	mesopallium
MCC	magnocellular cochlear nucleus
MCPI	magnocellular preisthmic nucleus
Me5	mesencephalic trigeminal nucleus
mes	mesenchyme
MG	medial geniculate nucleus (*nucleus ovoidalis*)
MJC	medial juxtacommissural nucleus of the pretectum
ML	molecular layer
mlf	medial longitudinal fasciculus
MnR	median raphe cells

MP	medial pallium
mr	median raphe
MS	medial septal nucleus
MSO	medial superior olivary nucleus (*laminaris nucleus*)
MT	medial terminal nucleus (*nucleus of the basal optic root*)
MV	mesopallium, ventral part
MVe	medial vestibular nucleus
NC	nidopallium, caudal part
NCcp	nidopallium, caudal part, corticoid plate
NCIF	nidopallium, caudal part, island field
NCL	nidopallium, caudal part, lateral region
ne	neuroepithelium
NF	frontal nidopallium
NICe	nidopallium, intermediate part, central region
NIS	nidopallium, intermediate part, superficial region
opt	optic tract
p1	prosomere 1 (pretectum)
p1Tg	prosomere 1 tegmentum
p2	prosomere 2 (thalamus)
p3	prosomere 3 (prethalamus)
pc	posterior commissure
Pal	pallidum
PalV	ventral pallidum
Pe	periventricular stratum
PG	pregeniculate nucleus (*ventral geniculate nucleus*)
PHi	parahippocampal area
PHiI	parahippocampal area, intermediate part
PHiM	parahippocampal area, medial part
Pi	pineal gland
Pk	Purkinje cell layer of the cerebellum
PO	preoptic nucleus
Pr5	principal sensory trigeminal nucleus
PrPT	principal pretectal nucleus

psp	pallial-subpallial boundary
r	raphe
RG	retrogeniculate nucleus (*retroovoidal nucleus*)
ro	roof
Rot	rotundus nucleus
Rt	reticular nucleus
SAC	stratum album centrale of the tectum
SCO	subcommissural organ
Se	septum
SGC	stratum griseum centrale of the tectum
SGFS	stratum griseum et fibrosum superficiale of the tectum
SLu	semilunar nucleus
sm	stria medullaris
SMi	superficial microcellular nucleus of the thalamus
SP	subpallium
SpL	lateral spiriform nucleus
SpM	medial spiriform nucleus
SpVe	spinal vestibular nucleus
SRot	subrotundus nucleus of the thalamus
SSp	supraspinal nucleus
St	striatum
StAm	strioamygdaloid transition area
STh	subthalamic nucleus
StPal	striopallidal area
SubG	subgeniculate nucleus (*ventrolateral nucleus*)
SuVe	superior vestibular nucleus
Tect	optic tectum
Tel	telencephalon
TGS	tectal gray, superficial stratum
ToSc	torus semicircularis, central part
ToSpe	torus semicircularis, periventricular part
VisCo	visual nidopallial nucleus, core region
VMH	ventralmedial hypothalamic nucleus

VP	ventral pallium
vpl	ventral pallial lamina
xc	cochlear decussation
xs	supraoptic decussation

[1] Alternative (traditional) terms are given in italic type.

Abstract

ADAMs (a disintegrin and metalloprotease) are a family of trans-membrane multi-domain metalloproteases with multiple functions. So far, more than 35 ADAM family members have been identified from mammalian and nonmammalian sources. Although some functions of ADAMs have been elucidated, their expression patterns remain poorly investigated, especially during CNS development. Here, we cloned the open reading frames or full-length cDNAs of ADAM9, ADAM10, ADAM12, ADAM22 and ADAM23 from chicken embryonic brain, analyzed their evolutionary relationship, and mapped their expression in the embryonic chicken brain by in situ hybridization for the first time. In general, each of the five ADAMs shows a spatially restricted and temporally regulated expression profile. However, the types of tissues and cells, which express each of the five ADAMs, differ from each other. ADAM9 is predominantly expressed in the choroid plexus and in the ventricular layer. ADAM10 is expressed by developing blood vessels, oligodendrocytes, and subsets of neurons and brain nuclei. ADAM12 is expressed by very few brain nuclei, cerebellar Purkinje cells, restricted regions of the neuroepithelium, and some neurons in the deep tectal layers. ADAM22 expression is strong in some brain nuclei and in the pineal gland. ADAM23 is expressed by most gray matter regions and the choroid plexus. The differential expression patterns suggest that the five ADAMs play multiple and versatile roles during brain development.

Key words: in situ hybridization, blood vessel, pineal gland, choroid plexus, neuroepithelium, oligodendrocytes.

Members of the ADAM (a disintegrin and a metalloprotease) family are type I transmembrane proteins. Another acronym for this protein family is MDC, which denotes their metalloproteinase-disintegrin-cysteine-rich domains (Wolfsberg et al., 1995; Black and White, 1998; Schlondorff and Blobel, 1999). ADAMs possess a multi-domain structure with a signal peptide, a prodomain, a metalloprotease domain, a disintegrin domain, a cysteine-rich domain, an epidermal growth factor (EGF)-like domain, a transmembrane domain and a cytoplasmic tail. The disintegrin domain can bind integrins or other receptors (Lu et al., 2007). The metalloprotease domain contains a consensus active-site sequence for a zinc-dependent metalloprotease; some ADAMs have been shown to be catalytically functional. In relation to these multiple domains, ADAMs were proposed to be involved in proteolysis, adhesion, cell fusion and cell signaling (Blobel, 2002, 2005; White, 2003). Specific biological processes, in which ADAMs have been implicated, include sperm-egg fusion, somatic cell-cell adhesion, cell-matrix interaction, ectodomain shedding, myoblast fusion, and neurogenesis (Seals and Courtneidge, 2003). Moreover, some ADAMs have been implicated in the control of membrane fusion, cytokine and cytokine receptor shedding, growth factor and their receptor processing, and cell migration, as well as in processes such as muscle development, fertilization, and cell fate determination (Huovila et al., 1996; Seals and Courtneidge, 2003). Up-regulation or inhibition of expression of specific ADAMs has been associated with a number of diseases, including inflammation, asthma, arthritis, atherosclerosis and cancer (Wolfsberg et al., 1995; Duffy et al., 2003; Moss and Bartsch, 2004).

The existence of ADAM genes has been confirmed in many animal species, including mammals, reptiles and invertebrates, but ADAMs have not been found in lower organisms like *Escherichia coli* and *Saccharomyces cerevisiae* or in plants (Seals and Courtneidge, 2003). So far, more than 35 ADAMs have been cloned from different species. For a short description of each member, consult the Cytokines & Cells Online Pathfinder Encyclopaedia website (COPE, http://www.copewithcytokines.de/cope.cgi?Key=ADAM%20protein%20family).

Individual members of the ADAM family show variable expression patterns that are developmentally regulated. Some ADAMs are expressed in highly restricted patterns in specific tissues and organs, whereas others are expressed more widely.

In the nervous system, ADAMs play a role in cell proliferation, migration, differentiation, apoptosis, myelination and axon guidance, as well as in some nervous diseases, such as Alzheimer’s disease and inflammatory responses (Novak, 2004; Yang et

al., 2006). For example, ADAM10 plays an important role in neurogenesis and axon extension; it is required for the formation of the optic projection to the tectum (Chen et al., 2007). ADAM10 was demonstrated to cleave axon guidance molecules like ephrin and cadherins (Janes et al., 2005; Maretzky et al., 2005, 2008; Reiss et al., 2005, 2006; Schulz et al., 2008).

Not much is known about the expression profiles of ADAMs in the CNS. Kärkkäinen et al. (2000) identified ten ADAM mRNAs and showed strikingly different expression profiles of six ADAM mRNAs in the major parts of the adult mouse brain by Northern analysis. Similar results were obtained for ADAM22 and ADAM23 in the human brain (Sagane et al., 1998). In situ hybridization with probes for ADAM10 and ADAM17 showed regional expression of these molecules in different regions of the adult brain (Kärkkäinen et al., 2000). However, the spatial and temporal expression patterns of ADAMs during vertebrate brain development remain unknown.

In the present study, we cloned the full-length or open reading frame (ORF) sequences of three novel members of the ADAM family from the chicken (ADAM12, ADAM22 and ADAM23) and investigated the spatiotemporal expression patterns of these and two other ADAMs (ADAM9 and ADAM10) in the embryonic chicken brain in detail. Our results reveal a spatially restricted and temporally regulated expression pattern for all five ADAMs. The general type of structures that express the individual ADAMs are, however, rather different. The results from the present study provide a basis for the investigation of possible functions of ADAMs in brain development.

Experimental procedures

Animals

Fertilized eggs of White Leghorn chicken (*Gallus gallus domesticus*) were purchased from a local farm and incubated in a forced-draft incubator (Ehret, Emmendingen, Germany) at 37°C and 65% humidity. Embryos were studied at embryonic day 6 (E6), E8, E10, E12, E14, E16, E18, and E19 (at least 3 embryos for each stage). Embryos were removed from the eggs after induction of deep anesthesia by cooling on ice. The brain was dissected carefully and fixed in formaldehyde solution (4% in Hepes-buffered salt solution; HBSS) on ice for 6 to 24 hours, depending on the stage. Older embryos (E14, E16, E18 and E19) were prefixed with 4% formaldehyde solution by intracardial perfusion. After fixation, the brains were immersed in graded sucrose solutions (12%, 15% and 18% in HBSS).

Specimens were embedded in TissueTec O.C.T. compound (Science Services, München, Germany), frozen in liquid nitrogen and stored at -80°C, as described previously (Lin et al., 2008).

RNA extraction and cDNA cloning

Total RNA from whole E12 brain was prepared using the TRIzol reagent, according to the manufacturer's instruction (Invitrogen, Karlsruhe, Germany). First-strand cDNA was synthesized in vitro using the SuperScript First-Strand Synthesis System (Invitrogen) with E12 brain total RNA. The ORF of ADAM9, ADAM10 and ADAM23 were cloned by RT-PCR. The full-length sequences of chicken ADAM12 and ADAM22 were cloned using the SMART RACE cDNA Amplification Kit (Takara Bio Europe/Clontech, Saint-Germain-en-Laye, France) and confirmed by sequencing (to be submitted to Genbank). Based on to the RACE results, the ORFs of ADAM12 and ADAM22 were cloned by One Step RT-PCR Kit (Qiagen, Hilden, Germany). The RT-PCR reaction was performed first at 50°C for 30 min for reverse transcription and at 95°C for 15 min for denaturation, followed by 30 cycles of amplification. The primers and PCR parameters are shown in Table 1. Finally, all of the obtained sequences were cloned into pCR-II vector (Invitrogen) and sequenced by a commercial company (MWG-Biotech AG, Ebersberg, Germany) with M13 forward, reverse and specific internal primers. The obtained sequences were compared to those of other published ADAM genes and were blasted against the chicken genome with the NCBI BLAST program (http://www.ncbi.nlm.nih.gov/BLAST). The nucleotide similarities and evolutionary relationships of the different ADAMs were analyzed using the Lasergene MegAlign program (DNASTAR, Madison, WI).

Probe synthesis and in situ hybridization

Digoxigenin-labeled sense and antisense cRNA probes were transcribed in vitro from the purified pCR-II plasmids containing the ORF of the different ADAMs, according to the manufacturer's instructions for probe synthesis (Roche, Mannheim, Germany). Sense cRNA probes were used as a negative control for in situ hybridization. Probes were purified by sodium acetate or LiCl/EtOH precipitation and by using Quick Spin Columns (Roche). Incorporation of label and correct size was verified by RNA formaldehyde denaturing gel electrophoresis, blotting, and detection of membrane-bound probes using alkaline phosphatase-conjugated anti-digoxigenin Fab fragments (Roche).

In situ hybridization on cryosection was performed according to Redies et al. (1993). In brief, cryostat sections of 20 µm thickness were fixed with 4% formaldehyde in PBS and pretreated with proteinase K and acetic anhydride. Sections were hybridized overnight with cRNA probe at a concentration of about 3 ng/µl at 70°C in hybridization solution (50% formamide, 3× SSC, 10mM EDTA, 10% dextran sulfate, 1× Denhardt's solution, 42 µg/ml yeast transfer RNA and 42 µg/ml salmon sperm DNA). After the sections were washed and the unbound cRNA was removed by RNase, the sections were incubated with alkaline phosphatase-coupled anti-digoxigenin Fab fragments (Roche) at 4°C overnight. For visualization of the labeled mRNA, a substrate solution of nitroblue tetrazolium salt and 5-bromo-4-chloro-3-indoyl phosphate was added.

Immunohistochemistry

In selected cases, sections adjacent to those used for in situ hybridization were processed for galactocerebroside (Galc) immunohistochemistry following the immunostaining protocol by Redies et al. (1993). In brief, the sections were fixed in ice-cold 4% formaldehyde in HBSS for 20 min and washed in Tris-buffered saline (TBS, pH 7.4) supplemented with 1 mM $CaCl_2$ and 1 mM $MgCl_2$. Endogenous peroxidase activity was suppressed by incubation with 0.3% H_2O_2 in methanol for 30 min. Unspecific binding of antibodies was blocked by incubating the sections with 5% skim milk powder in TBS for 30 min. A mouse monoclonal antibody against galactocerebroside (hybridoma supernatant; kind gift of B. Ranscht; Ranscht et al., 1982) was appropriately diluted in blocking solution (1:2). Sections were incubated with this solution at 4°C overnight. Three washing steps in TBS were followed by incubation of the sections with biotinylated goat anti-mouse secondary antibody (Jackson ImmunoResearch, Cambridgeshire, UK) for 30 min at RT. The sections were then incubated with avidin-biotin-horseradish peroxidase complex (ABC Kit, Vector Laboratories, Burlingame, CA, USA) and reacted with 0.03% 3,3´-diaminobenzidine, 0.04% $NiCl_2$ and 0.01% H_2O_2 as a substrate, according to the manufacturer's instructions.

Image analysis

For neuroanatomic orientation, sections adjacent to those used for in situ hybridization and immonohistochemistry were stained with thionine acetate for Nissl substance (Redies et al., 1993). All sections were viewed and photographed under a transmission light microscope (Olympus BX40, Hamburg, Germany) equipped with a digital camera

(Olympus DP70). Photomicrographs were adjusted in contrast and brightness by the Photoshop software (Adobe, Mountain View, CA) for optimal display of the staining patterns in the figures. For identification of neuroanatomical structures, the atlas by Puelles et al. (2007) was followed.

Results

Cloning and phylogenetic analysis of the five ADAM cDNAs from chicken

Based on the published sequences of chicken ADAM9 and ADAM10, and the predicted sequence of chicken ADAM23, we cloned their ORF by RT-PCR. For ADAM12 and ADAM22, the full-length sequences were obtained by the RACE method. The accession numbers of the sequences will be/were submitted to GenBank and are listed in Table 1.

The analysis of the evolutionary relationship amongst all eight known chicken ADAMs indicates a relatively high similarity for ADAM22 and ADAM23, and for ADAM9 and ADAM12, respectively, whereas ADAM10 and ADAM17 are more distant from the other ADAMs (Fig. 1).

Expression patterns in the embryonic brain

In general, each of the ADAMs investigated shows a spatially restricted and temporally regulated expression pattern. Strikingly, the type of tissues, cell types and the neuroanatomical structures, which express individual ADAMs, differ from each other (Table 2). Expression patterns are shown in Fig. 2 (ADAM9), Figs. 3 and 4 (ADAM10), Fig. 5 (ADAM12), Fig. 6 (ADAM22) and Fig. 7 (ADAM23). In the figures, the panels are arranged according to their developmental stage (early to late). For a negative control, sense RNA probes were used (Figs. 2L, 3P). With few exceptions, the nomenclature of Puelles at al. (2007) was used. Alternative (traditional) terms are given in the list of abbreviations used in the figures.

ADAM9

At E6 and E8, ADAM9 is expressed in the ventricular (neuroepithelial) layer (ne) of several brain regions, for example, in the hindbrain, the medial part of the tectal vesicle, the diencephalon (Di in Fig. 2A), the telencephalon and the roof (ro) of the third ventricle (3v in Fig. 2A). In addition, at E8, ADAM9 transcript is found in the ependymal layer of the primordial choroid plexus (chp) in the lateral ventricles (lv in Fig. 2B). Some blood

vessels express ADAM9 weakly. In the diencephalon and mesencephalon, expression in the ventricular layer is weak and more widespread at E8 than at E6.

At E10, expression is strong in the ependymal layer (ne), the hindbrain floor plate (fp) and the mesencephalic roof (ro in Fig. 2C). In addition, weak homogeneous staining is seen in the hindbrain (HBr) and cerebellar gray matter (Cb in Fig. 2D). The accessory oculomotor nucleus of Edinger-Westphal (EW in Fig. 2C) shows moderate staining. Expression by the mantle layer of the mid- and forebrain remains very weak. Moderate staining of blood vessel (Bv in Fig. 2E) is observed throughout the brain.

From E12 to E16, very strong expression in the choroid plexus (chp) of all ventricles predominates (Fig. 2F). Weak expression in almost all gray matter regions and moderate expression in blood vessels persists (Fig. 2G,H). In the diencephalon, the rotundus nucleus (Rot), the anterior pretectal nucleus (APT), and the dorsal anterior nuclear complex (DA) show moderate expression (Fig. 2H). In the mesencephalon and isthmic region (Fig. 2G), the magnocellular preisthmic nucleus (MCPI), the isthmic parvicellular nucleus (IsPC), the semilunar nucleus (SLu), the tectal gray matter (TGS in Fig. 2H) and the tectum (Tect) are also moderately positive.

At the prehatching stage (E19), the expression in the choroid plexus and the regionalized expression in the ependymal lining are weaker than at earlier stages. Blood vessels are no longer positive. Gray matter expression is also weaker and more heterogeneous. Purkinje cells (Pk) show relatively strong expression throughout the cerebellum (Fig. 2K). The supraspinal nucleus (SSp), the dorsal complex of the vagal nerve (10 in Fig. 2M,N), neurons of the hindbrain reticular formation, the lateral vestibular nucleus (LVe in Fig. 2I,J), and the nucleus rotundus show slightly stronger signal than surrounding gray matter.

ADAM10

At E6 and E8, the ventricular (neuroepithelial) layer (ne) of all parts of the brain is strongly positive, for example in the tectum (Fig. 3A,D,E), in the diencephalon (Fig. 3B) and in the hindbrain (Fig. 3C). The mantle layer shows weak to moderate signal; in some areas, for example in the dorsal thalamus (p2 in Fig. 3D), expression is stronger than in other regions. In the blood vessels throughout the mantle layer, ADAM10 expression is especially prominent (arrows in Fig. 3C,E). The choroid plexus (chp in Fig. 3D) also expresses ADAM10. At E10 and E12, strong ADAM10 expression by blood vessels

persists (arrows in Figs. 3G-K); this expression decreases at later stages and is no longer detectable in brain at E19.

At E12, most gray matter areas exhibit widespread and weak ADAM10 expression throughout the brain. Signal in some regions, however, increases to high levels from E8 to E14. In the diencephalon, mesencephalon and isthmic region, strongly positive structures at E12 include the anterior and posterior dorsal thalamic complex (DA in Fig. 3G; DP in Fig. 3H), the medial geniculate (ovoidal) nucleus (MG in Fig. 3H), the principal pretectal nucleus (PrPT in Fig. 3I), the intergeniculate leaflet (not shown), the lateral spiriform nucleus (SpL in Fig. 3I), the hypothalamic periventricular organ (HPO in Fig. 3H; at E14 in Fig. 3O,P), the ventromedial hypothalamic nucleus (VMH in Fig. 3H), the central core and central shell parts of the midbrain auditory torus (ToS in Fig. 3J), the isthmic parvicellular nucleus (IsPC in Fig. 3J), the magnocellular preisthmic nucleus (MCPI in Fig. 3J), and the semilunar nucleus (SLu in Fig. 3J). In the tectum, most cells in the stratum griseum centrale (SGC), the periventricular stratum (Pe) and the neuroepithelial stratum (ne) contain strongly positive cells, whereas cells in the stratum griseum et fibrosum superficiale (SGFS) are only weakly positive (Fig. 3K,L).

In the telencephalon at E14 (Fig. 3M,N), all structures express ADAM10, but at different levels ranging from weak to strong staining. The structures that are most strongly positive include the apical hyperpallium (HA), the intermediate parahippocampal area (PHiI), superficial parts of the mesopallium (M), and most of the nidopallium (NF, NICe, NIS, NCIF, NCL, NC) and the amygdala. In the subpallium, signal is weak in the globus pallidus (GP) to moderate in the striatum (St). A ventral and a dorsal subregion of the lateral septum (LS) express ADAM10 strongly.

Staining decreases from E14 to E19, with the exception of the telencephalon and the cerebellum. In the cerebellum, ADAM10 is expressed strongly by the Purkinje cell (Pk) layer and weakly by in the internal and external granule cell layer (EGL; E14 in Fig. 3Q,R).

At late stages of embryogenesis (E16-E19), numerous small ADAM10-positive cells are found in fiber tracts. For example at E16, ADAM10-positive cells that co-express galactocerebroside (Galc), a marker for oligodendrocytes (Ranscht et al., 1982), are observed around the auditory nuclei (MCC, magnocellular cochlear nucleus; MSO, medial superior olivary nucleus [nucleus laminaris]; Fig. 4A-C) and in the auditory projections that cross the midline (xc). Other structures that contain similar ADAM10-positive cells include the root of the oculomotor nerve (3n in Fig. 4D,E), the brachium of the superior

colliculus (BCS in Fig. 4F) and the medial longitudinal fasciculus (mlf in Fig. 4G-I). Finally, the pineal gland (Pi) expresses ADAM10 at E18 (Fig. 4J,K).

ADAM12

At E6 and E8, ADAM12 signal in the telencephalon is restricted to a few weakly labeled cells in the mantle layer of the medial pallium (MP in Fig. 5A). Regional expression in the ventricular layer is observed in the mesencephalic vesicle (Tect), except for the caudal regions, in the pretectum (p1) and in the epithalamus (ET in Fig. 5B). The dorsal thalamus (p2) contains ADAM12-positive cells in the mantle layer. There are also some dispersed ADAM12-positive cells in the mantle layer of the pretectum (arrow in Fig. 5B).

At E10, the mesencephalic ventricular layer is still positive (Fig. 5C). In addition, dispersed cells are seen in the deeper strata of the developing tectal mantle layer (arrows in Fig. 5C). The ependymal lining of the aqueduct (aq), including its dorsal recess (draq), expresses ADAM12 strongly, but the subcommissural organ (SCO) is negative (Fig. 5D). In the isthmus, the parvicellular nucleus expresses ADAM12 strongly (IsPC in Fig. 5C), but none of the other isthmic nuclei is positive. In the cerebellum (Fig. 5E), clusters of Purkinje cells (Pk) express ADAM12 in the flocculus (Fl). Also, the midline granule cell raphe (mr) and some cells in the external granular layer are positive in the vermal region (Fig. 5E). In the hindbrain, all parts of the floor plate (fp) and the median raphe cells (MnR) express ADAM12 (Fig. 5F).

In the E12 telencephalon, the visual core region of the nidopallial nucleus expresses ADAM12 (VisCo in Fig. 5G). ADAM12-positive cells are also found in the periventricular stratum (Pe) of the medial pallium (MP in Fig. 5G). In the dorsal thalamus, the superficial microcellular nucleus (SMi in Fig. 5I), the dorsal anterior nuclear complex (DA in Fig. 5I), the medial geniculate (ovoidal) nucleus (MG in Fig. 5J), the perirotundic area, and the intergeniculate leaflet are positive (not shown). More caudally, in the pretectum, the medial terminal nucleus expressed ADAM12 (MT in Fig. 5K). In the tectum, there are a few dispersed ADAM12-positive cells in the stratum griseum centrale (SGC in Fig. 5M). In their large size and deep position within SGC, these cells resemble the magnocellular SGC neurons described by Martinez-de-la-Torre et al. (1987). The isthmic parvicellular nucleus remains strongly positive (Fig. 5L).

At E14 and E16, the expression of ADAM12 is similar to E12. Strong staining is still seen in the tectum, the parvicellular isthmic nucleus, and the core nucleus of the nidopallium. Expression in the other structures has decreased. In the cerebellum, the

innermost (premigratory) sheet of the external granular layer (EGL) is positive, as well as almost the entire Purkinje cell (Pk) layer, except for a few small gaps (arrowheads in Fig. 5N). At E16, ADAM12 is expressed in the dorsal (motor) nucleus of the vagus nerve (10 in Fig. 5O). The floor plate is still positive (fp in Fig. 5O).

At E19, the staining observed at E16 persists. In addition, very small ADAM12-positive cells are seen almost everywhere. These cells are especially numerous in fiber tracts, for example in the brachium of the superior colliculus (BCS in Fig. 5P). The distribution and size of these cells is reminiscent of oligodendrocytes, which have been shown to express ADAM12 in the human and rat (Bernstein et al., 2004). Cerebellar Purkinje cells are now ubiquitously positive (not shown).

ADAM22

At E6, ADAM22 is expressed by the mesenchyme surrounding the brain (mes in Fig. 6A). In the brain, the neuroepithelial layer (ne) is negative except for some weak staining in the pretectal and basal mesencephalic region. The mantle layer shows diffuse and weak to moderate staining in some areas, for example, in the diencephalon (p2, p3 in Fig. 6A).

Expression at E8 is similar to that at E6, but the ventricular signal has become stronger in some areas, for example, in the mesencephalon and some diencephalic regions. The tectal midline (arrowhead in Fig. 6B), the neuroepithelium of the epithalamus (ET) and the roof of the third ventricle (3v) show very strong ADAM22 signal (Fig. 6B).

From E10 onwards, staining in gray matter is heterogeneous. Many gray matter structures express relatively high levels of ADAM22 while others are negative or show low signal. The expression patterns are relatively stable between E10 and E19. In the following paragraphs, expression patterns will be described for the fore- and midbrain at E10-E14 (Fig. 6C-J) and for the hindbrain at E16-E19 (Fig. 6K-P).

Telencephalic structures that express high levels of ADAM22 include superficial layers of the hippocampus (Hi in Fig. 6F), the medial parahippocampal area (PHiM in Fig. 6G), the caudodorsolateral pallium (CDL in Fig. 6F), the visual nidopallium, the anterior amygdaloid area (AA in Fig. 6F), the amygdaloid subnuclei surrounding the core nucleus of the amygdala (ACo in Fig. 6G), the amygdalohippocampal area (AHi in Fig. 6G), the amygdaloid taenial nucleus (ATn in Fig. 6G), the extended amygdala (EA in Fig. 6F), the lateral septum (LS in Fig. 6C), the medial septal nucleus (MS in Fig. 6G), the striatum (St in Fig. 6C,F), the intrapeduncular nucleus (InP in Fig. 6C) and the striopallidal area (StPal in Fig. 6C). In the diencephalon (Fig. 6I), the following nuclei show especially strong

ADAM22 expression: the superficial microcellular nucleus, the anterior dorsal thalamic complex, the posterior dorsal thalamic complex (DP), the reticular nucleus, the rotundus nucleus (Rot), the subrotundic nucleus (SRot), the perigeniculate nucleus (PG), and the anterior pretectal area (APT). The pineal gland (Pi), but not the choroid plexus (chp), expresses ADAM22 strongly (Fig. 6H).

In the mesencephalon, the mesencephalic nucleus of the trigeminal nerve (Me5 in Fig. 6D), the prosomere 1 tegmentum (p1Tg in Fig. 6D) and the trochlear nucleus (4 in Fig. 6E) are positive. In the tectum (Fig. 6J), the vast majority of cells in the stratum griseum centrale (SGC), a few cells in the stratum album centrale (SAC), and the neuroepithelial layer (ne) express ADAM22.

In the cerebellum, clusters of Purkinje cells (Pk) express ADAM22 at E14 and E16 while granule cells show weak expression (Fig. 6K). At E19, both Purkinje cells and granule cells express ADAM22 relatively strongly and ubiquitously (not shown). The deep cerebellar nuclei also express ADAM22, for example the lateral cerebellar nucleus (Lat in Fig. 6N).

Heterogenous expression of ADAM22 is also observed in the late embryonic hindbrain. In the isthmic region, the semilunar nucleus (SLu in Fig. 6E,L) expresses very high levels of ADAM22 throughout development. Other strongly positive hindbrain structures include the isthmooptic nucleus (IsO in Fig. 6L), the raphe nuclei (R in Fig. 6L), the reticular formation (Rt in Fig. 6L,M,O,P), the magnocellular cochlear nucleus (MCC in Fig. 6M), the medial superior olivary (laminar) nucleus (MSO in Fig. 6M), the lateral cerebellar nucleus (Lat in Fig. 6N), the lateral vestibular nucleus (LVe in Fig. 6N), the medial vestibular nucleus (MVe in Fig. 6O), and the inferior olivary nucleus (IO in Fig. 6P).

ADAM23

At E6, almost the entire mantle layer shows moderate signal, with some minor regional variations in staining intensity (Fig. 7A). The ventricular layer is stained weakly, if at all. The roof plate of the third ventricle is positive (ro in Fig. 7A).

At E8, staining of the mantle layer persists throughout the brain. There is also regional expression of ADAM23 in the periventricular layer of the lateral ventricles (Pe in Fig. 7B,C). The choroid plexus of the lateral ventricles shows strong staining (chp in Fig. 7B), but that of the third ventricle is stained weakly or not at all. The pineal gland is negative throughout development (Table 2).

At E10, the labeling of the mantle layer structures is still heterogeneous, but very widespread. Some nuclei are more strongly labeled than others (for example, see the gray matter of the mesencephalon and hindbrain in Fig. 7D,E). In the tectum, only the deep layers are positive (Tect in Fig. 7D).

From E12 to E19, the gray matter retains its heterogeneous and widespread expression (Fig. 7F-P). The most strongly labeled gray matter structures include, in the telencephalon, the hippocampus (Hi in Fig. 7H,N), the parahippocampal area (PHi in Fig. 7F,H), the strioamygdaloid transition area (StAM in Fig. 7F), the ventral mesopallium (MV in Fig. 7H), the caudal nidopallium, the amygdaloid complex, the amygdalohippocampal area, parts of the striatum (St in Fig. 7F,H,N), dispersed cells in the globus pallidus (GP in Fig. 7H,N), and the lateral septum (LS in Fig. 7F,H,N). The choroid plexus of the lateral ventricle (chp in Fig. 7F,H) remains positive, with regional variations in signal intensity. The lateral ventricle (lv) is bordered ventrally by an ADAM23-positive ependymal surface, but not dorsally (Fig. 7F,H). In the prethalamus of the diencephalon (Fig. 7G), strongly ADAM23-positive nuclei include the subgeniculate nucleus (SubG) and the pregeniculate nucleus (PG). In the thalamus (Fig. 7G,I,L), the dorsal anterior nuclear complex (DA), the dorsal lateral geniculate nucleus (DLG), the rotundus nucleus (Rot), the subrotundic nucleus (SRot), the medial geniculate nucleus, the retrogeniculate nucleus (RG) express ADAM23 strongly. In the pretectum, the medial juxtacommissural nucleus (MJC in Fig. 7L) and the medial spiriform nucleus (SpM in Fig. 7I) are strongly ADAM23 positive.

In the mesencephalon, the oculomotor complex (3 in Fig. 7J; see also 3 and EW in Fig. 7D for E10) and the trochlear nucleus (4 in Fig. 7J) exhibit strong signal. In the torus semicircularis (inferior colliculus), the periventricular part (ToSpe) is more strongly stained than the core part (ToSc), as already seen at E10 (Fig. 7D). The neurons of the mesencephalic nucleus of the trigeminal nerve (Me5 in Fig. 7L) express ADAM23 very strongly. In the deep layers of the tectum (SAC and SGC in Fig. 7M), most neurons show strong signal. In the superficial layers (SGFS), only a few cells are positive. The magnocellular preisthmic nucleus is more strongly positive than the isthmic nuclei.

The Purkinje cells of the cerebellum (Pk in Fig. 7P) express ADAM23 strongly and homogeneously while the expression in the internal granular layer (Gr) is weaker. All of the deep cerebellar nuclei exhibit very strong signal.

In the hindbrain, most nuclei are weakly to moderately positive. The nuclei that express high levels of ADAM23 mRNA include the magnocellular cochlear nucleus (MCC

in Fig. 7J,O), which shows a prominent gradient from low levels caudolaterally to high levels rostromedially (insert in Fig. 7O). The other cochlear nuclei (MSO and Ang in Fig. 7O), the vestibular nuclei (MVe, LVe, SuVe in Fig. 7J,O) and the principal sensory trigeminal nucleus (Pr5 in Fig. 7J) show moderate signal. More caudally, strongly positive nuclei include the motor nucleus of the trigeminal nerve, the nucleus of the lateral lemniscus and the motor nucleus of the vagal complex (data not shown). The entire hindbrain reticular formation (Rt in Fig. 7O), in particular in the gigantocellular neurons, show prominent signal.

Discussion

Although the function of some members of the ADAM family is well studied (see below), their expression pattern during vertebrate brain development is poorly understood. For the chicken embryo, only a few studies on the expression or function of ADAMs have been published. The chicken is an excellent animal model to study embryonic development. The complete sequencing of the chicken genome and the availability of the in vivo electroporation technique for genetic manipulation (Muramatsu et al., 1997; Luo and Redies, 2005) have enhanced the usefulness of the chicken embryo in developmental biology. Hall and Erickson (2003) reported that chicken ADAM10 is expressed in epithelial tissues and plays a role in their morphogenesis. The expression of ADAM13 in the chicken embryo was shown to be temporally and spatially regulated in different organs and tissues (Lin et al., 2007). ADAM17, a main proteolytic protease during embryonic development, was implicated in the non-amyloidogenic processing of beta-amyloid precursor protein in the chicken (Carrodeguas et al., 2005). Watabe-Uchida et al. (2004) reported that ADAM35 (also called meltrin-ε) is expressed in epithelial tissues during chicken embryogenesis. From the work in chicken and other species, it has become clear that ADAMs have diverse functions in many developmental processes, like cell adhesion, neurogenesis, axon guidance, protein shedding, signal transduction etc. (Seals and Courtneidge, 2003; Blobel, 2005). In order to propose and test the functional roles of ADAMs in brain development, it is necessary to know the precise expression patterns of these genes. We therefore cloned five ADAMs (ADAM9, ADAM10, ADAM12, ADAM22 and ADAM23) and analyzed their expression during chicken embryonic brain development for the first time. ADAM9, ADAM10 and ADAM12 have metalloprotease activity, whereas ADAM22 and ADAM23 do not. Our results show that the expression

patterns of the ADAMs are strikingly different, both at the level of brain regions (Figs. 2-7) and neural cell types (Table 2).

ADAM9

ADAM9 can mediate cell adhesion through binding to integrin α6β1 by the disintegrin domain (Nath et al., 2000). ADAM9 has been shown to cleave the insulin B-chain, pro-TNF-alpha, gelatin, beta-casein, fibronectin and APP (Roghani et al., 1999; Schwettmann and Tschesche, 2001; Asai et al., 2003). It appears that other members of the ADAM family may functionally replace ADAM9 because knock-out mice develop into fertile adults without major abnormalities (Weskamp et al., 2002). In the chicken embryo, ADAM9 is expressed by blood vessels, the choroid plexus, by parts of the neuroepithelium and in regions of differentiating gray matter, suggesting that ADAM9 plays multiple unknown roles during brain development.

ADAM10

ADAM10, named *Kuzbanian* in Drosophila (Rooke et al., 1996) is essential to embryonic development and controls neurogenesis and axon extension in the CNS (Fambrough et al., 1996; Pan and Rubin, 1997; Chen et al., 2007). ADAM10-deficient mice developed only to E9.5 with multiple defects in the CNS, somites and cardiovascular system (Hartmann et al., 2002). Also, ADAM10 has been confirmed as a candidate alpha-secretase responsible for shedding proteins as diverse as APP, heparin-binding EGF (HB-EGF), EGF receptor, E-cadherin, N-cadherin, protocadherin C3 and VE-cadherin (Yan et al., 2002; Sahin et al., 2004; Maretzky et al., 2005, 2008; Reiss et al., 2005, 2006; Schulz et al., 2008). Our results show that ADAM10 is mainly expressed by developing blood vessels as well as in restricted neuroepithelial regions and in differentiating gray matter. The latter finding suggests that the proposed role of ADAM10 in axon elongation (Chen et al., 2007) is confined to specific brain regions and/or fiber tracts. In this context, our novel finding that ADAM10 is also expressed by oligodendrocytes at later embryonic stages in many fiber tracts is of interest. Whether ADAM10-positive neurites and oligodendrocytes interact remains to be investigated. In neuroepithelial cells, growing blood vessels and during neurogenesis, ADAM10 may regulate cell differentiation, as proposed previously for other systems (Pan and Rubin, 1997).

ADAM12

ADAM12, also called meltrin-α, is a member of meltrin subfamily of ADAMs (Inoue et al., 1998). It can mediate cell adhesion by binding to integrin α9β1 (Eto et al., 2000). As an active metalloprotease, the potential physiological substrates of ADAM12 include insulin-like growth factor binding proteins IGFBP-3 and -5, placental leucine aminopeptidase (P-LAP), heparin binding EGF-like growth factor (HB-EGF), EGF, β-cellulin and S-carboxymethylated transferrin (Jacobsen et al., 2008). Although ADAM12 appears to play a role in myoblast fusion in embryonic development (Galliano et al., 2000), ADAM12-deficient mice, which are viable and fertile, have only minor muscular abnormalities (Kurisaki et al., 2003). ADAM12 is overexpressed in several human tumors such as breast carcinoma, colon carcinoma and gastric carcinoma (Iba et al., 1999) and is required for mouse prostate tumor progression (Peduto et al., 2006). Interestingly, ADAM12 is a marker of trisomy 18 in the first and second trimester of pregnancy (Spencer and Cowans, 2007). In quail, ADAM12 was reported to be expressed in dorsal root ganglia and the ventral spinal roots (Lewis et al., 2004). In the human and rat, ADAM12 is expressed by oligodendrocytes (Bernstein et al., 2004). The present study maps the expression of ADAM12 in the vertebrate brain for the first time. ADAM12 is expressed in restricted regions of the neuroepithelium, suggesting a role in brain regionalization. Especially striking is the highly restricted expression in very few gray matter structures. These structures belong to different functional systems, for example, to the visual system (visual nidopallial nucleus, tectum, isthmic parvicellular nucleus and medial terminal nucleus), the auditory system (medial geniculate nucleus), the cerebellar system (Purkinje cells) and the visceral nervous system (nucleus of the vagus nerve). It will be interesting to study what common role, if any, ADAM12 plays in these restricted gray matter regions.

ADAM22 and ADAM23

ADAM22 and ADAM23, which are closely related phylogenetically (Fig. 1), are uncatalytical members of the ADAM family. Their gene symbol and alternative names are MDC2 and MDC3, respectively (Sagane et al., 1998). Some of the binding partners of the two ADAMs are known. For example, the 14-3-3ζ protein can interact with the cytoplasmic domain of ADAM22; this interaction is required for cell spreading and cell adherence (Zhu et al., 2005). ADAM22 also serves as a receptor for LGI1 that regulates synaptic transmission (Fukata et al., 2006).

ADAM22-deficient mice show signs of severe ataxia and peripheral nerve hypomyelination (Sagane et al., 2005), whereas ADAM23-deficient mice show tremor and severe ataxia and die within two weeks of birth (Leighton et al., 2001). These neurological defects indicate that the two ADAMs are important for normal development and function of the nervous system (Yang et al., 2006). ADAM23 is expressed primarily as a cell-surface protein that appears to be localized to sites of intercellular contact where it serves to mediate cell-cell interactions. ADAM23 also regulates neuronal differentiation within the mammalian CNS (Goldsmith et al., 2004; Sun et al., 2007).

Both molecules are highly expressed in the human brain, as revealed by Northern blotting (Sagane et al., 1998). Novak (2004) mentioned unpublished observations that ADAM22 is expressed in Purkinje cells of the cerebellum and neurons of the neocortex. The present study reveals the complex expression patterns of the two ADAMs in developing brain for the first time. Both ADAMs are expressed in restricted regions of the neuroepithelium. In all major parts of brain, brain nuclei and layers with large differences in their ADAM expression are found adjacent to each other. The expression patterns of the two ADAMs in the neuroepithelium and gray matter differ from each other, but overlap partially. In some brain structures, for example, the pineal gland and the choroid plexus, the expression profile of the two ADAMs is opposite (Table 2). These results suggest that the two ADAMs, despite their closely homologous nucleotide sequence, play distinct roles in different brain structures. Interestingly, the magnocellular cochlear nucleus displays a rostromedial-to-caudolateral gradient of expression (Fig. 7O) that may relate to the tonotopic gradient found in this nucleus (Rubel and Parks, 1975).

In summary, the five ADAMs investigated in the present study differ in their regional expression in developing brain areas, both in the neuroepithelial domains and in gray matter. These results suggest that ADAMs, like many transcription factors and adhesion molecules, play a role in brain regionalization (for reviews, see Redies and Puelles, 2001; Puelles and Rubenstein, 2003). In addition, we confirm previous results by other groups (for reviews, see Novak, 2004; Yang et al., 2006) that the five ADAMs are expressed differentially by specific types of tissues and cells in the developing brain, like blood vessels, oligodendrocytes, pineal cells, floor plate ependymal cells and neurons (Table 2). Together, these results indicate multiple and diverse roles for each ADAM in brain development. The present results may provide the basis for studying these roles at the experimental level in the future.

Acknowledgements

We thank Dr. Cornelius Lemke for perfusion of older stage embryos and Ms. Jessica Heyder and Sylvia Hänßgen for their expert technical assistance. This work was supported by institute funds and a grant from the Deutsche Forschungsgemeinschaft (Lu 1455/1-1).

References

Asai M, Hattori C, Szabó B, Sasagawa N, Maruyama K, Tanuma S, Ishiura S (2003) Putative function of ADAM9, ADAM10, and ADAM17 as APP alpha-secretase. Biochem Biophys Res Commun 301:231-235.

Bernstein HG, Keilhoff G, Bukowska A, Ziegeler A, Funke S, Dobrowolny H, Kanakis D, Bogerts B, Lendeckel U (2004) ADAM (a disintegrin and metalloprotease) 12 is expressed in rat and human brain and localized to oligodendrocytes. J Neurosci Res 75:353-360.

Black RA, White JM (1998) ADAMs: focus on the protease domain. Curr Opin Cell Biol 10:654-659.

Blobel CP (2002) Functional and biochemical characterization of ADAMs and their predicted role in protein ectodomain shedding. Inflamm Res 51:83-84.

Blobel CP (2005) ADAMs: key components in EGFR signalling and development. Nat Rev Mol Cell Biol 6:32-43.

Carrodeguas JA, Rodolosse A, Garza MV, Sanz-Clemente A, Pérez-Pé R, Lacosta AM, Domínguez L, Monleón I, Sánchez-Díaz R, Sorribas V, Sarasa M (2005) The chick embryo appears as a natural model for research in beta-amyloid precursor protein processing. Neuroscience 134:1285-1300.

Chen YY, Hehr CL, Atkinson-Leadbeater K, Hocking JC, McFarlane S (2007) Targeting of retinal axons requires the metalloproteinase ADAM10. J Neurosci 27:8448-8456.

Duffy MJ, Lynn DJ, Lloyd AT, O'Shea CM (2003) The ADAMs family of proteins: from basic studies to potential clinical applications. Thromb Haemost 89:622–631.

Eto K, Puzon-McLaughlin W, Sheppard D, Sehara-Fujisawa A, Zhang XP, Takada Y (2000) RGD-independent binding of integrin alpha9beta1 to the ADAM-12 and -15 disintegrin domains mediates cell-cell interaction. J Biol Chem 275:34922-34930.

Fambrough D, Pan D, Rubin GM, Goodman CS (1996) The cell surface metalloprotease/ disintegrin Kuzbanian is required for axonal extension in Drosophila. Proc Natl Acad Sci USA 93:13233-13238.

Fukata Y, Adesnik H, Iwanaga T, Bredt DS, Nicoll RA, Fukata M (2006) Epilepsy-related ligand/receptor complex LGI1 and ADAM22 regulate synaptic transmission. Science 313:1792-1795.

Galliano MF, Huet C, Frygelius J, Polgren A, Wewer UM, Engvall E (2000) Binding of ADAM12, a marker of skeletal muscle regeneration, to the muscle-specific actin-

Binding protein, alpha -actinin-2, is required for myoblast fusion. J Biol Chem 275:13933-13939.

Goldsmith AP, Gossage SJ, ffrench-Constant C (2004) ADAM23 is a cell-surface glycoprotein expressed by central nervous system neurons. J Neurosci Res 78:647-658.

Hall RJ, Erickson CA (2003) ADAM 10: an active metalloprotease expressed during avian epithelial morphogenesis. Dev Biol 256:146-159.

Hartmann D, de Strooper B, Serneels L, Craessaerts K, Herreman A, Annaert W, Umans L, Lübke T, Lena Illert A, von Figura K, Saftig P (2002) The disintegrin/ metalloprotease ADAM 10 is essential for Notch signalling but not for alpha-secretase activity in fibroblasts. Hum Mol Genet 11:2615-2624.

Huovila AP, Almeida EA, White JM (1996) ADAMs and cell fusion. Curr Opin Cell Biol 8:692-699.

Iba K, Albrechtsen R, Gilpin BJ, Loechel F, Wewer UM (1999) Cysteine-rich domain of human ADAM 12 (meltrin alpha) supports tumor cell adhesion. Am J Pathol 154:1489-1501.

Inoue D, Reid M, Lum L, Krätzschmar J, Weskamp G, Myung YM, Baron R, Blobel CP (1998) Cloning and initial characterization of mouse meltrin beta and analysis of the expression of four metalloprotease-disintegrins in bone cells. J Biol Chem 273:4180-4187.

Jacobsen J, Visse R, Sørensen HP, Enghild JJ, Brew K, Wewer UM, Nagase H (2008) Catalytic properties of ADAM12 and its domain deletion mutants. Biochemistry 47:537-547.

Janes PW, Saha N, Barton WA, Kolev MV, Wimmer-Kleikamp SH, Nievergall E, Blobel CP, Himanen JP, Lackmann M, Nikolov DB (2005) Adam meets Eph: an ADAM substrate recognition module acts as a molecular switch for ephrin cleavage in trans. Cell 123:291-304.

Kärkkäinen I, Rybnikova E, Pelto-Huikko M, Huovila AP (2000) Metalloprotease-disintegrin (ADAM) genes are widely and differentially expressed in the adult CNS. Mol Cell Neurosci 15:547-560.

Kurisaki T, Masuda A, Sudo K, Sakagami J, Higashiyama S, Matsuda Y, Nagabukuro A, Tsuji A, Nabeshima Y, Asano M, Iwakura Y, Sehara-Fujisawa A (2003) Phenotypic analysis of Meltrin alpha (ADAM12)-deficient mice: involvement of Meltrin alpha in adipogenesis and myogenesis. Mol Cell Biol 23:55-61.

Leighton PA, Mitchell KJ, Goodrich LV, Lu X, Pinson K, Scherz P, Skarnes WC, Tessier-

Lavigne M (2001) Defining brain wiring patterns and mechanisms through gene trapping in mice. Nature 410:174-179.

Lewis SL, Farlie PG, Newgreen DF (2004) Isolation and embryonic expression of avian ADAM 12 and ADAM 19. Gene Expr Patterns 5:75-79.

Lin J, Luo J, Redies C (2008) Molecular cloning and expression analysis of three cadherin-8 isoforms in the embryonic chicken brain. Brain Res 1201:1-14.

Lin J, Redies C, Luo J (2007) Regionalized expression of ADAM13 during chicken embryonic development. Dev Dyn 236:862-870.

Lu X, Lu D, Scully MF, Kakkar VV (2007) Structure-activity relationship studies on ADAM protein-integrin interactions. Cardiovasc Hematol Agents Med Chem 5:29-42.

Luo J, Redies C (2005) Ex ovo electroporation for gene transfer into older chicken embryos. Dev Dyn 233:1470-1477.

Maretzky T, Reiss K, Ludwig A, Buchholz J, Scholz F, Proksch E, de Strooper B, Hartmann D, Saftig P (2005) ADAM10 mediates E-cadherin shedding and regulates epithelial cell-cell adhesion, migration, and beta-catenin translocation. Proc Natl Acad Sci USA 102:9182-9187.

Maretzky T, Scholz F, Köten B, Proksch E, Saftig P, Reiss K (2008) ADAM10-mediated E-cadherin release is regulated by proinflammatory cytokines and modulates keratinocyte cohesion in eczematous dermatitis. J Invest Dermatol 128:1737-1746.

Martinez-de-la-Torre M, Martinez S, Puelles L (1987) Solitary magnocellular neurons in the avian optic tectum: cytoarchitectonic, histochemical and [3H]thymidine autoradiographic characterization. Neurosci Lett 74:31-36.

Moss ML, Bartsch JW (2004) Therapeutic benefits from targeting of ADAM family members. Biochemistry 43:7227-7235.

Muramatsu T, Mizutani Y, Ohmori Y, Okumura J (1997) Comparison of three nonviral transfection methods for foreign gene expression in early chicken embryos in ovo. Biochem Biophys Res Commun 230:376-380.

Nath D, Slocombe PM, Webster A, Stephens PE, Docherty AJ, Murphy G (2000) Meltrin gamma (ADAM-9) mediates cellular adhesion through alpha(6)beta(1)integrin, leading to a marked induction of fibroblast cell motility. J Cell Sci 113:2319-2328.

Novak U (2004) ADAM proteins in the brain. J Clin Neurosci 11:227-235.

Pan D, Rubin GM (1997) Kuzbanian controls proteolytic processing of Notch and mediates lateral inhibition during Drosophila and vertebrate neurogenesis. Cell 90:271-280.

Peduto L, Reuter VE, Sehara-Fujisawa A, Shaffer DR, Scher HI, Blobel CP (2006) ADAM12 is highly expressed in carcinoma-associated stroma and is required for mouse prostate tumor progression. Oncogene 25:5462-5466.

Puelles L, Martinez-de-la-Torre M, Paxinos G, Watson C, Martinez S (2007) The chick brain in stereotaxic coordinates. An atlas featuring neuromeric subdivisions and mammalian homologies. San Diego, Academic Press.

Puelles L, Rubenstein JL (2003) Forebrain gene expression domains and the evolving prosomeric model. Trends Neurosci 26:469-476.

Ranscht B, Clapshaw PA, Price J, Noble M, Seifert W (1982) Development of oligodendrocytes and Schwann cells studied with a monoclonal antibody against galactocerebroside. Proc Natl Acad Sci USA 79:2709-2713.

Redies C, Engelhart K, Takeichi M (1993) Differential expression of N- and R-cadherin in functional neuronal systems and other structures of the developing chicken brain. J Comp Neurol 333:398-416.

Redies C, Puelles L (2001) Modularity in vertebrate brain development and evolution. Bioessays 23:1100-1111.

Reiss K, Maretzky T, Ludwig A, Tousseyn T, de Strooper B, Hartmann D, Saftig P (2005) ADAM10 cleavage of N-cadherin and regulation of cell-cell adhesion and beta-catenin nuclear signalling. EMBO J 24:742-752.

Reiss K, Maretzky T, Haas IG, Schulte M, Ludwig A, Frank M, Saftig P (2006) Regulated ADAM10-dependent ectodomain shedding of gamma-protocadherin C3 modulates cell-cell adhesion. J Biol Chem 281:21735-21744.

Roghani M, Becherer JD, Moss ML, Atherton RE, Erdjument-Bromage H, Arribas J, Blackburn RK, Weskamp G, Tempst P, Blobel CP (1999) Metalloprotease-disintegrin MDC9: intracellular maturation and catalytic activity. J Biol Chem 274:3531-3540.

Rooke J, Pan D, Xu T, Rubin GM (1996) KUZ, a conserved metalloprotease-disintegrin protein with two roles in Drosophila neurogenesis. Science 273:1227-1231.

Rubel EW, Parks TN (1975) Organization and development of brain stem auditory nuclei of the chicken: tonotopic organization of n. magnocellularis and n. laminaris. J Comp Neurol 164:411-433.

Sagane K, Hayakawa K, Kai J, Hirohashi T, Takahashi E, Miyamoto N, Ino M, Oki T, Yamazaki K, Nagasu T (2005) Ataxia and peripheral nerve hypomyelination in ADAM22-deficient mice. BMC Neurosci 6:33.

Sagane K, Ohya Y, Hasegawa Y, Tanaka I (1998) Metalloproteinase-like, disintegrin-like,

cysteine-rich proteins MDC2 and MDC3: novel human cellular disintegrins highly expressed in the brain. Biochem J 334:93-98.

Sahin U, Weskamp G, Kelly K, Zhou HM, Higashiyama S, Peschon J, Hartmann D, Saftig P, Blobel CP (2004) Distinct roles for ADAM10 and ADAM17 in ectodomain shedding of six EGFR ligands. J Cell Biol 164:769-779.

Schlöndorff J, Blobel CP (1999) Metalloprotease-disintegrins: modular proteins capable of promoting cell-cell interactions and triggering signals by protein-ectodomain shedding. J Cell Sci 112:3603-3617.

Schulz B, Pruessmeyer J, Maretzky T, Ludwig A, Blobel CP, Saftig P, Reiss K (2008) ADAM10 regulates endothelial permeability and T-cell transmigration by proteolysis of vascular endothelial cadherin. Circ Res 102:1192-1201.

Schwettmann L and Tschesche H (2001) Cloning and expression in Pichia pastoris of metalloprotease domain of ADAM 9 catalytically active against fibronectin. Protein Expr Purif 21:65-70.

Seals DF, Courtneidge SA (2003) The ADAMs family of metalloproteases: multidomain proteins with multiple functions. Genes Dev 17:7-30.

Spencer K, Cowans NJ (2007) ADAM12 as a marker of trisomy 18 in the first and second trimester of pregnancy. J Matern Fetal Neonatal Med 20:645-650.

Sun Y, Wang Y, Zhang J, Tao J, Wang C, Jing N, Wu C, Deng K, Qiao S (2007) ADAM23 plays multiple roles in neuronal differentiation of P19 embryonal carcinoma cells. Neurochem Res 32:1217-1223.

Watabe-Uchida M, Masuda A, Shimada N, Endo M, Shimamura K, Yasuda K, Sehara-Fujisawa A (2004) Novel metalloprotease-disintegrin, meltrin epsilon (ADAM35), expressed in epithelial tissues during chick embryogenesis. Dev Dyn 230:557-568.

Weskamp G, Cai H, Brodie TA, Higashyama S, Manova K, Ludwig T, Blobel CP (2002) Mice lacking the metalloprotease-disintegrin MDC9 (ADAM9) have no evident major abnormalities during development or adult life. Mol Cell Biol 22:1537-1544.

White JM (2003) ADAMs: modulators of cell-cell and cell-matrix interactions. Curr Opin Cell Biol 15:598-606.

Wolfsberg TG, Straight PD, Gerena RL, Huovila AP, Primakoff P, Myles DG, White JM (1995) ADAM, a widely distributed and developmentally regulated gene family encoding membrane proteins with a disintegrin and metalloprotease domain. Dev Biol 169:378-383.

Yan Y, Shirakabe K, Werb Z (2002) The metalloprotease Kuzbanian (ADAM10) mediates the transactivation of EGF receptor by G protein-coupled receptors. J Cell Biol 158:221-226.

Yang P, Baker KA, Hagg T (2006) The ADAMs family: coordinators of nervous system development, plasticity and repair. Prog Neurobiol 79:73-94.

Zhu P, Sang Y, Xu H, Zhao J, Xu R, Sun Y, Xu T, Wang X, Chen L, Feng H, Li C, Zhao S (2005) ADAM22 plays an important role in cell adhesion and spreading with the assistance of 14-3-3. Biochem Biophys Res Commun 331:938-946.

Legends

Figure 1. Evolutionary relationships among the eight known chicken ADAMs, based on multiple nucleotide sequence alignment of their ORFs. The length of each pair of branches represents the distance between sequence pairs, while the units at the bottom of the figure indicate the number of substitution events.

Figure 2. ADAM9 expression in the chicken brain at embryonic day (E) 8 (**A,B**), E10 (**C-E**), E14 (**F-H**) and E19 (**I-N**). In situ hybridization results are shown for frontal sections, except for **G** that shows a horizontal section. **A**, diencephalon (Di); **B**, choroid plexus (chp) in the lateral ventricle (lv); **C**, midbrain; **D**, cerebellum (Cb) and hindbrain (HBr); **E,** higher magnification of the boxed area in D to show an ADAM9-positive blood vessel (Bv); **F**, pineal gland (Pi) and choroid plexus (chp) in the third ventricle (3v); **G**, tectum (Tect) and isthmic region; **H**, dorsal thalamus; **I**, lateral vestibular nucleus (LVe) in hindbrain; **J**, thionine staining of a section adjacent to **I**; **K**, cerebellar cortex with ADAM9-positive Purkinje cells (Pk); **L**, negative control (sense probe); **M**, vagal motor complex (10) and supraspinal nucleus (SSp) in the hindbrain; **N,** thionine staining of a section adjacent to **M**. For other abbreviations, see separate list. Scale bars, 100µm (in E), 200µm (in A-C,F,I-N), and 500µm (in D,G,H).

Figure 3. ADAM10 expression in the chicken brain at embryonic day (E) 6 (**A-C**), E8 (**D-F**), E12 (**G-L**) and E14 (**M-R**). In situ hybridization results are shown for frontal sections, except for **D**, **J** and **N** that show horizontal sections. **A**, neuroepithelium (ne) of the tectum; **B**, dorsal thalamus; **C**, hindbrain; **D**, telencephalon (Tel), dorsal thalamus (p2) and tectum; **E**, tectum; **F**, thionine staining of a section adjacent to **E**; **G-I**, sections through the diencephalon in a rostral-to-caudal series; **J**, mesencephalon; **K**, tectum; **L**, thionine staining of a section adjacent to **K**; **M**, frontal section through the telencephalon; **N**, horizontal section through the telencephalon; **O**, periventricular organ of the hypothalamus (HPO); **P**, negative control (sense probe); **Q**, granule cell raphe (r) and Purkinje cells (Pk) in cerebellum; **R**, thionine staining of a section adjacent to **Q**. For other abbreviations, see separate list. Arrows point at blood vessels. Scale bars, 100µm (in A-C,E,F,K,L,O-R), and 500µm (in all other panels).

Figure 4. ADAM10 expression (**A,D,F,H,J**), immunostaining results for galactocerebroside (Galc, a marker for oligodendrocytes; **B,I**), and thionine stains (**C,E,G,K**) in frontal sections through the chicken brain at embryonic day (E) 16 (**A-C**), E18 (**D,E,J,K**) and E19 (**F-I**). **A-C**, medial superior olivary (laminaris) nucleus in the hindbrain (adjacent sections); **D,E,** oculomotor nerve (3n) in the mesencephalon; **F**, brachium of the superior colliculus (BCS) in the tectum; **G-I**, medial longitudinal fasciculus (mlf) in the hindbrain; **J,K**, pineal gland (Pi). A-C, D/E, G-I and J/K represent adjacent sections, respectively. For other abbreviations, see separate list. Scale bars, 100µm (in D,E), and 200µm (in all other panels).

Figure 5. ADAM12 expression in the chicken brain at embryonic day (E) 8 (**A,B**), E10 (**C-F**), E12 (**G-M**), E16 (**N,O**) and E19 (**P,Q**). In situ hybridization results are shown for frontal sections, except for **A**, **B**, **G**, **H, K** and **L** that show horizontal sections. **A**, telencephalon (Tel); **B**, telencephalon, thalamus and tectum (Tect); **C**, tectum; **D**, mesencephalon; **E**, cerebellum and hindbrain; **F**, floor plate (fp) and median raphe nucleus (MnR); **G**, visual nidopallial nucleus, core region (VisCo) of the telencephalon; **H**, thionine staining of a section adjacent to **G**; **I**, dorsal thalamus; **J**, diencephalon at the level of the medial geniculate nucleus (MG); **K**, medial terminal nucleus (MT) in the mesencephalon; **L**, isthmic parvicellular nucleus (IsPC); **M**, tectum; **N**, Purkinje cells (Pk) in the cerebellum (Cb); **O,** dorsal motor nucleus of the vagus nerve (10); **P**, isthmic parvicellular nucleus (IsPC) and brachium of the superior colliculus (BCS); **Q**, thionine staining of a section adjacent to **P**. Arrows in **B** and **C** indicate the periventricular stratum (Pe). For other abbreviations, see separate list. Scale bars, 200µm (in A,D,F,I-Q), and 500µm (in all other panels).

Figure 6. ADAM22 expression in the chicken brain at embryonic day (E) 6 (**A**), E8 (**B**), E10 (**C**), E12 (**D,E**), E14 (**F-J**), E16 (**K**) and E19 (**L-P**). In situ hybridization results are shown for frontal sections, except for **B** that shows a horizontal section. **A**, diencephalon; **B**, telencephalon and tectum (arrowhead indicates the tectal midline); **C**, telencephalon; **D**, tegmentum of prosomere 1 (p1Tg) and hypothalamus (HT); **E**, isthmic region and rostral hindbrain; **F**, telencephalon (rostral section); **G**, telencephalon (caudal section); **H**, pineal gland (Pi) and choroid plexus (chp); **I**, tectum and diencephalon; **J**, tectum; **K**, Purkinje cells (Pk) in cerebellum; **L**, hindbrain; **M**, magnocellular cochlear nucleus (MCC) and medial superior olivary nucleus (MSO) in the hindbrain; **N**, deep cerebellar and vestibular

nuclei; **O**, hindbrain (rostral section); **P**, hindbrain (caudal section). For other abbreviations, see separate list. Scale bars, 200µm (in A,H,J,K), and 500µm (in all other panels).

Figure 7. ADAM23 expression in the chicken brain at embryonic day (E) 6 (**A**), E8 (**B,C**), E10 (**D,E**), E12 (**F,G**), E14 (**H-L**), E16 (**M**) and E19 (**N-P**). In situ hybridization results are shown for frontal sections, except for **J** and **K** that show horizontal sections. **A**, diencephalon; **B**, choroid plexus (chp) in the forebrain; **C**, periventricular stratum (Pe) of the telencephalon; **D**, tectum (Tect) and mesencephalic tegmentum; **E**, cerebellum and hindbrain; **F**, telencephalon; **G**, dorsal thalamus; **H**, telencephalon; **I**, diencephalon; **J**, hindbrain; **K**, thionine staining of a section adjacent to **J**; **L**, diencephalon; **M**, tectum; **N**, telencephalon; **O**, cerebellum (Cb) and hindbrain; the insert shows the ADAM23 expression gradient in the magnocellular cochlear nucleus (MCC); **P**, Purkinje cells (Pk) in cerebellum. For other abbreviations, see separate list. Scale bars, 200µm (in B,C,M,P), and 500µm (in all other panels).

Table 1. Primers and parameters for PCR and GenBank accession numbers for chicken ADAM9, ADAM10, ADAM12, ADAM22 and ADAM23.

Name	Primer	PCR parameter	GenBank accession No.
ADAM9	5'- atg gct cgg gcg gcg cgg a -3'	30 sec at 94°C, 30 sec at 60°C,	NM_001031396
	5'- cta taa gga gtg gta gga cca -3'	3 min at 68°C	
ADAM10	5'- atg gat cta gcg agg acg at -3'	30 sec at 94°C, 30 sec at 58°C,	AY077631
	5'- tca atg tct cat atg tcc ca -3'	3 min at 68°C	
ADAM12	5'- atg tca aag cgt ctc ctt gcg -3'	45 sec at 94°C, 45 sec at 58°C,	FJ188468
	5'- atc att tca cat cag cag tag c -3'	2.5 min at 72°C	
ADAM22	5'- atg aat gct aca tca cag aag ttt g -3'	45 sec at 94°C, 45 sec at 60°C,	FJ188469
	5'- gca gaa cag cct tgt cac gtc c -3'	2.5 min at 72°C	
ADAM23	5'- atg ccg cag aaa gac tac aa -3'	30 sec at 94°C, 30 sec at 55°C,	FJ188470
	5'- tta ctt aaa gcc cca tcc tg -3'	2.5 min at 68°C	

Table 2. Comparison of the expression of ADAM9, ADAM10, ADAM12, ADAM22 and ADAM23 in tissues and cell types of the embryonic chicken brain*

	ADAM9	ADAM10	ADAM12	ADAM22	ADAM23
Blood vessels	++[1]	+++[1]	-	-	-
Oligodendrocytes	-	++[2]	+[2]	-	-
Pineal gland	+	+	-	+++	-
Choroid plexus	+++	+[3]	+[3]	-	+++[3]
Neuroepithelium	+++[3]	++	++[3]	++[3]	+[3]
Gray matter[3]	++	++	-	++	++
Floor plate	++	+	+++	-	-

* -, negative, +, weakly positive; ++, moderately positive; +++, strongly positive. The table lists the highest expression levels observed.

[1] negative at older stages

[2] positive from E16 to E19

[3] regional expression

Figure 1. Evolutionary relationships among the eight known chicken ADAMs, based on multiple nucleotide sequence alignment of their ORFs

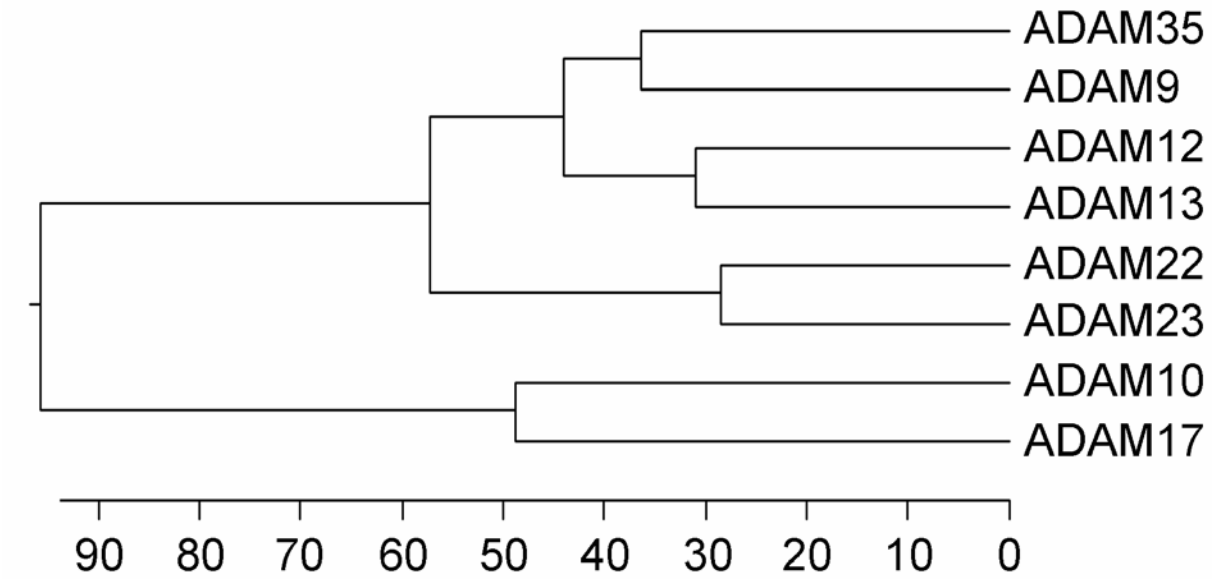

Figure 2. ADAM9 expression

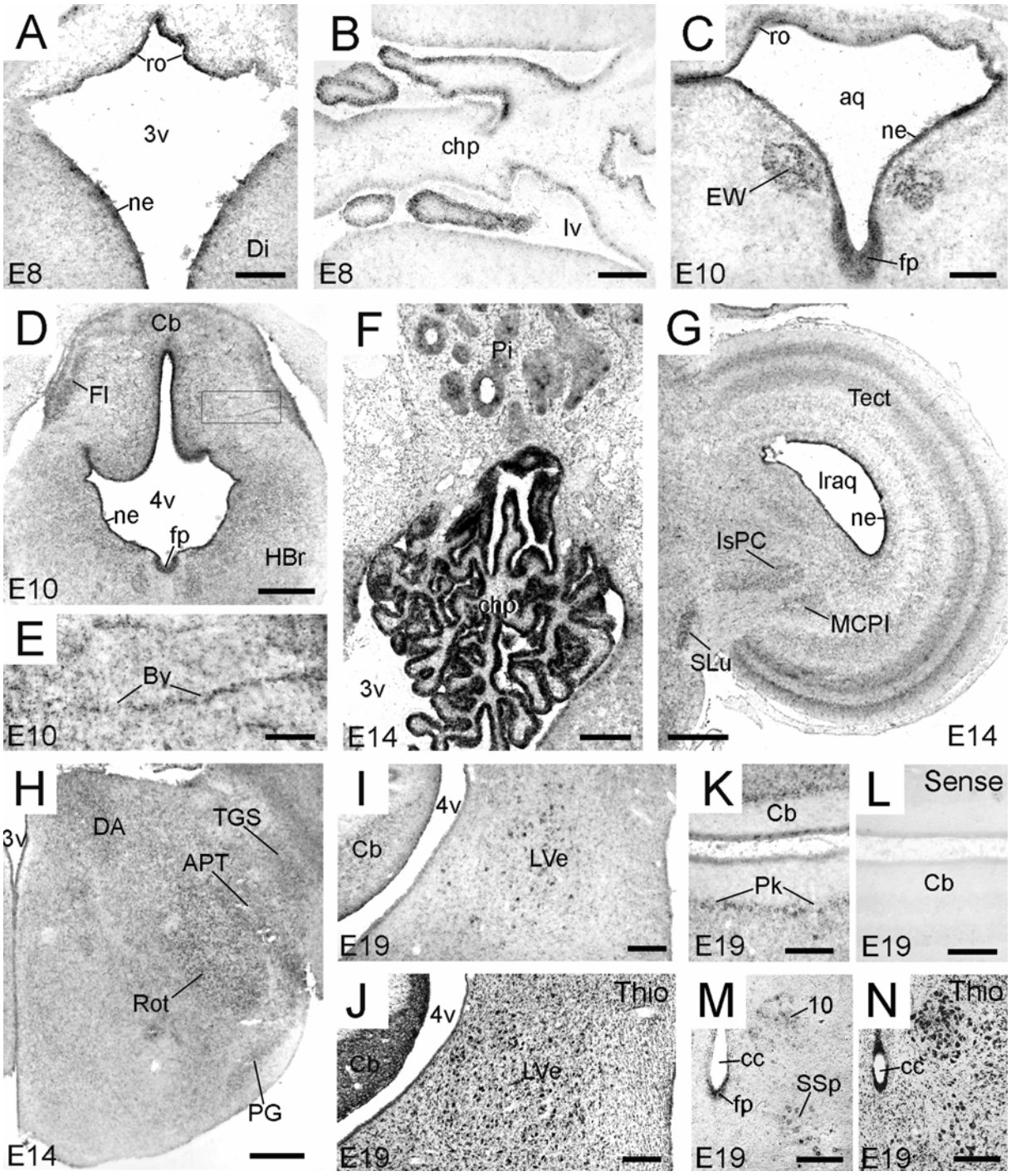

Figure 3. ADAM10 expression (1)

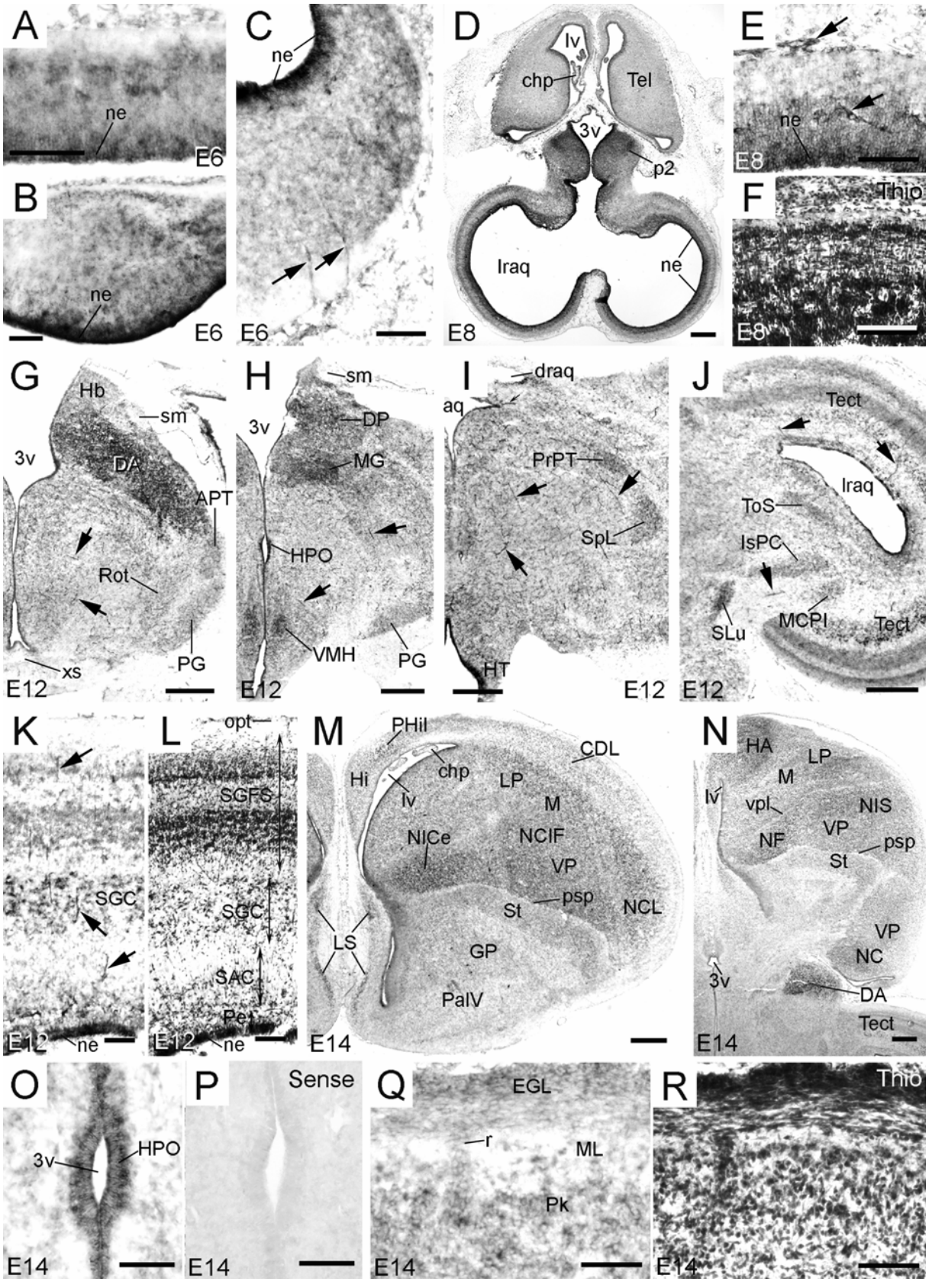

Figure 4. ADAM10 expression (2)

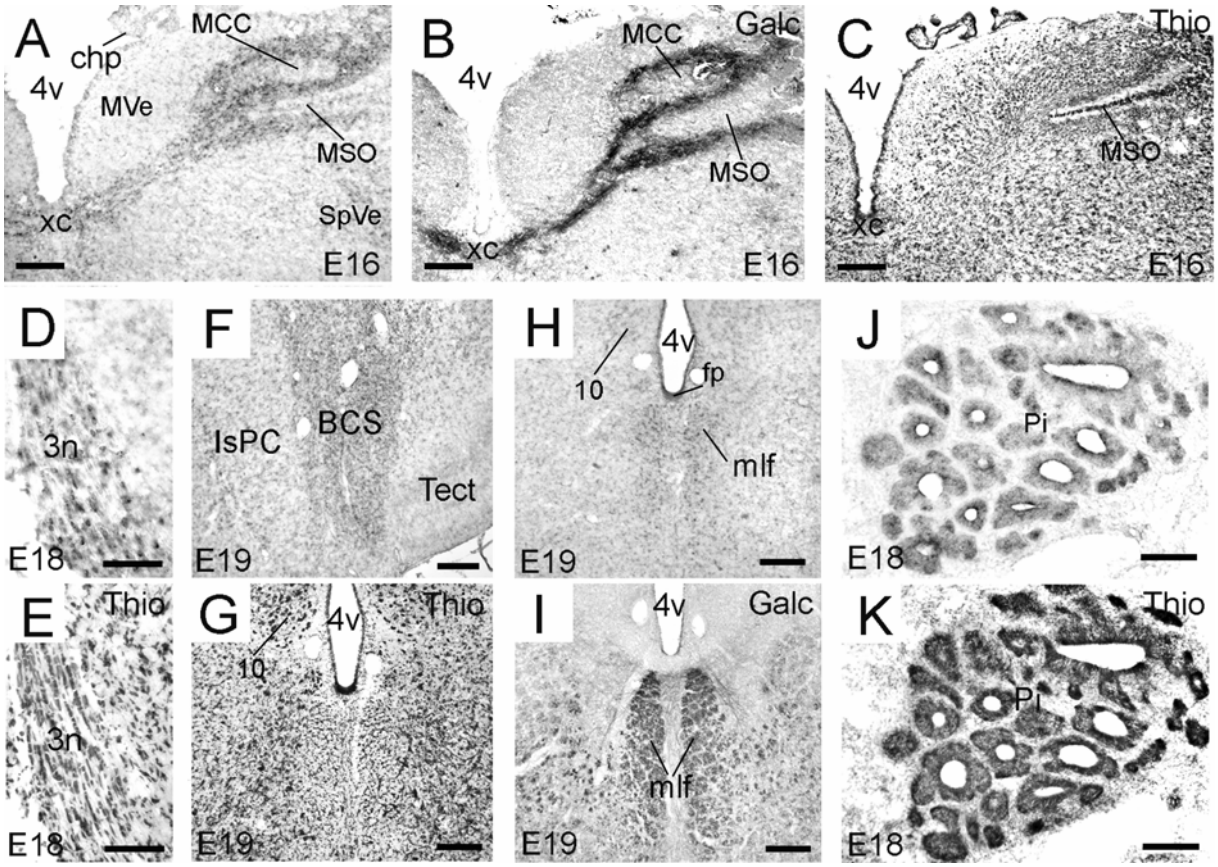

Figure 5. ADAM12 expression

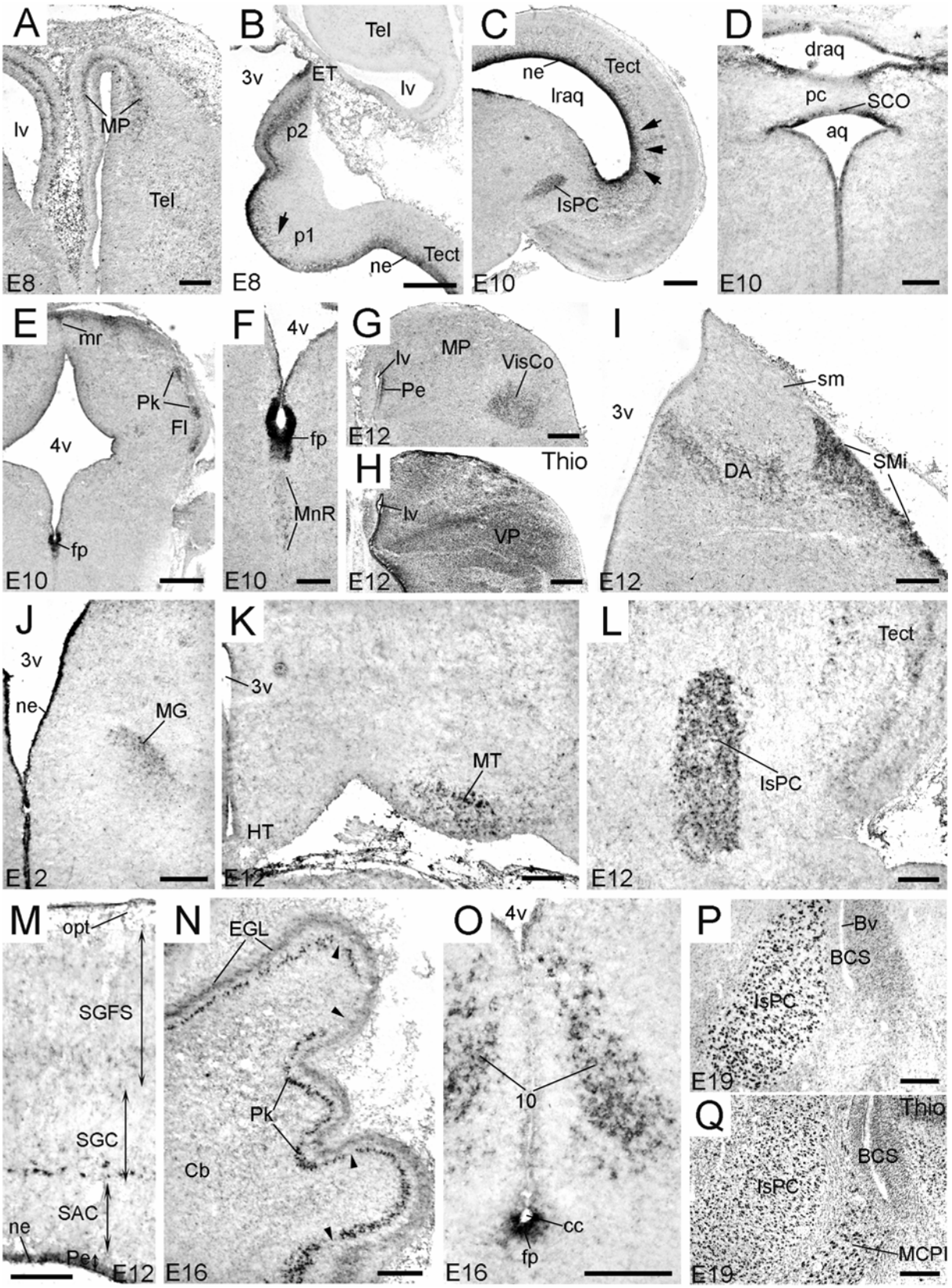

Figure 6. ADAM22 expression

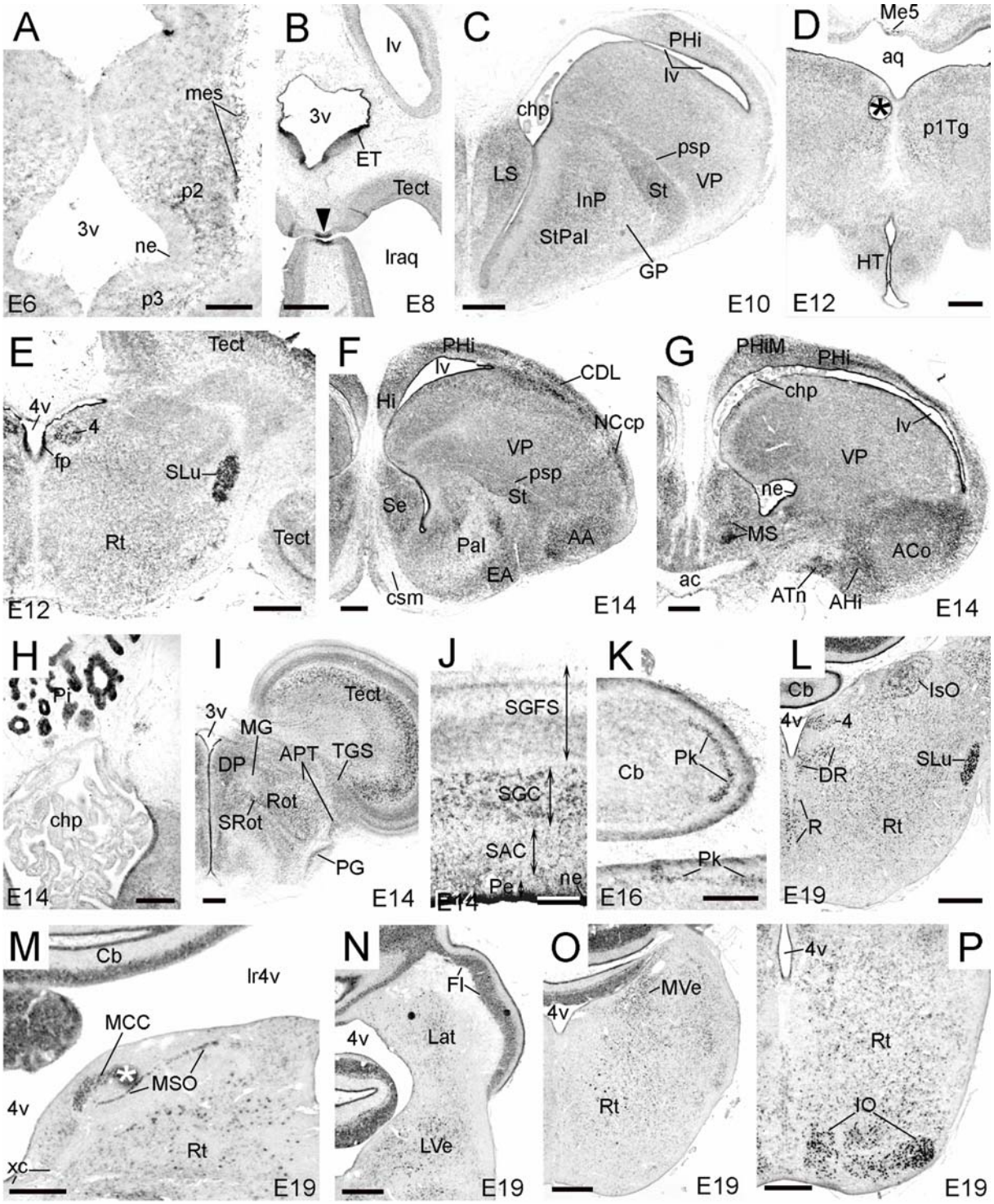

Figure 7. ADAM23 expression

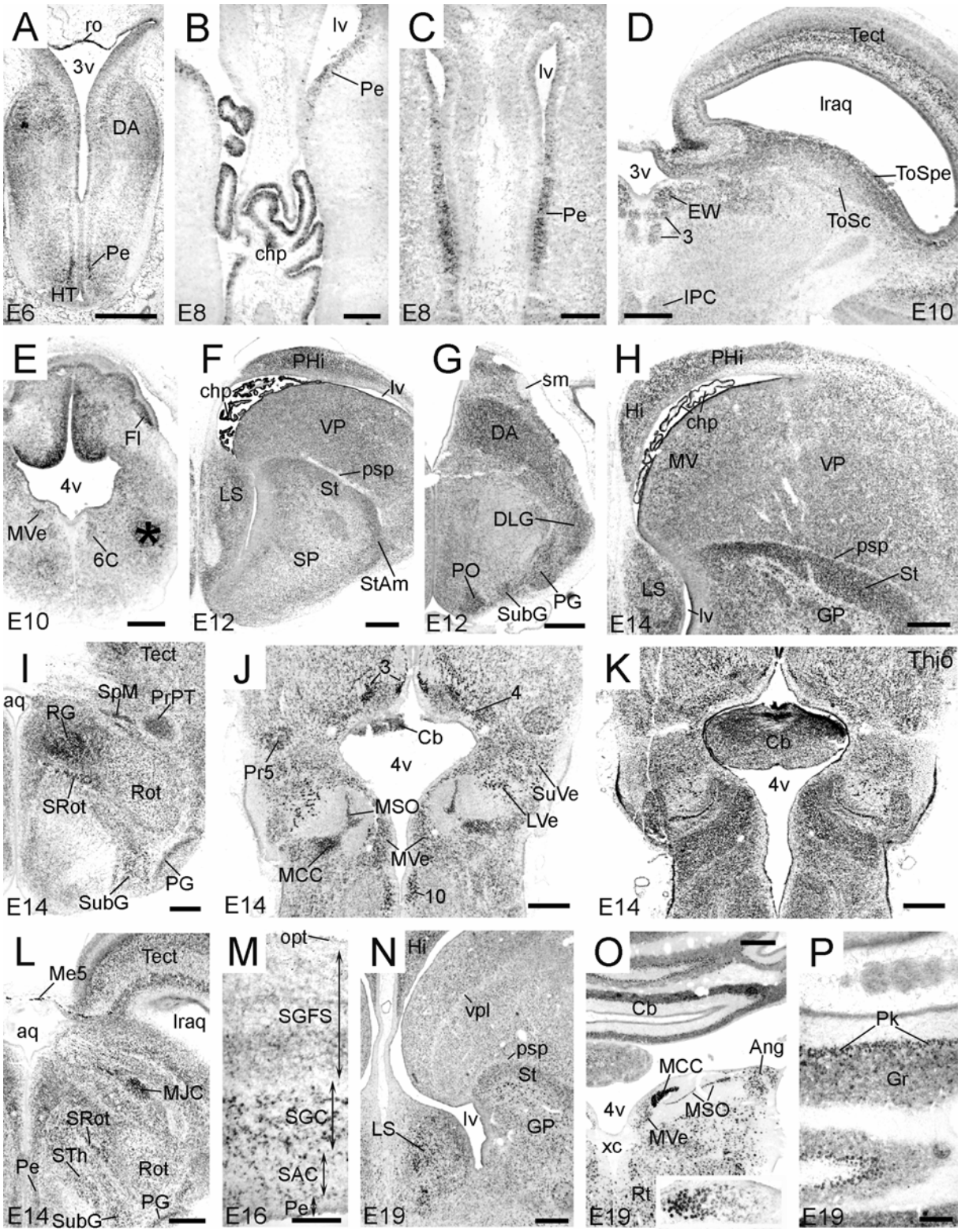

4. ADDITIONAL RESULTS

Overexpression of ADAM17 remodels blood vessels in the developing chicken tectum

Introduction

A detailed account on the expression and roles of ADAMs is given in Chapter 1.3. In brief, ADAM proteins possess multiple domains that are potentially involved in proteolysis, adhesion, cell fusion and cell signalling (Blobel, 2002, 2005). Altered expression of some members of the ADAM family has been associated with a number of diseases including inflammation, asthma, arthritis, Alzheimer's disease, atherosclerosis and cancer (Duffy et al., 2003; Vincent, 2004). In the brain, ADAMs play a role in neural development, axon guidance and some nervous diseases (Yang et al., 2006).

ADAM17, also named TACE (TNF alpha converting enzyme), is the best-characterized member of the ADAM family. In the nomenclature of CD antigens, ADAM17 has been given the designation CD156b. ADAM17 protein is a major sheddase that releases the extracellular domain of many proteins, including receptors and preforms of cytokines and growth factors (Novak, 2004). ADAM17 is up-regulated in human colon carcinoma (Blanchot-Jossic et al., 2005). In the brain, ADAM17 mRNA is expressed ubiquitously. Proteolytic cleavage of the neural cell adhesion molecule (N-CAM) by ADAM17 has an effect on neurite outgrowth (Kalus et al., 2006). ADAM17 is also involved in human CNS inflammation (Kieseier et al., 2003), and in the cleavage of amyloid precursor protein (APP) in Alzheimer's disease (Asai et al., 2003). During chicken embryonic development, ADAM17 has been implicated in the non-amyloidogenic processing of beta-amyloid precursor protein as a main proteolytic protease (Carrodeguas et al., 2005). Mice that are catalytically deficient of ADAM17 have been generated. Heterozygous mice developed normally and were fertile; however, the homozygous siblings were underrepresented at birth and most died within 24 hours (Peschon et al., 1998). Moreover, the inhibition of ADAM17 expression reduces hypoxia-induced brain tumor cell invasiveness (Zheng et al., 2007).

The blood-brain barrier (BBB) of the brain vasculature segregates the CNS milieu from the systemic blood circulation and helps to maintain the delicate homeostasis of the CNS environment (Lai and Kuo, 2005). The BBB is a highly regulated membranous barrier of the CNS capillaries; it is composed of endothelial cells and pericytes (Engelhardt, 2003; Lai and Kuo, 2005). Endothelial cells with their tight junctions

constitute the main element of the BBB. The surrounding pericytes are essential toward the microvascular endothelial wall for the formation, maturation, and maintenance of the normal microvascular structure and function. The molecular mechanisms regulating BBB permeability are poorly understood.

In this study, we analyzed the effect of ADAM17 overexpression on blood vessel formation in the chicken embryonic brain. We chose the midbrain tectum for electroporation because it is easily accessible for ex ovo electroporation, as shown by previous studies from our laboratory (Treubert-Zimmermann et al., 2002; Luo and Redies, 2005). In the present study, the cDNA of chicken ADAM17 was cloned and its expression was analyzed during chicken embryonic development for the first time. Results from semi-quantitative RT-PCR suggest that expression levels are similar at different stages, except for somewhat lower expression at later stages (E16-E20). In situ hybridization (ISH) results revealed that ADAM17 is expressed widely throughout the developing brain. In the optic tectum, ADAM17 is expressed strongly in the neuroepithelium and the periventricular stratum (Pe), moderately in the stratum griseum centrale (SGC), and weakly in the stratum griseum et fibrosum superficiale (SGFS). Expression is low or absent in the stratum album centrale (SAC) and blood vessels. Furthermore, by in vivo (ex ovo) electroporation, we overexpressed ADAM17 in the developing chicken tectum and analyzed the resulting morphological changes by fluorescence immunostaining and transmission electron microscopy (TEM). Compared to wild-type blood vessels, the morphology of blood vessel in the electroporated tecta is dramatically changed; the thickness of the blood vessel walls is increased in parallel to the number of pericytes. Together, our results indicate that the overexpression of ADAM17 remodels the morphology of the developing vasculature, possibly through an ADAM17-induced change in the extracellular matrix environment of the brain vasculature.

Materials and Methods

Animals

Chicken embryos were obtained and prepared as described in Publications 1-4.

RNA isolation and cDNA cloning

Total RNA from whole chicken embryos or embryonic brains were prepared using TRIzol reagent according to the manufacturer’s instruction (Invitrogen, Karlsruhe, Germany). For

embryos at 1.5 days' incubation (E1.5), E2, E2.5, E3 and E4, total RNA was isolated from whole embryos; for E5, E6 and E8, total RNA was only extracted from the heads; and for E10, E12, E14, E16, E18 and E20, total RNA was extracted from isolated brains. The quality of total RNA was examined by ethidium bromide-stained denaturing agarose gel electrophoresis and RNA concentration determined by a spectrophotometer.

First strand cDNA was synthesized in vitro using the SuperScript First-Strand Synthesis System (Invitrogen) with total RNA from E12 brain. Then the full-length cDNA and a partial cDNA sequence of ADAM17 were cloned by PCR. The PCR reaction was performed first for 2 min at 94°C for denaturing, followed by 30 cycles of amplification (denaturing for 30 sec at 94°C, annealing for 30 sec at 59°C, and extension for 2.5 min at 68°C). The last extension was for 10 min at 68°C. The primers for full-length cDNA of ADAM17 were 5'-ATGAGACTCCGGCTGTGG-3' (upper) and 5'-TCAGCACTCCGTCT CCTTGC-3' (lower). The primers for the partial cDNA sequence were 5'-TCCCGCGT GCTAAAGTTCCTCTGG-3' (upper) and 5'-GGCACTCGCGCTCCTCTCATCAC-3' (lower). At last, the sequences were cloned into pCR-II vector (Invitrogen) and sequenced by a commercial company (MWG-Biotech AG, Ebersberg, Germany) with M13 forward, reverse and specific internal primers.

Semi-quantitative RT-PCR

Semi-quantitative RT-PCR was performed using the One Step RT-PCR Kit (Qiagen, Hilden, Germany). Samples with water only or without reverse transcriptase served as negative controls. The same amount of total RNA was used for each reaction. Glyceraldehyde-3-phosphate dehydrogenase (GAPDH) was used as an internal control to monitor the amount of RNA. The forward primer for GAPDH was 5'-GGGCTCATCTGAAGGGTGGTGCTA-3' and the reverse primer was 5'-GTGGGGGAGACAGAAGGGAACAGA-3' (expected length 810 bp). The ratio between the primer concentrations for ADAM17 (primer for partial sequence, expected length 1070 bp) and GAPDH was 5:1. The one step RT-PCR reaction was performed in the same tube for both ADAM17 and GAPDH first at 50°C for 30 min for reverse transcription and at 95°C for 15 min for denaturing, followed by 30 cycles of amplification (denaturing for 45 sec at 94°C, annealing for 45 sec at 59°C [ADAM17 and GAPDH], and extension for 1.5 min at 72°C). The RT-PCR fragments were analyzed on 1.5% agarose gels.

Plasmids and antibodies

Full-length and partial sequences of ADAM17 were cloned into pCR-II vector (see above) for cRNA probe synthesis. Then the full-length sequence of ADAM17 was subcloned from pCR-II-ADAM17 into the eukaryotic expression vector pCAGGS that carries a CMV/chicken beta-actin promoter as pCAGGS-ADAM17. Full-length GFP cDNA in pCAGGS (pCAGGS-GFP) was a kind gift of Dr. H. Ogawa (Momose et al., 1999). All plasmids were purified from Topo10 strain of Escherichia coli (Invitrogen) with the Maxi Plasmid Purification Kit (Qiagen).

The following antibodies were used for immunostaining of sections: rat polyclonal antibody HT7 that serves as a marker for blood-brain barrier (BBB)-forming endothelial cells (dilution 1:200; kind gift of H. Gerhardt, Institute of Pathology, University of Tübingen, Germany; Risau et al., 1986; Gerhardt et al., 1996); Cy3-labeled mouse monoclonal antibody against smooth muscle actin (SMA), a marker for smooth muscle cells or pericytes (1:300, Sigma); rabbit polyclonal antiserum against human fibronectin, used as a marker for blood vessels in the brain (1:2000, kind gift of R. Hynes, MIT, Cambridge); rabbit polyclonal antibody M12K against alpha-catenin (1:50; kind gift of W. Schneider, Max-Planck-Institut for Developmental Biology, Tübingen, Germany; Schneider et al., 1993), which is present in brain vasculature (Miskevich et al., 1998); and rat monoclonal antibody against CD31 (PECAM-1), a marker for endothelial cell-cell interactions involved in angiogenesis (1:10; Abcam ab7388; DeLisser et al., 1997). Primary antibodies were followed by incubation with secondary antibodies (Cy3-labelled AffiniPure goat anti-mouse, rat or rabbit IgG antisera, respectively; Jackson ImmunoResearch).

In vivo (ex ovo) electroporation

The method for ex ovo culture was modified after Luo and Redies (2004). The contents of fertilized eggs, incubated at 37°C in a forced-draft egg incubator (BSS160, Ehret, Germany), were put into petri dishes at E3, and then transferred into an incubator (B6120, Heraeus, Germany) for further incubation at 37°C ("shell-less" culture). For ex ovo electroporation, E6 embryos were chosen (Momose et al., 1999; Treubert-Zimmermann et al., 2002; Luo and Redies, 2005). The vitelline and amnion membranes were torn carefully with fine forceps over the tectum. About 0.5-1µl pCAGGS-GFP plasmid in Gey's buffered salt solution (GBSS, Invitrogen, concentration of plasmid about 0.5µg/µl and 2µg/µl), together with 0.1% Fast Green (Sigma) and similar amounts of pCAGGS-ADAM17

(concentration of plasmid 0.5µg/µl or 2µg/µl, compared to 0.25µg/µl of pCAGGS-GFP plasmid) were injected into the right tectal ventricle. Immediately following injection, electric pulses (25V, 60 ms pulse length, six pulses, 100 ms intervals) were applied by an electroporator (CUY 21, TR Tech, Japan). Transfected embryos were returned to the incubator until E8, E10 and E12. Brains with positive GFP signal were isolated, fixed and embedded, as described (Publications 1-4). All sections used were cut in frontal plate.

Probe synthesis and in situ hybridization (ISH)

Digoxigenin-labeled sense and antisense cRNA probes were transcribed in vitro from the purified pCR-II plasmids containing the full-length or partial sequence of ADAM17, according to the manufacturer's instructions for probe synthesis (Roche, Mannheim, Germany). Sense cRNA probes were used as a negative control for ISH. Hybridized probes were detected using alkaline phosphatase-conjugated anti-digoxigenin Fab fragments (Roche Diagnostics GmbH, Germany). ISH on cryosection was performed according to the method described in Publications 1-4. Photomicrographs, including those for gels, were adjusted in contrast and brightness by the Photoshop software (Adobe, Mountain View, CA) for optimal display of the staining patterns in the figures.

Apoptosis analysis with TUNEL assay

Apoptosis was compared between transfected and untransfected areas in the same electroporated embryos. To detect apoptotic cells, cryostat sections were stained using the In Situ Cell Death Detection Kit/TMR Red (Roche) according to the manufacturer’s instructions.

Immunohistochemistry

For immunofluorescence staining, sections adjacent to those used for ISH were preincubated with skimmed milk solution (5% skimmed milk, 0.3% Triton X-100, and 0.04% sodium azide in TBS) at room temperature for 60 min, then incubated sequentially with the primary antibodies against HT7, SMA, fibronectin, alpha-catenin or CD31, respectively, appropriately diluted in the skimmed milk solution at 4^{o}C overnight, and with Cy3-labeled secondary antibody against the IgGs of the appropriate species (1:300 dilution) at room temperature for 60 min each. Finally, dye Hoechst 33258 (Molecular Probes) was used for staining of cell nuclei. Fluorescence was visualized and photographed

under a transmission fluorescence microscope (Olympus BX40, Hamburg, Germany) equipped with a digital camera (Olympus DP70).

Transmission electron microscopy (TEM)

Electroporated embryos were perfusion fixed at E12 via the heart with 2.5% glutardialdehyde /2% formaldehyde solution for 5 min. The following embryos were used: 2 embryos for pCAGGS-ADAM17/pCAGGS-GFP co-electroporation, 2 embryos for pCAGGS-GFP electroporation alone, and 2 normal embryos without electroporation (serving as negative controls). The brains were dissected carefully after perfusion and fixed in the above fixative at 4^{o}C overnight. Under a fluorescence stereomicroscope (Leica, Mannhein, Germany), the GFP-positive area in each tectum was then dissected and fixed further in 1% osmium tetroxide. Vibratom sections were prepared from this specimen, dehydrated in ethanol and embedded in Durcupan ACM (Fluka, Switzerland). Ultrathin sections were examined in an electron microscope (EM900, Zeiss, Oberkochen, Germany) after counterstaining with uranyl acetate and lead citrate (Roberts, 2002). Pictures were taken with a CCD camera (FastScan–F 114, TVIPS GmbH, Gauting, Germany).

Morphometry and statistical analysis

The intensity of individual bands from semi-quantitative RT-PCR was quantified using the software ImageQuant TL (Amersham Biosciences). The intensity value of each band was normalized to the value of the corresponding GAPDH band. Each experiment was repeated three times (n=3). In the figures, all data are shown with the standard error of the mean (S.E.M). Statistical analysis was performed by two-tailed *t* test using PRISM 4 software (GraphPad, San Diego, CA, USA). A value of $p<0.05$ was considered as a statistically significant difference for the different experiments in the same experimental group.

For analysis of the transmission electron microscope images of tectal blood vessels, the area occupied by the blood vessel walls was measured from digital images by using the NIH image program (ImageJ) and expressed in number of pixels. In the same measured areas, the number of cross-sections through pericyte nuclei and endothelial cell nuclei were counted, respectively. All calculations were performed with SPSS 11.0 for Windows (SPSS Inc., Chicago, IL, USA). Student's *t* test was used to compare quantitative differences between areas of the vessel walls, and between the numbers of pericyte nuclei from different samples, respectively.

Results and discussion

To study ADAM17 mRNA expression, semi-quantitative RT-PCR was performed from E1.5 to E20. Our results show that ADAM17 began to be transcribed as early as at E1.5 or even earlier. Expression is maintained at high levels until E20 (Fig. 5A). A statistic analysis of the semi-quantitative RT-PCR results failed to reveal any significant differences for the different stages, except for a small decrease at later stages (E16-E20; Fig. 5B). Overall, results demonstrate a relatively stable expression of ADAM17 throughout the chicken embryonic development.

The results from in situ hybridization indicate that ADAM17 (AM17) expression is visualized in the deep layers of the tectum at E8 (Fig. 5C). At E10 and E12, ADAM17 is expressed strongly in the neuroepithelium (ne in Fig. 5D,E) and the periventricular stratum (Pe), moderately in the stratum griseum centrale (SGC), weakly in the stratum griseum et fibrosum superficiale (SGFC), and absent in the stratum album centrale (SAC in Fig. 5D). ADAM17 sense probe was taken as a negative control (Fig. 5F).

To study the function of ADAM17 during tectal development, ADAM17-containing plasmid (ADAM17-pCAGGS) was injected and electroporated into the tectum at E6 to induce ADAM17 overexpression. Positive specimens were collected at E8, E10 and E12. ADAM17 overexpression changed the morphology of the tectum at E10 and E12 (Fig. 5I and Figs. 6,7). Control electroporation experiments (GFP alone) did not result in morphological changes in the tectum (Fig. 5G). To study whether the thinning of the tectal layers observed with ADAM17 overexpression was due to apoptosis, a TUNEL essay was performed. A comparison of the number of apoptotic cells between ADAM17 overexpression and control specimens revealed a very low number of apoptotic cells in both cases (Fig. 5H,J). We conclude that the change in tectal morphology induced by ADAM17 overexpression did not result from a marked increase in apoptosis.

Figure 6A shows that GFP-positive control cells can be visualized in the tectum (Tect) under the fluorescence microscope. ISH with ADAM17 antisense probe (AM17 in Fig. 6) was performed on sections from E8 embryos (Fig. 6B), E10 embryos (Fig. 6C), and E12 embryos (Fig. 6D). Results show that ADAM17 was successfully overexpressed in the GFP-positive tectal area at all three stages (Fig. 6B-D). At E10 and E12, the thickness of the tectum was decreased and the gross morphology of tectal blood vessels was altered in the electroporated area (Fig. 6C,D).

In this study, I focus on the morphology of the blood vessels. To define the morphological change induced by overexpression of ADAM17 in the developing tectum in

more detail, I used different blood vessel markers. HT7 is a marker for blood-brain barrier (BBB)-forming endothelial cells (Gerhardt, 1996). Compared to the non-electroporated area, the ADAM17/GFP-positive area showed a similar staining pattern for HT7 (Fig. E-G'). Fig. 6G and G' display the merged images for the HT7 staining (red), Hoechst 33258 (nuclear) staining (blue) and GFP staining (green) in the same section. Moreover, the following additional markers were used: alpha-smooth muscle actin (SMA) is a marker for smooth muscle cells or pericytes (Fig. 6H-K); fibronectin (Fn) is a marker for basement membranes in the blood vessels (O'Shea, 1987) (Fig. 6L-O); alpha-catenin is a general marker for vasculature in the brain (Miskevich et al., 1998) (Fig. 6P-S); and PECAM-1/CD31 is a marker that mediates endothelial cell-cell interactions involved in angiogenesis (DeLisser et al., 1997) (Fig. 6T-W). From the immunostaining of these four antibodies, we can see that the size of the blood vessels in the ADAM17/GFP-positive area is much larger than that in the non-electroporated area. The inserts at the lower left side of Figure 6H,L,P,T (for E10) and Figure 6J,N,R,V (for E12) show magnifications of the areas boxed in these figures. Figure 6I,M,Q,U (for E10) and Figure 6K,O,S,W (for E12) represent the merged images for GFP (green) and Cy3 (red) fluorescence staining with the respective antibodies. A comparison of the results for HT7 (endothelial marker) and SMA (pericyte marker) suggest that the hypertrophy of the blood vessels in the ADAM17/GFP-positive area is due to a change in the number and size of pericytes, but not of endothelial cells.

To study the change in the pericytes in more detail, transmission electron microscope (TEM) experiments were performed. In the regions where the tectum overexpressed ADAM17, the number of pericytes in the wall of the vessels was increased (Fig. 7B), compared to control samples of the non-electroporated adjacent areas or the areas that were electroporated with GFP alone (Fig. 7A). In Figure 7A,B, arrowheads show the endothelial cells, and arrows show the pericytes. For quantification of this result, we measured the areas occupied by the brain vessel wall in tectal regions with pCAGGS-ADAM17/pCAGGS-GFP co-expression samples (ADAM17/GFP, n=55) and the two types of controls, i.e. non-electroporated adjacent regions (ØADAM17/ØGFP, n=26) and electroporation with GFP alone (GFP, n=20). A *t* test showed a significant difference of the mean values for the vessel walls between the experimental group and both control groups ($p<0.05$ and $p<0.02$, respectively; Fig. 7C). There was also a significant difference in the number of the pericyte nuclei between experimental and control groups ($p<0.02$ and $p<0.01$, respectively; Fig. 7D). However, there was no significant difference in the number

of the endothelial cell nuclei between all three groups (data not shown). The cell-cell contact between endothelial cells and pericytes was not investigated in this study. However, it is known that reciprocal interactions between pericytes and endothelial cells regulate the development, stabilization, maturation and remodeling of vasculature (Choi and Kim, 2008).

During CNS development, the vascular system in the brain is derived from the leptomeningeal blood vessels through angiogenesis. The capillaries from the perineural vascular plexus penetrate neural tissue and form the brain microvessels. The walls of typical angiogenic microvessels are composed of two types of cells, endothelial cells and pericytes. Endothelial cells form the inner lining of the vascular tube; pericytes form an outer sheath around the endothelium (Risau, 1997). Also, pericytes are in active communication with the cells of the neurovascular unit and make fine-tuned regulatory adjustments in response to stress stimuli in the brain (Dore-Duffy, 2008). Disruption of the extracellular matrix (ECM) is combined with an enhanced BBB permeability in pathological states (Rosenberg et al., 1993; Rascher et al., 2002). In vitro experiments support that differentiation of pericytes in culture is accompanied by changes in the extracellular matrix (Schor et al., 1991). Matrix metalloproteases (MMPs) were shown to regulate the structure and function of ECM molecules under normal and pathological conditions (Sternlicht and Werb, 2001). ADAM17 has been hypothesized to regulate angiogenesis based on its proteolytic activity in matrix degradation, although it has not yet been investigated sufficiently (van Hinsbergh et al., 2006). Based to the above results, I speculate that the increase in the number of pericytes in the developing tectum is due to a change in the ECM environment of the blood vessels in the areas of ADAM17 overexpression.

Furthermore, ADAM17 mRNA is strongly present in the ventricular layer (neuroepithelium) that is composed of radial glial cells whose processes span the entire thickness of the neural tube wall. Because of the lack of antibodies against ADAM17, I was unable to study whether the radial glial processes express ADAM17. This question remains to be answered in a future study.

Conclusion

My results show that ADAM17 is expressed at relatively high levels throughout embryonic brain development. Overexpression of ADAM17 leads to an increase in the thickness of the blood vessel wall, due to an increase in the number of pericytes. The mechanism of this

change remains unknown. Here, I speculate that the overexpression of ADAM17 remodels the developing brain vasculature through a change in the ECM environment of the brain blood vessels.

Legends for the additional figures

Fig. 5. ADAM17 expression in the embryonic chicken brain.

A. Result from semi-quantitative RT-PCR analysis showing the expression of ADAM17 at different stages of chicken embryonic development (upper bands; E1.5-E4, whole embryos; E5-E8, whole heads; E10-E20, brain). GAPDH (lower bands) served as an internal control to monitor the amount of RNA.

B. The measured intensity values of the ADAM17 bands shown in A were normalized to the GAPDH value. The error bars represent means +/- S.E.M. (n=3).

C-F. Results from in situ hybridization (ISH) with ADAM17 antisense probe on cross-sections through the tectum at E8 (C), E10 (D), and E12 (E). ISH with ADAM17 sense probe served as a negative control (F).

G-J. TUNEL assay on cross-sections through the E12 tectum. G,I. GFP signal in a specimen electroporated with GFP plasmid alone (control; GFP), and co-electroporated with ADAM17 plasmid (AM17/GFP), respectively. H,J. TUNEL assays showing the apoptotic cells (red points) in the same sections as in G and I, respectively. Scale bars, 200μm in F for D-F, in J for C and G-J.

Fig. 6. ADAM17 overexpression mediated by in vivo (ex ovo) electroporation in the developing tectum. All specimens were electroporated at E6.

A. Fluorescence microphotographs of an embryonic chicken tectum at E8 (whole mount preparation). B-C. Results from ADAM17 in situ hybridization (ISH) showing ADAM17 overexpression in the electroporated area at E8 (B), E10 (C), and E12 (D).

E-G'. Fluorescence photomicrographs of HT7 immunoreactivity at E12. E. HT7 immunostaining. F. GFP fluorescence of the same section as E. G. Merged images for HT7 (red), GFP (green) and nuclear stain Hoechst 33258 (blue). G' shows a higher magnification of the electroporated area.

H-K. Fluorescence photomicrographs of alpha-smooth muscle actin (SMA) immunoreactivity at E10 (H,I) and at E12 (J,K). H,J. SMA immunoreactivity; I,K. Merged images for SMA immunoreactivity (red) and GFP fluorescence (green) for the same sections as shown in H and J, respectively.

L-O. Fluorescence photomicrographs of fibronectin (Fn) immunoreactivity at E10 (L,M) and at E12 (N,O). L,N. Fibronectin immunoreactivity. M,O. Merged images for fibronectin immunoreactivity (red) and GFP fluorescence (green) for the same sections as shown in L and N, respectively.

P-S. Fluorescence photomicrographs of alpha-catenin immunoreactivity at E10 (P,Q) and at E12 (R,S). P,R. Alpha-catenin immunoreactivity. Q,S. Merged images for alpha-catenin immunoreactivity (red) and GFP fluorescence (green) for the same sections as shown in P and R, respectively.

T-W. Fluorescence photomicrographs of PECAM-1/CD31 immunoreactivity at E10 (T,U) and at E12 (V,W). T,V. CD31 immunoreactivity. U,W. Merged images for CD31 immunoreactivity (red) and GFP fluorescence (green) for the same sections as shown in T and V, respectively.

The inserts in H,J,L,N,P,R,T and V are higher magnifications of the areas boxed in the respective figures. Scale bars, 100μm in the insert of V for all of the inserts; 200μm in B and in W (for all other panels, except A).

Fig. 7. Results from transmission electron microscopy and the statistical analysis.

A,B. Results from transmission electron microscopy at E12. A, GFP electroporation alone (control); B, ADAM17 overexpression sample. The arrowheads show the nuclei of endothelial cells, and the arrows show the nuclei of the pericytes. Scale bars, 4μm in A for B as well.

C,D. Results of the statistical analysis. C shows for the mean values for the area occupied by the blood vessels walls in the electroporated area or wild type (n=55 for ADAM17/GFP co-electroporation; n=20 for electroporation of GFP alone; and n=26 for the wild type control).

D shows for the mean values for the number of the pericyte nuclei in the blood vessels walls in the electroporated area or wild type (n=55 for ADAM17/GFP co-electroporation; n=20 for electroporation of GFP alone; and n=26 for the wild type control).

Figure 5. ADAM17 expression in the embryonic chicken brain

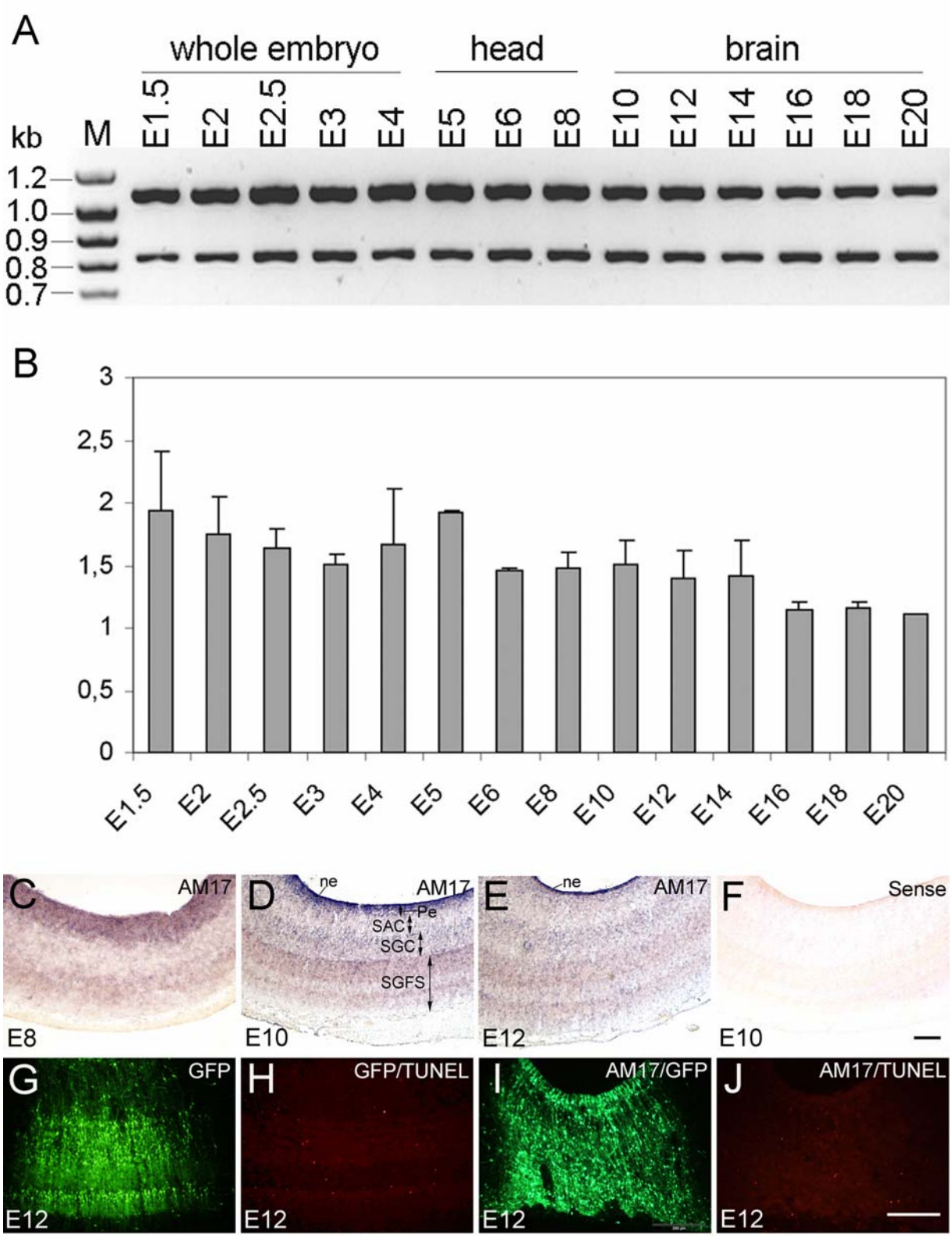

Figure 6. ADAM17 overexpression mediated by in vivo (ex ovo) electroporation in the developing tectum. All specimens were electroporated at E6.

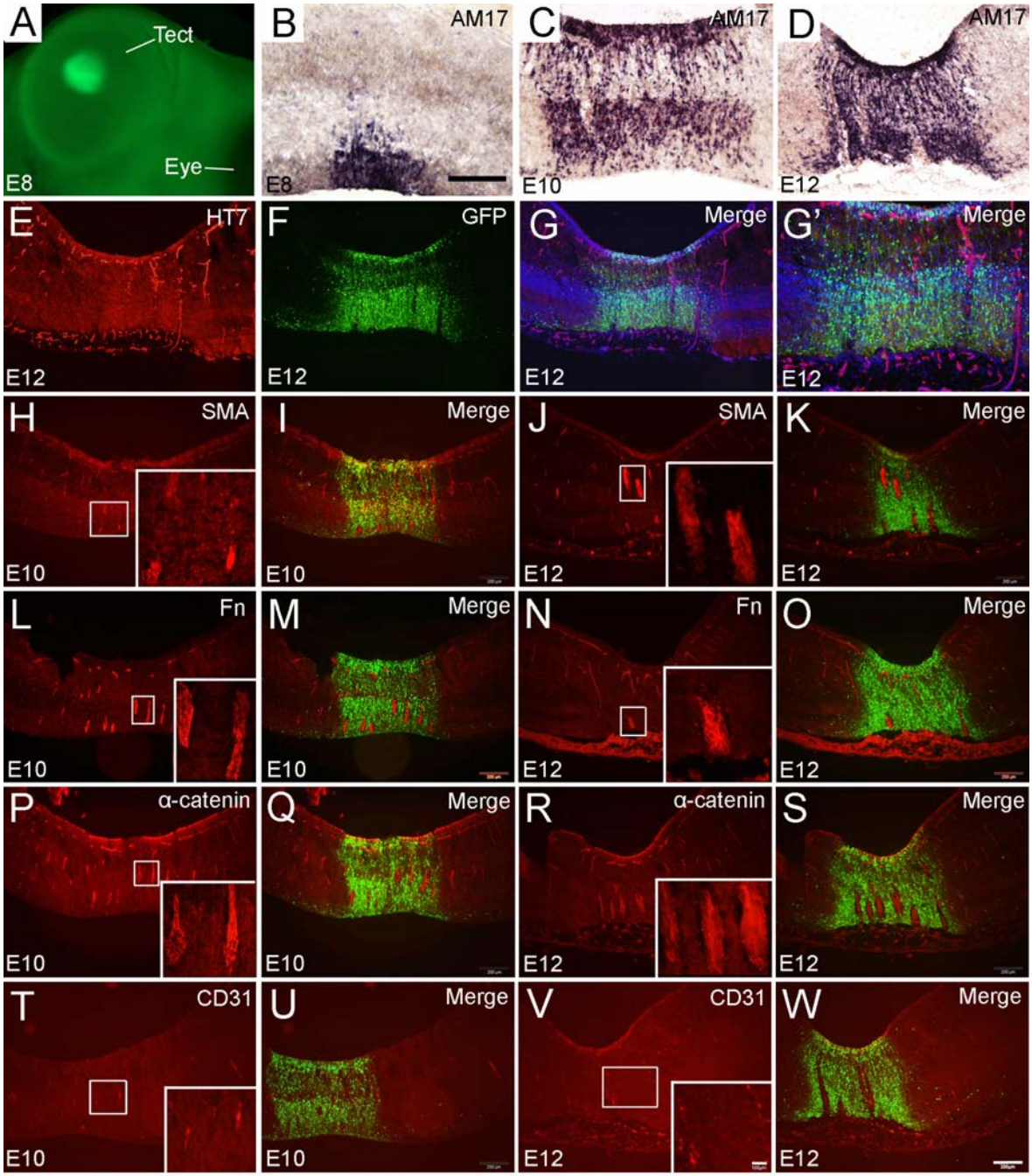

Figure 7. Results from transmission electron microscopy and the statistical analysis.

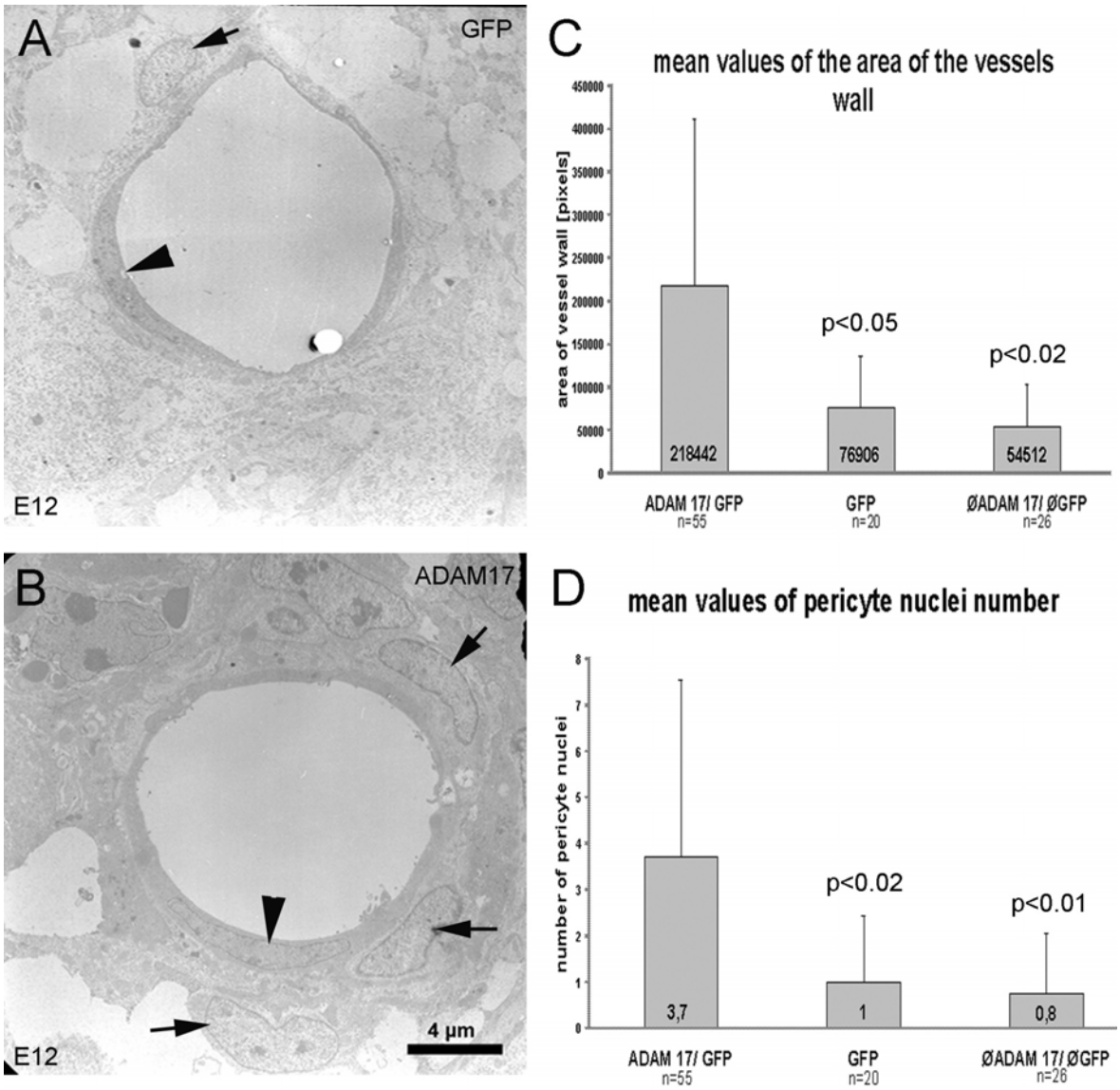

5. DISCUSSION

As outlined in the Introduction section, cell adhesion molecules have various functions during embryonic development. Cadherins, one of the best investigated families of cell adhesion molecules, were first cloned and studied in chicken embryos (Hatta and Takeichi, 1986; Napolitano et al., 1991). Like cadherins, ADAMs play important roles during embryonic development (Blobel, 2005; Yang et al., 2006), but few studies were performed in the chicken system to date. There are still many unexplored questions with regard to the temporal and spatial expression and functions of cadherins and ADAMs during the vertebrate development and evolution. The cloning and expression analysis of different cadherins or ADAMs during chicken embryogenesis will be a first step to answer these questions. Based on the expression patterns of cadherins and ADAMs, hypotheses about their functions can be formulated and tested experimentally. In my doctoral study, I firstly cloned the full-length cDNA sequences of five new chicken genes, ADAM12, ADAM13, ADAM22, Cdh8 and Cdh19, using the method of rapid amplification of cDNA ends (RACE). Results from mapping the expression of these genes show that

- ADAM13 is expressed in a well-defined spatiotemporal pattern during chicken embryonic development (Publication 1);
- eight classical cadherins (N-Cdh, R-Cdh, Cdh6, Cdh7, Cdh8, Cdh11, Cdh19 and Cdh20) are expressed in spatially restricted expression patterns in the developing chicken cochlea (Publication 2);
- Cdh8 has three isoforms in chicken embryonic system and each isoform shows a spatiotemporal expression profile (Publication 3);
- ADAM9, ADAM10, ADAM12, ADAM22 and ADAM23 all are expressed in the developing chicken brain, and each of the five members has its own restricted expression pattern in specific types of tissues and cells (Publication 4); and
- overexpression of ADAM17 remodels blood vessels in the developing chicken tectum by increasing the number of pericytes (Additional Results).

Together, these results indicate multiple and diverse roles for each ADAM and cadherin in embryonic development.

5.1 Expression of ADAMs in the developing chicken embryo

The existence of ADAM genes has been confirmed in many animal species, including mammals, reptiles and invertebrates (Seals and Courtneidge, 2003). Individual members of the ADAM family show variable expression patterns that are developmentally regulated. Some ADAMs are expressed in highly restricted patterns in specific tissues and organs, whereas others are expressed more widely. Most studies about ADAMs investigated human, mouse or rat. Only a few papers reported the functions or expression profiles of ADAMs in avian species. In this study, seven ADAMs (ADAM9, ADAM10, ADAM12, ADAM13, ADAM17, ADAM22 and ADAM23) were cloned, and their expression patterns were analyzed during embryonic development of the chicken brain. ADAM13 was also studied in organs other than the brain (Publication 1). Each member has its own expression pattern in the developing brain, though the expression patterns of some ADAMs display varying degrees of overlap (Publication 4). Moreover, to obtain insight into the function of ADAMs in brain development, ADAM17 was overexpressed in the developing tectum. As a result, the morphology of blood vessels in the developing chicken tectum was remodelled through an increase in the number of pericytes (Additional Results). These findings will be discussed in more detail in the following sections.

5.1.1 ADAM13 expression during chicken embryonic development

Based on the predicted chicken ADAM13 sequence, a full-length sequence, which encodes 947 amino acids, was obtained by RACE method. This chicken cDNA sequence was analyzed from different aspects, such as sequencing, BLAST, deduced protein structure analysis, and the evolutionary relationship analysis with other known ADAMs. The obtained chicken gene shares the highest similarity with *Xenopus* ADAM13, and a relatively high identity with human and mouse ADAM33. It can therefore be considered as the orthologous gene of *Xenopus* ADAM13 or human and mouse ADAM33. The obtained molecule was designated as chicken ADAM13 (Publication 1).

From semi-quantitative RT-PCR result, ADAM13 began to be transcribed weakly at E1.5. As embryo develops, the transcription of ADAM13 increased gradually and reached the highest at E10, then decreased sequentially and was still detectable at E20. This result suggested that the expression of ADAM13 is temporally changed during chicken embryonic development.

The results from the section and whole mount in situ hybridization indicate that ADAM13 is expressed strongly in the chicken embryo, but only in specific regions. Firstly,

ADAM13 is expressed in structures derived from the cranial neural crest. The expression of ADAM13 in cranial neural crest cells suggests that ADAM13 might play a role in guiding cranial neural cells to their destination during migration. Secondly, ADAM13 is expressed strongly in the mesenchyme around the brain that will form the meninges later in development. Interestingly, the expression in the meninges or the prospective meninges decreases gradually from earlier to older stages, but can be still seen until E10 at least. Thirdly, ADAM13 is expressed in the somites and its derived structures. The expression of ADAM13 in somitic mesoderm was also described in *Xenopus*, but only at early stages of development and not in somite-derived structures (Alfandari et al., 1997). Extending these results, I described the expression of ADAM13 also at relatively late stages. Forthly, ADAM13 is expressed strongly in the dorsal aorta and the developing kidney. Note that the expression of ADAM13 in the glomeruli is associated with the vascular tuft. It will be of interest to study whether ADAM13 expression in the mesenchyme around the mesonephric tubules and the nephric duct also reflects expression by vascular cells. Fifthly, ADAM13 is expressed in digestive organs, such as the esophagus, the proventriculus, the gizzard, and the intestines. Together, these results extend previous results from *Xenopus* for early stages of development (Alfandari et al., 1997, 2001) and show in detail that ADAM13 is expressed also at later stages of development and in organs that were not previously known to express ADAM13. For example, at E10, ADAM13 mRNA was transcribed widely in muscles, e.g., of the limbs, the thorax, and the abdominal wall, as well as in condensed sheets of chondroblasts around cartilage, e.g., around the vertebrae, the ribs and the sternum (Publication 1).

Like *Xenopus* ADAM13, chicken ADAM13 has a molecular structure similar to members of the meltrin subfamily of ADAMs, which comprises ADAM9, ADAM12, ADAM19 and ADAM35. These genes are involved in muscle development (Yagami-Hiromasa et al., 1995; Weskamp et al., 2002; Lewis et al., 2004; Watabe-Uchida et al., 2004). The expression of some members of the meltrin subfamily has been described in avian embryos (Lewis et al., 2004; Watabe-Uchida et al., 2004). In the quail, ADAM12 is expressed in the cranial ganglia, in the mesenchyme of the limb bud, and in the mesenchyme surrounding the dorsal aorta, whereas ADAM19 is expressed in the cranial and dorsal root ganglia and in the allantois (Lewis et al., 2004). ADAM35 is expressed in the chicken myotome and several epithelial tissues, such as the otic vesicles and gut epithelia (Watabe-Uchida et al., 2004). The full-length sequence of chicken ADAM9 was reported, but its expression pattern has not been described to date (Caldwell et al., 2005). It

will be interesting to investigate the functional relation between chicken ADAM13 and other members of the meltrin subfamily during the embryonic development.

Some functional studies on the roles of ADAM13 have been published. For example, the migration of cranial neural crest cells requires the metalloprotease activity of ADAM13 in *Xenopus* (Alfandari et al., 2001). ADAM13 cleaves fibronectin in vitro and remodels a fibronectin substrate in vivo; furthermore, its disintegrin and cysteine-rich domains can bind the second heparin-binding domain of fibronectin (Gaultier et al., 2002). However, other roles of ADAM13 during chicken embryonic development remain unexplored. According to my present results, the migration of the neural crest cells in chicken embryos may also require the metalloprotease activity of ADAM13. Last but not least, strong expression of ADAM13 by other types of tissues and cells, for example the developing meninges, dorsal aorta, kidney, muscle and digestive organs, suggests that ADAM13 may play multiple roles during embryonic chicken development.

As mentioned, the gene orthologous to chicken ADAM13 in human and mouse is ADAM33, which has been confirmed as a susceptibility gene for asthma (Holgate et al., 2006). The restricted expression of ADAM33 in mesenchymal cells and its association with bronchial hyperresponsiveness and accelerated decline in lung function strongly indicate that ADAM33 is involved in the structural airway components of asthma. Chicken ADAM13 is also expressed by the bronchial mesenchyme in the developing lung. It remains obscure whether ADAM expression is associated with avian respiratory disease.

5.1.2 ADAM expression in the CNS

Only little was known about the expression profiles of ADAMs in the CNS. Kärkkäinen et al. (2000) identified ten ADAM mRNAs and showed strikingly different expression profiles of six of these mRNAs in the major parts of the adult mouse brain by Northern analysis. Similar results were obtained for ADAM22 and ADAM23 in the human brain (Sagane et al., 1998). In situ hybridization with probes for ADAM10 and ADAM17 showed regional expression of these molecules in the adult mouse brain (Kärkkäinen et al., 2000). However, the spatiotemporal expression patterns of ADAMs during brain development remain largely unknown.

Results from my study (Publication 4) show that, in the developing brain, the general types of structures that express individual ADAMs are rather different. ADAM9 is predominantly expressed in the choroid plexus and in the ventricular layer; ADAM10 is expressed by developing blood vessels, oligodendrocytes, and subsets of neurons and brain

nuclei; ADAM12 is expressed by a few brain nuclei, cerebellar Purkinje cells, restricted regions of the neuroepithelium, and deep layer of tectum; ADAM22 expression is strongly in some brain nuclei and pineal gland, but negative in choroid plexus; and ADAM23 is expressed by most gray matter regions and the choroid plexus.

These results differ from the expression patterns of other families of adhesion molecules. For example, the expression patterns of individual classic cadherins in the developing chicken brain are less variable (Redies, 2000; Redies et al., 2005). Although each classic cadherin shows a regionally restricted pattern that differs from that of other cadherins, most classic cadherins are expressed in the same types of tissues (ventricular layer, subsets of neurons and brain nuclei, and specific fiber tracts). Very few classic cadherins are known to be expressed by oligodendrocytes and blood vessels (for example, VE-cadherin in blood vessels). Moreover, the expression of cadherins is regionally restricted in general, while that of some ADAMs (for example, ADAM10 and ADAM23) is more widespread. These results suggest that most cadherins play similar roles but at different locations in the brain. In contrast, the relatively variable expression patterns of ADAMs suggest that they play versatile roles in different types of brain tissues, either in highly restricted brain regions (for example, ADAM12 in brain nuclei) or more widespread throughout the brain (for example, ADAM10, ADAM22 and ADAM23).

As mentioned in the Introduction, possible roles for ADAMs in brain development include cell proliferation, migration, differentiation, apoptosis, myelination, as well as axon guidance (Novak, 2004; Yang et al., 2006). The expression patterns revealed in my study (Publication 4) will provide a basis for further experimental studies that investigate the functional role of ADAMs during brain development.

5.1.3 ADAM17 overexpression enlarges the blood vessel wall through increasing the number of pericytes in the developing optic tectum

ADAM17 has been well investigated in human and mouse. Results from my study (Additional Results) show that it is expressed widely in the developing chicken brain with relatively little differences at different developmental stages, except for slightly weaker expression at later stages (E16-E20). In the chicken optic tectum, ADAM17 is expressed strongly in the neuroepithelium and the periventricular stratum and moderately in the neurons of the stratum griseum centrale, but weakly or not at all in the other more superficial tectal strata and in blood vessels.

When ADAM17 was overexpressed in the chicken developing optic tectum by ex ovo electroporation (gain-of-function study), the morphology of blood vessel dramatically changed compared to the wild-type. We showed that the observed thickening of the blood vessel wall was due to a significant increase in the number of pericytes surrounding the endothelial cells. My results indicate that ADAM17 overexpression can change the morphology of blood vessels and, as a consequence, possibly remodel the blood-brain barrier (BBB) in the developing tectum. Because ADAM17 is a protease for many substrates, it is conceivable that the overexpression of ADAM17 might change the extracellular matrix environment of the CNS blood vessels, which, in turn, may result in the observed hypertrophy of the blood vessel wall. Of course, additional experiments will have to confirm this hypothesis.

Pericytes have an important role in the formation of the BBB, a highly regulated membranous barrier of CNS capillaries (Engelhardt, 2003; Lai and Kuo, 2005). The main function of the BBB is to protect the brain from the intrusion of harmful substances. Changes in the BBB are observed in different kinds of nervous system diseases. Endothelial cells with their tight junctions constitute the main component of the BBB. However, pericytes are essential for the formation, maturation, and maintenance of the normal microvascular structure of the endothelial wall and its function. The molecular mechanisms, which regulate BBB permeability, remain poorly understood. My results suggest that ADAM17 may be a candidate molecule to contribute to the formation of the BBB.

Not only ADAM17, but also ADAM10 and ADAM15 are known to be involved in angiogenesis (van Hinsbergh et al., 2006). For example, ADAM15 is strongly expressed in endothelial cells; however, there is no major developmental defect or pathological phenotype in ADAM15-deficient mice, which prompted an evaluation of its role in neovascularization (Horiuchi et al., 2003, 2005). My results have confirmed that ADAM9 and ADAM10 are both expressed in blood vessels of the developing brain, but not in the mature brain (Publication 4). It will be interesting to investigate the angiogenetic function of these additional ADAM members.

To study gene function, the overexpression (gain-of-function) strategy was used successfully in our group in the electroporated chicken embryo (Treubert-Zimmermann et al., 2002; Luo and Redies, 2004, 2005; Luo et al., 2004, 2006). Analysis of loss-of-function experiments is a more common approach to study gene function. For example, in our group, Gänzler-Odenthal and Redies (1998) blocked successfully the function of N-

cadherin in the embryonic chicken brain with a specific antiserum, but this method depends on the availability of a functionally blocking antibody. Luo and Redies (2004) tried the plasmid-mediated antisense expression of Cdh6 and Cdh7 by electroporation as well, but they did not find a striking difference in mRNA levels between the wild type and the antisense expression. Recently, double-stranded RNA (dsRNA) has been shown to mediate sequence-specific post-transcription gene silencing. This methodology has become well known as RNA interference (RNAi; Caplen, 2002; Hannon, 2002). Recently, RNAi has been established as a convenient tool to analyze the function of genes of interest in invertebrates and vertebrates (Sato et al., 2004). Most RNAi experiments are being performed at the cellular level in combination with cell culture. As described in the Introduction, chicken embryos provide an ideal model system to investigate vertebrate embryogenesis. Thus, the establishment of RNAi in chicken embryos in combination with in vivo electroporation would provide a powerful method to analyze the function of genes expressed during embryogenesis. Small interfering RNA (siRNA) as a quick and simple method has been used for silencing the exogenous and endogenous gene expression in chicken embryogenesis (Rao et al., 2004). Vector-based RNAi has been used in different reports (Katahira and Nakamura, 2003; Chesnutt and Niswander, 2004; Dai et al., 2005; Das et al., 2006). Virus-based RNAi, using the replication-competent avian splice (RCAS) retrovirus, was successfully applied to the developing chicken retina (Harpavat and Cepko, 2006). In the future, these or similar plasmid-based RNAi approaches combined with in vivo electroporation will provide a powerful tool to investigate gene function in the chicken embryo.

5.2 Cadherins are markers to analyze functional pattern formation in the nervous system

The precise and complicated structure of the CNS is intimately associated with its mature functions and requires a multitude of cell-cell interactions. Many cell recognition molecules that mediate cell-cell interactions are implicated in neural development. Therefore, isolating and understanding these cell adhesion molecules will help us to elucidate the mechanisms of brain development. Cadherins are one of the largest and best-investigated families of cell adhesion molecules. As surface glycoproteins, which are critical to normal embryonic development, cadherins are directly involved in a wide variety of processes such as cell adhesion, cell sorting, cell survival, morphogenesis, formation of intercellular junctions, maintenance of tissue integrity and tumorigenesis.

Both reduced and inappropriate expression of cadherins has been associated with abnormal tissue formation in embryos and tumorigenesis in mature organisms (Takeichi, 1991; Hirano et al., 2003; Redies et al, 2005).

The expression of the various cadherin family members is regulated in a complex pattern during embryogenesis. For example, Kim et al. (2007) examined the spatiotemporal distribution of mRNAs for 12 delta-protocadherins (non-clustered Pcdhs) in rat brain using in situ hybridization. Some of them (Pcdh1, Pcdh7, Pcdh9, Pcdh10, Pcdh11, Pcdh17, and Pcdh20) showed region-dependent expression patterns in the brain during the early postnatal stage. Hertel et al. (2008) analyzed the expression patterns of 12 different classic cadherins and delta-protocadherins in the basal ganglia of the postnatal and adult mouse by in situ hybridization, and their results suggest that cadherins provide a code of potentially adhesive cues, which specify not only patch and matrix compartments but also multiple molecular gradients within the mouse basal ganglia. Krishna et al. (2008) cloned 16 members of the classic cadherin and delta-protocadherin subfamilies from ferret brain. They demonstrated that almost all of these molecules are expressed in spatiotemporally restricted profiles throughout visual cortical development. Differential expression was observed not only in the layers of the developing visual cortex but also in subsets of neurons within the cortical layers.

In chicken embryos, the expression patterns and possible functions of N-Cdh, R-Cdh, Cdh6, Cdh7, Cdh8, Cdh10, Pcdh7 and Pcdh10 have been investigated in the CNS by several groups, including our own group (Redies et al., 2002a,b; Treubert-Zimmermann et al., 2002; Heyers et al., 2003, 2004; Becker and Redies, 2003; Müller et al., 2004; Luo et al., 2004; Luo and Redies, 2004; Neudert and Redies, 2008; Publication 3). Chicken Cdh20 (MN-cadherin) is expressed exclusively in lateral motor column of lumbar region in the spinal cord from E4 to E10 (Shirabe et al., 2005). In the spinal cord, chicken Pcdh10 (OL-protocadherin) was specifically expressed in motor neurons, and the protein was distributed along motor nerves (Nakao et al., 2005). For a few cadherins, their regulation by gene regulatory factors has also been studied. For example, the regionalized expression of Cdh7 in a restricted region of the spinal cord neuroepithelium is regulated by Shh and Pax7 during development (Luo et al., 2006). However, there are still some members of cadherin family that are poorly understood at both the expression level and the functional level in the CNS.

In conclusion, the regionally restricted expression of individual cadherins in the developing brain is well established. Other organs, such as the kidney, also express

multiple cadherins in differential patterns, but in different types of tissues (Perantoni, 1999). In this work, I mapped the expression of multiple cadherins in an organ that undergoes a highly complex morphogenesis during its development, the inner ear. Although some cadherins have been shown to be expressed during inner ear development, my study is the first to systematically compare the expression patterns of multiple cadherins in the inner ear (Publication 2). My results show that the neural tube and the ear vesicle, which both derive from the ectoderm, are subject to a similarly complex spatiotemporal regulation of expression. In another project, I asked whether three isoforms of a classic cadherin (Cdh8) also differ in their spatiotemporal regulation in the developing brain and possibly contribute to nervous system complexity (Publication 3). The answer to this question, however, was negative.

5.2.1 Cadherin expression in the developing chicken cochlea

The expression of the eight classic cadherins (N-Cdh, R-Cdh, Cdh6B, Cdh7, Cdh8, Cdh11, Cdh19 and Cdh20) was investigated in the developing chicken cochlea (Publication 2). Respectively, the expression of Cdh6B and N-Cdh was demonstrated in the hair cells, while Cdh8, Cdh11, and N-Cdh mRNAs were present in the supporting cells of the basilar papilla. Hair cells and supporting cells share a common progenitor cell during chicken cochlear development (Weisleder et al., 1995; Fekete et al., 1998). Supporting cells can differentiate into hair cells when hair cells are destroyed by acoustic noise or ototoxic drugs (Girod et al., 1989; Adler and Raphael, 1996; Roberson et al., 2004; Yamagata et al., 2006). It is remarkable that N-Cdh signalling can induce cell proliferation of both hair cells and supporting cells. The blocking of N-Cdh function results in an inhibition of the proliferation of hair cells and supporting cells (Warchol, 2002). Therefore, the expression of cadherins in the supporting cells and the hair cells may have an effect on the differentiation of the supporting cells and the hair cells during normal chicken cochlear development.

However, R-Cdh and Cdh11 were exclusively expressed by the homogene cells of the chicken cochlea, which are involved in the formation of the tectorial membrane during chicken cochlear development (Tanaka and Smith, 1975; Cohen and Fermin, 1985). The temporal profile of R-Cdh and Cdh11 expression in the homogene cells may relate to the generation of the tectorial membrane. Interestingly, Cdh7, Cdh19, and Cdh20 were expressed in an overlapping manner during cochlear development in the chicken. Cdh19 was transcribed by the spindle-shaped cells, Cdh20 in the acoustic ganglion cells, and

Cdh7 in both of them. This result suggests that the regulation of gene expression for these three closely related cadherins, which are located at the same chromosomal location of the human genome (Kools et al., 2000), is only partially diverged in the cochlea and may coregulate the development of the spindle-shaped cells and the acoustic ganglion cells. In the cochlea, the projection of peripheral receptive regions onto auditory structures of the CNS is tonotopically organized. The guidance of the nerve fibres mediating this tonotopic projection is therefore of special interest. Several CAMs have been found to be involved in the guidance of the extension of the neurites from the acoustic ganglion to their target hair cells (Richardson et al., 1987; Kajikawa et al., 1997). The present study reveals that R-Cdh, N-Cdh, and Cdh7 are coexpressed by the neurites of the acoustic ganglion axons and that N-Cdh and R-Cdh are also coexpressed in the areas of contact between the neurite terminals and the hair cells. Previous studies have demonstrated that R-Cdh, N-Cdh, and Cdh7 play an important role in neurite outgrowth and fasciculation, in synaptogenesis and/or in synaptic plasticity during embryonic development (Redies et al., 1992, Redies, 1995; Fannon and Colman, 1996; Riehl et al., 1996; Tanaka et al., 2000; Treubert-Zimmermann et al., 2002). Therefore, the three cadherins may be involved in the guidance of neurites from the acoustic ganglion to the sensory epithelium and in synaptogenesis with the target cells. Together, the expression of the eight classic cadherins in the developing cochlea suggests a role for cadherins in the genesis of the auditory system, for example, in the formation of hair cells and in the guidance of the neurites of acoustic ganglion to their target hair cells.

5.2.2 Cadherin 8 expression in the embryonic chicken brain

Cdh8 has been identified in human (Shimoyama et al., 2000), mouse (Korematsu and Redies, 1997a, b), and rat (Kido et al., 1998). The complete chicken Cdh8 cDNA sequence (Cdh8-3) was published in Publication 2. Chicken Cdh8-3 cDNA has high similarity with human, mouse, and rat Cdh8 (80% identities and higher); similarity to human Cdh8 is highest. The structural similarity between the Cdh8 genes of these species demonstrates that Cdh8 is a gene highly conserved between higher vertebrates. From RACE results, I found that chicken Cdh8 has two other isoforms (Cdh8-1 and Cdh8-2) generated by alternative mRNA splicing. It has been reported previously that Cdh8 is expressed in two isoforms in rat, a complete isoform and a truncated isoform that lacks the trans-membrane domain and the cytoplasmic tail (Kido et al., 1998). Isoforms of some other type II classic cadherins have also been reported (PB-Cdh, Sugimoto et al., 1996; Cdh11, Kawaguchi et

al., 1999; and Cdh7, Kawano et al., 2002). The function of all these short variants of classic cadherins remains to be investigated. Shimoyama et al. (2000) demonstrated that, like other classic cadherins, the long isoform of Cdh8 regulates cell-cell binding. The two short isoforms of chicken Cdh8 might also have adhesive function because the extracellular domain of classic cadherins serves as the interface for cell-cell binding and determines binding specificity (Takeichi, 1991).

Structural analysis revealed that the extracellular domains form structural units whose dimerization is crucial for their adhesive activity (Shapiro et al., 1995; Nagar et al., 1996; Elste and Benson, 2006; Pokutta and Weis, 2007). Whether the short unique sequences of the short isoforms at the site of truncation have a special role in cell adhesion or other functions of Cdh8 remains unclear. For rat Cdh8, Kido et al. (1998) did not demonstrate an adhesive function of the truncated isoform.

The complete Cdh8 isoform (Cdh8-3) is expressed in the supporting cells of the basilar papilla in the chicken developing cochlea (Publication 2), and expression is temporally and spatially regulated also in the embryonic brain (Publication 3). The in situ hybridization study revealed a restricted pattern of Cdh8-3 expression in a subset of gray matter structures in the late embryonic chicken brain. Other classic cadherins are expressed in a similarly restricted pattern in the embryonic chicken brain, for example N-Cdh, R-Cdh, Cdh6B, Cdh7 (Redies et al., 2000, 2001), and Cdh10 (Fushimi et al., 1997). The Cdh8-3 expression pattern is different from that of these other cadherins, although there is a partial overlap in some areas. According to the expression pattern of chicken Cdh8 in the developing brain, Cdh8 can possibly contribute to the adhesive code that is postulated to regulate morphogenesis and functional differentiation of the chicken brain during embryogenesis.

The two shorter isoforms (Cdh8-1 and Cdh8-2) are expressed weakly compared to the long isoform (Cdh8-3). Although some evidence for a differential regulation of the three isoforms in the major brain regions was obtained by semi-quantitative RT-PCR, I could not observe a differential expression of the two shorter isoforms at the regional level by in situ hybridization because expression levels of Cdh8-1 and Cdh8-2 were too low to be detected by this method. Consequently, it remains unclear whether all three isoforms contribute to the adhesive code of developing brain structures to the same degree or in a similar way.

A function of Cdh8 in neural circuit formation and synaptogenesis has been demonstrated in the somatosensory system of Cdh8-deficient mice (Suzuki et al., 2007).

Their results showed that Cdh8 is essential for establishing the physiological coupling between cold-sensitive sensory neurons and their target neurons in dorsal horn of the spinal cord. There is a relatively large degree of phylogenetic conservation of Cdh8 expression between chicken and mouse. It will be interesting to analyze the possible functions of the three Cdh8 isoforms during chicken embryonic development by appropriate experimental methods also in chicken. Suitable methods of investigation would be gain-of-function or loss-of-function studies of these isoforms in conjunction with in vivo electroporation.

5.3 Interaction between ADAMs and cadherins

The main identified functions of ADAMs are substrate shedding through the metalloprotease domain and cell-cell or cell-matrix adhesion mediated by the disintegrin domain (Blobel, 2005; Lu et al., 2007). For the function of cadherins, the release of their extracellular domain containing the homophilic binding cites is important to regulate cell adhesion, cell migration, and neurite outgrowth (Paradies and Grunwald, 1993; Nakagawa and Takeichi, 1998). For N-Cdh, this ectodomain cleavage is inhibited by tissue inhibitors of metalloproteinases (TIMPs). Furthermore, TIMPs promote fibroblast adhesion through stabilization of focal adhesion contacts. This stabilization was correlated with an increase of N-Cdh expression (Ho et al., 2001). Recently, it has been found that ADAM10 is responsible for the shedding of different cadherins (Reiss et al., 2005, 2006; Maretzky et al., 2005, 2008; Schulz et al., 2008). The knock-down of ADAM10 expression by different methods (in ADAM10-deficient mice, or with siRNA or a specific inhibitor) results in an increase of cell adhesion. As mentioned in the Introduction, ADAM10 can not only shed N-Cdh to decrease cell adhesion, but also affect its distribution in fibroblasts (Reiss et al., 2005). ADAM10 is also responsible for E-Cdh cleavage, which regulates epithelial cell adhesion and migration and affects E-Cdh subcellular localization (Maretzky et al., 2005). Maretzky et al. (2008) also revealed that ADAM10 is involved in regulating E-Cdh cell-surface expression in the diseased human skin. An increase in the level of active ADAM10 leads to a loss of E-Cdh from the cell surface and decreases keratinocyte cohesion. In another experimental study, ADAM10 inhibitor and siRNA transfection both were able to block the constitutive shedding of gamma-Pcdh C3 and modulated the cell adhesion (Reiss et al., 2006). Moreover, through the shedding of VE-Cdh, ADAM10 can regulate the endothelial permeability and T-cell transmigration (Schulz et al., 2008). Interestingly, it is ADAM10, not ADAM9, ADAM15 or ADAM17, that sheds these cadherins and regulates cell adhesion. Because half of all members of the ADAM family display metalloprotease

activity, we must ask whether other ADAMs have the same or a similar function as ADAM10, or if ADAM10 can shed other cadherins. The present results on the distribution of ADAMs in the developing chicken brain and similar expression data on cadherins may help to put forward specific hypotheses on possible interactions between members of the two gene families and the role of these interactions in regional brain development.

6. SUMMARY

Introduction: Cell adhesion molecules (CAMs) play various roles during embryonic development. Cadherins are a large superfamily of CAMs that mediate cell-cell adhesion and signaling transduction by a calcium-dependent mechanism. The ADAM family of genes can also be considered a family of CAMs, because their disintegrin domain binds integrin to mediate cell-cell or cell-matrix interactions, and their cysteine-rich domain and epidermal growth factor-like domain both are able to modify cell-cell adhesion. Moreover, many ADAMs are metalloproteases that shed different trans-membrane proteins, such as cadherins. However, the expression patterns and potential functions of most ADAMs and some cadherins remain poorly understood. In the present thesis, I cloned seven members of the ADAM family and a multiple cadherins from the chicken embryo, and investigated their molecular characteristics and expression profiles during chicken embryonic development.

Methods: Fertilized eggs were incubated in a forced-draft incubator at 37°C and 65% humidity until the embryos reached the desired stage. Total RNA was isolated from different stages and partial or full-length cDNAs of the ADAMs and cadherins of interest were cloned by RT-PCR or RACE. The temporal expression profiles of each gene were analyzed with semi-quantitative RT-PCR during chicken embryonic development. Northern blot was performed to determine the amount and size of chicken cadherin-8 isoforms as well. Results from semi-quantitative RT-PCR and Northern blot were further analyzed by appropriate statistic methods. The temporal and spatial expression patterns of the cloned molecules were investigated using in situ hybridization of sections or whole mount specimens. Appropriate protein markers helped to confirm the identity of expression areas by immunostaining. To investigate the function of chicken ADAM17, an overexpression (gain-of-function) experiment was performed using in vivo (ex ovo) electroporation of the embryonic chicken tectum.

Results: I obtained the novel full-length sequences of chicken ADAM12, ADAM13, ADAM22, Cdh8 and Cdh19. The expression pattern of ADAM13 was investigated in detail in the chicken embryo throughout the developing organism. The expression patterns of eight chicken cadherins (N-Cdh, R-Cdh, Cdh6, Cdh7, Cdh8, Cdh11, Cdh18 and Cdh20) were analyzed in the developing cochlea at older embryonic stages. I confirmed that

chicken Cdh8 possesses three isoforms from mRNA alternative splicing and analyzed their temporal and spatial expression in the chicken embryonic brain. Five ADAMs investigated (ADAM9, ADAM10, ADAM12, ADAM22, ADAM23) show different types of expression patterns in the developing chicken brain. Finally, ADAM17 overexpression (gain-of-function) resulted in a morphological change of the blood vessels in the developing tectum. This change coincided with an increase in the number of pericytes.

Conclusions: Our results indicate that chicken ADAM13 is expressed more widely during embryonic development than was previously known for *Xenopus* ADAM13. In the developing cochlea, different classic cadherins show restricted expression patterns, similar to their expression in the brain. Cdh8 has three transcript variants from mRNA alternative splicing, all of which show temporal and spatial expression profiles during chicken embryonic brain development by RT-PCR, but only the long isoform was expressed in amounts high enough to be detected by in situ hybridization. Unlike cadherins, the five investigated ADAMs exhibit general spatiotemporal expression patterns in brain tissue that are rather different for each ADAM, suggesting various roles for different ADAMs in brain development. Additionally, I show that ADAM17 overexpression increases the wall thickness of the blood vessels in the tectum by increasing the number of pericytes. I speculate that the observed increase in the number of pericytes is caused by a remodeling of the extra-cellular matrix environment of vascular cells due to ADAM17-induced changes in cell-matrix interactions, matrix protein shedding, or cell signal transduction.

7. ZUSAMMENFASSUNG

Einleitung: Zelladhäsionsmoleküle (CAMs) spielen in der Embryonalentwicklung vielfältige Rollen. Cadherine, eine Großfamilie der CAMs, vermitteln in Abhängigkeit von Calciumionen Zell-Zell-Adhäsion und Signaltransduktion. Die ADAM-Gen-Familie kann ebenfalls als eine Familie der CAMs angesehen werden, da ihre Disintegrin-Domäne durch Bindung an Integrin Zell-Zell-Adhäsion und Zell-Matrix-Adhäsion vermittelt. Mit Hilfe ihrer Cystein-reichen Domäne und der Epidermal-Growth-Factor-Domäne können ADAMs die Zell-Zell-Adäsion auch modulieren. Die überwiegende Anzahl von ADAMs sind Metalloproteinasen, die verschiedene transmembranäre Proteine, wie zum Beispiel Cadherine, spalten können. Jedoch sind die Expressionsmuster und mögliche Funktionen der meisten ADAMs und einiger Cadherine nicht gut erforscht. Daher klonierte ich in meiner Dissertation sieben Mitglieder der ADAM-Familie und mehrere Cadherine aus dem Huhnembryo und untersuchte ihre molekularen Eigenschaften und Expressionsprofile während der embryonalen Entwicklung des Huhns.

Methoden: Befruchtete Hühnereier wurden in einem Frischluftinkubator bei 37°C und 65% Luftfeuchtigkeit inkubiert, bis die Embryonen das gewünschte Altersstadium erreicht hatten. Die gesamte RNA wurde für unterschiedliche Stadien isoliert und cDNA-Fragmente oder cDNAs gesamter Länge von ADAM-Molekülen und Cadherinen wurden mit RT-PCR oder RACE kloniert. Das zeitliche Expressionsprofil jedes isolierten Genes wurde mit semi-quantitativer RT-PCR bestimmt. Mit der Northern-Blot-Methode wurde für Cadherin-8 auch die Menge und Länge der im Huhn auftretenden Isoformen bestimmt. Die Ergebnisse der semi-quantitativen RT-PCR und der Northern-Blots wurden mit geeigneten statistischen Methoden ausgewertet. Das zeitlich-räumliche Expressionsmuster der klonierten Moleküle analysierte ich mittels *In situ*-Hybridisierung sowohl auf Gewebeschnitten als auch an kompletten Embryonen. Verschiedene molekulare Marker dienten dazu, die Identität von anatomischen Strukturen zu verifizieren. Um die Funktion von ADAM17 zu untersuchen, wurde dieses Gen im Huhnembryo durch *In vivo*-(*Ex ovo*-)Elektroporation im Tectum des Huhnembryos überexprimiert.

Ergebnisse: Ich klonierte bisher unbekannte cDNA-Sequenzen gesamter Länge von ADAM12, ADAM13, ADAM22, Cdh8 und Cdh19 des Huhns. Das Expressionsmuster von ADAM13 untersuchte ich im Detail während der gesamten Entwicklung des

Huhnembryos. Die Expressionsprofile acht verschiedener Cadherine (N-Cdh, R-Cdh, Cdh6, Cdh7, Cdh8, Cdh11, Cdh18 und Cdh20) wurden in der sich entwickelnden Cochlea in späten Entwicklungsstadien des Huhns näher betrachtet. Ich bestätigte, dass es im Huhn drei Isoformen von Cdh8 gibt, die aufgrund von alternativem mRNA-Splicing entstehen, und untersuchte deren räumlich-zeitliche Expression im Gehirn des Huhnembryos. Fünf von mir untersuchte ADAMs (ADAM9, ADAM10, ADAM12, ADAM22 und ADAM23) wiesen unterschiedliche Expressionsprofile im Gehirn des Huhnembryos auf. Die Überexpression von ADAM17 im sich entwickelnden Tectum des Huhns resultierte in einer morphologischen Veränderung der Blutgefäßwände, die mit einer Vermehrung von Perizyten einherging.

Schlussfolgerungen: Die Ergebnisse zeigen, dass ADAM13 im Huhnembryo in mehr Organen exprimiert wird, als bisher für ADAM13 in der *Xenopus*-Entwicklung bekannt war. In der sich entwickelnden Cochlea des Huhns weisen verschiedene klassische Cadherine räumlich beschränkte Expressionsmuster auf und ähneln darin den Expressionsmustern im Gehirn. Cdh8 kommt in drei verschiedenen mRNA-Transkripten vor, die alle spezifische räumlich-zeitlich beschränkte Expressionsmuster im embryonalen Gehirn des Huhns aufweisen, wobei allerdings nur die lange Isoform so stark exprimiert ist, das es für den Nachweis mit der *In situ*-Hybridisierung ausreicht. Anders als die Cadherine besitzen die fünf untersuchten ADAMs zeitlich-räumliche Expressionsmuster, die sich voneinander generell unterscheiden, was auf unterschiedliche Funktionen dieser ADAMs bei der Gehirnentwicklung hinweist. Des weiteren konnte ich durch die Überexpression von ADAM17 zeigen, dass die morphologische Veränderung in den Wänden der Blutgefäße auf eine größere Anzahl von Perizyten zurückzuführen ist. Dieser Anstieg lässt sich möglicherweise auf Veränderungen der extrazellulären Matrix in der Umgebung der Blutgefäße zurückführen, welche wiederum durch ADAM17-induzierte Modifikationen der Zell-Matrix-Interaktionen, Matrix-Proteinspaltung oder Signaltransduktion hervorgerufen sein können.

8. REFERENCES

Adler HJ, Raphael Y. 1996. New hair cells arise from supporting cell conversion in the acoustically damaged chick inner ear. *Neurosci Lett,* 205:17-20.

Agiostratidou G, Hulit J, Phillips GR, Hazan RB. 2007. Differential cadherin expression: potential markers for epithelial to mesenchymal transformation during tumor progression. *J Mammary Gland Biol Neoplasia,* 12:127-133.

Alfandari D, Cousin H, Gaultier A, Smith K, White JM, Darribère T, DeSimone DW. 2001. Xenopus ADAM 13 is a metalloprotease required for cranial neural crest-cell migration. *Curr Biol,* 11:918-930.

Alfandari D, Wolfsberg TG, White JM, DeSimone DW. 1997. ADAM 13: a novel ADAM expressed in somitic mesoderm and neural crest cells during Xenopus laevis development. *Dev Biol,* 182:314-330.

Anders A, Gilbert S, Garten W, Postina R, Fahrenholz F. 2001. Regulation of the alpha-secretase ADAM10 by its prodomain and proprotein convertases. *FASEB J,* 15:1837-1839.

Arndt K, Nakagawa S, Takeichi M, Redies C. 1998. Cadherin-defined segments and parasagittal cell ribbons in the developing chicken cerebellum. *Mol Cell Neurosci,* 10:211-228.

Arndt K, Redies C. 1996. Restricted expression of R-cadherin by brain nuclei and neural circuits of the developing chicken brain. *J Comp Neurol,* 373:373-399.

Arndt K, Redies C. 1998. Development of cadherin-defined parasagittal subdivisions in the embryonic chicken cerebellum. *J Comp Neurol,* 401:367-381.

Asai M, Hattori C, Szabó B, Sasagawa N, Maruyama K, Tanuma S, Ishiura S. 2003. Putative function of ADAM9, ADAM10, and ADAM17 as APP alpha-secretase. *Biochem Biophys Res Commun,* 301:231-235.

Asayesh A, Alanentalo T, Khoo NK, Ahlgren U. 2005. Developmental expression of metalloproteases ADAM 9, 10, and 17 becomes restricted to divergent pancreatic compartments. *Dev Dyn,* 232:1105-1114.

Becker T, Redies C. 2003. Internal structure of the nucleus rotundus revealed by mapping cadherin expression in the embryonic chicken visual system. *J Comp Neurol,* 467:536-548.

Bellairs R, Osmond M. 2005. The atlas of chicken development. Second edition, Elsevier Academic Press. San Diego, USA.

Bernstein HG, Keilhoff G, Bukowska A, Ziegeler A, Funke A, Dobrowony H, Kanakis D, Bogerts B, Lendeckel U. 2004. ADAM (a disintegrin and metalloprotease) 12 is expressed in rat and human brain and localized to oligodendrocytes. *J Neurosci Res,* 75:353-360.

Black RA, White JM. 1998. ADAMs: focus on the protease domain. *Curr Opin Cell Biol,* 10:654-659.

Blanchot-Jossic F, Jarry A, Masson D, Bach-Ngohou K, Paineau J, Denis MG, Laboisse CL, Mosnier JF. 2005. Up-regulated expression of ADAM17 in human colon carcinoma: co-expression with EGFR in neoplastic and endothelial cells. *J Pathol,* 207:156-163.

Blobel CP. 2002. Functional and biochemical characterization of ADAMs and their predicted role in protein ectodomain shedding. *Inflamm Res,* 51:83-84.

Blobel CP. 2005. ADAMs: key components in EGFR signalling and development. *Nat Rev Mol Cell Biol,* 6:32-43.

Boissy P, Lenhard TR, Kirkegaard T, Peschon JJ, Black RA, Delaisse JM, del Carmen Ovejero M. 2003. An assessment of ADAMs in bone cells: absence of TACE activity prevents osteoclast recruitment and the formation of the marrow cavity in developing long bones. *FEBS Lett,* 553:257-261.

Bosse F, Petzold G, Greiner-Petter R, Pippirs U, Gillen C, Muller HW. 2000. Cellular localization of the disintegrin CRII-7/rMDC15 mRNA in rat PNS and CNS and regulated expression in postnatal development and after nerve injury. *Glia,* 32:313-327.

Brown WR, Hubbard SJ, Tickle C, Wilson SA. 2003. The chicken as a model for large-scale analysis of vertebrate gene function. *Nat Rev Genet,* 4:87-98.

Caldwell RB, Kierzek AM, Arakawa H, Bezzubov Y, Zaim J, Fiedler P, Kutter S, Blagodatski A, Kostovska D, Koter M, Plachy J, Carninci P, Hayashizaki Y, Buerstedde JM. 2005. Full-length cDNAs from chicken bursal lymphocytes to facilitate gene function analysis. *Genome Biol,* 6:R6.

Caplen NJ. 2002. A new approach to the inhibition of gene expression. *Trends Biotechnol,* 20:49-51.

Carrodeguas JA, Rodolosse A, Garza MV, Sanz-Clemente A, Pérez-Pé R, Lacosta AM, Domínguez L, Monleón I, Sánchez-Díaz R, Sorribas V, Sarasa M. 2005. The chick embryo appears as a natural model for research in beta-amyloid precursor protein processing. *Neuroscience,* 134:1285-1300.

Chantry A, Gregson N, Glynn P. 1992. Degradation of myelin basic protein by a

membrane-associated metalloprotease: neural distribution of the enzyme. *Neurochem Res,* 17:861-867.

Chen YY, Hehr CL, Atkinson-Leadbeater K, Hocking JC, McFarlane S. 2007. Targeting of retinal axons requires the metalloproteinase ADAM10. *J Neurosci,* 27:8448-8456.

Chesnutt C, Niswander L. 2004. Plasmid-based short-hairpin RNA interference in the chicken embryo. *Genesis,* 39:73-78.

Choi YK, Kim KW. 2008. Blood-neural barrier: its diversity and coordinated cell-to-cell communication. *BMB Rep,* 41:345-352.

Cohen GM, Fermin CD. 1985. Development of the embryonic chick's tectorial membrane. *Hear Res,* 18:29-39.

Dai F, Yusuf F, Farjah GH, Brand-Saberi B. 2005. RNAi-induced targeted silencing of developmental control genes during chicken embryogenesis. *Dev Biol,* 285:80-90.

Das RM, Van Hateren NJ, Howell GR, Farrell ER, Bangs FK, Porteous VC, Manning EM, McGrew MJ, Ohyama K, Sacco MA, Halley PA, Sang HM, Storey KG, Placzek M, Tickle C, Nair VK, Wilson SA. 2006. A robust system for RNA interference in the chicken using a modified microRNA operon. *Dev Biol,* 294:554-563.

DeLisser HM, Christofidou-Solomidou M, Strieter RM, Burdick MD, Robinson CS, Wexler RS, Kerr JS, Garlanda C, Merwin JR, Madri JA, Albelda SM. 1997. Involvement of endothelial PECAM-1/CD31 in angiogenesis. *Am J Pathol,* 151:671-677.

Dore-Duffy P. 2008. Pericytes: pluripotent cells of the blood brain barrier. *Curr Pharm Des,* 14:1581-1593.

Duffy MJ, Lynn DJ, Lloyd AT, O'Shea CM. 2003. The ADAMs family of proteins: from basic studies to potential clinical applications. *Thromb Haemost,* 89:622-631.

Elste AM, Benson DL. 2006. Structural basis for developmentally regulated changes in cadherin function at synapses. *J Comp Neurol,* 495:24-35.

Engelhardt B. 2003. Development of the blood-brain barrier. *Cell Tissue Res,* 314:119-129.

Fambrough D, Pan D, Rubin GM, Goodman CS. 1996. The cell surface etalloprotease/ disintegrin Kuzbanian is required for axonal extension in Drosophila. *Proc Natl Acad Sci USA,* 93:13233-13238.

Fannon AM, Colman DR. 1996. A model for central synaptic junctional complex formation based on the differential adhesive specificities of the cadherins. *Neuron,* 17:423-434.

Fekete DM, Muthukumar S, Karagogeos D. 1998. Hair cells and supporting cells share a common progenitor in the avian inner ear. *J Neurosci,* 18:7811-7821.

Fushimi D, Arndt K, Takeichi M, Redies C. 1997. Cloning and expression analysis of cadherin-10 in the CNS of the chicken embryo. *Dev Dyn,* 209:269-285.

Gänzler-Odenthal SI, Redies C. 1998. Blocking N-cadherin function disrupts the epithelial structure of differentiating neural tissue in the embryonic chicken brain. *J Neurosci,* 18:5415-5425.

Gaultier A, Cousin H, Darribère T, Alfandari D. 2002. ADAM13 disintegrin and cysteine-rich domains bind to the second heparin-binding domain of fibronectin. *J Biol Chem,* 277:23336-23344.

Gerhardt H, Liebner S, Redies C, Wolburg H. 1999. N-cadherin expression in endothelial cells during early angiogenesis in the eye and brain of the chicken: relation to blood-retina and blood-brain barrier development. *Eur J Neurosci,* 11:1191-1201.

Gerhardt H, Liebner S, Wolburg H. 1996. The pecten oculi of the chicken as a new in vivo model of the blood-brain barrier. *Cell Tissue Res,* 285:91-100.

Gerhardt H, Rascher G, Schuck J, Weigold U, Redies C, Wolburg H. 2000a. R- and B-cadherin expression defines subpopulations of glial cells involved in axonal guidance in the optic nerve head of the chicken. *Glia,* 31:131-143.

Gerhardt H, Wolburg H, Redies C. 2000b. N-cadherin mediates pericytic-endothelial interaction during brain angiogenesis in the chicken. *Dev Dyn,* 218:472-479.

Gerst JL, Raina AK, Pirim I, McShea A, Harris PL, Siedlak SL, Takeda A, Petersen RB, Smith MA. 2000. Altered cell-matrix associated ADAM proteins in Alzheimer disease. *J Neurosci Res,* 59:680-684.

Gilpin BJ, Loechel F, Mattei MG, Engvall E, Albrechtsen R, Wewer UM. 1998. A novel secreted form of human ADAM 12 (meltrin alpha) provokes myogenesis in vivo. *J Biol Chem,* 273:157-166.

Girod DA, Duckert LG, Rubel EW. 1989. Possible precursors of regenerated hair cells in the avian cochlea following acoustic trauma. *Hear Res,* 42:175-194.

Goddard DR, Bunning RA, Woodroofe MN. 2001. Astrocyte and endothelial cell expression of ADAM 17 (TACE) in adult human CNS. *Glia,* 34:267-271.

Goichberg P, Geiger B. 1998. Direct involvement of N-cadherin-mediated signaling in muscle differentiation. *Mol Biol Cell,* 9:3119-3131.

Goldsmith AP, Gossage SJ, ffrench-Constant C. 2004. ADAM23 is a cell-surface glycoprotein expressed by central nervous system neurons. *J Neurosci Res,* 78:647-

658.

Gunn TM, Azarani A, Kim PH, Hyman RW, Davis RW, Barsh GS. 2002. Identification and preliminary characterization of mouse ADAM33. *BMC Genet,* 3:2.

Hall RJ, Erickson CA. 2003. ADAM 10: an active metalloprotease expressed during avian epithelial morphogenesis. *Dev Biol,* 256:146-159.

Ham C, Levkau B, Raines EW, Herren B. 2002. ADAM15 is an adherens junction molecule whose surface expression can be driven by VE-cadherin. *Exp Cell Res,* 279:239-247.

Hamburger V, Hamilton HL. 1951. A series of normal stages in the development of the chick embryo. *J. Morphol,* 88, 49-92.

Hannon GJ. 2002. RNA interference. *Nature,* 418:244-251.

Harpavat S, Cepko CL. 2006. RCAS-RNAi: a loss-of-function method for the developing chick retina. *BMC Dev Biol,* 6:2.

Hartmann D, de Strooper B, Serneels L, Craessaerts K, Herreman A, Annaert W, Umans L, Lubke T, Lena Illert A, von Figura K, Saftig P. 2002. The disintegrin/metalloprotease ADAM 10 is essential for Notch signalling but not for α-secretase activity in fibroblasts. *Hum Mol Genet,* 11:2615-2624.

Hatta K, Takeichi M. 1986. Expression of N-cadherin adhesion molecules associated with early morphogenetic events in chick development. *Nature,* 320:447-449.

Hattori M, Osterfield M, Flanagan JG. 2000. Regulated cleavage of a contact-mediated axon repellent. *Science,* 289:1360-1365.

Hertel N, Krishna-K, Nuernberger M, Redies C. 2008. A cadherin-based code for the divisions of the mouse basal ganglia. *J Comp Neurol,* 508:511-528.

Heyers D, Kovjanic D, Redies C. 2003. Cadherin expression coincides with birth-dating patterns in patchy compartments of the developing chicken telencephalon. *J Comp Neurol,* 460:155-166.

Heyers D, Luksch H, Redies C. 2004. Selective synaptic cadherin expression by traced neurons of the chicken visual system. *Neuroscience,* 127:901-912.

Hirano S, Suzuki ST, Redies C. 2003. The cadherin superfamily in neural development: diversity, function and interaction with other molecules. *Front Biosci,* 8:d306-355.

Ho AT, Voura EB, Soloway PD, Watson KL, Khokha R. 2001. MMP inhibitors augment fibroblast adhesion through stabilization of focal adhesion contacts and up-regulation of cadherin function. *J Biol Chem,* 276:40215-40224.

Holgate ST, Yang Y, Haitchi HM, Powell RM, Holloway JW, Yoshisue H, Pang YY,

Cakebread J, Davies DE. 2006. The genetics of asthma: ADAM33 as an example of a susceptibility gene. *Proc Am Thorac Soc,* 3:440-443.

Horiuchi K, Weskamp G, Lum L, Hammes HP, Cai H, Brodie TA, Ludwig T, Chiusaroli R, Baron R, Preissner KT, Manova K, Blobel CP. 2003. Potential role for ADAM15 in pathological neovascularization in mice. *Mol Cell Biol,* 23:5614-5624.

Horiuchi K, Zhou HM, Kelly K, Manova K, Blobel CP. 2005. Evaluation of the contributions of ADAMs 9, 12, 15, 17, and 19 to heart development and ectodomain shedding of neuregulins beta1 and beta2. *Dev Biol,* 283:459-471.

Hotoda N, Koike H, Sasagawa N, Ishiura S. 2002. A secreted form of human ADAM9 has an alpha-secretase activity for APP. *Biochem Biophys Res Commun,* 293:800-805.

Huang X, Huang P, Robinson MK, Stern MJ, Jin Y. 2003. UNC-71, a disintegrin and metalloprotease (ADAM) protein, regulates motor axon guidance and sex myoblast migration in C. elegans. *Development,* 130:3147-3161.

Ju MJ, Aroca P, Luo J, Puelles L. and Redies, C. 2004. Molecular profiling indicates avian branchiomotor nuclei invade the hindbrain alar plate. *Neuroscience,* 128:785-796.

Kajikawa H, Umemoto M, Taira E, Miki N, Mishiro Y, Kubo T, Yoneda Y. 1997. Expression of neurite outgrowth factor and gicerin during inner ear development and hair cell regeneration in the chick. *J Neurocytol,* 26:501-509.

Kalus I, Bormann U, Mzoughi M, Schachner M, Kleene R. 2006. Proteolytic cleavage of the neural cell adhesion molecule by ADAM17/TACE is involved in neurite outgrowth. *J Neurochem,* 98:78-88.

Kärkkäinen I, Rybnikova E, Pelto-Huikko M, Huovila AP. 2000. Metalloprotease-disintegrin (ADAM) genes are widely and differentially expressed in the adult CNS. *Mol Cell Neurosci,* 15:547-560.

Katahira T, Nakamura H. 2003. Gene silencing in chick embryos with a vector-based small interfering RNA system. *Dev Growth Differ,* 45:361-367.

Kawaguchi J, Takeshita S, Kashima T, Imai T, Machinami R, Kudo A. 1999. Expression and function of the splice variant of the human cadherin-11 gene in subordination to intact cadherin-11. *J Bone Mineral Res,* 14:764-775.

Kawaguchi M, Mitsuhashi Y, Kondo S. 2004. Localization of tumour necrosis factor-alpha converting enzyme in normal human skin. *Clin Exp Dermatol,* 29:185-187.

Kawaguchi N, Xu X, Tajima R, Kronqvist P, Sundberg C, Loechel F, Albrechtsen R, Wewer UM. 2002. ADAM 12 protease induces adipogenesis in transgenic mice. *Am J Pathol,* 160:1895-1903.

Kawano R, Matsuo N, Tanaka H, Nasu M, Yoshioka H, Shirabe K. 2002. Identification and characterization of a soluble cadherin-7 isoform produced by alternative splicing. *J Biol Chem,* 277:47679-47685.

Kelly K, Hutchinson G, Nebenius-Oosthuizen D, Smith AJ, Bartsch JW, Horiuchi K, Rittger A, Manova K, Docherty AJ, Blobel CP. 2005. Metalloprotease-disintegrin ADAM8: expression analysis and targeted deletion in mice. *Dev Dyn,* 232:221-231.

Kerrigan JJ, McGill JT, Davies JA, Andrews L, Sandy JR. 1998. The role of cell adhesion molecules in craniofacial development. *J R Coll Surg Edinb,* 43:223-229.

Kheradmand F, Werb Z. 2002. Shedding light on sheddases: role in growth and development. *Bioessays,* 24:8-12.

Kido M, Obata S, Tanihara H, Rochelle JM, Seldin MF, Taketani S, Suzuki ST. 1998. Molecular properties and chromosomal location of cadherin-8. *Genomics,* 48:186-194.

Kieseier BC, Pischel H, Neuen-Jacob E, Tourtellotte WW, Hartung HP. 2003. ADAM-10 and ADAM-17 in the inflamed human CNS. *Glia,* 42:398-405.

Kim SY, Chung HS, Sun W, Kim H. 2007. Spatiotemporal expression pattern of non-clustered protocadherin family members in the developing rat brain. *Neuroscience,* 147:996-1021.

Kools P, Van Imschoot G, van Roy F. 2000. Characterization of three novel human cadherin genes (CDH7, CDH19, and CDH20) clustered on chromosome 18q22-q23 and with high homology to chicken cadherin-7. *Genomics,* 68:283-295.

Korematsu K, Redies C. 1997a. Cadherin-8 mRNA expression in the developing mouse central nervous system. *J Comp Neurol,* 387:291-306.

Korematsu K, Redies C. 1997b. Restricted expression of cadherin-8 in segmental and functional subdivisions of the embryonic mouse brain. *Dev Dyn,* 208:178-189.

Kovjanic D, Redies C. 2003. Small-scale pattern formation in a cortical area of the embryonic chicken telecephalon. *J Comp Neurol,* 456:95-104.

Krishna-K, Nuernberger M, Weth F, Redies C. 2008. Layer-specific expression of multiple cadherins in the developing visual cortex (V1) of the ferret. *Cereb Cortex,* Jun 4. [Epub ahead of print] doi:10.1093/cercor/bhn090.

Kronqvist P, Kawaguchi N, Albrechtsen R, Xu X, Schroder HD, Moghadaszadeh B, Nielsen FC, Frohlich C, Engvall E, Wewer UM. 2002. ADAM12 alleviates the skeletal muscle pathology in mdx dystrophic mice. *Am J Pathol,* 161:1535-1540.

Kurisaki T, Masuda A, Osumi N, Nabeshima Y, Fujisawa-Sehara A. 1998. Spatially- and temporally-restricted expression of meltrin alpha (ADAM12) and beta (ADAM19) in

mouse embryo. *Mech Dev,* 73:211-215.

Kurohara K, Komatsu K, Kurisaki T, Masuda A, Irie N, Asano M, Sudo K, Nabeshima Y, Iwakura Y, Sehara-Fujisawa A. 2004. Essential roles of Meltrin beta (ADAM19) in heart development. *Dev Biol,* 267:14-28.

Lai CH, Kuo KH. 2005. The critical component to establish in vitro BBB model: Pericyte. *Brain Res Brain Res Rev,* 50:258-265.

Leighton PA, Mitchell KJ, Goodrich LV, Lu X, Pinson K, Scherz P, Skarnes WC. Tessier-Lavigne M. 2001. Defining brain wiring patterns and mechanisms through gene trapping in mice. *Nature,* 410:174-179.

Lewis SL, Farlie PG, Newgreen DF. 2004. Isolation and embryonic expression of avian ADAM 12 and ADAM 19. *Gene Expr Patterns,* 5:75-79.

Lu X, Lu D, Scully MF, Kakkar VV. 2007. Structure-activity relationship studies on ADAM protein-integrin interactions. *Cardiovasc Hematol Agents Med Chem,* 5:29-42.

Luo J, Ju MJ, Redies C. 2006. Regionalized cadherin-7 expression by radial glia is regulated by Shh and Pax7 during spinal cord development. *Neuroscience,* 142:1133-1143.

Luo J, Redies C. 2004. Overexpression of genes in Purkinje cells in the embryonic chicken cerebellum by in vivo electroporation. *J Neurosci Meth,* 139:241-245.

Luo J, Redies C. 2005. Ex ovo electroporation for gene transfer into older chicken embryos. *Dev Dyn,* 233:1470-1477.

Luo J, Treubert-Zimmermann U, Redies C. 2004. Cadherins guide migrating Purkinje cells to specific parasagittal domains during cerebellar development. *Mol Cell Neurosci,* 25:138-152.

Luo Y, Ferreira-Cornwell M, Baldwin H, Kostetskii I, Lenox J, Lieberman M, Radice G. 2001. Rescuing the N-cadherin knockout by cardiac-specific expression of N- or E-cadherin. *Development,* 128:459-469.

Marcinkiewicz M, Seidah NG. 2000. Coordinated expression of betaamyloid precursor protein and the putative beta-secretase BACE and alpha-secretase ADAM10 in mouse and human brain. *J Neurochem,* 75:2133-2143.

Maretzky T, Reiss A, Ludwig A, Buchholz J, Felix Scholz F, Proksch E, Bart de Strooper, Hartmann H and Saftig P. 2005. ADAM10 mediates E-cadherin shedding and regulates epithelial cell-cell adhesion, migration, and β-catenin translocation. *Proc Natl Acad Sci USA,* 102:9182-9187.

Maretzky T, Scholz F, Köten B, Proksch E, Saftig P, Reiss K. 2008. ADAM10-mediated

E-cadherin release is regulated by proinflammatory cytokines and modulates keratinocyten cohesion in eczematous dermatitis. *J Invest Dermatol,* 128:1737-1746.

Miskevich F, Zhu Y, Ranscht B, Sanes JR. 1998. Expression of multiple cadherins and catenins in the chick optic tectum. *Mol Cell Neurosci,* 12:240-255.

Mitchell KJ, Pinson KI, Kelly OG, Brennan J, Zupicich J, Scherz P, Leighton PA, Goodrich LV, Lu X, Avery BJ, Tate P, Dill K, Pangilinan E, Wakenight P, Tessier-Lavigne M, Skarnes WC. 2001. Functional analysis of secreted and transmembrane proteins critical to mouse development. *Nat Genet,* 28:241-249.

Momose T, Tonegawa A, Takeuchi J, Ogawa H, Umesono K, Yasuda K. 1999. Efficient targeting of gene expression in chick embryos by microelectroporation. *Dev Growth Differ,* 41:335-344.

Müller K, Hirano S, Puelles L, Redies C. 2004. OL-protocadherin expression in the visual system of the chicken embryo. *J Comp Neurol,* 470:240-255.

Muramatsu T, Mizutani Y, Ohmori Y, Okumura J. 1997. Comparison of three nonviral transfection methods for foreign gene expression in early chicken embryos in ovo. *Biochem Biophys Res Commun,* 230:376-380.

Muramatsu T, Nakamura A, Park HM. 1998. In vivo electroporation: a powerful and convenient means of nonviral gene transfer to tissues of living animals. *Int J Mol Med,* 1:55-62.

Murase S, Cho C, White JM, Horwitz AF. 2008. ADAM2 promotes migration of neuroblasts in the rostral migratory stream to the olfactory bulb. *Eur J Neurosci,* 27:1585-1595.

Nagar B, Overduin M, Ikura M, Rini JM. 1996. Structural basis of calcium-induced E-cadherin rigidification and dimerization. *Nature,* 380:360-364.

Nakagawa S, Takeichi M. 1998. Neural crest emigration from the neural tube depends on regulated cadherin expression. *Development,* 125:2963-2971.

Nakao S, Uemura M, Aoki E, Suzuki ST, Takeichi M, Hirano S. 2005. Distribution of OL-protocadherin in axon fibers in the developing chick nervous system. *Brain Res Mol Brain Res,* 134:294-308.

Napolitano EW, Venstrom K, Wheeler EF, Reichardt LF. 1991. Molecular cloning and characterization of B-cadherin, a novel chick cadherin. *J Cell Biol,* 113:893-905.

Neudert F, Redies C. 2008. Neural circuits revealed by axon tracing and mapping cadherin expression in the embryonic chicken cerebellum. *J Comp Neurol,* 509:283-301.

Nishimura H, Kim E, Nakanishi T, Baba T. 2004. Possible function of the

ADAM1a/ADAM2 Fertilin complex in the appearance of ADAM3 on the sperm surface. *J Biol Chem,* 279:34957-34962.

Novak U. 2004. ADAM proteins in the brain. *J Clin Neurosci,* 11:227-235.

Novince ZM, Azodi E, Marrs JA, Raymond PA, Liu Q. 2003. Cadherin expression in the inner ear of developing zebrafish. *Gene Expr Patterns,* 3:337-339.

Ortiz RM, Karkkainen I, Huovila AP, Honkaniemi J. 2005. ADAM9, ADAM10, and ADAM15 mRNA levels in the rat brain after kainic acidinduced status epilepticus. *Brain Res Mol Brain Res,* 137:272-275.

O'Shea KS. 1987. Differential deposition of basement membrane components during formation of the caudal neural tube in the mouse embryo. *Development,* 99:509-519.

Paradies NE, Grunwald GB. 1993. Purification and characterization of NCAD90, a soluble endogenous form of N-cadherin, which is generated by proteolysis during retinal development and retains adhesive and neurite-promoting function. *J Neurosci Res,* 36:33-45.

Peinado H, Portillo F, Cano A. 2004. Transcriptional regulation of cadherins during development and carcinogenesis. *Int J Dev Biol,* 48:365-375.

Perantoni AO. 1999. Cell adhesion molecules in the kidney: from embryo to adult. *Exp Nephrol,* 7:80-102.

Peschon JJ, Slack JL, Reddy P, Stocking K L, Sunnarborg SW, Lee DC, Russell WE, Castner BJ, Johnson RS, Fitzner JN, Boyce RW, Nelson N, Kozlosky CJ, Wolfson MF, Rauch CT, Cerretti DP, Paxton RJ, March CJ, Black RA. 1998. An essential role for ectodomain shedding in mammalian development. *Science,* 282:1281-1284.

Pokutta S, Weis WI. 2007. Structure and mechanism of cadherins and catenins in cell-cell contacts. *Annu Rev Cell Dev Biol,* 23:237-261.

Primakoff P, Myles DG. 2000. The ADAM gene family: surface proteins with adhesion and protease activity. *Trends Genet,* 16:83-87.

Rao M, Baraban JH, Rajaii F, Sockanathan S. 2004. In vivo comparative study of RNAi methodologies by in ovo electroporation in the chick embryo. *Dev Dyn,* 231:592-600.

Rascher G, Fischmann A, Kroger S, Duffner F, Grote EH, Wolburg H. 2002. Extracellular matrix and the blood-brain barrier in glioblastoma multiforme: spatial segregation of tenascin and agrin. *Acta Neuropathol (Berl),* 104:85-91.

Redies C. 1995. Cadherin expression in the developing vertebrate CNS: from neuromeres to brain nuclei and neural circuits. *Exp Cell Res,* 220:243-256.

Redies C. 2000. Cadherins in the central nervous system. *Prog Neurobiol,* 61:611-648.

Redies C, Arndt K, Ast M. 1997. Expression of the cell adhesion molecule axonin-1 in neuromeres of the chicken diencephalon. *J Comp Neurol,* 381:230-252.

Redies C, Ast M, Nakagawa S, Takeichi M, Martínez-de-la-Torre M, Puelles L. 2000. Morphological fate of diencephalic neuromeres and their subdivisions revealed by mapping cadherin expression. *J Comp Neurol,* 421:481-514.

Redies C, Inuzuka H, Takeichi M. 1992. Restricted expression of N- and R-cadherin on neurites of the developing chicken CNS. *J Neurosci,* 12:3525-3534.

Redies C, Kovjanic D, Heyers D, Medina L, Hirano S, Suzuki ST, Puelles L. 2002a. Patch/matrix patterns of gray matter differentiation in the telencephalon of the chicken and mouse. *Brain Res Bull,* 57:489-493.

Redies C, Luckner R, Arndt K. 2002b. Granule cell raphes in the cerebellar cortex of chicken and mouse. *Brain Res Bull,* 57:341-343.

Redies C, Medina L, Puelles L. 2001. Cadherin expression by embryonic divisionsand derived gray matter structures in the telencephalon of the chicken. *J Comp Neurol,* 438:253-285.

Redies C, Takeichi M. 1996. Cadherins in the developing central nervous system: an adhesive code for segmental and functional subdivisions. *Dev Biol,* 180:413-423.

Redies C, Treubert-Zimmermann U, Luo J. 2003. Cadherins as regulators for the emergence of neural nets from embryonic divisions. *J Physiol Paris,* 97:5-15.

Redies C, Vanhalst K, Roy F. 2005. delta-Protocadherins: unique structures and functions. *Cell Mol Life Sci,* 62:2840-2852.

Reiss K, Maretzky T, Haas IG, Schulte M, Ludwig A, Frank M, Saftig P. 2006. Regulated ADAM10-dependent ectodomain shedding of gamma -protocadherin C3 modulates cell-cell adhesion. *J Biol Chem,* 281:21735-21744.

Reiss K, Maretzky T, Ludwig A, Tousseyn T, de Strooper B, Hartmann D, Saftig P. 2005. ADAM10 cleavage of N-cadherin and regulation of cell-cell adhesion and beta-catenin nuclear signalling. *EMBO J,* 24:742-752.

Richardson GP, Crossin KL, Chuong CM, Edelman GM. 1987. Expression of cell adhesion molecules during embryonic induction. III. Development of the otic placode. *Dev Biol,* 119:217-230.

Riehl R, Johnson K, Bradley R, Grunwald GB, Cornel E, Lilienbaum A, Holt CE. 1996. Cadherin function is required for axon outgrowth in retinal ganglion cells in vivo. *Neuron,* 17:837-848.

Risau W. 1997. Mechanisms of angiogenesis. *Nature,* 386:671-674.

Risau W, Hallmann R, Albrecht U, Henke-Fahle S. 1986. Brain induces the expression of an early cell surface marker for blood-brain barrier-specific endothelium. *EMBO J,* 5:3179-3183.

Roberson DW, Alosi JA, Cotanche DA. 2004. Direct transdifferentiation gives rise to the earliest new hair cells in regenerating avian auditory epithelium. *J Neurosci Res,* 78:461-471.

Roberts IM. 2002. Iso-butanol saturated water: a simple procedure for increasing staining intensity of resin sections for light and electron microscopy. *J Microsc,* 207:97-107.

Rosenberg GA, Estrada E, Kelley RO, Kornfeld M. 1993. Bacterial collagenase disrupts extracellular matrix and opens blood-brain barrier in rat. *Neurosci Lett,* 160:117-119.

Rybnikova E, Karkkainen I, Pelto-Huikko M, Huovila AP. 2002. Developmental regulation and neuronal expression of the cellular disintegrin ADAM11 gene in mouse nervous system. *Neuroscience,* 112:921-934.

Sagane K, Hayakawa K, Kai J, Hirohashi T, Takahashi E, Miyamoto N, Ino M, Oki T, Yamazaki K, Nagasu T. 2005. Ataxia and peripheral nerve hypomyelination in ADAM22-deficient mice. *BMC Neurosci,* 6:33.

Sagane K, Ohya Y, Hasegawa Y, Tanaka I. 1998. Metalloproteinase-like, disintegrin-like, cysteine-rich proteins MDC2 and MDC3: novel human cellular disintegrins highly expressed in the brain. *Biochem J,* 334:93-98.

Sagane K, Yamazaki K, Mizui Y, Tanaka I. 1999. Cloning and chromosomal mapping of mouse ADAM11, ADAM22 and ADAM23. *Gene,* 236:79-86.

Sato F, Nakagawa T, Ito M, Kitagawa Y, Hattori MA. 2004. Application of RNA interference to chicken embryos using small interfering RNA. *J Exp Zoolog A Comp Exp Biol,* 301:820-827.

Schlomann U, Rathke-Hartlieb S, Yamamoto S, Jockusch H, Bartsch JW. 2000. Tumor necrosis factor alpha induces a metalloprotease-disintegrin, ADAM8 (CD156): implications for neuron-glia interactions during neurodegeneration. *J Neurosci,* 20:7964–7971.

Schlöndorff J, Blobel CP. 1999. Metalloprotease-disintegrins: modular proteins capable of promoting cell-cell interactions and triggering signals by protein-ectodomain shedding. *J Cell Sci,* 112:3603-3617.

Schneider S, Herrenknecht K, Butz S, Kemler R, Hausen P. 1993. Catenins in Xenopus embryogenesis and their relation to the cadherin-mediated cell-cell adhesion system. *Development,* 118:629-640.

Schor AM, Canfield AE, Sloan P, Schor SL. 1991. Differentiation of pericytes in culture is accompanied by changes in the extracellular matrix. *In Vitro Cell Dev Biol,* 27A:651-659.

Schulz B, Pruessmeyer J, Maretzky T, Ludwig A, Blobel CP, Saftig P, Reiss K. 2008. ADAM10 regulates endothelial permeability and T-cell transmigration by proteolysis of vascular endothelial cadherin. *Circ Res,* 102:1139-1142.

Seals DF, Courtneidge SA. 2003. The ADAMs family of metalloproteases: multidomain proteins with multiple functions. *Genes Dev,* 17:7-30.

Shapiro L, Fannon AM, Kwong PD, Thompson A, Lehmann MS, Grubel G, Legrand JF, Als-Nielsen J, Colman DR, Hendrickson WA. 1995. Structural basis of cell-cell adhesion by cadherins. *Nature,* 374:327-337.

Shimoyama Y, Tsujimoto G, Kitajima M, Natori M. 2000. Identification of three human type-II classic cadherins and frequent heterophilic interactions between different subclasses of type-II classic cadherins. *Biochem J,* 349:159-167.

Shirabe K, Kimura Y, Matsuo N, Fukushima M, Yoshioka H, Tanaka H. 2005. MN-cadherin and its novel variant are transiently expressed in chick embryo spinal cord. *Biochem Biophys Res Commun,* 334:108-116.

Six E, Ndiaye D, Laabi Y, Brou C, Gupta-Rossi N, Israel A, Logeat F. 2003. The Notch ligand Delta1 is sequentially cleaved by an ADAM protease and gamma-secretase. *Proc Natl Acad Sci USA,* 100:7638-7643.

Skovronsky DM, Fath S, Lee VM, Milla ME. 2001. Neuronal localization of the TNF alpha converting enzyme (TACE) in brain tissue and its correlation to amyloid plaques. *J Neurobiol,* 49:40-46.

Sotillos S, Roch F, Campuzano S. 1997. The metalloprotease-disin-tegrin Kuzbanian participates in Notch activation during growth and patterning of Drosophila imaginal discs. *Development,* 124:4769-4779.

Sternlicht MD, Werb Z. 2001. How matrix metalloproteinases regulate cell behavior. *Annu Rev Cell Dev Biol,* 17:463-516.

Stone AL, Kroeger M, Sang QX. 1999. Structurefunction analysis of the ADAM family of disintegrin-like and metalloproteinase-containing proteins. *J Protein Chem,* 18:447-465.

Sugimoto K, Honda S, Yamamoto T, Ueki T, Monden M, Kaji A, Matsumoto K, Nakamura T. 1996. Molecular cloning and characterization of a newly identified member of the cadherin family, PB-cadherin. *J Biol Chem,* 271:11548-11556.

Suzuki SC, Furue H, Koga K, Jiang N, Nohmi M, Shimazaki Y, Katoh-Fukui Y, Yokoyama M, Yoshimura M, Takeichi M. 2007. Cadherin-8 is required for the first relay synapses to receive functional inputs from primary sensory afferents for cold sensation. *J Neurosci,* 27:3466-3476.

Suzuki SC, Takeichi M. 2008. Cadherins in neuronal morphogenesis and function. *Dev Growth Differ,* 1:S119-130.

Takahashi E, Sagane K, Nagasu T, Kuromitsu J. 2006. Altered nociceptive response in ADAM11-deficient mice. *Brain Res,* 1097:39-42.

Takeichi M. 1988. The cadherins: cell-cell adhesion molecules controlling animal morphogenesis. *Development,* 102:639-655.

Takeichi M. 1991. Cadherin cell adhesion receptors as a morphogenetic regulator. *Science,* 251:1451-1455.

Takeichi M. 1995. Morphogenetic roles of classic cadherins. *Cur Opin Cell Biol,* 7:619-627.

Takeichi M. 2007. The cadherin superfamily in neuronal connections and interactions. *Nature Rev Neurosci,* 8:11-20.

Tanabe C, Hotoda N, Sasagawa N, Sehara-Fujisawa A, Maruyama K, Ishiura S. 2007. ADAM19 is tightly associated with constitutive Alzheimer's disease APP alpha-secretase in A172 cells. *Biochem Biophys Res Commun,* 352:111-117.

Tanaka H, Shan W, Phillips GR, Arndt K, Bozdagi O, Shapiro L, Huntley GW, Benson DL, Colman DR. 2000. Molecular modification of N-cadherin in response to synaptic activity. *Neuron,* 25:93-107.

Tanaka K, Smith CA. 1975. Structure of the avian tectorial membrane. *Ann Otol Rhinol Laryngol,* 84:287-296.

Thiery JP. 2003. Cell adhesion in development: a complex signaling network. *Curr Opin Genet Dev,* 13:365-371.

Treubert-Zimmermann U, Heyers D, Redies C. 2002. Targeting axons to specific fiber tracts in vivo by altering cadherin expression. *J Neurosci,* 22:7617-7626.

van Hinsbergh VW, Engelse MA, Quax PH. 2006. Pericellular proteases in angiogenesis and vasculogenesis. *Arterioscler Thromb Vasc Biol,* 26:716-728.

Vanhalst K, Kools P, Staes K, van Roy F, Redies C. 2005. delta-Protocadherins: a gene family expressed differentially in the mouse brain. *Cell Mol Life Sci,* 62:1247-1259.

Vincent B. 2004. ADAM proteases: protective role in Alzheimer's and prion diseases? *Curr Alzheimer Res,* 1:165-174.

Vleminckx K, Kemler R. 1999. Cadherins and tissue formation: integrating adhesion and signaling. *BioEssays,* 21:211-220.

Warchol ME. 2002. Cell density and N-cadherin interactions regulate cell proliferation in the sensory epithelia of the inner ear. *J Neurosci,* 22:2607-2616.

Watabe-Uchida M, Masuda A, Shimada N, Endo M, Shimamura K, Yasuda K, Sehara-Fujisawa A. 2004. Novel metalloprotease-disintegrin, meltrin epsilon (ADAM35), expressed in epithelial tissues during chick embryogenesis. *Dev Dyn,* 230:557-568.

Weisleder P, Tsue TT, Rubel EW. 1995. Hair cell replacement in avian vestibular epithelium: supporting cell to type I hair cell. *Hear Res,* 82:125-133.

Weskamp G, Cai H, Brodie TA, Higashyama S, Manova K, Ludwig T, Blobel CP. 2002. Mice lacking the metalloprotease-disintegrin MDC9 (ADAM9) have no evident major abnormalities during development or adult life. *Mol Cell Biol,* 22:1537-1544.

Winklbauer R, Selchow A, Nagel M, Angres B. 1992. Cell interaction and its role in mesoderm cell migration during Xenopus gastrulation. *Dev Dyn,* 195:290-302.

Wöhrn JC, Nakagawa S, Ast M, Takeichi M, Redies C. 1999. Combinatorial expression of cadherins in the tectum and the sorting of neurites in the tectofugal pathways of the chicken embryo. *Neuroscience,* 90:985-1000.

Wöhrn JC, Puelles L, Nakagawa S, Takeichi M, Redies C. 1998. Cadherin expression in the retina and retinofugal pathways of the chicken embryo. *J Comp Neurol,* 396:20-38.

Wolfsberg TG, Bazan JF, Blobel CP, Myles DG, Primakoff P, White JM. 1993. The precursor region of a protein active in sperm-egg fusion contains a metalloprotease and a disintegrin domain: structural, functional, and evolutionary implications. *Proc Natl Acad Sci USA,* 90:10783-10787.

Wolfsberg TG, Primakoff P, Myles DG, White JM. 1995a. ADAM, a novel family of membrane proteins containing a disintegrin and metalloprotease domain: multipotential functions in cell–cell and cell–matrix interactions. *J Cell Biol,* 131:275-278.

Wolfsberg TG, Straight PD, Gerena RL, Huovila AP, Primakoff P, Myles DG, White JM. 1995b. ADAM, a widely distributed and developmentally regulated gene family encoding membrane proteins with a disintegrin and metalloprotease domain. *Dev Biol,* 169:378-383.

Yagami-Hiromasa T, Sato T, Kurisaki T, Kamijo K, Nabeshima Y, Fujisawa-Sehara A. 1995. A metalloprotease-disintegrin participating in myoblast fusion. *Nature,* 377:652-656.

Yamagata M, Weiner JA, Dulac C, Roth KA, Sanes JR. 2006. Labeled lines in the

retinotectal system: markers for retinorecipient sublaminae and the retinal ganglion cell subsets that innervate them. *Mol Cell Neurosci,* 33:296-310.

Yang P, Baker KA, Hagg T. 2005. A disintegrin and metalloprotease 21 (ADAM21) is associated with neurogenesis and axonal growth in developing and adult rodent CNS. *J Comp Neurol,* 490:163-179.

Yang P, Baker KA, Hagg T. 2006. The ADAMs family: coordinators of nervous system development, plasticity and repair. *Prog Neurobiol,* 79:73-94.

Zhao Z, Gruszczynska-Biegala J, Cheuvront T, Yi H, von der Mark H, von der Mark K, Kaufman SJ, Zolkiewska A. 2004. Interaction of the disintegrin and cysteine-rich domains of ADAM12 with integrin alpha7beta1. *Exp Cell Res,* 298:28-37.

Zheng X, Jiang F, Katakowski M, Kalkanis SN, Hong X, Zhang X, Zhang ZG, Yang H, Chopp M. 2007. Inhibition of ADAM17 reduces hypoxia-induced brain tumor cell invasiveness. *Cancer Sci,* 98:674-684.

Zhou HM, Weskamp G, Chesneau V, Sahin U, Vortkamp A, Horiuchi K, Chiusaroli R, Hahn R, Wilkes D, Fisher P, Baron R, Manova K, Basson CT, Hempstead BL, Blobel CP. 2004. Essential role for ADAM19 in cardiovascular morphogenesis. *Mol Cell Biol,* 24:96-104.

Zhu GZ, Lin Y, Myles DG. Primakoff P. 1999. Identification of four novel ADAMs with potential roles in spermatogenesis and fertilization. *Gene,* 234:227-237.

Zigrino P, Steiger J, Fox JW, Löffek S, Schild A, Nischt R, Mauch C. 2007. Role of ADAM-9 disintegrin-cysteine-rich domains in human keratinocyte migration. *J Biol Chem,* 282:30785-30793.

9. APPENDIX

NCBI GenBank information for the submitted full-length cDNA sequences

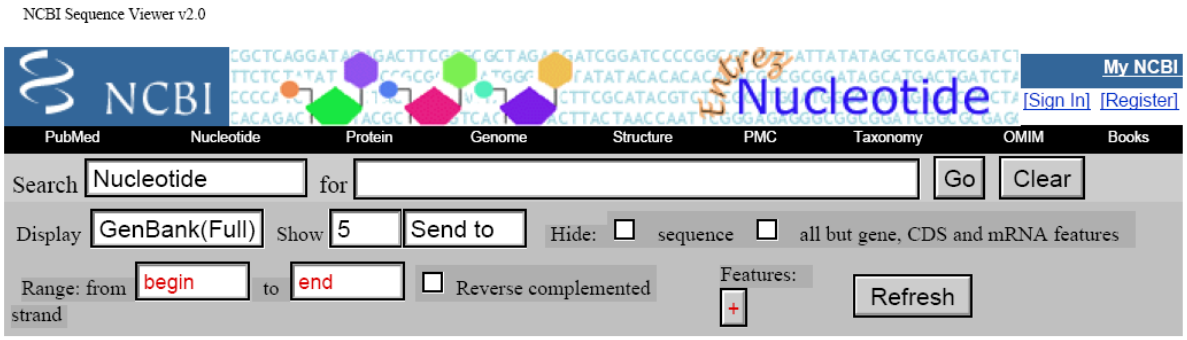

1: EF136663. Reports Gallus gallus a d...[gi:125434893] Links

Features Sequence

```
LOCUS       EF136663               2978 bp    mRNA    linear   VRT 27-FEB-2007
DEFINITION  Gallus gallus a disintegrin and metalloprotease 13 (ADAM13) mRNA,
            complete cds.
ACCESSION   EF136663
VERSION     EF136663.1  GI:125434893
KEYWORDS    .
SOURCE      Gallus gallus (chicken)
  ORGANISM  Gallus gallus
            Eukaryota; Metazoa; Chordata; Craniata; Vertebrata; Euteleostomi;
            Archosauria; Dinosauria; Saurischia; Theropoda; Coelurosauria;
            Aves; Neognathae; Galliformes; Phasianidae; Phasianinae; Gallus.
REFERENCE   1  (bases 1 to 2978)
  AUTHORS   Lin,J., Redies,C. and Luo,J.
  TITLE     Regionalized expression of ADAM13 during chicken embryonic
            development
  JOURNAL   (er) Dev. Dyn. 236 (3), 862-870 (2007)
   PUBMED   17245702
REFERENCE   2  (bases 1 to 2978)
  AUTHORS   Lin,J., Redies,C. and Luo,J.
  TITLE     Direct Submission
  JOURNAL   Submitted (22-NOV-2006) Institute of Anatomy I, Friedrich Schiller
            University of Jena, Teichgraben 7, Jena 07743, Germany
FEATURES             Location/Qualifiers
     source          1..2978
                     /organism="Gallus gallus"
                     /mol_type="mRNA"
                     /db_xref="taxon:9031"
                     /chromosome="4"
                     /dev_stage="embryonic stage 24"
     gene            1..2978
                     /gene="ADAM13"
     CDS             35..2878
                     /gene="ADAM13"
                     /codon_start=1
                     /product="a disintegrin and metalloprotease 13"
                     /protein_id="ABN42206.1"
                     /db_xref="GI:125434894"
                     /translation="MARLAPHVSPKWRGFAVIFGDHVLLLGLLLLPGHGGAAGTRGPM
                     SHGERVTPHWLLGGRSRRAVSLDDEVPAPARAEVAVMAEGRELILVLERNQLLAPGYT
```

NCBI Sequence Viewer v2.0

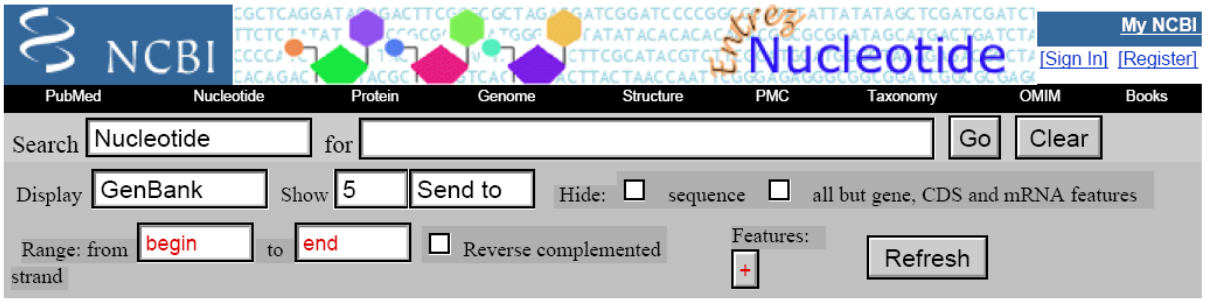

1: NM_001100289. Reports Gallus gallus cad...[gi:154152106] Links

Comment Features Sequence

```
LOCUS       NM_001100289            3676 bp    mRNA    linear   VRT 13-APR-2008
DEFINITION  Gallus gallus cadherin 8, type 2 (CDH8), mRNA.
ACCESSION   NM_001100289 XM_425125
VERSION     NM_001100289.1  GI:154152106
KEYWORDS    .
SOURCE      Gallus gallus (chicken)
  ORGANISM  Gallus gallus
            Eukaryota; Metazoa; Chordata; Craniata; Vertebrata; Euteleostomi;
            Archosauria; Dinosauria; Saurischia; Theropoda; Coelurosauria;
            Aves; Neognathae; Galliformes; Phasianidae; Phasianinae; Gallus.
REFERENCE   1  (bases 1 to 3676)
  AUTHORS   Lin,J., Luo,J. and Redies,C.
  TITLE     Molecular cloning and expression analysis of three cadherin-8
            isoforms in the embryonic chicken brain
  JOURNAL   Brain Res. 1201, 1-14 (2008)
   PUBMED   18336799
REFERENCE   2  (bases 1 to 3676)
  AUTHORS   Luo,J., Wang,H., Lin,J. and Redies,C.
  TITLE     Cadherin expression in the developing chicken cochlea
  JOURNAL   Dev. Dyn. 236 (8), 2331-2337 (2007)
   PUBMED   17654718
COMMENT     PROVISIONAL REFSEQ: This record has not yet been subject to final
            NCBI review. The reference sequence was derived from EF608154.1.
            On Jul 31, 2007 this sequence version replaced gi:118096458.
FEATURES             Location/Qualifiers
     source          1..3676
                     /organism="Gallus gallus"
                     /mol_type="mRNA"
                     /db_xref="taxon:9031"
                     /chromosome="11"
                     /map="11"
     gene            1..3676
                     /gene="CDH8"
                     /note="cadherin 8, type 2"
                     /db_xref="GeneID:427553"
     CDS             517..2916
                     /gene="CDH8"
                     /codon_start=1
                     /product="cadherin 8, type 2"
```

NCBI Sequence Viewer v2.0

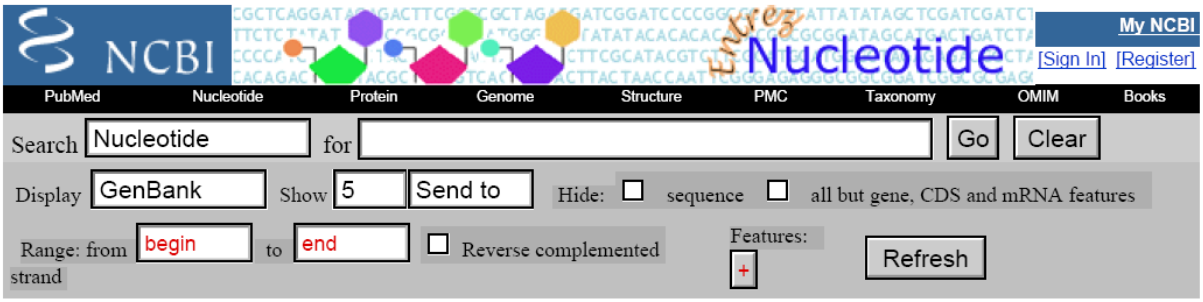

1: EU035636. Reports Gallus gallus cad...[gi:157932069] Links

Features Sequence

```
LOCUS       EU035636               2570 bp    mRNA    linear   VRT 10-APR-2008
DEFINITION  Gallus gallus cadherin 8 isoform 1 mRNA, complete cds.
ACCESSION   EU035636
VERSION     EU035636.1  GI:157932069
KEYWORDS    .
SOURCE      Gallus gallus (chicken)
  ORGANISM  Gallus gallus
            Eukaryota; Metazoa; Chordata; Craniata; Vertebrata; Euteleostomi;
            Archosauria; Dinosauria; Saurischia; Theropoda; Coelurosauria;
            Aves; Neognathae; Galliformes; Phasianidae; Phasianinae; Gallus.
REFERENCE   1  (bases 1 to 2570)
  AUTHORS   Lin,J., Luo,J. and Redies,C.
  TITLE     Molecular cloning and expression analysis of three cadherin-8
            isoforms in the embryonic chicken brain
  JOURNAL   Brain Res. 1201, 1-14 (2008)
   PUBMED   18336799
REFERENCE   2  (bases 1 to 2570)
  AUTHORS   Lin,J., Luo,J. and Redies,C.
  TITLE     Direct Submission
  JOURNAL   Submitted (16-JUL-2007) Institute of Anatimy I, Friedrich Schiller
            University Jena, Teichgraben 7, Jena D-07743, Germany
FEATURES             Location/Qualifiers
     source          1..2570
                     /organism="Gallus gallus"
                     /mol_type="mRNA"
                     /db_xref="taxon:9031"
                     /chromosome="11"
     CDS             517..2097
                     /note="Cdh8-1"
                     /codon_start=1
                     /product="cadherin 8 isoform 1"
                     /protein_id="ABW05086.1"
                     /db_xref="GI:157932070"
                     /translation="MPERLTEMLMDTWTPLIILWITVLPSIYMAPMNQSQVLPSGSST
                     GLKRLTEEQRILNRSKRGWVWNQMFVLEEFSGPEPILVGRLHTDLDPGSSKIKYILSG
                     DGAGTIFVINDKTGDIHAMKRLDREEKAEYTLTAQAVDRDTNKPLEPPSEFIIKVQDI
                     NDNAPEFVDGPYHATVPEMSVVGTFVTKVTATDADDPVYGNSAKLVYSILEGQPYFSI
                     EPHTAIIKTALPNMDREAKEEYFVVIQAKDMGGHMGGLSGTTTVTITLTDVNDNPPKF
                     AQSLYHFSVMEDVALGEPIGRVKANDLDIGENAKSSYDIIEGDGMDIFEITTDAQTQD
                     GVIRVRKPLDFETKKSYTLKVEAANIHIDPRFISGGPFKDTATVKIVVEDADEPPVFS
```

NCBI Sequence Viewer v2.0

NCBI Nucleotide

My NCBI [Sign In] [Register]

PubMed Nucleotide Protein Genome Structure PMC Taxonomy OMIM Books

Search Nucleotide for Go Clear

Display GenBank Show 5 Send to Hide: sequence all but gene, CDS and mRNA features

Range: from begin to end Reverse complemented strand Features: + Refresh

1: EU035637. Reports Gallus gallus cad...[gi:157932071] Links

Features Sequence

```
LOCUS       EU035637               2771 bp    mRNA    linear   VRT 10-APR-2008
DEFINITION  Gallus gallus cadherin 8 isoform 2 mRNA, complete cds.
ACCESSION   EU035637
VERSION     EU035637.1  GI:157932071
KEYWORDS    .
SOURCE      Gallus gallus (chicken)
  ORGANISM  Gallus gallus
            Eukaryota; Metazoa; Chordata; Craniata; Vertebrata; Euteleostomi;
            Archosauria; Dinosauria; Saurischia; Theropoda; Coelurosauria;
            Aves; Neognathae; Galliformes; Phasianidae; Phasianinae; Gallus.
REFERENCE   1  (bases 1 to 2771)
  AUTHORS   Lin,J., Luo,J. and Redies,C.
  TITLE     Molecular cloning and expression analysis of three cadherin-8
            isoforms in the embryonic chicken brain
  JOURNAL   Brain Res. 1201, 1-14 (2008)
   PUBMED   18336799
REFERENCE   2  (bases 1 to 2771)
  AUTHORS   Lin,J., Luo,J. and Redies,C.
  TITLE     Direct Submission
  JOURNAL   Submitted (16-JUL-2007) Institute of Anatimy I, Friedrich Schiller
            University Jena, Teichgraben 7, Jena D-07743, Germany
FEATURES             Location/Qualifiers
     source          1..2771
                     /organism="Gallus gallus"
                     /mol_type="mRNA"
                     /db_xref="taxon:9031"
                     /chromosome="11"
     CDS             517..2211
                     /note="Cdh8-2"
                     /codon_start=1
                     /product="cadherin 8 isoform 2"
                     /protein_id="ABW05087.1"
                     /db_xref="GI:157932072"
                     /translation="MPERLTEMLMDTWTPLIILWITVLPSIYMAPMNQSQVLPSGSST
                     GLKRLTEEQRILNRSKRGWVWNQMFVLEEFSGPEPILVGRLHTDLDPGSSKIKYILSG
                     DGAGTIFVINDKTGDIHAMKRLDREEKAEYTLTAQAVDRDTNKPLEPPSEFIIKVQDI
                     NDNAPEFVDGPYHATVPEMSVVGTFVTKVTATDADDPVYGNSAKLVYSILEGQPYFSI
                     EPHTAIIKTALPNMDREAKEEYFVVIQAKDMGGHMGGLSGTTTVTITLTDVNDNPPKF
                     AQSLYHFSVMEDVALGEPIGRVKANDLDIGENAKSSYDIIEGDGMDIFEITTDAQTQD
                     GVIRVRKPLDFETKKSYTLKVEAANIHIDPRFISGGPFKDTATVKIVVEDADEPPVFS
```

NCBI Sequence Viewer v2.0

NCBI Entrez Nucleotide

My NCBI [Sign In] [Register]

PubMed Nucleotide Protein Genome Structure PMC Taxonomy OMIM Books

Search Nucleotide for Go Clear

Display GenBank Show 5 Send to Hide: sequence all but gene, CDS and mRNA features

Range: from begin to end Reverse complemented strand Features: + Refresh

1: EF608155. Reports Gallus gallus cad...[gi:150416781] Links

Features Sequence

```
LOCUS       EF608155               2852 bp    mRNA    linear   VRT 08-AUG-2007
DEFINITION  Gallus gallus cadherin 19 mRNA, complete cds.
ACCESSION   EF608155
VERSION     EF608155.1  GI:150416781
KEYWORDS    .
SOURCE      Gallus gallus (chicken)
  ORGANISM  Gallus gallus
            Eukaryota; Metazoa; Chordata; Craniata; Vertebrata; Euteleostomi;
            Archosauria; Dinosauria; Saurischia; Theropoda; Coelurosauria;
            Aves; Neognathae; Galliformes; Phasianidae; Phasianinae; Gallus.
REFERENCE   1  (bases 1 to 2852)
  AUTHORS   Luo,J., Wang,H., Lin,J. and Redies,C.
  TITLE     Cadherin expression in the developing chicken cochlea
  JOURNAL   Dev. Dyn. 236 (8), 2331-2337 (2007)
   PUBMED   17654718
REFERENCE   2  (bases 1 to 2852)
  AUTHORS   Luo,J., Wang,H., Lin,J. and Redies,C.
  TITLE     Direct Submission
  JOURNAL   Submitted (12-MAY-2007) Neurobiological Laboratary, University of
            Rostock, Gehlsheimerstr. 20, Rostock 18147, Germany
FEATURES             Location/Qualifiers
     source          1..2852
                     /organism="Gallus gallus"
                     /mol_type="mRNA"
                     /db_xref="taxon:9031"
     CDS             307..2637
                     /codon_start=1
                     /product="cadherin 19"
                     /protein_id="ABR68860.1"
                     /db_xref="GI:150416782"
                     /translation="MNCSTFLSLVLALVQLQLCSPTTQIFSAQKTDQSYTTIRRVKRG
                     WVWEPLFVTEEETSTMPMYVGQLKSDLDKEDGSLQYILTGEGADSIFFINEHGKIYVR
                     QKLDREKKSFYILRAQVINRKTRHPIEPDSEFIIKVRDINDHEPQFLDGPYVATVPEM
                     SPEGTSVTQVTATDGDDPSYGNNARLLYSLIQGQPYFSVEPKTGVIRMTSQMDRETKD
                     QYLVVIQAKDMVGQAGAFSATATVTINLSDVNDNPPKFQQRLYYLNVSEEAPVGTTVG
                     RLLAEDSDIGENAAMNYFIEEDSSDVFGIITDRETQEGIIILKKRVDYESKRKHSVRV
                     KAVNRYIDDRFLKEGPFEDITIVQISVVDADEPPVFTLESYVMEIAEGVVSGSLVGTV
                     SARDLDNDDSSVRYSIVQGLHLKRLFSINEHNGTIITTEPLDREKASWHNITVTATET
                     RNPEKISEANVYIQVLDVNDHAPEFSKYYETFVCENAVPGQLIQNISAVDKDDSAENH
                     RFYFSLAQATNSSHFTVKDNQDNTAGIFTAGSGFSRKEQFYFFLPILILDNGSPPLTS
```

10. ACKNOWLEDGEMENTS

Prof. Christoph Redies introduced me to the field of embryonic development and neuroscience. I thank him sincerely for his kind advice, friendly help and perfect supervision of my dissertation. He always tried to fully develop my potential and encouraged me to explore open questions in neuroanatomy. Very frequent and intense discussions with him, even at lunchtime, made my work go into depth and helped me to become a mature researcher.

I am very grateful to Dr. Jiankai Luo, who supervised the initial stage of my doctoral research. Jiankai was not only an excellent advisor in my research work, but also he warmheartedly introduced me to living in Germany. I learnt a lot from him about experimental work in the laboratory, including the powerful method of in vivo electroporation. Although Jiankai left our group in March 2007, he continued to care for my ongoing work and often gave perfect advice to me. Thank you!

I am lucky to have had Franziska Neudert, Monique Nürnberger, Krishna Muthukumarappan, Nicole Hertel, Sylvia Hänßgen, Jessica Heyder and Silke Schreiber as my colleagues in the laboratory. I fondly remember working with them. The discussions with Franziska, Monique, Krishna and Nicole and their assistance in the laboratory helped to advance my experiments. I am very grateful to Sylvia, Jessica and Silke, who shared responsibility for making sure that routine procedures in the laboratory were always running well.

My sincere thanks to Dr. Cornelius Lemke for his help in performing the perfusion of the embryos and electron microscopic experiments, as well as for valuable discussions. I am sorry that I could not talk with him in German although he always encouraged me to continue learning this language.

I will never forget all my good friends in Jena. Here, I will not list their names. Without them, my life would lose much color.

Finally, I would like to express my gratitude to my family, my parents, my sisters and my brother. They always supported and encouraged me to study abroad. I would like to dedicate this thesis to my wife and my son. There are many thanks and apologies to them in my heart. Without their selfless support and deep love, this dissertation could not have been finished on time.

CURRICULUM VITAE

Personal Data:

Name:	Juntang Lin
Sex:	Male
Date of Birth:	08 August 1976
Place of Birth:	Henan Province, P. R. China
Nationality:	Chinese

Research experience:

07. 2005-present:

Ph.D. student and research fellow in the Institute of Anatomy I, Klinikum der Friedrich-Schiller-Universität, Teichgraben 7, 07743 Jena, Germany

07. 2002-07. 2005:

Research assistant in the Department of Cell Biology, Xinxiang Medical University, Henan Province, P. R. China

Education:

09. 1999-06. 2002:

College of Life Science, Henan Normal University, Henan Province, P. R. China
Master of Science

09. 1995-07. 1999:

College of Life Science, Henan Normal University, Henan Province, P. R. China
Bachelor of Science

PUBLICATIONS AND POSTER PRESENTATIONS

Publications:

1. **Juntang Lin**, Christoph Redies, Jiankai Luo. Regionalized expression of ADAM13 during chicken embryonic development. *Developmental Dynamics*, 2007, 236:862-870.
2. Jiankai Luo, Hong Wang, **Juntang Lin**, Christoph Redies. Cadherin expression in the developing chicken cochlea. *Developmental Dynamics*, 2007, 236:2331-2337.
3. **Juntang Lin**, Jiankai Luo, Christoph Redies. Molecular cloning and expression analysis of three cadherin-8 isoforms in the embryonic chicken brain. *Brain Research*, 2008, 1201:1-14.
4. **Juntang Lin**, Jiankai Luo, Christoph Redies. Differential expression of five members of the ADAM family in the developing chicken brain. *Neuroscience*, 2008 (in press)
5. Jiankai Luo, Min-Jeong Ju, **Juntang Lin**, Christoph Redies. Cadherin-20 expression by motor neurons is regulated by Sonic hedgehog during spinal cord development. Submitted to *NeuroReport*.
6. **Juntang Lin**, Cornelius Lemke, Christoph Redies, Xin Yan, Annett Markus, Eilhard Mix, Peter Kropp, Arndt Rolfs, Jiankai Luo. ADAM17 induces angiogenesis by increasing the proliferation of pericytes during chicken brain microvessel development. Manuscript in preparation.

Poster presentations:

1. **Juntang Lin**, Christoph Redies, Jiankai Luo. Transcription of ADAM13 during chicken embryonic development. 23. Arbeitstagung der Anatomischen Gesellschaft in Würzburg. 27-29 September, 2006.
2. **Juntang Lin**, Jiankai Luo, Christoph Redies. Expression of ADAM10 during chicken brain development. Seventh Göttingen Meeting of the German Neuroscience Society. 29 March -1 April, 2007.
3. **Juntang Lin**, Jiankai Luo, Christoph Redies. Expression of ADAMs in embryonic chicken brain. 24. Arbeitstagung der Anatomischen Gesellschaft in Würzburg. 26-28 September, 2007.

Statement

I am familiar with the Promotionsordnung of the Faculty of Biology and Pharmacy of the University of Jena. All parts of the dissertation were produced by myself. I hereby declare that this thesis does not contain any material previously submitted for a degree or diploma at another university or any material previously written or published by any other person, except where due acknowledgment or reference is made in the text. I also declare that I did not obtain the assistance of a dissertation counseling agent and that I did not provide any direct or indirect financial remuneration to any third party in connection with the content of my dissertation.

Jena, 01. October. 2008 …….

Juntang Lin